Lipids and inflammation in health and disease,
volume II

Edited by
Michael Bukrinsky, Alexander Nikolaevich Orekhov, Mirza S. Baig,
Veronika Myasoedova, Alessio Ravani, Vasily Sukhorukov and
Dongwei Zhang

About Frontiers

Frontiers is more than just an open access publisher of scholarly articles: it is a pioneering approach to the world of academia, radically improving the way scholarly research is managed. The grand vision of Frontiers is a world where all people have an equal opportunity to seek, share and generate knowledge. Frontiers provides immediate and permanent online open access to all its publications, but this alone is not enough to realize our grand goals.

Frontiers journal series

The Frontiers journal series is a multi-tier and interdisciplinary set of open-access, online journals, promising a paradigm shift from the current review, selection and dissemination processes in academic publishing. All Frontiers journals are driven by researchers for researchers; therefore, they constitute a service to the scholarly community. At the same time, the *Frontiers journal series* operates on a revolutionary invention, the tiered publishing system, initially addressing specific communities of scholars, and gradually climbing up to broader public understanding, thus serving the interests of the lay society, too.

Dedication to quality

Each Frontiers article is a landmark of the highest quality, thanks to genuinely collaborative interactions between authors and review editors, who include some of the world's best academicians. Research must be certified by peers before entering a stream of knowledge that may eventually reach the public - and shape society; therefore, Frontiers only applies the most rigorous and unbiased reviews. Frontiers revolutionizes research publishing by freely delivering the most outstanding research, evaluated with no bias from both the academic and social point of view. By applying the most advanced information technologies, Frontiers is catapulting scholarly publishing into a new generation.

What are Frontiers Research Topics?

Frontiers Research Topics are very popular trademarks of the *Frontiers journals series*: they are collections of at least ten articles, all centered on a particular subject. With their unique mix of varied contributions from Original Research to Review Articles, Frontiers Research Topics unify the most influential researchers, the latest key findings and historical advances in a hot research area.

Find out more on how to host your own Frontiers Research Topic or contribute to one as an author by contacting the Frontiers editorial office: frontiersin.org/about/contact

Lipids and inflammation in health and disease, volume II

Topic editors

Michael Bukrinsky — George Washington University, United States
Alexander Nikolaevich Orekhov — Institute for Aterosclerosis Research, Russia
Mirza S. Baig — Indian Institute of Technology Indore, India
Veronika Myasoedova — Monzino Cardiology Center (IRCCS), Italy
Alessio Ravani — Monzino Cardiology Center (IRCCS), Italy
Vasily Sukhorukov — Research Institute of Human Morphology, Russia
Dongwei Zhang — Beijing University of Chinese Medicine, China

Citation

Bukrinsky, M., Orekhov, A. N., Baig, M. S., Myasoedova, V., Ravani, A., Sukhorukov, V., Zhang, D., eds. (2023). *Lipids and inflammation in health and disease, volume II*. Lausanne: Frontiers Media SA. doi: 10.3389/978-2-8325-2258-5

Table of
contents

Editorial: Lipids and inflammation in health and disease, volume II

Evgeny Bezsonov[1,2,3,4]*, Mirza S. Baig[5], Michael Bukrinsky[6], Veronika Myasoedova[7], Alessio Ravani[7], Vasily Sukhorukov[2], Dongwei Zhang[8], Victoria Khotina[1,2] and Alexander Orekhov[9]*

[1]Laboratory of Angiopathology, Institute of General Pathology and Pathophysiology, Moscow, Russia, [2]Laboratory of Cellular and Molecular Pathology of the Cardiovascular System, Avtsyn Research Institute of Human Morphology, Petrovsky National Research Centre of Surgery, Moscow, Russia, [3]Department of Biology and General Genetics, I.M. Sechenov First Moscow State Medical University (Sechenov University), Moscow, Russia, [4]The Cell Physiology and Pathology Laboratory, Orel State University Named After I.S.Turgenev, Orel, Russia, [5]Department of Biosciences and Biomedical Engineering (BSBE), Indian Institute of Technology Indore (IITI), Simrol, India, [6]Department of Microbiology, Immunology and Tropical Medicine, School of Medicine and Health Sciences, The George Washington University, Washington, DC, United States, [7]Monzino Cardiology Center (IRCCS), Milan, Italy, [8]Diabetes Research Center, Beijing University of Chinese Medicine, Beijing, China, [9]Institute for Atherosclerosis Research, Skolkovo Innovative Center, Moscow, Russia

Editorial on the Research Topic
Lipids and inflammation in health and disease, volume II

The focus of this Research Topic is a continuation of the previous one and is devoted to the study of the role of lipids in inflammation in health and disease. Atherosclerosis is a classic example of how lipids involved in the normal functioning of cells and tissues can also induce inflammatory responses. Atherogenesis is far from being completely understood, and here we summarize the main pathological factors contributing to the development of this disease, focusing on the role of lipids.

Atherosclerosis is a disease of the intima of the arteries, leading to pathological thickening of the arterial wall with other secondary negative effects on the health of patients. The problem with this disease is that the exact causes of atherosclerosis are still not clarified, which limits the development of effective anti-atherosclerotic therapy. Thus, the identification of key molecular changes happening during the initiation and further progression of atherosclerosis, including the understanding of the role of lipids in this process, is a task of vital importance.

Atherosclerosis is an inflammatory disease associated with the infiltration of immune cells into the arterial wall (1, 2). Atherogenic factors (such as desialylated, oxidized, and electronegative LDL) (3, 4) are thought to be one of the main reasons for the accumulation of lipids in cells of the intima and macrophages, leading to the formation of so-called foam cells and further progression of atherosclerosis. There are gender differences in the development of atherosclerosis, including differences in lipid profiles (5).

Mitochondrial DNA mutations have been shown to be associated with atherosclerotic lesions, leading to the idea of a possible role of these mutations in the development of atherosclerosis (6). It should be noted that mitochondrial DNA mutations and mitochondrial dysfunction are associated not only with atherosclerosis (6), but also with a plethora of different diseases: non-alcoholic fatty liver disease, diabetes, polycystic ovarian syndrome, cancer, and various neurological diseases (7–9).

The components involved in the regulation of cholesterol metabolism (such as LDLR and PCSK9) can be considered potential targets for the development of drugs for the prevention of LDL-induced accumulation of cholesterol in cells (10, 11). It should also be noted also that PCSK9 may be associated with mitochondrial dysfunction (12), and even cancer in some cases (13).

In addition, atherosclerosis can be considered an autoimmune disease (14), and thus certain approaches used for the treatment of autoimmune and autoinflammatory diseases (15–17) may be potentially applicable to the cure of atherosclerosis.

Evidence is accumulating that non-coding RNAs are involved in the development of cardiovascular diseases including atherosclerosis (1), and, in addition to that, exosomes may also be involved in the progression of this disease (18).

Current pathological factors contributing to the development of atherosclerosis are shown in Figure 1.

This Research Topic collects 10 articles and reviews that are briefly discussed below.

A review by Poznyak et al. summarizes all known data on hypertension as a risk factor for atherosclerosis and risk assessment. The role of lipids in hypertension is discussed.

Data on oxidative stress as a primary factor linking lipids, inflammation, and atherosclerosis, in addition to therapeutic approaches to reduce oxidative stress were reviewed by Bale et al.

The reduction of plasma and liver lipid levels and atherosclerosis was discovered by Padalkar et al. in combined adenine-induced chronic kidney disease and diet-induced atherosclerosis in mice with a familial hypercholesterolemia
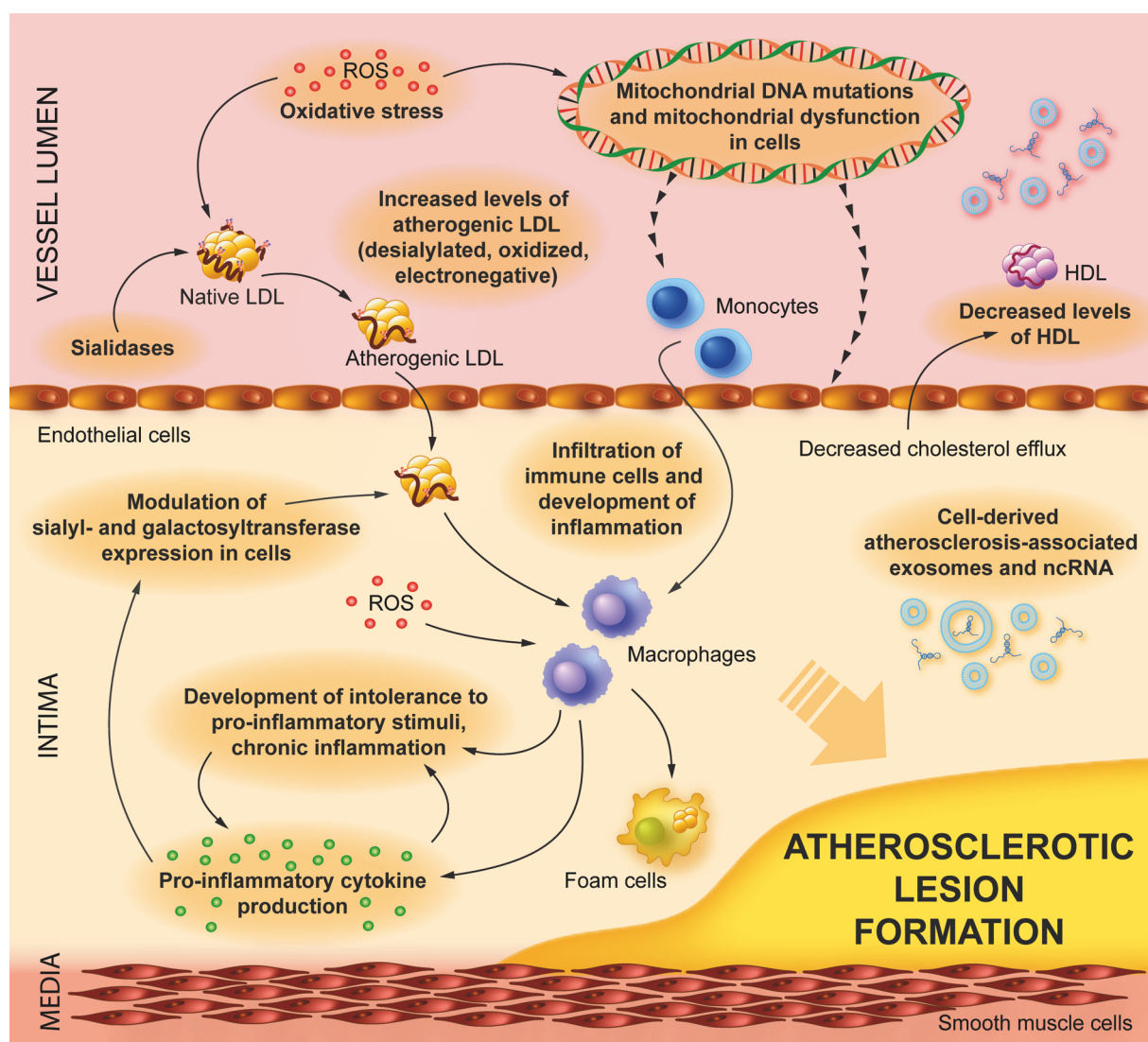
FIGURE 1
Pathological factors contributing to the development of atherosclerosis. Atherogenic LDL (desialylated, oxidized, and electronegative ones) induces lipid accumulation in endothelial cells and infiltrating macrophages, leading to foam cell formation, inflammation, and further progression of atherosclerosis. There are additional factors that contribute (or potentially contribute) to the development of atherogenesis, such as low levels of HDL, sialidase, and sialyl/galactosyltransferase activities leading to the generation of atherogenic LDL, intolerance to pro-inflammatory stimulation (including stimulation by atherogenic LDL), atherosclerosis-associated non-coding RNA (ncRNA), and exosomes.

mutation in the *ldlr* gene, leading to the conclusion that excessive adenine affects lipid metabolism.

The association of monomeric C-reactive protein (which is produced at sites of local inflammation) with carotid plaque number was found in patients with subclinical atherosclerosis in the study done by Melnikov et al.

The effects of lipoproteins, membranes, and extracellular vesicles on the structure and function of C-reactive protein were reviewed by Potempa et al.

Recent advances and future directions of research on the Von Willebrand factor (which may contribute to inflammation in atherosclerosis) with a focus on the diagnosis and treatment of cardiovascular diseases were reviewed by Kozlov et al.

The effect of Bie-Jia-Ruan-Mai-Tang (BJ, a traditional Chinese medicine formula) on proliferative diabetic retinopathy (the disease closely associated with inflammation) was investigated by Liu et al. using *in vitro* [human retinal capillary endothelial cells (HRCECs)] and *in vivo* (a diabetic mouse model) experiments.

The effects of forsythiasides [phenylethanol glycosides from the plant *Forsythia suspensa (Thunb.) Vahl*] on cardiovascular protection, anti-inflammation, antioxidation, and neuroprotection were reviewed by Yang et al.

The mechanism of action of monocyte locomotion inhibitory factor (MLIF) related to the reduction of ischemic stroke-induced inflammatory injury was investigated by Lv et al. with the conclusion about the anti-inflammatory effect of MLIF through the suppression of JNK/AP-1.

The attempt to identify molecular mechanisms of osteogenic differentiation of human valve interstitial cells (VIC) isolated from healthy donors or patients with calcific aortic valve disease associated with inflammation by RNA-seq transcriptomics and by shotgun proteomics was conducted by Semenova et al. with the finding of pro-osteogenic role of upregulated ZBTB16 gene.

The editors of Research Topic hope that the high standard of publications established in the first two volumes will be maintained in the third one.

Author contributions

EB and AO: writing and editing of the manuscript. MSB, MB, VM, AR, VS, VK, and DZ: editing of the manuscript. All authors contributed to the article and approved the submitted version.

Funding

Conflict of interest

The authors declare that the research was conducted in the absence of any commercial or financial relationships that could be construed as a potential conflict of interest.

Publisher's note

All claims expressed in this article are solely those of the authors and do not necessarily represent those of their affiliated organizations, or those of the publisher, the editors and the reviewers. Any product that may be evaluated in this article, or claim that may be made by its manufacturer, is not guaranteed or endorsed by the publisher.

References

1. Malekmohammad K, Bezsonov EE, Rafieian-Kopaei M. Role of lipid accumulation and inflammation in atherosclerosis: focus on molecular and cellular mechanisms. *Front Cardiovasc Med*. (2021) 8:707529. doi: 10.3389/fcvm.2021.707529

2. Poznyak AV, Bezsonov EE, Popkova TV, Starodubova AV, Orekhov AN. Immunity in atherosclerosis: focusing on T and B cells. *IJMS*. (2021) 22:8379. doi: 10.3390/ijms22168379

3. Mezentsev A, Bezsonov E, Kashirskikh D, Baig MS, Eid AH, Orekhov A. Proatherogenic sialidases and desialylated lipoproteins: 35 years of research and current state from bench to bedside. *Biomedicines*. (2021) 9:600. doi: 10.3390/biomedicines9060600

4. Mushenkova NV, Bezsonov EE, Orekhova VA, Popkova TV, Starodubova AV, Orekhov AN. Recognition of oxidized lipids by macrophages and its role in atherosclerosis development. *Biomedicines*. (2021) 9:915. doi: 10.3390/biomedicines9080915

5. Vakhtangadze T, Singh Tak R, Singh U, Baig MS, Bezsonov E. Gender differences in atherosclerotic vascular disease: from lipids to clinical outcomes. *Front Cardiovasc Med*. (2021) 8:707889. doi: 10.3389/fcvm.2021.707889

6. Bezsonov E, Sobenin I, Orekhov A. Immunopathology of atherosclerosis and related diseases: focus on molecular biology. *IJMS*. (2021) 22:4080. doi: 10.3390/ijms22084080

7. Dabravolski SA, Bezsonov EE, Baig MS, Popkova TV, Nedosugova LV, Starodubova AV, et al. Mitochondrial mutations and genetic factors determining NAFLD risk. *IJMS*. (2021) 22:4459. doi: 10.3390/ijms22094459

8. Dabravolski SA, Orekhova VA, Baig MS, Bezsonov EE, Starodubova AV, Popkova TV, et al. The role of mitochondrial mutations and chronic inflammation in diabetes. *IJMS*. (2021) 22:6733. doi: 10.3390/ijms22136733

9. Dabravolski SA, Nikiforov NG, Eid AH, Nedosugova LV, Starodubova AV, Popkova TV, et al. Mitochondrial dysfunction and chronic inflammation in polycystic ovary syndrome. *IJMS*. (2021) 22:3923. doi: 10.3390/ijms22083923

10. Puteri MU, Azmi NU, Kato M, Saputri FC. PCSK9 Promotes cardiovascular diseases: recent evidence about its association with platelet activation-induced myocardial infarction. *Life*. (2022) 12:190. doi: 10.3390/life12020190

11. Scharnagl H, März W. New lipid-lowering agents acting on LDL receptors. *Curr Top Med Chem*. (2005) 5(3):233–42. doi: 10.2174/1568026053544524

12. Ding Z, Liu S, Wang X, Mathur P, Dai Y, Theus S, et al. Cross-Talk between PCSK9 and damaged MtDNA in vascular smooth muscle cells: role in apoptosis. *Antioxid Redox Signaling*. (2016) 25:997–1008. doi: 10.1089/ars.2016.6631

13. Mahboobnia K, Pirro M, Marini E, Grignani F, Bezsonov EE, Jamialahmadi T, et al. PCSK9 And cancer: rethinking the link. *Biomed Pharmacother*. (2021) 140:111758. doi: 10.1016/j.biopha.2021.111758

14. Sima P, Vannucci L, Vetvicka V. Atherosclerosis as autoimmune disease. *Ann Transl Med*. (2018) 6(7):116. doi: 10.21037/atm.2018.02.02

15. El-Shebiny EM, Zahran ES, Shoeib SA, Habib ES. Bridging autoinflammatory and autoimmune diseases. *Egypt J Intern Med*. (2021) 33:11. doi: .org/10.1186/s43162-021-00040-5

16. Koushki K, Keshavarz Shahbaz S, Keshavarz M, Bezsonov EE, Sathyapalan T, Sahebkar A. Gold nanoparticles: multifaceted roles in the management of autoimmune disorders. *Biomolecules*. (2021) 11(9):1289. doi: .org/10.3390/biom11091289

17. Ghobadinezhad F, Ebrahimi N, Mozaffari F, Moradi N, Beiranvand S, Pournazari M, et al. The emerging role of regulatory cell-based therapy in

autoimmune disease. *Front Immunol*. (2022) 13:1075813. doi: 10.3389/fimmu.2022. 1075813

18. Wang C, Li Z, Liu Y, Yuan L. Exosomes in atherosclerosis: performers, bystanders, biomarkers, and therapeutic targets. *Theranostics*. (2021) 11 (8):3996–4010. doi: 10.7150/thno.56035

Bie-Jia-Ruan-Mai-Tang, a Chinese Medicine Formula, Inhibits Retinal Neovascularization in Diabetic Mice Through Inducing the Apoptosis of Retinal Vascular Endothelial Cells

Qiu-Ping Liu[1†], Yu-Ying Chen[1†], Yuan-Yuan Yu[1†], Pei An[1], Yi-Zhuo Xing[1], Hong-Xuan Yang[1], Yin-Jian Zhang[2], Khalid Rahman[3], Lei Zhang[4*], Xin Luan[1*] and Hong Zhang[1*]

[1] Shanghai Frontiers Science Center of TCM Chemical Biology, Institute of Interdisciplinary Integrative Medicine Research, Shanghai University of Traditional Chinese Medicine, Shanghai, China, [2] Ophthalmology Department of Longhua Hospital, Shanghai University of Traditional Chinese Medicine, Shanghai, China, [3] School of Pharmacy and Biomolecular Sciences, Faculty of Science, Liverpool John Moores University, Liverpool, United Kingdom, [4] Department of Vascular Surgery, Yueyang Hospital of Integrated Traditional Chinese and Western Medicine, Shanghai University of Traditional Chinese Medicine, Shanghai, China

Proliferative diabetic retinopathy (PDR) is one of the main complications of diabetes, mainly caused by the aberrant proliferation of retinal vascular endothelial cells and the formation of new blood vessels. Traditional Chinese medicines possess great potential in the prevention and treatment of PDR. Bie-Jia-Ruan-Mai-Tang (BJ), a Chinese medicine formula, has a good therapeutic effect on PDR clinically; however, the mechanism of action involved remains unclear. Therefore, we investigated the effect of BJ on PDR through *in vitro* and *in vivo* experiments. A diabetic mouse model with PDR was established by feeding a high-fat–high-glucose diet combined with an intraperitoneal injection of streptozotocin (STZ), while high-glucose-exposed human retinal capillary endothelial cells (HRCECs) were employed to mimic PDR *in vitro*. The *in vivo* experiments indicated that BJ inhibited the formation of acellular capillaries, decreased the expression of VEGF, and increased the level of ZO-1 in diabetic mice retina. *In vitro* experiments showed that high glucose significantly promoted cell viability and proliferation. However, BJ inhibited cell proliferation by cycle arrest in the S phase, thus leading to apoptosis; it also increased the production of ROS, decreased the mitochondrial membrane potential, reduced the ATP production, and also reduced the expressions of p-PI3K, p-AKT, and Bcl-xL, but increased the expressions of Bax and p-NF-κB. These results suggest that BJ induces the apoptosis of HRCECs exposed to high glucose through activating the mitochondrial death pathway by decreasing the PI3K/AKT signaling and increasing the NF-κB signaling to inhibit the formation of acellular capillaries in the retina, thus impeding the development of PDR.

Keywords: Chinese medicine formula, neovascularization, mitochondrial pathway, apoptosis, diabetic retinopathy

INTRODUCTION

Diabetes mellitus is a common metabolic disease characterized by chronic hyperglycemia, which can cause multiple organ damage (1). The development of hyperglycemia into diabetic complications is a complex process involving a series of mechanisms, and currently, no specific treatment is available (2). It was reported that there were 382 million diabetic patients worldwide in 2013, and moreover, this number is expected to increase to 592 million by 2035 (3). Diabetes can elicit a variety of complications, such as cardiovascular, kidney, and eye diseases, resulting in great inconvenience, economic pressure, and a sharp decline in the quality of life for the patients (4). A total of 14.8% of diabetic patients have eye complications, among which diabetic retinopathy (DR) is the most common and can lead to blindness (5). In total, 35% of patients eventually develop some form of retinopathy, suggesting that DR has the potential to be the leading cause of visual impairment and blindness worldwide (6). Therefore, it is essential to develop drugs for the prevention and treatment of DR. At present, panretinal photocoagulation (PRP) and anti-VEGF chemical drugs are the main treatment. Although these therapies indeed play a positive role in some aspects, however, the associated side effects cannot be ignored. For example, PRP can cause peripheral vision loss, night blindness, choroidal effusion, and macular edema, while the persistent effect is limited for the anti-VEGF chemical drugs. The current therapies still need to be improved for efficacy, safety, and persistence (7).

Owing to the characteristics of multiple targets, active components, and good safety, Chinese medicines have received increasing attention from clinicians and researchers worldwide (8). Numerous investigations have shown that Chinese medicines have great potential in the prevention and treatment of diabetes (9). Bie-Jia-Ruan-Mai-Tang (BJ) is an empirical prescription based on traditional Chinese medicine theory and long-term clinical practice, which is well summarized by Professor Jiu-Yi Xi, a famous expert in the treatment of peripheral vascular disease from the Yueyang Hospital of Integrated Traditional Chinese and Western Medicine Affiliated to the Shanghai University of Traditional Chinese Medicine. BJ is composed of *Trionyx sinensis* Wiegmann, the rhizome of *Acorus tatarinowii*, the whole plant of *Sedum sarmentosum*, and the root of *Paeonia lactiflora*, and has been clinically used for decades for the treatment of diabetic vascular complications in the Yueyang Hospital of Integrated Traditional Chinese and Western Medicine and Longhua Hospital affiliated to the Shanghai University of Traditional Chinese Medicine because of its good efficacies in softening hardness, relieving spasm, clearing heat,

detoxifying, invigorating qi, and promoting blood circulation (10, 11).

Endothelial dysfunction reflects an imbalance of endothelial cell-derived active substances, which can elicit injury, activation, and inflammation of endothelial cells. In addition, the dysfunction of endothelial cells is one of the main reasons for DR (12, 13). Although BJ has been used clinically for decades, the related mechanism of action still remains unclear. Accordingly, the present investigation aimed to verify the effects of BJ on diabetic mice with retinopathy and HRCECs exposed to high glucose, and to explore the possible mechanism of action involved.

MATERIALS AND METHODS

Preparation of Bie-Jia-Ruan-Mai-Tang Extract

The raw herbal materials comprising (BJ; the composition is shown in **Table 1**) were provided by the Ophthalmology Department of Longhua Hospital affiliated to the Shanghai University of Traditional Chinese Medicine, which were identified by Professor Hai-Liang Xin, a pharmacognosist in the Naval Military Medical University (Shanghai, China). The voucher specimen was deposited in the System Pharmacology Research Center, Institute of Interdisciplinary Integrative Medicine Research, Shanghai University of Traditional Chinese Medicine (SP2020016). These herbal materials were extracted twice for 1.5 h by refluxing with eight times the amount of 75% ethanol. The extracted solution was concentrated in a rotating evaporator after filtering with a four-layer gauze, and then pre-freeze at $-50°C$ for 5 h of vacuum dry in the material tray of a freeze-dryer. The temperature was finally fixed at $-40°C$ for 72 h to make a lyophilized powder. Finally, the extract with a yield of 18% was obtained and stored in a refrigerator at $-80°C$ until used.

Reagent

The cell-counting kit-8 (CCK-8) was purchased from the Meilun Biotechnology Co., Ltd. (Dalian, China). The ATP assay kit, the mitochondrial membrane potential kit, and the ROS assay kit were obtained from the Beyotime Biotechnology (Shanghai, China). The kits for the detection of cell apoptosis and cycle were provided by the KeyGen Biotechnology Co.,

TABLE 1 | The raw herbal material composition of Bie-Jia-Ruan-Mai-Tang.

Name of herbal material	Proportion
Shell of *Trionyx sinensis* Wiegmann	10
Whole plant of *Sedum sarmentosum* Bunge	6
Rhizome of *Acorus tatarinowii* Schott	6
Root of *Paeonia lactiflora* Pall	9
Root of *Astragalus mongholicus* Bunge	9
Root of *Dipsacus eroides* C. Y. Cheng et T. M.	6
Root and rhizome of *Glycyrrhiza uralensis* Fisch.	3
Flower bud and inflorescence of *Buddleja officinalis* Maxim.	6

Ltd. (Nanjing, China). Primary antibodies of p-NF-κB, NF-κB, p-PI3K, PI3K, p-AKT, AKT, BCL-XL, BAX, and GAPDH for Western blot were bought from the Cell Signaling Technology (Danvers, United States).

Animal Experiment

Male C57BL/6J mice (8 weeks of age) weighing 22–24 g were provided by the Shanghai Model Organisms Center, Inc. The animals were housed in a temperature-controlled room (23 ± 2°C) under a 12:12 h light–dark cycle of artificial light, with free access to food and water. The establishment of the mice model with DR was conferred with previous reports with slight alterations (14). Briefly, after 1 week of adaptive feeding, the animals were fed a high-fat–high-glucose diet (comprising 58.8% high-nutrition base feed, 20% glucose, 20% lard, 1% total cholesterol, and 0.2% sodium cholate, and purchased from the Nanjing Shengmin Scientific Research Animal Farm) for 17 weeks. Another eight mice given an ordinary diet were used as normal control. After 4 weeks, mice fed a high-fat–high-glucose diet were intraperitoneally injected with 50 mg/kg STZ (Sigma-Aldrich, St. Louis, MO, United States) for 5 consecutive days, while those in the normal control were injected with the same volume of normal saline. Four weeks after injection, the mice with blood glucose concentration above 16.7 mmol/L were considered to be type 2 diabetics [Shen et al. (15)]. The diabetic mice were divided into five different groups (n = 8 each group), including control group (Diabetic group), calcium dobesilate group (CAD, 0.25 g/kg.day^{-1}), low-dose group (LDG, 1.6 g/kg.day^{-1} BJ) group, medium-dose group (MDG, 3.2 g/kg.day^{-1} BJ), and high-dose group (HDG, 6.4 g/kg.day^{-1} BJ). Eight weeks after the administration of the above compounds, the mice were sacrificed by ether anesthesia, and the eyeballs were removed and stained with hematoxylin and eosin (H and E) and PAS (Periodic Acid-Schiff), and immunohistochemistry analyses were performed.

All animal experiments were approved by the Experimental Animal Ethics Committee of the Shanghai University of Traditional Chinese Medicine and performed in compliance with the University's Guidelines for the Care and Use of Laboratory Animals. The ethical number PZSHUTCM200814008 was adopted on 14 August 2020.

Cell Culture

Human retinal capillary endothelial cells (HRCECs) were purchased from the Cell Bank of Shanghai Academy of Chinese Sciences (Shanghai, China) and maintained in DMEM (HyClone, United States) supplemented with 10% FBS (GIBCO, United States) in an incubator of 5% CO$_2$ at 37°C. The HRCECs were then divided into two groups, *viz*. normal group of cells cultured in 5.5 mM glucose medium (NG) and a high-glucose group of cells cultured in 35 mM glucose medium (HG). In subsequent experiments, high-glucose-cultured cells were treated with BJ extract. A total of 0.1 g BJ extract was dissolved in 1 mL dimethyl sulfoxide, and the solution was filtered with a 0.22 µm sterile microporous membrane and diluted to the corresponding concentrations with the medium.

Cell-Counting Kit-8 Assay

Human retinal capillary endothelial cells cultured in NG and HG were, respectively, seeded into 96-well plates (5 × 10^3 cells/well), incubated at 37°C and 5% CO$_2$ for 24 h. The supernatant was discarded, and then the corresponding medium and different concentrations of BJ (10, 25, 50, 100, and 150 µg/mL) were added. After treatment with BJ for 24 h or 48 h, the supernatant was discarded, 100 µL of 10% CCK8 was added and incubated at 37°C for 30 min, and the absorbance was measured at 450 nm using a microplate reader. Cell viability was calculated as follows: Cell viability rate (%) = (absorbance of the experimental group–absorbance of the blank group)/(absorbance of the control group–absorbance of the blank group) × 100%.

Cell Colony Formation

Human retinal capillary endothelial cells cultured in NG and HG were, respectively, seeded into the 6-well plates (600 cells/well) and incubated at 37°C and 5% CO$_2$ for 24 h. The supernatant was discarded and the different concentrations of BJ (50, 100 µg/mL) were added to six-well plates for 8 consecutive days of incubation. Following this, HRCECs were fixed with 4% paraformaldehyde for 30 min and stained with crystal violet for 15 min, HRCECs cultured in NG were used as control.

Clone formation rate (%) = (Number of clones/number of inoculated cells) × 100%.

Cell Cycle Analysis

Human retinal capillary endothelial cells cultured in NG and HG were, respectively, harvested and seeded into six-well plates (5 × 10^5 cells/well) and incubated at 37°C for 24 h in the presence of 5% CO$_2$. After discarding the supernatant, different concentrations of BJ (50 and 100 µg/mL) or corresponding medium were added for another 24 h of incubation. One milliliter of precooled 70% ethanol was added to each well, and the cells were fixed at 4°C for 2 h. The cells were then collected, mixed with 0.5 mL PI, and the samples were incubated in the dark for 30 min, and the Beckman flow cytometer was used for detection.

Apoptosis Detection

Human retinal capillary endothelial cells cultured in NG and HG were, respectively, harvested and seeded into six-well plates (5 × 10^5 cells/well) and incubated at 37°C, for 24 h, in the presence of 5% CO$_2$. The different concentrations of BJ (50 and 100 µg/mL) were added for another 24 h of incubation. The cells were digested and centrifuged at 2,000 rpm for 10 min, 100 µL 1 × FITC binding solution was added to each well, mixed, and then 5 µL FITC dye was added for 10 min of incubation at room temperature in the dark. Finally, 5 µL PI dye was added for 5 min and the samples were incubated in the dark. HRCECs cultured in NG were used as control and the Beckman flow cytometer was used for detection.

JC-1 Mitochondrial Membrane Potential

Human retinal capillary endothelial cells cultured, respectively, in NG and HG were harvested and seeded into 24-well plates (5 × 10^4 cells/well) and incubated at 37°C, for 24 h, in the

presence of 5% CO_2. After removing the supernatant, the corresponding medium or different concentrations of BJ (50 and 100 μg/mL) were added for another 24 h of incubation. The transformation from red fluorescence to green fluorescence was used as one of the early detection indicators for cell apoptosis, and the fluorescence quantification was carried out using the Image J software.

Adenosine Triphosphate Detection

Adenosine triphosphate concentration in HRCECs was detected by the use of an ATP Assay Kit. Briefly, HRCECs cultured in NG and HG were, respectively, harvested, seeded into six-well plates (5×10^5 cells/well), and incubated at 37°C for 24 h in the presence of 5% CO_2. The corresponding medium or different concentrations of BJ were then added for 24 h of incubation. Cell lysis solution was added and the samples were centrifugated for 10 min at 12,000 $\times$ g at 4°C. A total of 20 μL sample or standard solution was added to 100 μL of ATP detection solution, mixed, and then luminescence was measured with a multifunctional enzyme plate analyzer.

Cell Nuclear Staining

Human retinal capillary endothelial cells cultured, respectively, in NG and HG were harvested, seeded into 24-well plates (5×10^4 cells/well), and incubated at 37°C for 24 h in the presence of 5% CO_2. The corresponding medium or different concentrations of BJ (50 and 100 μg/mL) were added for another 24 h of incubation. The HRCRCs were then washed with PBS three times, and 150 μL of 4% paraformaldehyde was added to fix for 30 min at room temperature. After abandoning the supernatant, 150 μL of 0.1% Triton X-100 was added and the samples were incubated for 10 min. Finally, 150 μL of DAPI solution was added to each well and incubated for 10 min at room temperature in the dark. The samples were photographed by the Operetta CLS high-content analysis system.

Intracellular Reactive Oxygen Species Detection

Intracellular ROS was detected with a ROS assay kit. Briefly, HRCECs cultured, respectively, in NG and HG were harvested, seeded into 6-well plates (5×10^5 cells/well), and incubated at 37°C for 24 h in the presence of 5% CO_2. DCFH-DA was added and the samples were incubated for 0.5 h. The different concentrations of BJ (50 and 100 μg/mL) or corresponding medium were added for 6 h, and the Beckman flow cytometer was used for detection.

Western Blot

Human retinal capillary endothelial cells cultured, respectively, in NG and HG were harvested, seeded into six-well plates (5×10^5 cells/well), and incubated at 37°C for 24 h in the presence of 5% CO_2. The different concentrations of BJ (50 and 100 μg/mL) and the corresponding medium were added for another 24 h of incubation. NP-40 cell lysate was added to split the cells. Protein concentration was determined with a BCA

Protein Concentration Assay Kit. The proteins were separated by 10% SDS-polyacrylamide electrophoresis, transferred to PVDF membrane, and sealed with 5% BSA at room temperature for 1 h. After incubation with the corresponding primary antibody overnight at 4°C, the membrane was washed three times with TBST, and the second antibody was used for another 1 h of incubation at room temperature. Then, the membrane was washed three times with TBST. Finally, the protein bands were detected and photographed using the Chemi Scope Mini (Tanon-4600SF).

Tandem Mass Tag Quantitative Proteomic Analysis

Human retinal capillary endothelial cells cultured, respectively, in NG and HG were seeded into 100 mm culture dishes. When the cells were about 60% confluent, 100 μg/mL BJ was added. After 24 h, NP-40 cell lysate was added to split the cells. Protein concentration was determined with a BCA Protein Concentration Assay Kit. Subsequently, 300 μg of protein was taken from each sample, diluted to 100 μL with PBS, and 500 μL of pre-cooled acetone was added. After mixing, the protein was placed in a −20°C refrigerator and frozen overnight. Then, the supernatant was discarded by centrifugation, 500 μL precooled acetone was added, protein precipitate was collected by centrifugation, and concentrated by vacuum for 5 min. A total of 20 μL of UA solution (8 M urea, 100 mM Tris, PH 7.6) was added and dissolved at room temperature for 1.5 h. A total of 50 mM DTT solution was added until a final concentration of 10 mM, and placed at 30°C for 1.5 h. IAA buffer was added (500 mM IAA in 50 mM TEAB) until a final concentration of 55 mM was obtained, left at room temperature for 40 min avoiding light, and then 50 mM TEAB was added until the urea concentration of lower than 1 M was obtained. Trypsin buffer (4 μg Trypsin in 40 μL and 50 mM TEAB buffer, 1:50 ratio of Trypsin: protein) was added and placed at 37°C for 16–18 h. The C18 Cartridge (3 M, 7 mm/3 ml) was used to desalt the peptide, which was lyophilized and redissolved with 40–50 uL 0.1% formic acid solution, and the thermo quantitative colorimetric assay was performed. This was done by adding 100 μL 50 mM TEAB buffer to the lyophilized sample, which was vortexed mixed, followed by the addition of a 50 μL sample to a 1.5 mL Ep tube for labeling reaction, which was performed by adding and vortex mixing 50 μL 50 mM TEAB, and vortex mixing. After balancing the Tandem mass tag (TMT) reagent to room temperature, 41 μL anhydrous acetonitrile was added, vortex mixed for 5 min, and centrifuged. A total of 41 μL TMT reagent was then added to the sample, mixed vortically, and placed at room temperature for 1 h. The reaction was stopped by the addition of 8 μL 5% hydroxylamine for 15 min, all samples were merged into a 1.5 mL Ep tube, lyophilized after desalting (3 m, 7 mm/3 mL), and stored at −80°C. The samples were separated by reversed-phase chromatography and analyzed by LC-MS/MS. Proteins with fold changes of quantification >1.5 and P-value < 0.05 were considered as differential expression. After obtaining the differentially expressed proteins, GO/KEGG

analyses were performed to describe the related functions, and the interaction network analysis was also carried out by using the STRING database.

Statistical Analysis

All data were analyzed using the SPSS 25.0 statistical software, and the data are expressed as mean ± standard deviation. The comparison of the mean between two groups was performed by *T*-test, and the comparison of multiple groups was performed by one-way analysis of variance. $P < 0.05$ was considered statistically significant.

RESULTS

Main Components of Bie-Jia-Ruan-Mai-Tang

Bie-Jia-Ruan-Mai-Tang consists of eight raw herbal materials, whose chemical composition is rather complex, so it is necessary to identify its major ingredients. The main components of extract (BJ) were detected by HPLC-Q-TOF-MS in positive and negative ion mode. As demonstrated in **Figure 1**, a total of 20 compounds were identified as follows: Luteolin (1), L-tert-Leucine (2), Vanillic acid (3), 5-Hydroxymethylfurfural (4), Loganic acid (5), Loganin (6), Sweroside (7), Albiflorin (8), Paeoniflorin (9), Calycosin 7-O-Glucoside (10), isoliquiritin apioside (11), Liquiritigenin (12), Isorhamnetin (13), Cynaroside (14), Dipsacoside B (15), Akebia saponin D (16), Benzoylpaeoniflorin (17), Apigenin (18), Liguiritigenin-7-O-D-apiosyl-4′-O-D-glucoside (19), and Quercitrin (20).

Bie-Jia-Ruan-Mai-Tang Does Not Reduce Blood Glucose in Diabetic Mice

The *in vivo* experiment process is displayed in **Figure 2A**. During the experiment, the body weight of mice was measured weekly. As shown in **Figure 2B**, the weight of mice in the normal group was higher than that of diabetic mice, while there was no obvious difference among the control, CAD, and BJ groups. The bodyweight of each group remained stable during the experiment. As shown in **Figure 2C**, in the 9th week, the diabetic mice were grouped randomly and hierarchically according to blood glucose concentration, and there was no significant difference in blood glucose between each group. The blood glucose concentration was measured at the 4th week and at the end of the experiment after the administration of the drugs. The results showed that after 8 weeks of administration, the blood glucose of mice in the CAD group decreased markedly, while BJ had no significant effect on blood glucose in diabetic mice.

Bie-Jia-Ruan-Mai-Tang Inhibits Retinal Angiogenesis in Diabetic Mice

To investigate the effects of BJ on retinal structure, acellular capillaries formation, and related protein expression in PDR mice, H and E, PAS, and immunohistochemistry techniques were carried out; the results are displayed in **Figure 3**. Compared with

the normal group, the layers of retinal structures in the control group were blurred, and the outer nuclear layer (ONL) and inner nuclear layer (INL) were arranged loosely. However, these changes were reversed after 8 weeks of BJ administration. PAS staining was used to analyze the formation of acellular capillaries in the retina, and the number of acellular capillaries in each field was counted. As a result, the number of acellular capillaries was significantly increased in the control group when compared with the normal group, but sharply reduced by BJ in a dose-dependent manner, suggesting that BJ inhibited the formation of acellular capillaries in the retina. The immunohistochemical staining was quantified by calculating the positive area, and the result exhibited that the expression of VEGF decreased and tight junction protein ZO-1 increased after 8 weeks of BJ administration.

Bie-Jia-Ruan-Mai-Tang Decreases the Proliferation of High-Glucose-Exposed Human Retinal Capillary Endothelial Cells

The assays for cell counting and plate cloning were used to verify the inhibitory effect of BJ on the viability and proliferation of HRCECs exposed to high glucose. High glucose significantly promoted cell viability, which could be reversed after treatment with different concentrations of BJ for 24 h (**Figure 4A**) and 48 h (**Figure 4C**). The IC_{50} values of BJ for 24 h and 48 h were calculated according to the cell-counting assay, which were 220.294 and 20.256 µg/mL, respectively (**Figures 4B,D**). In the plate cloning test, after treatment with BJ for 8 consecutive days, HRCECs were stained with crystal violet for 15 min and the purple area was counted. As revealed in **Figures 4E,F**, BJ markedly inhibited the proliferation of HRCECs in a dose-dependent manner. Cell cycle arrest plays an important role in the inhibition of cell proliferation. Therefore, we performed cell cycle analysis to further evaluate the effect of BJ in high-glucose-cultured HRCECs. Propidium iodide (PI) is a fluorescent dye that can produce fluorescence after binding with double-stranded DNA, and the fluorescence intensity is proportional to the content of double-stranded DNA. After the intracellular DNA is stained with PI, the DNA content of the cells is determined by flow cytometry, and then the cell cycle can be analyzed according to the DNA content. As expected, the cell cycle was arrested in the S phase after treatment with different concentrations of BJ for 24 h (**Figures 4G,H**), indicating that BJ inhibited the proliferation of HRCECs exposed to high glucose through arresting the cell cycle.

Bie-Jia-Ruan-Mai-Tang Promotes Apoptosis of High-Glucose-Exposed Human Retinal Capillary Endothelial Cells

Apoptosis can also reduce the number of cells; therefore, a flow cytometry analysis was used to detect the apoptosis of HRCECs cultured with high glucose after treatment with different concentrations of BJ for 24 h. Annexin V labeled with
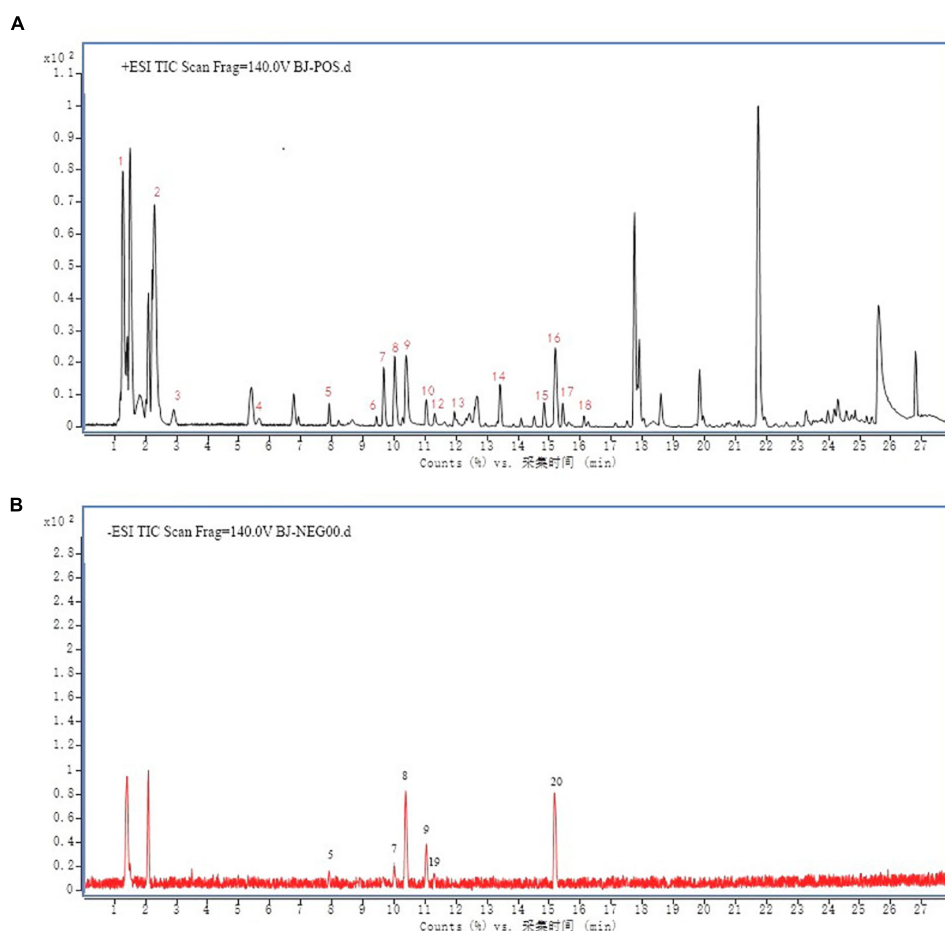
FIGURE 1 | Twenty compounds from BJ were detected by LC-MS/MS analysis in positive and negative ion mode. The chromatographic conditions were as follows: **(A)** Positive ion mode. **(B)** Negative ion mode. Agilent 6530 quadrupole-time of flight mass spectrometry (Q-TOF-MS) system, ACQUITY UPLC HSS T3 (2.1 mm × 150 mm, 1.7 μm) column temperature 60°C. 1. Luteolin, 2. L-tert-Leucine, 3. Vanillic acid, 4. 5-Hydroxymethylfurfural, 5. Loganic acid, 6. Loganin, 7. Sweroside, 8. Albiflorin, 9. Paeoniflorin, 10. Calycosin 7-O-Glucoside, 11. isoliquiritin apioside, 12. Liquiritigenin, 13. Isorhamnetin, 14. Cynaroside, 15. Dipsacoside B, 16. Akebia saponin D, 17. Benzoylpaeoniflorin, 18. Apigenin, 19. Liguiritigenin-7-O-D-apiosyl-4'-O-D-glucoside, 20. Quercitrin.

FITC fluorescent probe was employed to detect apoptosis, and the FITC positive cells were considered apoptotic cells. The results indicated that BJ increased apoptosis of the cells in a dose-dependent manner compared with the HG group (**Figure 5A**). We further evaluated the effect of BJ on nucleus morphology by DAPI staining, which can produce high-intensity fluorescence by binding to DNA. Therefore, the morphology of the nucleus can be observed through a fluorescence microscope. The nucleus is oval under normal circumstances, but showed irregular shapes after BJ treatment for 24 h (**Figure 5B**), indicating that BJ promoted the nuclear condensation and fragmentation.

Bie-Jia-Ruan-Mai-Tang Increases Mitochondrial Dysfunction of High-Glucose-Exposed Human Retinal Capillary Endothelial Cells

Mitochondrial membrane potential (MMP) is an indicator of mitochondrial membrane permeability, which is decreased during early apoptosis (16). MMP changes can be detected with the fluorescent probe JC-1 and are high under normal circumstances. After BJ treatment, the Operetta CLS high-content analysis system was used to observe the red and green fluorescence in the HRCECs, and the ratio of red to green fluorescence was quantified. After 24 h of BJ treatment, the proportion of green fluorescence evidently increased, suggesting the reduction of MMP in HRCECs (**Figures 6A,C**). ATP production is closely related to mitochondrial function (17). Besides, the production of ROS is closely associated with mitochondria as well (18), which are composed of superoxide radical anions, hydrogen peroxide (H_2O_2), and hydroxyl radicals. Excessive ROS causes DNA damage and cell death (19). Therefore, we further evaluated the effects of BJ on mitochondria by detecting the production of ATP and ROS in HRCECs. It was found that high glucose markedly promoted the production of ROS and ATP. After treatment with BJ, ROS increased obviously (**Figures 6B,D**), while ATP (**Figure 6E**) significantly decreased when compared with the HG group.
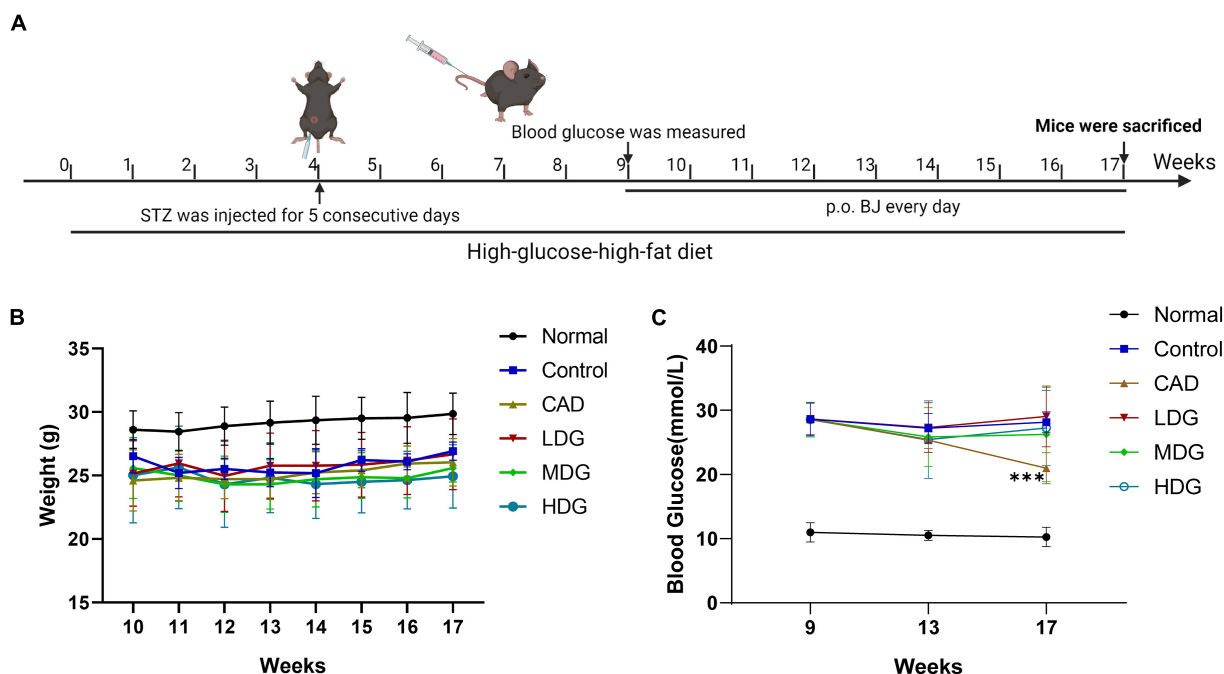
FIGURE 2 | Effect of BJ on the bodyweight and blood glucose in diabetic mice. **(A)** *In vivo* experiment process. Mice were fed a high-fat–high-glucose diet for 17 weeks. In the 4th week, mice were intraperitoneally injected with 50 mg/kg STZ for 5 consecutive days. In the 9th week, mice with blood glucose concentration above 16.7 mmol/L were considered type 2 diabetic. BJ was given for 8 consecutive weeks. Mice were weighed once a week **(B)**, and in the 13th and 17th week, the blood glucose was measured **(C)**. Data are represented as means ± SD ($n = 8$). ***$P < 0.001$ vs. control.
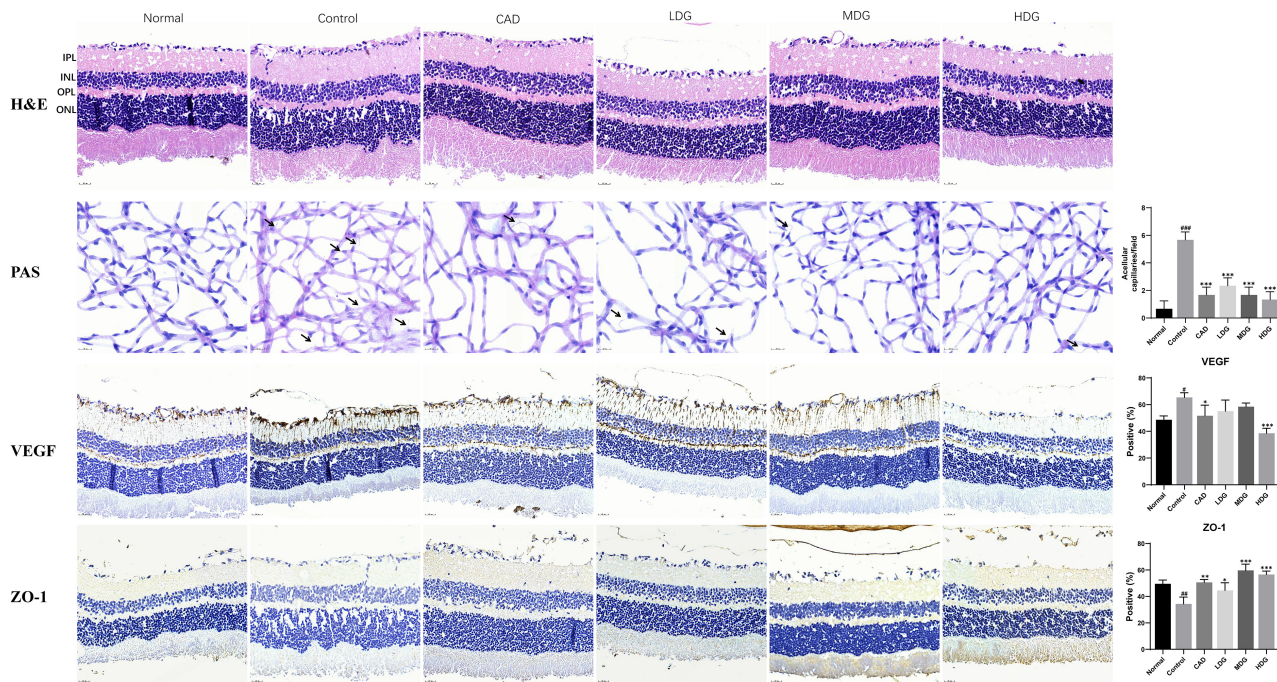
FIGURE 3 | Bie-Jia-Ruan-Mai-Tang (BJ) inhibits retinal angiogenesis in diabetic mice. The H and E, PAS, and immunohistochemistry staining were used to investigate the effects of BJ on retinal structure, acellular capillaries formation, and related protein expression in diabetic mice. The acellular capillaries in each field were counted, and the immunohistochemistry staining for VEGF and ZO-1 was quantified by calculating the positive area. IPL: inner plexiform layer, INL: inner nuclear layer, OPL: outer plexiform layer, ONL: outer nuclear layer. The arrows indicate acellular capillaries. Data are represented as mean ± SD ($n = 8$). #$P < 0.05$, ##$P < 0.01$, ###$P < 0.001$ vs. Normal; *$P < 0.05$, **$P < 0.01$, ***$P < 0.001$ vs. control.

FIGURE 4 | Bie-Jia-Ruan-Mai-Tang (BJ) represses the viability and proliferation of high-glucose-exposed HRCECs. After treatment with BJ for 24 h **(A)** and 48 h **(C)**, respectively, the CCK-8 kit was used to detect the cell viability of HRCECs ($n = 6$). The corresponding IC_{50} values were calculated according to the results of the cell counting assay, which were 220.294 μg/mL **(B)** and 20.256 μg/mL **(D)**, respectively. Cell colony formation assay **(E,F)** was performed to detect the proliferation of cells ($n = 3$). Cell cycle analysis **(G,H)** indicated that high-glucose-exposed HRCECs were arrested at the S phase by BJ ($n = 3$). HRCECs cultured with normal-glucose (NG) were used as control. All data are expressed as mean ± SD. $^{\#\#}P < 0.01$, $^{\#\#\#}P < 0.001$ vs. NG; $^{**}P < 0.01$, $^{***}P < 0.001$ vs. HG.

Bie-Jia-Ruan-Mai-Tang Depresses PI3K/AKT Signal Pathway Activation

Western blot was performed to study the mechanism of BJ against HRCECs exposed to high glucose. As shown in **Figure 7**, BJ significantly inhibited the expression of p-PI3K and p-AKT when compared with the HG group, indicating that the proliferation inhibition of HRCECs by BJ was related to suppressing activation of the PI3K/AKT signal pathway. Besides, apoptosis is also associated with the NF-κB signaling pathway (20), hence, the expression of NF-κB was detected. The results revealed that BJ significantly promoted the phosphorylation of NF-κB. As BJ was responsible for the collapse of MMP, we examined the expression of mitochondrial apoptosis-related proteins. As a result, high glucose promoted the expression of BCL-XL and inhibited BAX expression, while BJ treatment reversed these changes.

TMT Quantitative Proteomic Analysis

TMT quantitative proteomic analysis was carried out to detect the differentially expressed proteins after treatment with BJ. The screening conditions were set as p-value < 0.05 and quantification fold changes >1.5. After 100 μg/mL BJ treatment for 24 h, 403 differentially expressed proteins were screened out, of which 335 were downregulated and 69 upregulated as compared with the control. Then, the analyses of GO (Gene Ontology), PPI (Protein–Protein Interaction Network Analysis), and KEGG (Kyoto Encyclopedia of Genes and Genomes) were performed to find out the main functions of these differential proteins and the potential targets of BJ.

Gene Ontology analysis divided the function of protein into three parts, *viz.* cellular component, molecular function, and biological process. The function of most differential proteins is related to cellular component, among which, the main proteins are related to the nucleus, extracellular exosome, and membrane (**Figure 8A**). The GO enrichment chord diagram shows the GO term involved in the differential proteins (**Figure 8B**), indicating that their functions are mainly related to extracellular exosomes and cadherin binding. String database can be used to predict functional correlations between proteins. PPI are composed of proteins interacting with each other to participate in biological signal transmission, gene expression regulation, energy and substance metabolism, cell cycle regulation, and other life processes. The differentially expressed proteins were analyzed using the String database to obtain the interaction between them. Twenty-five proteins with the highest connectivity were selected to draw the interaction network diagram (**Figure 8C**), and the top five proteins in connectivity were listed as follows: HSPA4, ENO1, SOD1, PARK7, and PRDX6. KEGG analysis can help to understand the pathways changed after BJ treatment by analyzing the signaling pathways that are significantly
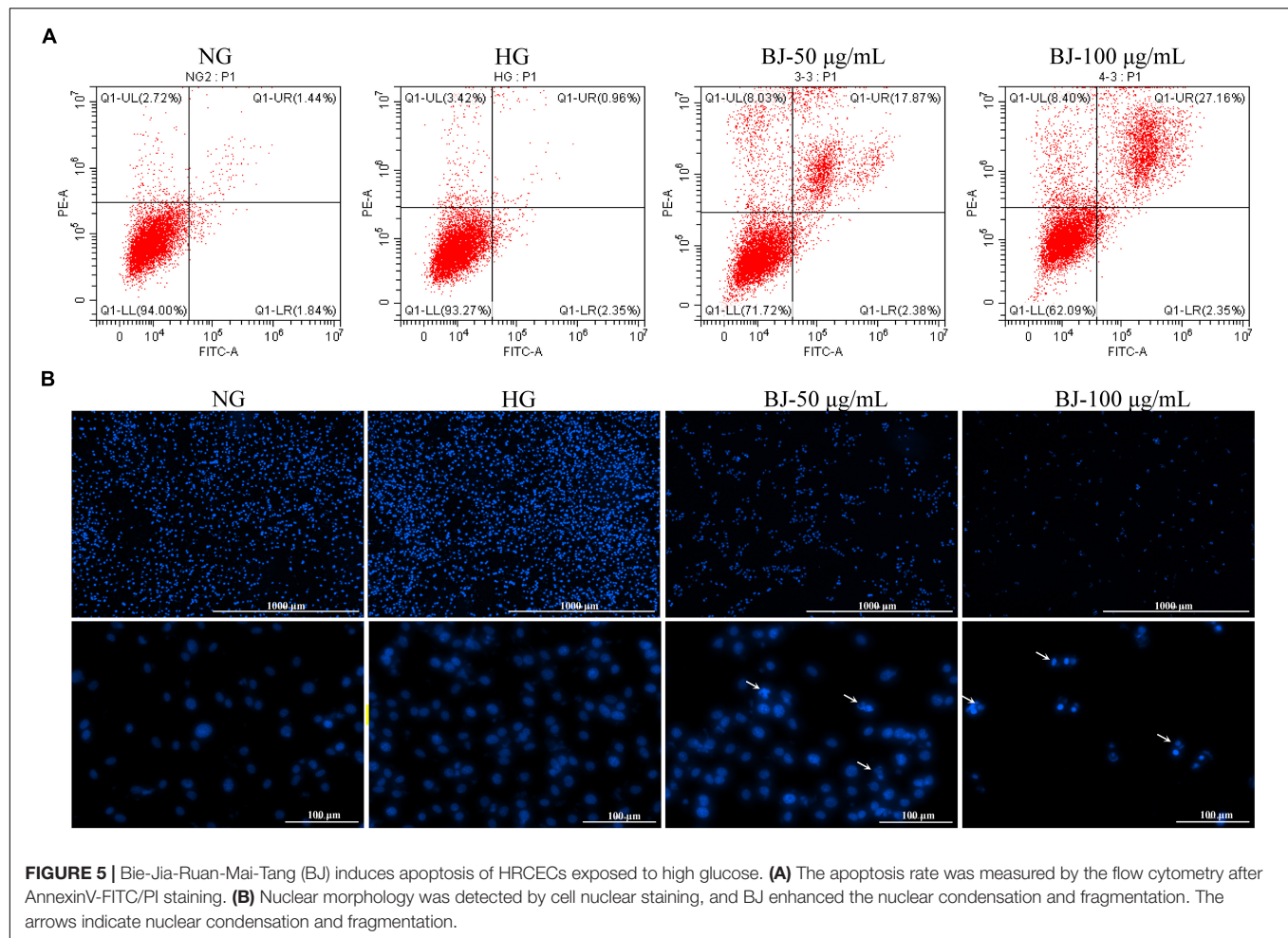
FIGURE 5 | Bie-Jia-Ruan-Mai-Tang (BJ) induces apoptosis of HRCECs exposed to high glucose. **(A)** The apoptosis rate was measured by the flow cytometry after AnnexinV-FITC/PI staining. **(B)** Nuclear morphology was detected by cell nuclear staining, and BJ enhanced the nuclear condensation and fragmentation. The arrows indicate nuclear condensation and fragmentation.

enriched in differentially expressed proteins. KEGG enrichment analysis demonstrated that most of the differential proteins were related to metabolism, including the pentose phosphate pathway, glycolysis, and purine metabolism (**Figures 8D–F**). As BJ reduced the ATP production, we speculate that BJ inhibits the proliferation of the cells by regulating cell metabolism.

DISCUSSION

The incidence of DR is continuing to rise (21). There are two main types of DR: early non-proliferative diabetic retinopathy (NPDR) and proliferative diabetic retinopathy (PDR). The main features of NPDR include microaneurysms, retinal hemorrhage, intraretinal microvascular abnormalities (IRMA), and changes in venous diameter, while PDR is characterized by pathological preretinal neovascularization (22). The abnormal proliferation of retinal vascular endothelial cells is closely related to PDR. Since its onset occurs after many years of diabetes progression, there is an opportunity to take steps to prevent vision loss (23). Therefore, drugs that inhibit retinal vascular endothelial cell proliferation are expectedly used to prevent further deterioration of DR. PDR is closely associated with the formation of acellular

capillaries, which is obviously promoted by VEGF (24, 25). Additionally, hyperglycemia also impairs the expression of tight-junction protein zonula occludens-1 (ZO-1) in the retina, which will increase the permeability of retinal capillaries, leading to blood extravasation and deterioration of DR (26). In this study, a diabetes model of mice was established through feeding a high-fat–high-glucose diet and intraperitoneal injection of STZ. The results showed that BJ significantly inhibited the formation of acellular capillaries in the retina of model mice, reduced the expression of VEGF, and promoted the expression of ZO-1, thus hindering the development of DR. After we conferred with the relevant literature, calcium dobesilate (CAD) was selected as a positive drug *in vivo* experiments (27, 28), which has antioxidant, free radical, and vascular protection effects. Many randomized controlled clinical trials have confirmed the efficacy and safety of CAD in the treatment of DR (29). In this study, CAD reduced the concentration of blood glucose, thus inhibited the formation of acellular capillaries and the expression of VEGF in the retina of model mice, indicating that CAD has a protective effect on retinal lesions. The *in vitro* experiments were carried out further to explore the related mechanism of action. HRCECs cultured in high-glucose condition were used to mimic DR *in vitro*. High glucose can obviously promote cell proliferation.

FIGURE 6 | Bie-Jia-Ruan-Mai-Tang (BJ) elicits mitochondrial dysfunction. **(A)** Representative images. JC-1 staining was used to evaluate the MMP change after treatment of the cells with BJ. The normal MMP shows red fluorescence, while green fluorescence represents the decreased membrane potential, indicating mitochondrial dysfunction. The ratio of red to green fluorescence was quantified **(C)**. The level of ROS in HRCECs was measured by a flow cytometer **(B,D)**. The ATP concentration was detected by the ATP assay kit **(E)**. Data are represented as mean ± SD ($n = 3$). $^{\#\#}P < 0.01$, $^{\#\#\#}P < 0.001$ vs. NG; $^{*}P < 0.05$, $^{***}P < 0.001$ vs. HG.

FIGURE 7 | Effect of BJ on protein expression of PI3K/AKT and NF-κB signal pathways in HRCECs exposed to high glucose. Representative images are displayed for p-PI3K, PI3K, p-AKT, AKT, p-NF-κB, NF-κB, Bax, Bcl-xL, and GAPDH protein bands.

FIGURE 8 | TMT quantitative proteomic analysis. The differentially expressed proteins were divided into three categories by GO analysis, and each category was divided into multiple items. Then top 10 differential proteins in each category were mapped **(A)**. **(B)** GO enrichment chord graph. Red on the left indicates upregulated proteins while blue downregulated proteins. The right represents the GO corresponding items. **(C)** PPI network analysis. Twenty-five proteins with the highest connectivity were selected to draw the interaction network diagram. **(D)** KEGG pathway classification. The percentage of differentially expressed proteins in pathways and metabolism is indicated. **(E,F)** Top 20 pathways and metabolisms with the highest enrichment scores in KEGG enrichment analysis.

Bie-Jia-Ruan-Mai-Tang was found to possess the abilities of proliferation inhibition and apoptosis induction in HRCECs exposed to high glucose.

BJ, a Chinese medicine formula composed of eight raw herbal materials, has been verified to have a good therapeutic effect on DR after decades of clinical application. Some of these raw herbal materials have previously been reported to be effective in treating diabetes as well. Turtle shell decoct pill, a formula with the shell of *Trionyx sinensis* as King medicine, can inhibit tumor angiogenesis (30), indicating that the shell possesses the potential to treat vascular diseases. Besides, the formula comprising *Astragalus mongholicus* Bunge and *Panax notoginseng* (*Burkill*) F.H. Chen protects the kidney from inflammatory damage in diabetic nephropathy, possibly by inhibiting mTOR and activating PINK1/Parkin signaling to promote autophagy (31). There are 20 compounds detected in BJ, and many of them have previously been reported to have therapeutic effects on diabetes. Akebia saponin D prevents renal injury in diabetic mice through activating the NRF2/HO-1 pathway and inhibiting the NF-κB pathway (32). Quercitrin can significantly reduce fasting blood glucose concentration and increase insulin level to improve the antioxidant status of diabetic rats (33). Isorhamnetin has a renal protective role by regulating autophagy epigenetic regulators in type 2 diabetes model rats (34). Vanillic acid regulates diabetic hypertension by adjusting blood glucose, insulin, and blood pressure (35).

Luteolin alleviates inflammation and oxidative stress through inhibiting NF-κB and upregulating Nrf2, thereby promoting wound recovery in diabetic rats (36). Apigenin ameliorates diabetic nephropathy by depressing oxidative stress and the MAPK pathway (37).

PI3K-dependent AKT activation affects several downstream pathways, which involves cell proliferation, angiogenesis, senescence, apoptosis, and cell survival (38, 39). BCL-XL and BAX are associated with the mitochondrial apoptosis pathway. Under normal circumstances, the apoptotic regulator BAX is mediated primarily by continuous reverse-transcriptional translocation elicited by BCL2L1/BCL-XL from mitochondria to the cytoplasm, thus avoiding the accumulation of BAX on the mitochondrial outer membrane (40). BCL-XL is an anti-apoptotic protein belonging to the Bcl-2 family, which helps to maintain the normal membrane state under stress conditions through direct pore-forming of the mitochondrial outer membrane (41). NF-κB, a type of DNA-binding eukaryotic cell transcription factor, is involved in normal physiological processes such as immune and inflammatory responses. The NF-κB signaling pathway is closely related to the development, proliferation, differentiation, and apoptosis of immune cells, and plays a major role in the regulation of inflammatory cytokine gene expression (42). Besides, NF-κB promotes apoptosis by triggering a series of events (24). The present investigation indicates that BJ promotes
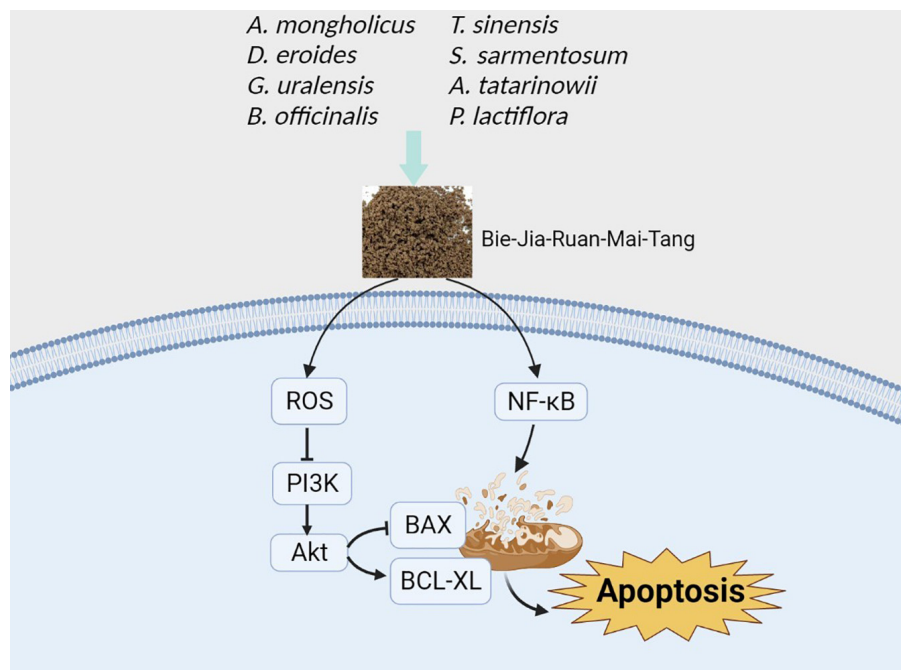
FIGURE 9 | Suggested mechanism of action of BJ eliciting the apoptosis of HRCECs exposed to high glucose. Created with BioRender.com.

apoptosis of HRCRCs exposed to high glucose, possibly through inhibition of PI3K/AKT signaling. Furthermore, BJ induces the mitochondrial dysfunction by interfering with the expression of mitochondrial function-related proteins, such as BAX and BCL-XL (**Figure 9**).

Proteome provides the current expression level of protein molecules, which can help us to understand the mechanism of action of medicines (43). One of the leading causes for diabetes is persistent hyperglycemia. We performed proteomics research on high-glucose-incubated HRCECs after BJ treatment. KEGG enrichment analysis showed that most of the differential proteins were related to metabolism, which was mainly involved in glucose metabolism, such as the pentose phosphate pathway, galactose metabolism, and pyruvate metabolism (**Figure 8E**). In addition, the pentose phosphate pathway has a higher enrichment score and lower p-value (**Figure 8F**). This suggests that BJ plays a therapeutic role probably by interfering with intracellular glucose metabolism. Although BJ displayed no hypoglycemic effect on the peripheral blood of model mice *in vivo* experiments, this does not prevent its therapeutic effect on PDR.

Currently, there still exist many limitations in the treatment of PDR with surgery and chemicals, such as many adverse reactions and expensive fees. Chinese medicines have attracted great attention owing to their good efficacy, low toxicity, and convenient use. Our study displayed that BJ retarded the development of DR by inhibiting the proliferation of acellular capillaries and promoting the stability of the retina. To further investigate the related mechanism of action, we established an *in vitro* model

of retinal endothelial cells cultured with high glucose. The findings indicated that BJ inhibited proliferation and induced apoptosis in the cells by eliciting cycle arrest and decreasing mitochondrial membrane potential *via* inactivation of the PI3K/AKT signaling pathway and activation of the NF-κ B pathway.

CONCLUSION

Bie-Jia-Ruan-Mai-Tang inhibits the formation of acellular capillary in the retina and the instability of retinal structure in DR mice, suppresses proliferation, and induces apoptosis in HRCECs exposed to high glucose through inducing cell cycle arrest and reducing mitochondrial membrane potential, indicating that BJ has the potential to treat DR.

DATA AVAILABILITY STATEMENT

The data presented in the study are deposited in the ProteomeXchange repository, accession number PXD012393.

ETHICS STATEMENT

The animal study was reviewed and approved by the Experimental Animal Ethics Committee of Shanghai University of Traditional Chinese Medicine.

AUTHOR CONTRIBUTIONS

HZ, XL, and LZ contributed to the conception and design of the experiments. Q-PL, Y-YC, and Y-YY performed the experiments and wrote the draft. PA, Y-ZX, and H-XY performed the statistical analysis and interpreted the data. Y-JZ and LZ provided the raw herbal materials. HZ and KR revised the manuscript. All authors agreed to be accountable for all aspects of the work, ensuring integrity and accuracy.

FUNDING

REFERENCES

1. Ma R. Epidemiology of diabetes and diabetic complications in China. *Diabetologia.* (2018) 61:1249–60. doi: 10.1007/s00125-018-4557-7

2. Laddha A, Kulkarni Y. Tannins and vascular complications of diabetes: an update. *Phytomedicine.* (2019) 56:229–45. doi: 10.1016/j.phymed.2018.10.026

3. Guariguata L, Whiting D, Hambleton I, Beagley J, Linnenkamp U, Shaw J. Global estimates of diabetes prevalence for 2013 and projections for 2035. *Diabetes Res Clin Pract.* (2014) 103:137–49. doi: 10.1016/j.diabres.2013.11.002

4. Darenskaya M, Kolesnikova L, Kolesnikov S. Oxidative stress: pathogenetic role in diabetes mellitus and its complications and therapeutic approaches to correction. *Bull Exp Biol Med.* (2021) 171:179–89. doi: 10.1007/s10517-021-05191-7

5. Simó-Servat O, Hernández C, Simó R. Diabetic retinopathy in the context of patients with diabetes. *Ophthalmic Res.* (2019) 62:211–7. doi: 10.1159/000499541

6. Yau J, Rogers S, Kawasaki R, Lamoureux E, Kowalski J, Bek T, et al. Global prevalence and major risk factors of diabetic retinopathy. *Diabetes Care.* (2012) 35:556–64. doi: 10.2337/dc11-1909

7. Le N, Kroeger Z, Lin W, Khanani A, Weng C. Novel treatments for diabetic macular edema and proliferative diabetic retinopathy. *Curr Diab Rep.* (2021) 21:43. doi: 10.1007/s11892-021-01412-5

8. Wang N, Yang B, Zhang X, Wang S, Zheng Y, Li X, et al. Network pharmacology-based validation of caveolin-1 as a key mediator of Ai Du Qing inhibition of drug resistance in breast cancer. *Front Pharmacol.* (2018) 9:1106. doi: 10.3389/fphar.2018.01106

9. Wang J, Ma Q, Li Y, Li P, Wang M, Wang T, et al. Research progress on traditional Chinese medicine syndromes of diabetes mellitus. *Biomed Pharmacother.* (2020) 121:109565. doi: 10.1016/j.biopha.2019.109565

10. Xu H, Tang W, Zhang L. Effect of "Tangzu formula"on latent syndrome of diabetic foot tendon gangrene. *Shanghai J Tradit Chin Med.* (2016) 50:38–40. doi: 10.16305/j.1007-1334.2016.01.013

11. Yan S, Liu G, Li W, Zhang L. Clinical observation of "Tangzu formula"in treating diabetic foot ulcers: a randomized and placebo-controlled trial. *Shanghai J Tradit Chin Med.* (2016) 50:55–7. doi: 10.16305/j.1007-1334.2016.06.018

12. Mrugacz M, Bryl A, Zorena K. Retinal vascular endothelial cell dysfunction and neuroretinal degeneration in diabetic patients. *J Clin Med.* (2021) 10:458. doi: 10.3390/jcm10030458

13. Hamilton S, Watts G. Endothelial dysfunction in diabetes: pathogenesis, significance, and treatment. *Rev Diabet Stud.* (2013) 10:133–56. doi: 10.1900/rds.2013.10.133

14. Wang M, Fang G, Culver D, Davis A, Rich M, Glass J. The wlds protein protects against axonal degeneration: a model of gene therapy for peripheral neuropathy. *Ann Neurol.* (2001) 50:773–9. doi: 10.1002/ana.10039

15. Shen YL, Jiang YP, Li XQ, Wang SJ, Ma MH, Zhang CY, et al. Erhuang formula improves renal fibrosis in diabetic nephropathy rats by inhibiting CXCL6/JAK/STAT3 signaling pathway. *Front Pharmacol.* (2020) 10:1596. doi: 10.3389/fphar.2019.01596

16. Yue J, Jin S, Li Y, Zhang L, Jiang W, Yang C, et al. Magnesium inhibits the calcification of the extracellular matrix in tendon-derived stem cells *via* the ATP-P2R and mitochondrial pathways. *Biochem Biophys Res Commun.* (2016) 478:314–22. doi: 10.1016/j.bbrc.2016.06.108

17. Zorova L, Popkov V, Plotnikov E, Silachev D, Pevzner I, Jankauskas S, et al. Mitochondrial membrane potential. *Anal Biochem.* (2018) 552:50–9. doi: 10.1016/j.ab.2017.07.009

18. Indo H, Davidson M, Yen H, Suenaga S, Tomita K, Nishii T, et al. Evidence of ROS generation by mitochondria in cells with impaired electron transport chain and mitochondrial DNA damage. *Mitochondrion.* (2007) 7:106–18. doi: 10.1016/j.mito.2006.11.026

19. Evens A, Prachand S, Shi B, Paniaqua M, Gordon L, Gartenhaus R. Imexon-induced apoptosis in multiple myeloma tumor cells is caspase-8 dependent. *Clin Cancer Res.* (2004) 10:1481–91. doi: 10.1158/1078-0432.ccr-1058-03

20. Pai P, Sukumar S. HOX genes and the NF-κB pathway: a convergence of developmental biology, inflammation and cancer biology. *Biochim Biophys Acta Rev Cancer.* (2020) 1874:188450. doi: 10.1016/j.bbcan.2020.188450

21. Duh E, Sun J, Stitt A. Diabetic retinopathy: current understanding, mechanisms, and treatment strategies. *JCI Insight.* (2017) 2:e93751. doi: 10.1172/jci.insight.93751

22. Stitt A, Curtis T, Chen M, Medina R, McKay G, Jenkins A, et al. The progress in understanding and treatment of diabetic retinopathy. *Prog Retin Eye Res.* (2016) 51:156–86. doi: 10.1016/j.preteyeres.2015.08.001

23. Tolentino MS, Tolentino AJ, Tolentino MJ. Current and investigational drugs for the treatment of diabetic retinopathy. *Expert Opin Investig Drugs.* (2016) 25:1011–22. doi: 10.1080/13543784.2016.1201062

24. Chen J, Stark L. Insights into the relationship between nucleolar stress and the NF-κB pathway. *Trends Genet.* (2019) 35:768–80. doi: 10.1016/j.tig.2019.07.009

25. Du A, Xie Y, Ouyang H, Lu B, Jia W, Xu H, et al. In vivosi-miao-yong-an decoction for diabetic retinopathy: a combined network pharmacological and approach. *Front Pharmacol.* (2021) 12:763163. doi: 10.3389/fphar.2021.763163

26. Tien T, Barrette K, Chronopoulos A, Roy S. Effects of high glucose-induced Cx43 downregulation on occludin and Zo-1 expression and tight junction barrier function in retinal endothelial cells. *Invest Ophthalmol Vis Sci.* (2013) 54:6518–25. doi: 10.1167/iovs.13-11763

27. Fang Y, Shi K, Lu H, Lu L, Qiu B. Mingmu xiaomeng tablets restore autophagy and alleviate diabetic retinopathy by inhibiting PI3K/Akt/mTOR signaling. *Front Pharmacol.* (2021) 12:632040. doi: 10.3389/fphar.2021.632040

28. Pang B, Ni Q, Di S, Du L, Qin Y, Li Q, et al. Luo tong formula alleviates diabetic retinopathy in rats through micro-200b target. *Front Pharmacol.* (2020) 11:551766. doi: 10.3389/fphar.2020.551766

29. Zhang X, Liu W, Wu S, Jin J, Li W, Wang N. Calcium dobesilate for diabetic retinopathy: a systematic review and meta-analysis. *Sci China Life Sci.* (2015) 58:101–7. doi: 10.1007/s11427-014-4792-1

30. Chen D, Zhang X. Experimental study on antitumor angiogenesis of turtle shell decoct pill. *J Zhejiang Tradit Chin Med.* (2004) 12:32–4.

31. Wen D, Tan R, Zhao C, Li J, Zhong X, Diao H, et al. *Astragalus mongholicus* bunge and panax notoginseng (Burkill) F.H. Chen formula for renal injury in diabetic nephropathy- *in vivo* and *in vitro* evidence for autophagy regulation. *Front Pharmacol.* (2020) 11:732. doi: 10.3389/fphar.2020.00732

32. Lu C, Fan G, Wang D. Akebia saponin D ameliorated kidney injury and exerted anti-inflammatory and anti-apoptotic effects in diabetic nephropathy by activation of NRF2/HO-1 and inhibition of NF-KB pathway. *Int Immunopharmacol.* (2020) 84:106467. doi: 10.1016/j.intimp.2020.106467

33. Babujanarthanam R, Kavitha P, Mahadeva Rao U, Pandian M. Quercitrin a bioflavonoid improves the antioxidant status in streptozotocin: induced

diabetic rat tissues. *Mol Cell Biochem.* (2011) 358:121–9. doi: 10.1007/s11010-011-0927-x

34. Matboli M, Ibrahim D, Hasanin A, Hassan M, Habib E, Bekhet M, et al. Epigenetic modulation of autophagy genes linked to diabetic nephropathy by administration of isorhamnetin in type 2 diabetes mellitus rats. *Epigenomics.* (2021) 13:187–202. doi: 10.2217/epi-2020-0353

35. Vinothiya K, Ashokkumar N. Modulatory effect of vanillic acid on antioxidant status in high fat diet-induced changes in diabetic hypertensive rats. *Biomed Pharmacother.* (2017) 87:640–52. doi: 10.1016/j.biopha.2016.12.134

36. Chen L, Cheng H, Kuan Y, Liang T, Chao Y, Lin H. Therapeutic potential of luteolin on impaired wound healing in streptozotocin-induced rats. *Biomedicines.* (2021) 9:761. doi: 10.3390/biomedicines9070761

37. Malik S, Suchal K, Khan S, Bhatia J, Kishore K, Dinda A, et al. Apigenin ameliorates streptozotocin-induced diabetic nephropathy in rats *via* MAPK-NF-κB-TNF-α and TGF-β1-MAPK-fibronectin pathways. *Am J Physiol Renal Physiol.* (2017) 313:F414–22. doi: 10.1152/ajprenal.00393.2016

38. Hoke G, Ramos C, Hoke N, Crossland M, Shawler L, Boykin J. Atypical diabetic foot ulcer keratinocyte protein signaling correlates with impaired wound healing. *J Diabetes Res.* (2016) 2016:1586927. doi: 10.1155/2016/1586927

39. Li T, Wang G. Computer-aided targeting of the PI3K/AKT/mTOR pathway: toxicity reduction and therapeutic opportunities. *Int J Mol Sci.* (2014) 15:18856–91. doi: 10.3390/ijms151018856

40. Edlich F, Banerjee S, Suzuki M, Cleland M, Arnoult D, Wang C, et al. Bcl-x(L) retrotranslocates bax from the mitochondria into the cytosol. *Cell.* (2011) 145:104–16. doi: 10.1016/j.cell.2011.02.034

41. Rochette P, Brash D. Progressive apoptosis resistance prior to senescence and control by the anti-apoptotic protein BCL-xL. *Mech Ageing Dev.* (2008) 129:207–14. doi: 10.1016/j.mad.2007.12.007

42. Taniguchi K, Karin M. NF-κB, inflammation, immunity and cancer: coming of age. *Nat Rev Immunol.* (2018) 18:309–24. doi: 10.1038/nri.2017.142

43. Jackson C, Gundersen K, Tong L, Utheim T. Dry eye disease and proteomics. *Ocul Surf.* (2022) 24:119–28. doi: 10.1016/j.jtos.2022.03.001

The monomeric C-reactive protein level is associated with the increase in carotid plaque number in patients with subclinical carotid atherosclerosis

Ivan Melnikov[1,2]*, Sergey Kozlov[3], Olga Pogorelova[4], Maria Tripoten[4], Leyla Khamchieva[4], Olga Saburova[1], Yuliya Avtaeva[1], Maria Zvereva[1], Evgeny Matroze[1,5], Tatiana Kuznetsova[6], Lyudmila Prokofieva[1], Tatiana Balakhonova[4,7] and Zufar Gabbasov[1]*

[1]Laboratory of Cell Hemostasis, National Medical Research Centre of Cardiology named after academician E.I. Chazov of the Ministry of Health of the Russian Federation, Moscow, Russia, [2]Laboratory of Gas Exchange, Biomechanics and Barophysiology, State Scientific Center of the Russian Federation − The Institute of Biomedical Problems of the Russian Academy of Sciences, Moscow, Russia, [3]Laboratory of Problems of Atherosclerosis, National Medical Research Centre of Cardiology named after academician E.I. Chazov of the Ministry of Health of the Russian Federation, Moscow, Russia, [4]Department of Ultrasound Diagnostics, National Medical Research Centre of Cardiology named after academician E.I. Chazov of the Ministry of Health of the Russian Federation, Moscow, Russia, [5]Department of Innovative Pharmacy, Medical Devices and Biotechnology, Moscow Institute of Physics and Technology, Moscow, Russia, [6]Laboratory of Neurohormonal Regulation of Cardiovascular Diseases, National Medical Research Centre of Cardiology named after academician E.I. Chazov of the Ministry of Health of the Russian Federation, Moscow, Russia, [7]Department of Cardiology, Functional and Ultrasound Diagnostics, Sechenov University, Moscow, Russia

The high-sensitivity C-reactive protein (hsCRP) assay measures the level of the pentameric form of CRP in blood. Currently, there are no available assays measuring the level of the monomeric form of CRP (mCRP), produced at sites of local inflammation. We developed an assay measuring the mCRP level in blood plasma with functional beads for flow cytometry. The assay was used to measure the mCRP level in 80 middle-aged individuals with initially moderate cardiovascular SCORE risk. By the time of the mCRP measurement, the patients have been followed up for subclinical carotid atherosclerosis progression for 7 years. Ultrasound markers of subclinical atherosclerosis, which included plaque number (PN) and total plaque height (PH), were measured at baseline and at the 7th-year follow-up survey. Inflammatory biomarkers, including mCRP, hsCRP, inteleukin-6 (IL-6) and von Willebrand factor (VWF) level, were measured at the 7th-year follow-up survey. The median level of mCRP was 5.2 (3.3; 7.1) μg/L, hsCRP 1.05 (0.7; 2.1) mg/L, IL-6 0.0 (0.0; 2.8) pg/mL, VWF 106 (77; 151) IU/dL. In the patients with the mCRP level below median vs. the patients with the median mCRP level or higher, change from baseline in PN was 0.0 (0.0; 1.0) vs. 1.0 (1.0; 2.0) and PH 0.22 (−0.24; 1.91) mm vs. 1.97 (1.14; 3.14) mm, respectively ($p < 0.05$). The adjusted odds ratio for the formation

of new carotid atherosclerotic plaques was 4.7 (95% CI 1.7; 13.2) for the patients with the median mCRP level or higher. The higher mCRP level is associated with the more pronounced increase in PN and PH in patients with normal level of traditional inflammatory biomarkers and initially moderate cardiovascular SCORE risk.

Introduction

The complications of atherosclerosis are among the leading causes of disability and mortality worldwide. One of the most advocated measures to prevent or delay atherosclerosis development is the reduction of the low-density lipoprotein cholesterol (LDL-C) level in blood (1). Yet, even extreme reduction in the LDL-C level cannot prevent major adverse cardiovascular events (MACE) (2). A crucial contributor to cardiovascular risk that remains in spite of aggressive lipid-lowering and control of other modifiable risk factors is low-grade inflammation in atherosclerotic plaques (3). Currently, the level of the main inflammatory biomarker C-reactive protein measured by the high-sensitivity assay (hsCRP) $\geq$ 2.0 mg/L is considered as a factor increasing estimated cardiovascular risk (4). Large randomized controlled clinical trials CANTOS, COLCOT, LoDoCo2 demonstrated that the reduction of the hsCRP level below 2.0 mg/L with anti-inflammatory agents decreased the MACE frequency by 23–29% (5). The hsCRP assays detect the plasma concentration of the pentameric form of CRP (pCRP), which is synthesized in hepatocytes under stimulation by proinflammatory cytokines, predominantly interleukin-6 (IL-6) (3). At sites of local inflammation pCRP binds to its specific ligand, lysophosphatidylcholine, on membranes of damaged or apoptotic cells and microparticles, as well as oxidized LDL, and undergoes dissociation to the monomeric form of CRP (mCRP) (6, 7). Dissociation opens up terminal octapeptide (Phe-Thr-Lys-Pro-Gly-Leu-Trp-Pro) on the C-terminal end of monomeric subunits, giving mCRP its antigenic specificity (6, 8, 9). After dissociation mCRP remains predominantly bound to cell membranes (10, 11). mCRP was found on circulating microparticles in blood of patients with acute myocardial infarction (12) and peripheral artery disease (13). The mCRP deposits were found in carotid atherosclerotic plaque tissue, but not in the intact vessel wall (14, 15). The mCRP deposits were localized to the necrotic core, neovessels, areas of macrophage, T-cells and smooth muscle cells accumulation in atherosclerotic plaques (14, 15). A range of proinflammatory actions of mCRP was shown *in vitro*. It stimulated monocyte and lymphocyte recruitment and synthesis of proinflammatory cytokines IL-6, IL-8, macrophage and T-cell polarization into proinflammatory phenotype, promoted angiogenesis (10, 16).

However, a feasible commercially available assay measuring the mCRP level in blood plasma or serum is lacking. To date, there are four published papers that describe measuring the mCRP level in blood plasma or serum (17–20). In all these studies the assays were performed with enzyme immunoassay (ELISA) technique. In 2015 Wang et al. produced a monoclonal antibody (mAb) to mCRP and developed an assay for measuring the mCRP level in blood plasma (17). The assay was used to measure the mCRP level in patients with acute myocardial infarction, unstable and stable angina pectoris (17). In 2018 Zhang et al. used the mAb clone 8C8 to measure the mCRP level in blood plasma of patients with autoimmune skin diseases (eczema, psoriasis and urticaria) and healthy controls (18). In 2020 Williams et al. used the mAb clone 8C8 to measure the mCRP level in serum of patients with acute inflammation and the hsCRP level more than 100 mg/L (19). In 2021 Munuswamy et al. used an aptamer-based mCRP competition ELISA to measure the mCRP level in patients with chronic obstructive pulmonary disease (COPD) (20). Previously, the mAb clone 8C8 was used to detect the mCRP deposits in atherosclerotic plaque samples by Jabs et al. (21) and Krupinski et al. (15). Schwedler et al. demonstrated that the mAb clone 8C8 was highly specific to mCRP (22). So far, there were no studies evaluating the association of the mCRP level with ultrasound markers of carotid atherosclerosis.

Materials and methods

Study design

The level of mCRP and other inflammatory biomarkers was measured in blood plasma from patients enrolled in the study of subclinical carotid atherosclerosis progression that has been going in the National Medical Research Center of Cardiology, Moscow, Russia, since 2012. This study was initially designed to investigate the benefit of different statin doses in middle-aged persons with moderate cardiovascular SCORE risk,

mildly elevated LDL-C level and subclinical non-stenotic carotid atherosclerotic plaques.

Patients of both sexes 40–65 years old with moderate cardiovascular SCORE risk, the LDL-C level 2.7–4.8 mmol/L and subclinical low-grade carotid stenoses narrowing the arterial lumen < 50% were eligible for the enrollment.

The study excluded from the enrollment patients with coronary artery disease (CAD), transient ischemic attacks and history of cerebrovascular accidents, symptomatic atherosclerosis of peripheral arteries, atherosclerosis of the carotid and peripheral arteries narrowing the arterial lumen ≥ 50%, aortic aneurysm, diabetes mellitus types 1 and 2, familial hypercholesterolemia, arterial hypertension, chronic kidney disease (GFR < 60 ml/min/1.73 m^2 or serum creatinine > 150 μmol/L), the LDL-C level ≥ 4.9 mmol/L and ≤2.6 mmol/L, the triglyceride (TG) level > 4.5 mmol/L, the three-fold or higher increase in the level of aspartate aminotransferase (AST) and/or alanine aminotransferase (ALT) above the upper limit of normal, cardiovascular SCORE risk ≥ 5%, chronic inflammatory diseases (including autoimmune disorders), malignant neoplasms, allergic reactions, lipid-lowering therapy in the previous 12 months, contraindications to statin administration.

Patients underwent an interview, physical examination, full blood count and biochemical blood test, the lipid panel test, electrocardiogram, echocardiogram and carotid ultrasonography. Patients meeting the inclusion criteria were offered to participate in the study. Recruited patients were prescribed atorvastatin with the individual dose adjustment to achieve the target LDL-C level < 2.6 mmol/L according to ESC/EAS Guidelines for the Management of Dyslipidaemias that were applicable at the time of enrollment (23). The target LDL-C level was shifted to < 1.8 mmol/L in 2019 according to the updated ESC/EAS Guidelines for the Management of Dyslipidaemias (24). The follow-up surveys included annual lipid panel tests and consultations of the same supervising physician. At the 7th-year follow-up survey, all the patients underwent carotid ultrasonography. Assessment of the level of inflammatory biomarkers (mCRP, hsCRP, IL-6) and von Willebrand factor (VWF) in blood plasma was also performed at the 7th-year follow-up survey.

Study enrollment began in 2012 and was completed in 2013. Of 379 consecutively screened individuals, 112 were included in the study. During the first year of the follow-up, 32 participants withdrew from the study. The resulting study population comprised 80 patients, including 47 men (59%) and 33 women (41%). All the patients completed the 7-year follow-up period.

Carotid ultrasonography

All scanning and reading procedures were identical at baseline and at the 7th-year follow-up survey. All measurements were performed with iU-22 (Phillips, the Netherlands) ultrasound system equipped with a 3–9 MHz linear-array transducer by the same operator at baseline and follow-up. Measurements were performed in B-mode imaging, Color Doppler imaging, Power doppler imaging and Pulsed Wave Doppler mode. The common carotid artery (CCA), the internal carotid artery (ICA) and the carotid artery bifurcation on both sides were scanned for atherosclerotic plaques (6 segments in total) in the anterior, lateral and posterior planes. According to the Mannheim Carotid Intima-Media and Plaque Consensus, a carotid atherosclerotic plaque was defined as a focal structure protruding into the arterial lumen at least 0.5 mm, or at least 50% compared to the adjacent intima-media thickness (IMT), or as a focal intima-media thickening > 1.5 mm (25). Plaque number (the total number of atherosclerotic plaques) and total plaque height (the sum of all plaque heights) were calculated in all 6 examined segments (26). IMT was defined as the distance between the lumen-intima and the media-adventitia interfaces. CCA-IMT was measured along the posterior wall of the distal segments of both CCAs at a distance 1 cm proximal to the bifurcation. Three measurements were performed with the anterior and lateral scanning approach on each side. The highest of 6 mean values calculated from 3 consecutive anterior and 3 consecutive lateral measurements was taken as right or left CCA-IMT. The mean CCA-IMT was calculated as half-sum of right and left CCA-IMT.

The assay measuring the mCRP level in blood plasma

The assay is based on the Cytometric Bead Array (CBA) kit (BD Biosciences, USA), containing fluorescent functional beads. This kit allows conjugating the beads to an antibody against a target protein. Covalent binding of an antibody to the beads is performed with Sulfo-SMCC (Sigma-Aldrich, USA) and dithiothreitol (Thermo Fisher, USA) according to the manufacturer's protocol. When the complex of antibody and beads is added into a sample of blood plasma, the antibody binds a ligand protein. Then, a fluorochrome-labeled second-layer developing antibody against the same protein is added into the sample. This antibody binds the target protein in the complex with the beads and primary antibody. The intensity of the fluorescence from the second-layer antibody allows quantifying the level of the target protein in the sample by a flow cytometer. The fluorescent spectra of the second-layer antibody and the beads must be different. The CBA beads series A5, C4, and E5 that have different fluorescence intensity in the APC-Cy7 channel were used in this study. The different fluorescence intensity of the beads allows distinguishing between the different series of the beads on a flow cytometry histogram. The A5 beads were conjugated to the anti-pCRP/mCRP mAb clone MOH328 (ImTek, Russia); the

C4 beads were conjugated to the anti-mCRP mAb clone 8C8 (Sigma-Aldrich, USA); the E5 beads were conjugated to the anti-pCRP mAb clone MOH372 (ImTek, Russia). The beads conjugated to the anti-pCRP antibodies were used to rule out cross-reactivity of the mAb clone 8C8 to pCRP. As a second-layer developing antibody a FITC-labeled polyclonal goat-antihuman antibody to CRP GAHCRP-FITC (ImTek, Russia) was used. To confirm specificity of the mAbs and construct a calibration curve, pCRP (Sigma-Aldrich, USA) and the recombinant mCRP (a gift by dr. L. Potempa, Roosevelt University, USA) solutions were used. Prior to flow cytometry analysis the beads-antibody conjugates were incubated with studied samples at room temperature for 1 h. All measurements were performed on the FACS CantoII (BD Biosciences, USA) flow cytometer.

Blood samples collection and analysis

Blood samples were collected from the cubital vein into the S-Monovette 3.8% sodium citrate vials (Sarstedt, Germany) after 12 h of fasting. Platelet poor plasma (PPP) was prepared by centrifugation for 20 min at 2,000 g and stored at −70°C. Before measurements plasma was thawed in an ultrasonic bath at 37°C. The level of hsCRP, IL-6, VWF and the lipid panel were measured at the laboratory of clinical biochemistry of the National Medical Research Centre of Cardiology named after academician E.I. Chazov of the Ministry of Health of the Russian Federation, Moscow, Russia.

Statistical analysis

The data are presented as mean ± standard deviation or median (lower quartile; upper quartile) as appropriate. The type of distribution was tested with the Shapiro-Wilk W test. Comparative analysis of two independent groups was performed with Mann-Whitney U test for quantitative data and Fisher's exact test for qualitative data. Comparative analysis of two dependent groups was performed with Wilcoxon signed-rank test. Spearman's rank correlation coefficient was used to assess correlation between the inflammatory biomarkers. Probability was considered significant at $p < 0.05$. All statistical tests were 2-tailed. Statistical analysis was performed with STATISTICA v. 7.0 (StatSoft Inc., USA) and IBM SPSS Statistics v. 26.0 (SPSS Inc., USA).

Ethical approval

The study followed the Good Clinical Practice (GCP) standards and the principles of the Declaration of Helsinki. The study was approved by the ethics committee of the National Medical Research Centre of Cardiology named after academician E.I. Chazov of the Ministry of Health of the Russian Federation, Moscow, Russia. Written informed consent was obtained from all the participants.

Results

The assay measuring the mCRP level in blood plasma

The assay measuring the mCRP level in blood plasma was developed for flow cytometry analysis. The assay utilized the CBA beads C4 conjugated to the anti-mCRP mAb clone 8C8. The beads A5, conjugated to the anti-pCRP/mCRP mAb clone MOH328, and E5, conjugated to the anti-pCRP mAb clone MOH372, were used to rule out cross-reactivity of the mAb clone 8C8 to pCRP. To detect pCRP or mCRP the beads-antibody conjugates were incubated with samples of pCRP or mCRP solution in concentration 0.25 mg/L at room temperature for 1 h. Figure 1A shows a diagram of the background fluorescence intensity from the beads A5, C4, and E5 in the APC-Cy7 channel. Figure 1B shows a histogram of the fluorescence intensity from the beads A5, C4, and E5 in the FITC channel in the presence of the second-layer polyclonal anti-CRP antibody GAHCRP-FITC. Without any form of CRP, the mean fluorescence intensity (MFI) registered in the samples was low: 157 arbitrary units (a.u.), 112 a.u. and 82 a.u. for the A5, C4, and E5 beads, respectively.

Figure 2 shows MFI from the A5, C4, and E5 beads in the presence of pCRP (Figure 2A) or mCRP (Figure 2B) in concentration 0.25 mg/L and the second-layer polyclonal anti-CRP antibody GAHCRP-FITC. The A5 beads (gate P1), conjugated to the mAb clone MOH 328, bound pCRP and mCRP equally well. The C4 beads (gate P2), conjugated to the mAb clone 8C8, predominantly bound mCRP. The E5 beads (gate P3), conjugated to the mAb clone MOH372, predominantly bound pCRP. MFI recorded in the pCRP or mCRP samples was, respectively, 3,261 a.u. and 3,127 a.u. from the A5 beads, 188 a.u. and 2,766 a.u. from the C4 beads, 2,486 a.u. and 313 a.u. from the E5 beads in the FITC channel. Additionally, the mAb clone 8C8 was tested in a sample with pCRP concentration 5.0 mg/L. MFI from the C4 beads was 204 a.u. in the FITC channel in the presence of the second-layer polyclonal anti-CRP antibody GAHCRP-FITC. After mCRP was added into the sample up to concentration 0.25 mg/L, MFI raised to 2,842 a.u. Therefore, the mAb clone 8C8, conjugated to the C4 beads, is highly specific for mCRP.

The serial dilutions method was used to construct a calibration curve. The stock solution of the recombinant mCRP with known concentration in µg/L was serially diluted and titrated from 0.25 to 250.0 µg/L. Each diluted sample was
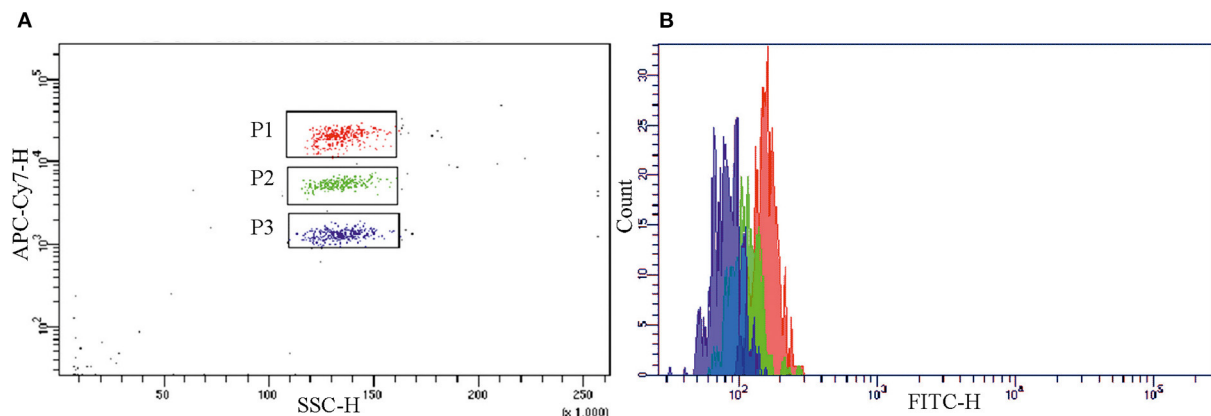
FIGURE 1

Background fluorescence intensity from the A5 (gate P1), C4 (gate P2) and E5 (gate P3) beads, conjugated to the monoclonal antibodies clones MOH 328 (anti-pCRP/mCRP), 8C8 (anti-mCRP), MOH372 (anti-pCRP), respectively, in **(A)** the APC-Cy7 channel and **(B)** the FITC channel in the absence of mCRP or pCRP and in the presence of polyclonal FITC-labeled antibody to CRP (GAHCRP-FITC). mCRP, monomeric C-reactive protein; pCRP, pentameric C-reactive protein.
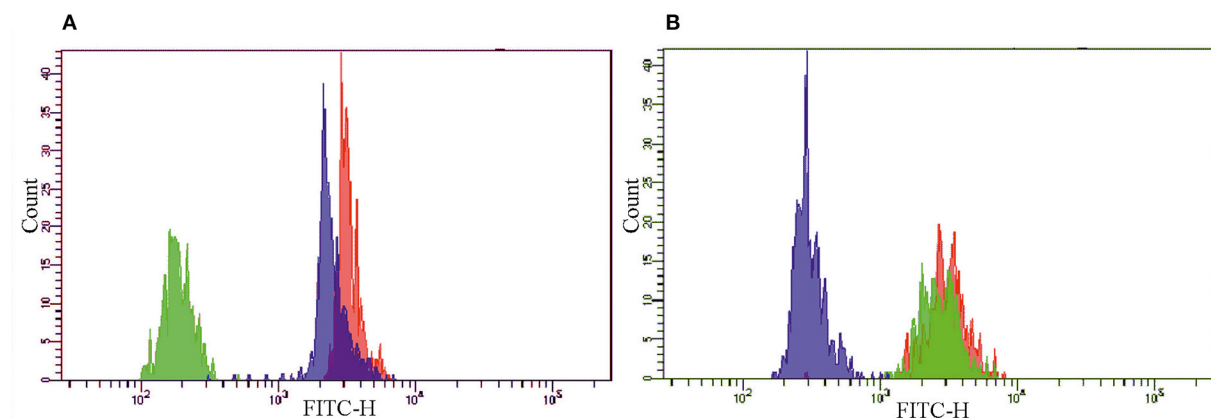
FIGURE 2

The histograms of the fluorescence intensity of the A5 (red), C4 (green) and E5 (blue) beads, conjugated to monoclonal antibodies clones MOH 328 (anti-pCRP/mCRP), 8C8 (anti-mCRP), MOH372 (anti-pCRP), respectively, in the presence of **(A)** pCRP or **(B)** mCRP in concentration 0.25 mg/L and polyclonal FITC-labeled antibody to CRP (GAHCRP-FITC). mCRP, monomeric C-reactive protein; pCRP, pentameric C-reactive protein.

incubated with the C4 beads and the second-layer polyclonal anti-CRP antibody GAHCRP-FITC. Then, MFI in the FITC channel from consecutively diluted samples was measured by flow cytometry. The relationship between MFI and the mCRP concentrations was linear at the mCRP concentrations from 1.0 to 100.0 µg/L. MFI did not differ significantly from the background fluorescence at the mCRP concentrations below 1.0 µg/L. Therefore, the mCRP concentration 1.0 µg/L shall be taken as a threshold value of the developed assay. The relationship between MFI and the mCRP concentrations above 100.0 µg/L was non-linear. Hence, to get a reliable result in a sample with the mCRP concentration more than 100.0 µg/L, this sample must be down-titrated until the mCRP concentration is

within the range from 1.0 to 100.0 µg/L. From this concentration the actual mCRP level can be calculated considering the sample dilution factor.

The association between the level of biomarkers (mCRP, hsCRP, IL-6, VWF) and the markers of subclinical carotid atherosclerosis

At the 7th-year follow-up survey plaque number increased in 45 (56%) patients (30 men and 15 women). Plaque number

TABLE 1 Baseline characteristics of the patients.

	Patients with increased plaque number (n = 45)	Patients without increased plaque number (n = 35)	p
Age, years	53 ± 6	53 ± 6	0.7
Men/women, no. (%)	30 (67%)/15 (33%)	17 (49%)/18 (51%)	0.1
Family history of premature CVD, no. (%)	9 (20%)	8 (23%)	0.8
Current smoking, no. (%)	12 (27%)	10 (29%)	0.5
Ex-smoker, no. (%)	6 (13%)	3 (9%)	0.9
BMI, kg/m^2	26.0 (24.1; 30.7)	25.7 (24.3; 28.6)	0.7
BMI ≥ 30 kg/m^2	14 (31%)	8 (23%)	0.4
TC, mmol/L	5.68 (5.12; 6.27)	5.70 (5.07; 6.25)	0.7
LDL-C, mmol/L	3.70 (3.20; 4.21)	3.80 (3.43; 4.34)	0.4
HDL-C, mmol/L	1.12 (1.0; 1.39)	1.10 (0.98; 1.32)	0.9
TG, mmol/L	1.54 (1.01; 2.10)	1.28 (1.0; 1.89)	0.5

CVD, cardiovascular disease; BMI, body mass index; TC, total cholesterol; LDL-C, low-density lipoprotein cholesterol; HDL-C, high-density lipoprotein cholesterol; TG, triglycerides.
Statistical analysis was performed with Mann-Whitney U test for quantitative data and Fisher's exact test for qualitative data.

did not change in 35 (44%) patients (17 men and 18 women). The baseline characteristics of the patients are shown in Table 1.

The groups did not differ in sex, current smokers, exsmokers and non-smokers, family history of cardiovascular diseases (CVD), body mass index (BMI) and obesity. The patients did not have overt arterial hypertension, diabetes mellitus, nor they received cardiovascular medications at baseline. The patients with increased plaque number received atorvastatin in the dose 20 (20; 40) mg daily; the patients without increased plaque number received atorvastatin in the dose 20 (20; 40) mg daily (p = 0.7). The characteristics of the patients at the 7th-year follow-up survey are shown in Table 2.

In the patients with increased plaque number MACE developed in 5 cases (2 cases of myocardial infarction, 2 cases of angina pectoris and 1 case of stroke) during the followup period. Moreover, diabetes mellitus type 2 developed in 6 cases and arterial hypertension requiring pharmacological treatment in 22 cases. In the patients without increased plaque number MACE developed in 2 cases (angina pectoris in both cases) during the follow-up period. Also, diabetes mellitus type 2 developed in 1 case and arterial hypertension requiring pharmacological treatment in 16 cases.

The groups were different only in the LDL-C level and the mCRP level. The level of biomarkers depending on the increase in plaque number is shown in Figure 3.

In all patients (n = 80) the level of mCRP was 5.2 (3.3; 7.1) μg/L, hsCRP 1.05 (0.7; 2.1) mg/L, IL-6 0.0 (0.0; 2.8) pg/mL, VWF 1.06 (0.77; 1.51) IU/dL. The mCRP level did not correlate with the hsCRP level (r = 0.006, p = 0.9) and the IL-6 level (r = 0.02; p = 0.9), but positively correlated with the VWF level (r = 0.3; p = 0.01). The hsCRP level positively correlated with the IL-6 level (r = 0.4; p = 0.001). The correlation matrix between mCRP and other biomarkers are shown in Table 3.

The patients were divided by the median mCRP level 5.2 (3.3; 7.1) μg/L. The group with the mCRP level < 5.2 μg/L comprised 39 patients (21 men and 18 women). The group with the mCRP level ≥ 5.2 μg/L comprised 41 patients (26 men and 15 women). The increase in plaque number was detected in 14 (36%) patients in the group with the mCRP level < 5.2 μg/L and in 31 (76%) patients in the group with the mCRP level ≥ 5.2 μg/L. The ultrasound markers of carotid atherosclerosis and CCA-IMT depending on the mCRP level are shown in Table 4.

The association between the mCRP level and the change in plaque number, total plaque height (Figure 4), left, right and mean CCA-IMT was significant for the patients with the mCRP level < 5.2 μg/L, as well as the patients with the mCRP level ≥ 5.2 μg/L, except for left CCA-IMT, which did not change significantly in the patients with the mCRP level ≥ 5.2 μg/L. However, the patients with the mCRP level ≥ 5.2 μg/L demonstrated a pronounced increase in the ultrasound markers of carotid atherosclerosis. In the patients with the mCRP level < 5.2 μg/L, the median percentage change in plaque number was 0%, total plaque height 4%, right CCA-IMT 7%, left CCA-IMT 5%, mean CCA-IMT 5%, whereas in the patients with the mCRP level ≥ 5.2 μg/L the median percentage change in plaque number was 50%, total plaque height 57%, right CCA-IMT 7%, mean CCA-IMT 7%.

The unadjusted odds ratio for the formation of new carotid atherosclerotic plaques was 5.5 [95% confidence interval (CI) 2.1; 14.6; p = 0.001] for the patients with the median mCRP level or higher. Logistic regression analysis was performed to adjust the odds ratio for other risk factors and biomarkers. Regression analysis was performed by stepwise inclusion or exclusion of factors in the model. The resulting logistic regression model included the mCRP level ≥ 5.2 μg/L, the hsCRP level, the LDL-C level at the 7th-year follow-up survey and male sex. Other risk

TABLE 2   The characteristics of the patients at the 7th-year follow-up survey.

	Patients with increased plaque number (n = 45)	Patients without increased plaque number (n = 35)	p
Age, years	60 ± 6	60 ± 6	0.7
Men/women, no. (%)	30 (67%)/15 (33%)	17 (49%)/18 (51%)	0.1
Family history of premature CVD, no. (%)	9 (20%)	8 (23%)	0.8
Current smoking, no. (%)	11 (24%)	6 (17%)	0.4
Ex-smoker, no. (%)	7 (16%)	7 (20%)	0.9
BMI, kg/m^2	27.1 (24.4; 31.4)	26.9 (25.2; 29.4)	0.7
BMI ≥ 30 kg/m^2	16 (36%)	8 (23%)	0.2
Arterial Hypertension, no. (%)	22 (51%)	16 (43%)	0.8
Diabetes mellitus type 2, no. (%)	6 (14%)	1 (3%)	0.1
MACE, total no. (%)	5 (11%)	2 (6%)	0.4
- Myocardial Infarction, no. (%)	2 (4%)	0	
- Angina Pectoris, no. (%)	2 (4%)	2 (6%)	
- Stroke, no. (%)	1 (2%)	0	
TC, mmol/L	4.14 (3.84; 4.35)	3.99 (3.63; 4.38)	0.2
LDL-C, mmol/L	2.33 (2.05; 2.44)	2.15 (1.82; 2.34)	0.04
HDL-C, mmol/L	1.24 (1.08; 1.46)	1.22 (1.02; 1.48)	0.4
TG, mmol/L	1.22 (0.95; 1.61)	1.11 (0.88; 1.35)	0.6
mCRP, µg/L	6.3 (4.2; 9.8)	4.0 (2.45; 5.35)	0.0006
hsCRP, mg/L	1.2 (0.7; 2.4)	0.9 (0.6; 1.6)	0.2
hsCRP ≥ 2.0 mg/L	18	8	0.1
IL-6, pg/mL	0.0 (0.0; 3.2)	0.0 (0.0; 2.14)	0.6
VWF, IU/dL	107 (77; 163)	103 (85; 124)	0.6

CVD, cardiovascular disease; BMI, body mass index; MACE, major adverse cardiovascular events; TC, total cholesterol; LDL-C, low-density lipoprotein cholesterol; HDL-C, high-density lipoprotein cholesterol; TG, triglycerides; mCRP, monomeric C-reactive protein; hsCRP, C-reactive protein measured with high-sensitivity test; IL-6, interleukin-6; VWF, von Willebrand factor. Statistical analysis was performed with Mann-Whitney U test for quantitative data and Fisher's exact test for qualitative data.

factors and biomarkers were excluded, because they decreased the predictive value of the model. The model was significant ($p = 0.001$) with 75.0% of correct predictions for the formation of new carotid atherosclerotic plaques. The model with the hsCRP level ≥ 2.0 mg/L as a categorical variable instead of the hsCRP level as a continuous variable was also significant ($p = 0.001$), but returned slightly less correct predictions (71.3%). The adjusted odds ratio for the formation of new carotid atherosclerotic plaques was 4.74 (95% CI 1.70–13.24) for the patients with the median mCRP level or higher. The results of the logistic regression model predicting the formation of new atherosclerotic plaques are shown in the Table 5.

Discussion

The assay measuring the mCRP level in blood plasma was developed in this study. The assay utilized the CBA beads conjugated to the mAb clone 8C8. Test measurements performed in samples of pCRP and the recombinant mCRP in the range of concentrations confirmed high specificity of the mAb clone 8C8 for mCRP. The calibration curve for the developed assay was constructed with the serial dilutions method in consecutively diluted samples of the recombinant mCRP. The relationship between MFI and the mCRP concentrations was linear in the range of the mCRP concentrations from 1.0 µg/L to 100.0 µg/L. At the mCRP concentrations below 1.0 µg/L, MFI did not differ from the background fluorescence. Therefore, the threshold sensitivity of the developed assay is 1.0 µg/L. The high specificity of the mAb clone 8C8 to mCRP was previously shown in a number of studies (15, 18, 19, 21, 22). The threshold sensitivity of assays measuring the mCRP level also was 1.0 µg/L for ELISA utilizing mAb clone 8C8 in the study of Zhang et al. (18) and for ELISA utilizing mAb produced by Wang et al. (17).

The presence of carotid atherosclerosis in asymptomatic individuals with low to moderate cardiovascular SCORE risk may reclassify them to a higher risk category. Such individuals may need a more aggressive approach to the modification of risk factors, including initiation of lipid-lowering therapy, to prevent or halt MACE development (4, 23). All the patients enrolled in the study had subclinical low-grade carotid stenoses, detected
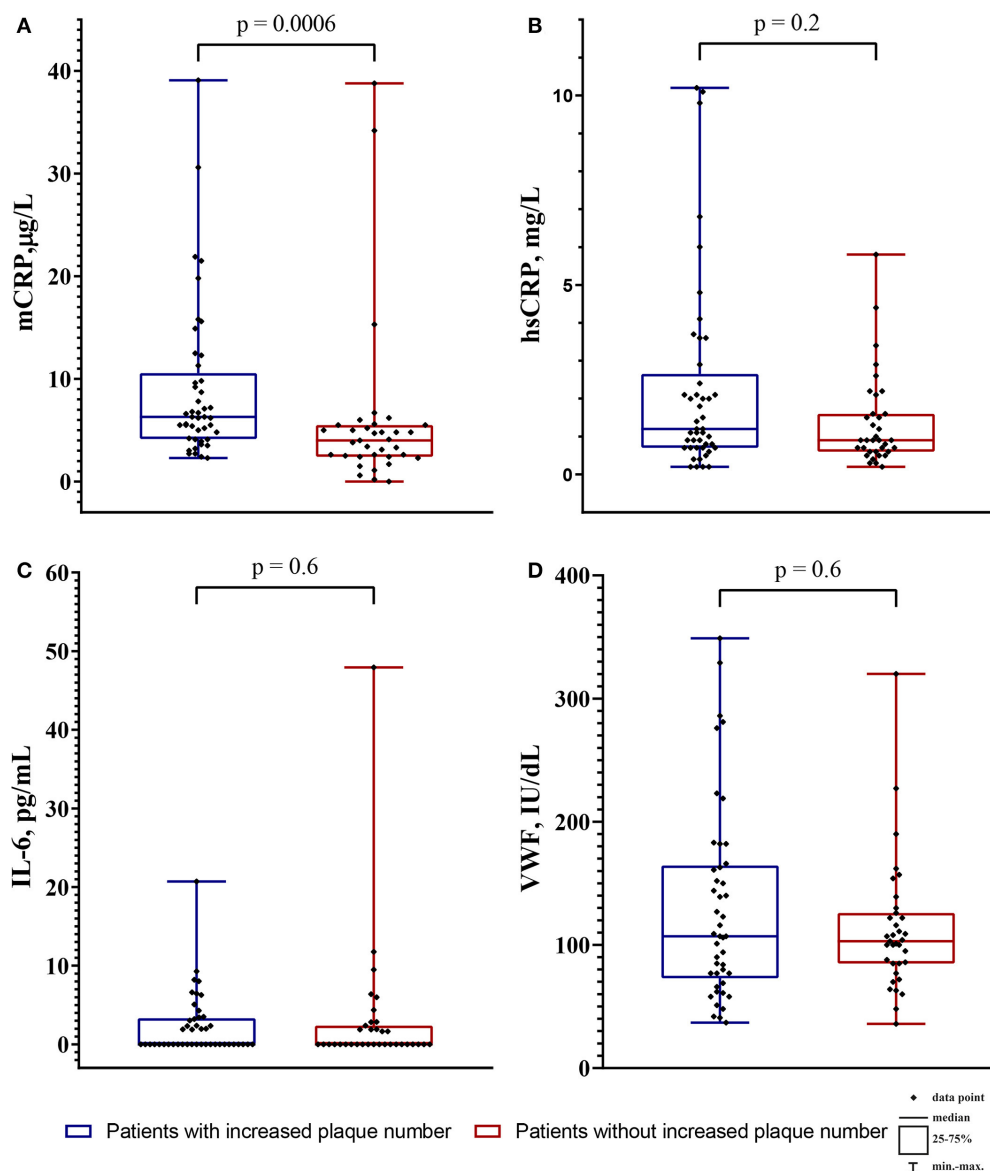
FIGURE 3
The level of biomarkers in the patients with increased plaque number (blue boxplots) and the patients without increased plaque number (red boxplots). **(A)** the monomeric C-reactive protein (mCRP) level in µg/L; **(B)** the high-sensitivity C-reactive protein (hsCRP) level in mg/L; **(C)** the interleukin-6 level (IL-6) in pg/mL; **(D)** the von Willebrand factor (VWF) level in IU/dL. The intergroup difference was analyzed by Mann-Whitney U test.

with ultrasonography, narrowing the arterial lumen < 50%, and the LDL-C level higher than 2.6 mmol/L. The risk category was reclassified to high cardiovascular SCORE risk according to ESC/EAS Guidelines for the Management of Dyslipidaemias that were applicable at the time of enrollment (23). The target LDL-C level in this risk category was <2.6 mmol/L. All the patients enrolled in the study were prescribed atorvastatin and achieved the target LDL-C level. Since the patients had no evidence of advanced carotid stenoses, assessment of atherosclerosis progression by change in blood flow parameters

was inapplicable. Therefore, the increase in plaque number was considered as the main ultrasound marker of carotid atherosclerosis progression in this study (27).

Despite lipid-lowering therapy, carotid plaque number increased in 45 (56%) patients by the 7th-year follow-up survey. The patients with and without increased plaque number were different only in the LDL-C level and the mCRP level. The median mCRP level 5.2 µg/L or higher corresponded with the pronounced increase in plaque number and total plaque height. The adjusted odds ratio for the formation of new carotid

TABLE 3 The correlation matrix between mCRP and other biomarkers.

Variables	mCRP		hsCRP		IL-6		VWF	
	r	p	r	p	r	p	r	p
mCRP	1	–	0.006	0.9	0.02	0.9	**0.3**	**0.01**
hsCRP	0.006	0.9	1	–	**0.4**	**0.001**	0.1	0.2
IL-6	0.02	0.9	**0.4**	**0.001**	1	–	−0.1	0.2
VWF	**0.3**	**0.01**	0.1	0.2	−0.1	0.2	1	–

mCRP, monomeric C-reactive protein; hsCRP, C-reactive protein measured with high-sensitivity test; IL-6, interleukin-6; VWF, von Willebrand factor. Spearman's rank correlation coefficient was used to measure r and p-values. The bold values mean the values with $p < 0.05$.

TABLE 4 The ultrasound markers of carotid atherosclerosis and CCA-IMT depending on the mCRP level.

	mCRP < 5.2 µg/L (n = 39)			mCRP ≥ 5.2 µg/L (n = 41)		
	Baseline	The 7th-year follow-up survey	Change	Baseline	The 7th-year follow-up survey	Change
Plaque number	3.0	3.0	0.0	2.0	3.0	1.0
	(1.0; 4.0)	(2.0; 4.0)	(0.0; 1.0)*	(1.0; 3.0)	(2.0; 4.0)	(1.0; 2.0)*
Total plaque height, mm	5.56	6.21	0.22	3.70	7.04	1.97
	(2.57; 8.13)	(3.97; 10.13)	(−0.24; 1.91)*	(2.34; 5.51)	(4.45; 11.30)	(1.14; 3.14)*
CCA-IMT right, mm	0.66	0.70	0.04	0.72	0.77	0.06
	(0.58; 0.71)	(0.61; 0.79)	(0.01; 0.09)*	(0.62; 0.81)	(0.65; 0.89)	(−0.01; 0.13)*
CCA-IMT left, mm	0.62	0.70	0.04	0.67	0.72	0.03
	(0.60; 0.75)	(0.61; 0.84)	(0.01; 0.09)*	(0.61; 0.78)	(0.61; 0.91)	(-0.04; 0.07)[NS]
CCA-IMT mean, mm	0.66	0.70	0.05	0.71	0.74	0.05
	(0.58; 0.72)	(0.63; 0.82)	(0.0; 0.1)*	(0.64; 0.80)	(0.65; 0.87)	(0.00; 0.1)*

mCRP, monomeric C-reactive protein; CCA-IMT, intima-media thickness of common carotid artery; *$p < 0.05$; [NS], not significant (Wilcoxon signed-rank test).

atherosclerotic plaques was 4.74 (95% CI 1.70–13.24) for the patients with the median mCRP level or higher. Higher plaque number was associated with increased stroke (28) and CAD (29) occurrence in asymptomatic individuals. An increase in maximum plaque thickness was associated with increased CAD (30) occurrence in asymptomatic individuals. The maximum plaque thickness was equal to the plaque burden in prediction of MACE in asymptomatic individuals (31). An association between the increase in CCA-IMT and higher cardiovascular risk in asymptomatic individuals was shown in large population studies (32, 33).

Correlation analysis showed that the mCRP level did not correlate with the hsCRP and IL-6 level, yet weakly correlated with the VWF level. Williams et al. also reported that the mCRP level did not correlate with the hsCRP level (19). Zhang et al. reported that in patients with autoimmune skin diseases and the elevated mCRP level, the hsCRP level was within the normal range (18). Munuswamy et al. also did not find correlation of the mCRP level with the hsCRP level in patients with COPD (20).

In this study population, the median hsCRP level was 1.05 (0.7; 2.1) mg/L, which was well below the 2.0 mg/L threshold for residual inflammatory cardiovascular risk (4). Of 26 patients

who had the hsCRP level ≥ 2.0 mg/L, 18 belonged to the group with increased plaque number and 8 to the group without change in plaque number. The median IL-6 level was 0.0 (0.0; 2.8) pg/mL. The median VWF level was 106 (77; 151) IU/dL, which was within normal limits.

To our knowledge, this is the first study evaluating the association of the mCRP level with ultrasound markers of carotid atherosclerosis. Previously, Wang et al. measured the mCRP level in blood plasma of patients with acute myocardial infarction, unstable and stable angina pectoris (17). The highest mCRP level was observed in patients with acute myocardial infarction (20.96 ± 1.64 µg/L), especially in those who died in 30 days after the event (36.70 ± 10.26 µg/L), whereas in patients with stable angina pectoris or healthy individuals mCRP was not detected (17). Zhang et al. reported the median mCRP level in blood plasma of patients with eczema, psoriasis, urticaria and healthy controls ranging from 15.2 to 59.8 µg/L (18). Williams et al. detected the mean mCRP level 1,030.0 ± 110.0 µg/L in serum of patients with acute inflammation and the hsCRP level more than 100 mg/L (19). Munuswamy et al. reported that the median mCRP level in patients with COPD was 660.0 µg/L, whereas in healthy
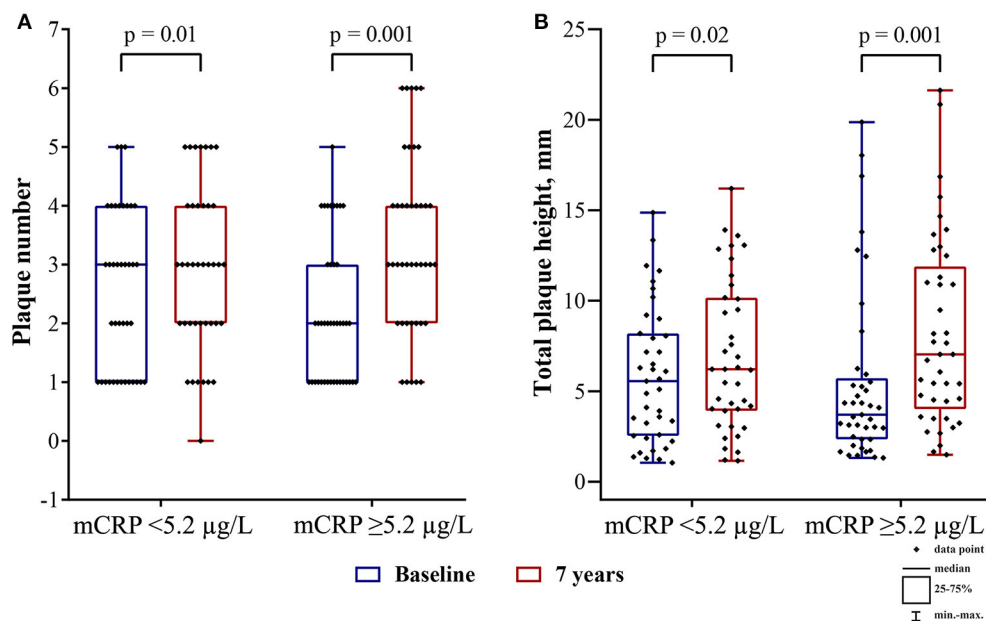
FIGURE 4
(A) plaque number and **(B)** total plaque height at baseline (blue boxplots) and the 7th-year follow-up survey (red boxplots) in the patients with the mCRP level below median or the median mCRP level or higher. At the 7th-year follow-up survey, the intragroup change in all markers was significant (Wilcoxon signed-rank test). mCRP, monomeric C-reactive protein.

TABLE 5 The results of the logistic regression model predicting the formation of new atherosclerotic plaques.

Predictor	Coefficient (β)	aOR (95% CI)	p
Intercept	−4.00	0.02	0.02
The mCRP level ≥ 5.2 μg/L	1.56	4.74 (1.70–13.24)	0.001
The hsCRP level, mg/L	0.30	1.35 (0.98–1.86)	0.06
The achieved LDL-C level, mmol/L	1.14	3.12 (0.69–14.08)	0.14
Male sex	0.94	2.57 (0.90–7.36)	0.08

aOR, adjusted odds ratio; CI, confidence interval; mCRP, monomeric C-reactive protein; hsCRP, C-reactive protein measured with high-sensitivity test; LDL-C, low-density lipoprotein cholesterol.

controls mCRP was not traceable (20). In our study, the mCRP level was lower: 6.3 (4.2; 9.8) μg/L vs. 4.0 (2.45; 5.35) μg/L in the patients with and without increased plaque number, respectively. This may be attributed to the absence of comorbidity, few traditional cardiovascular risk factors and statin treatment in the patients.

The association of the elevated hsCRP level with an increase in the degree of carotid artery stenoses, greater number, larger area and total height of carotid atherosclerotic plaques was shown in a number of studies (27, 34–36). The association of the hsCRP level with cardiovascular risk was shown in a number of large randomized controlled clinical trials, including JUPITER, CANTOS, PROVE-IT, and IMPROVE-IT (3). The association of the elevated IL-6 level with a greater plaque number (37) and a greater CCA-IMT (38) was reported in asymptomatic individuals. The IL-6 level was associated with the cardiovascular risk in the CANTOS trial (3). The elevated VWF level was associated with the endothelial disfunction (39, 40) and higher cardiovascular risk in individuals with subclinical carotid atherosclerosis (41). As it was already mentioned, the overall health status of the patients in our study was considerably mild, which may explain normal level of the inflammatory biomarkers and VWF. Moreover, the patients were prescribed statins, which reduce the hsCRP level (3). Based on the hsCRP level, the participants of this study should have been classified to the low residual inflammatory cardiovascular risk category. Yet, the mCRP level allowed to identify individuals with higher probability of formation of new carotid atherosclerotic plaques among the study participants.

Limitations of the study

The main limitation of this study is the absence of baseline measurement of the biomarkers and low rate of MACE. This precludes from correct assessment of the mCRP level as a biomarker of residual inflammatory risk.

Conclusion

Despite statin treatment, 56% of the patients with low-grade carotid stenoses and initially moderate cardiovascular SCORE risk demonstrated the increase in carotid plaque number. The patients with and without increased plaque number were different only in the LDL-C level and the mCRP level. The level of hsCRP, IL-6 and VWF was normal. The median mCRP level or higher allowed to identify individuals with higher probability of formation of new carotid atherosclerotic plaques among the study participants. The adjusted odds ratio for the formation of new carotid atherosclerotic plaques was 4.74 (95% CI 1.70–13.24) for the patients with the median mCRP level or higher. Therefore, this study for the first time shows that the higher mCRP level is associated with the more pronounced increase in plaque number and total plaque height in patients with normal level of traditional inflammatory biomarkers and initially moderate SCORE risk.

Data availability statement

The raw data supporting the conclusions of this article will be made available by the authors, without undue reservation.

Ethics statement

The studies involving human participants were reviewed and approved by the Ethics Committee of the National Medical Research Centre of Cardiology named after academician E.I. Chazov of the Ministry of Health of the Russian Federation. The patients/participants provided their written informed consent to participate in this study.

Author contributions

IM, SK, TB, and ZG: conceptualization. OP, LK, TB, YA, MZ, and EM: data curation. EM and ZG: formal analysis. IM, LP, and ZG: funding acquisition. IM, OP, MT, LK, OS, YA, MZ, and TK: investigation. SK, TB, OS, TK, and ZG: methodology. MT and ZG: project administration. LK and LP: resources. SK, TB, and ZG: supervision. OS, EM, and LP: validation. IM, MT, and OS: visualization. IM, YA, MZ, and TK: writing—original draft. IM, SK, OP, and ZG: writing—review and editing. All authors have read and agreed to the published version of the manuscript.

Conflict of interest

The authors declare that the research was conducted in the absence of any commercial or financial relationships that could be construed as a potential conflict of interest.

Publisher's note

All claims expressed in this article are solely those of the authors and do not necessarily represent those of their affiliated organizations, or those of the publisher, the editors and the reviewers. Any product that may be evaluated in this article, or claim that may be made by its manufacturer, is not guaranteed or endorsed by the publisher.

References

1. Borén J, Chapman MJ, Krauss RM, Packard CJ, Bentzon JF, Binder CJ, et al. Low-density lipoproteins cause atherosclerotic cardiovascular disease: pathophysiological, genetic, and therapeutic insights: a consensus statement from the European Atherosclerosis Society Consensus Panel. *Eur Heart J.* (2020) 41:2313–30. doi: 10.1093/eurheartj/ehz962

2. Dimmitt SB, Stampfer HG, Martin JH, Warren JB. Clinical benefits of evolocumab appear less than hoped. *Lancet.* (2018) 391:933–4. doi: 10.1016/S0140-6736(18)30530-0

3. Ridker PM. Anticytokine agents: targeting interleukin signaling pathways for the treatment of atherothrombosis. *Circ Res.* (2019) 124:437–50. doi: 10.1161/CIRCRESAHA.118.313129

4. Grundy SM, Stone NJ, Bailey AL, Beam C, Birtcher KK, Blumenthal RS, et al. 2018 AHA/ACC/AACVPR/AAPA/ABC/ACPM/ADA/AGS/APhA/ASPC/NLA/PCNA guideline on the management of blood cholesterol: a report of the American College of Cardiology/American Heart Association Task Force on Clinical Practice Guidelines. *Circulation.* (2019) 73:e285–350. doi: 10.1016/j.jacc.2018.11.003

5. Soehnlein O, Libby P. Targeting inflammation in atherosclerosis — from experimental insights to the clinic. *Nat Rev Drug Discov.* (2021) 20:589–610. doi: 10.1038/s41573-021-00198-1

6. Ji S, Wu Y, Zhu L, Potempa LA, Sheng F, Lu W, et al. Cell membranes and liposomes dissociate C-reactive protein (CRP) to form a new,

biologically active structural intermediate: mCRP ₘ. *FASEB J.* (2007) 21:284–94. doi: 10.1096/fj.06-6722com

7. Braig D, Nero TL, Koch H-G, Kaiser B, Wang X, Thiele JR, et al. Transitional changes in the CRP structure lead to the exposure of proinflammatory binding sites. *Nat Commun.* (2017) 8:14188. doi: 10.1038/ncomms14188

8. Potempa LA, Siegel JN, Fedel BA, Potempa RT, Gewurz H. Expression, detection and assay of a neoantigen (Neo-CRP) associated with a free, human C-reactive protein subunit. *Mol Immunol.* (1987) 24:531–41. doi: 10.1016/0161-5890(87)90028-9

9. Li H-Y, Wang J, Meng F, Jia Z-K, Su Y, Bai Q-F, et al. An intrinsically disordered motif mediates diverse actions of monomeric c-reactive protein. *J Biol Chem.* (2016) 291:8795–804. doi: 10.1074/jbc.M115.695023

10. Rajab IM, Hart PC, Potempa LA. How C-reactive protein structural isoforms with distinctive bioactivities affect disease progression. *Front Immunol.* (2020) 11:2126. doi: 10.3389/fimmu.2020.02126

11. Thiele JR, Habersberger J, Braig D, Schmidt Y, Goerendt K, Maurer V, et al. Dissociation of pentameric to monomeric C-reactive protein localizes and aggravates inflammation: in vivo proof of a powerful proinflammatory mechanism and a new anti-inflammatory strategy. *Circulation.* (2014) 130:35–50. doi: 10.1161/CIRCULATIONAHA.113.007124

12. Habersberger J, Strang F, Scheichl A, Htun N, Bassler N, Merivirta R-M, et al. Circulating microparticles generate and transport monomeric C-reactive protein in patients with myocardial infarction. *Cardiovasc Res.* (2012) 96:64–72. doi: 10.1093/cvr/cvs237

13. Crawford JR, Trial J, Nambi V, Hoogeveen RC, Taffet GE, Entman ML. Plasma levels of endothelial microparticles bearing monomeric C-reactive protein are increased in peripheral artery disease. *J Cardiovasc Trans Res.* (2016) 9:184–93. doi: 10.1007/s12265-016-9678-0

14. Eisenhardt SU, Habersberger J, Murphy A, Chen Y-C, Woollard KJ, Bassler N, et al. Dissociation of pentameric to monomeric C-reactive protein on activated platelets localizes inflammation to atherosclerotic plaques. *Circ Res.* (2009) 105:128–37. doi: 10.1161/CIRCRESAHA.108.190611

15. Krupinski J, Turu MM, Martinez-Gonzalez J, Carvajal A, Juan-Babot JO, Iborra E, et al. Endogenous expression of C-reactive protein is increased in active (ulcerated noncomplicated) human carotid artery plaques. *Stroke.* (2006) 37:1200–4. doi: 10.1161/01.STR.0000217386.37107.be

16. McFadyen JD, Kiefer J, Braig D, Loseff-Silver J, Potempa LA, Eisenhardt SU, et al. Dissociation of C-reactive protein localizes and amplifies inflammation: evidence for a direct biological role of c-reactive protein and its conformational changes. *Front Immunol.* (2018) 9:1351. doi: 10.3389/fimmu.2018.01351

17. Wang J, Tang B, Liu X, Wu X, Wang H, Xu D, et al. Increased monomeric CRP levels in acute myocardial infarction: a possible new and specific biomarker for diagnosis and severity assessment of disease. *Atherosclerosis.* (2015) 239:343–349. doi: 10.1016/j.atherosclerosis.2015.01.024

18. Zhang L, Li H-Y, Li W, Shen Z-Y, Wang Y-D, Ji S-R, et al. An ELISA assay for quantifying monomeric C-reactive protein in plasma. *Front Immunol.* (2018) 9:511. doi: 10.3389/fimmu.2018.00511

19. Williams RD, Moran JA, Fryer AA, Littlejohn JR, Williams HM, Greenhough TJ, et al. Monomeric C-reactive protein in serum with markedly elevated CRP levels shares common calcium-dependent ligand binding properties with an in vitro dissociated form of C-reactive protein. *Front Immunol.* (2020) 11:115. doi: 10.3389/fimmu.2020.00115

20. Munuswamy R, De Brandt J, Burtin C, Derave W, Aumann J, Spruit MA, et al. Monomeric CRP is elevated in patients with COPD compared to non-COPD control persons. *JIR.* (2021) Volume 14:4503–4507. doi: 10.2147/JIR.S320659

21. Jabs WJ, Theissing E, Nitschke M, Bechtel JFM, Duchrow M, Mohamed S, et al. Local generation of C-reactive protein in diseased coronary artery venous bypass grafts and normal vascular tissue. *Circulation.* (2003) 108:1428–1431. doi: 10.1161/01.CIR.0000092184.43176.91

22. Schwedler SB. Tubular staining of modified C-reactive protein in diabetic chronic kidney disease. *Nephrol Dial Trans.* (2003) 18:2300–7. doi: 10.1093/ndt/gfg407

23. Developed with the special contribution of: European Association for Cardiovascular Prevention & Rehabilitation, Authors/Task Force Members, Reiner Z, Catapano AL, De Backer G, Graham I, et al. ESC/EAS guidelines for the management of dyslipidaemias: the task force for the management of dyslipidaemias of the European Society of Cardiology (ESC) and the European Atherosclerosis Society (EAS). *Eur Heart J.* (2011) 32:1769–818. doi: 10.1093/eurheartj/ehr158

24. Mach F, Baigent C, Catapano AL, Koskinas KC, Casula M, Badimon L, et al. 2019 ESC/EAS guidelines for the management of dyslipidaemias:

lipid modification to reduce cardiovascular risk. *Eur Heart J.* (2020) 41:111–88. doi: 10.1093/eurheartj/ehz455

25. Touboul P-J, Hennerici MG, Meairs S, Adams H, Amarenco P, Bornstein N, et al. Mannheim carotid intima-media thickness and plaque consensus (2004-2006-2011). An update on behalf of the advisory board of the 3rd, 4th and 5th watching the risk symposia, at the 13th, 15th and 20th European Stroke Conferences, Mannheim, Germany, 2004, Brussels, Belgium, 2006, and Hamburg, Germany, 2011. *Cerebrovasc Dis.* (2012) 34:290–6. doi: 10.1159/000343145

26. Sakaguchi M, Kitagawa K, Nagai Y, Yamagami H, Kondo K, Matsushita K, et al. Equivalence of plaque score and intima-media thickness of carotid ultrasonography for predicting severe coronary artery lesion. *Ultrasound Med Biol.* (2003) 29:367–71. doi: 10.1016/S0301-5629(02)00743-3

27. Hashimoto H, Kitagawa K, Hougaku H, Shimizu Y, Sakaguchi M, Nagai Y, et al. C-reactive protein is an independent predictor of the rate of increase in early carotid atherosclerosis. *Circulation.* (2001) 104:63–7. doi: 10.1161/hc2601.091705

28. Hollander M, Bots ML, del Sol AI, Koudstaal PJ, Witteman JCM, Grobbee DE, et al. Carotid plaques increase the risk of stroke and subtypes of cerebral infarction in asymptomatic elderly: the Rotterdam study. *Circulation.* (2002) 105:2872–7. doi: 10.1161/01.CIR.0000018650.58984.75

29. Mehta A, Rigdon J, Tattersall MC, German CA, Barringer TA, Joshi PH, et al. Association of carotid artery plaque with cardiovascular events and incident coronary artery calcium in individuals with absent coronary calcification: the MESA. *Circ Cardiovasc Imaging.* (2021) 14:e011701. doi: 10.1161/CIRCIMAGING.120.011701

30. Adams A, Bojara W, Schunk K. Early diagnosis and treatment of coronary heart disease in asymptomatic subjects with advanced vascular atherosclerosis of the carotid artery (type III and IV b findings using ultrasound) and risk factors. *Cardiol Res.* (2018) 9:22–27. doi: 10.14740/cr667w

31. Sillesen H, Sartori S, Sandholt B, Baber U, Mehran R, Fuster V. Carotid plaque thickness and carotid plaque burden predict future cardiovascular events in asymptomatic adult Americans. *Eur Heart J Cardiovasc Imaging.* (2018) 19:1042–50. doi: 10.1093/ehjci/jex239

32. Sillesen H, Muntendam P, Adourian A, Entrekin R, Garcia M, Falk E, et al. Carotid plaque burden as a measure of subclinical atherosclerosis. *JACC Cardiovasc Imaging.* (2012) 5:681–9. doi: 10.1016/j.jcmg.2012.03.013

33. de Weerd M, Greving JP, de Jong AWF, Buskens E, Bots ML. Prevalence of asymptomatic carotid artery stenosis according to age and sex: systematic review and metaregression analysis. *Stroke.* (2009) 40:1105–13. doi: 10.1161/STROKEAHA.108.532218

34. Halvorsen DS, Johnsen SH, Mathiesen EB, Njølstad I. The association between inflammatory markers and carotid atherosclerosis is sex dependent: the Tromsø study. *Cerebrovasc Dis.* (2009) 27:392–7. doi: 10.1159/000207443

35. Ojima S, Kubozono T, Kawasoe S, Kawabata T, Miyata M, Miyahara H, et al. Association of risk factors for atherosclerosis, including high-sensitivity C-reactive protein, with carotid intima-media thickness, plaque score, and pulse wave velocity in a male population. *Hypertens Res.* (2020) 43:422–30. doi: 10.1038/s41440-019-0388-2

36. Arthurs ZM, Andersen C, Starnes BW, Sohn VY, Mullenix PS, Perry J. A prospective evaluation of C-reactive protein in the progression of carotid artery stenosis. *J Vasc Surg.* (2008) 47:744–51. doi: 10.1016/j.jvs.2007.11.066

37. Amar J, Fauvel J, Drouet L, Ruidavets JB, Perret B, Chamontin B, et al. Interleukin 6 is associated with subclinical atherosclerosis: a link with soluble intercellular adhesion molecule 1. *J Hypertens.* (2006) 24:1083–8. doi: 10.1097/01.hjh.0000226198.44181.0c

38. Lee W-Y, Allison MA, Kim D-J, Song C-H, Barrett-Connor E. Association of interleukin-6 and c-reactive protein with subclinical carotid atherosclerosis (the Rancho Bernardo Study). *Am J Cardiol.* (2007) 99:99–102. doi: 10.1016/j.amjcard.2006.07.070

39. Páramo JA, Beloqui O, Colina I, Diez J, Orbe J. Independent association of von Willebrand factor with surrogate markers of atherosclerosis in middle-aged asymptomatic subjects: association of VWF with surrogate markers of atherosclerosis. *J Thrombosis Haemostasis.* (2005) 3:662–4. doi: 10.1111/j.1538-7836.2005.01305.x

40. Horvath B, Hegedus D, Szapary L, Marton Z, Alexy T, Koltai K, et al. Measurement of von Willebrand factor as the marker of endothelial dysfunction in vascular diseases. *Exp Clin Cardiol.* (2004) 9:31–4.

41. Kovacevic KD, Mayer FJ, Jilma B, Buchtele N, Obermayer G, Binder CJ, et al. Von Willebrand factor antigen levels predict major adverse cardiovascular events in patients with carotid stenosis of the ICARAS study. *Atherosclerosis.* (2019) 290:31–6. doi: 10.1016/j.atherosclerosis.2019.09.003

Check for updates

Forsythiasides: A review of the pharmacological effects

Hong-Xuan Yang[1], Qiu-Ping Liu[1], Yan-Xi Zhou[2,3],
Yu-Ying Chen[1], Pei An[1], Yi-Zhuo Xing[1], Lei Zhang[4]*, Min Jia[5]*
and Hong Zhang[1]*

[1]Institute of Interdisciplinary Integrative Medicine Research, Shanghai University of Traditional
Chinese Medicine, Shanghai, China, [2]State Key Laboratory of Characteristic Chinese Medicine
Resources in Southwest China, College of Pharmacy, Chengdu University of Traditional Chinese
Medicine, Chengdu, China, [3]Library, Chengdu University of Traditional Chinese Medicine, Chengdu,
China, [4]Yueyang Hospital of Integrated Traditional Chinese and Western Medicine, Shanghai
University of Traditional Chinese Medicine, Shanghai, China, [5]Department of Chinese Medicine
Authentication, School of Pharmacy, Naval Medical University, Shanghai, China

Forsythiasides are a kind of phenylethanol glycosides existing in *Forsythia suspensa* (Thunb.) Vahl, which possesses extensive pharmacological activities. According to the different groups connected to the nucleus, forsythiasides can be divided into A-K. In recent years, numerous investigations have been carried out on forsythiasides A, B, C, D, E, and I, which have the effects of cardiovascular protection, anti-inflammation, anti-oxidation, neuroprotection, et al. Mechanistically, forsythiasides regulate toll-like receptor 4 (TLR4)/myeloid differentiation factor 88 (MyD88)/nuclear factor kappaB (NF-κB), nuclear factor-erythroid 2-related factor 2 (Nrf2)/heme oxygenase-1 (HO-1) and other signaling pathways, as well as the expression of related cytokines and kinases. Further exploration and development may unearth more treatment potential of forsythiasides and provide more evidence for their clinical applications. In summary, forsythiasides have high development and application value.

KEYWORDS

forsythiasides, *Forsythia suspensa*, cardiovascular protection, anti-inflammation, anti-oxidation

Introduction

Forsythiae Fructus (Chinese name连翘) is the dried fruit of *Forsythia suspensa* (Thunb.) Vahl, a medicinal plant (Oleaceae) widely distributed in Shanxi, Henan, Shaanxi, and other provinces in China. It is commonly used not only in the clinical practice of traditional Chinese medicine (TCM), but also as an important raw material of many Chinese patent drugs due to its traditional efficacies of clearing heat and detoxification, detumescence and dispersing knot, dispelling wind, and clearing heat.

Forsythiae Fructus possesses a variety of pharmacological activities, such as anti-inflammation, antioxidation, anti-virus, and anti-bacteria. Numerous compounds are isolated from *F. suspensa*, including phenylethanol glycosides, lignans, flavonoids, terpeniods, volatile oils, etc. (1–3). Forsythiasides are the main components of phenylethanol glycosides which have the highest content in *F. suspensa*.

As the important ingredients for Forsythiae Fructus to exert various pharmacological activities, forsythiasides A-K have been isolated from *F. suspensa* (4–6). Forsythiasides is a kind of glycosides formed by phenylethanol and sugar and have the stem nucleus as shown in **Table 1**. The glucose can connect with aglycone, rhamnose, xylose, apinose, and caffeoyl. The structures of forsythiasides A-K are displayed in **Table 1**, and the structures of forsythoside A and B are shown in **Figure 1**.

Pharmacological activities

Cardiovascular protection

Forsythiaside A and forsythiaside B can reduce cardiovascular disease damage and exert cardiovascular protection due to their extensive anti-inflammatory and antioxidant effects. Intravenous injection of 5–20 mg/kg forsythoside B dose-dependently reduced polymorph nuclear leukocyte (PMN) infiltration and myeloperoxidase (MPO) activity in a rat model of myocardial ischemia-reperfusion injury (7). The former releases inflammatory factors to damage cardiomyocytes after being activated by ischemic injury, while the latter is considered to be related to the occurrence of cardiovascular disease (8, 9). High-mobility group box 1 (HMGB1) is an inflammatory mediator released by necrotic cells or activated innate immune cells and can activate the NF-κB signaling pathway (10). Forsythoside B could attenuate the expression of HMGB1 and NF-κB in myocardial tissue, decrease the levels of troponin-T, TNF-α, and IL-6 in serum, and reduce the severity of myocardial injury (7). After 40 mg/kg of forsythiaside A was injected intraperitoneally into heart failure mice, the protein expression of NF-κB was decreased, and the levels of inflammatory factors TNF-α, IL-6, and IL-1β in serum were reduced, displaying the cardioprotective effect of forsythiaside A (11).

Nuclear factor-erythroid 2-related factor 2 (Nrf2) is a cytoprotective factor that can regulate the expression of genes encoding antioxidant, anti-inflammatory, and other related proteins. It could bind to antioxidant response elements (AREs) to initiate the transcription of downstream antioxidant genes (12). Forsythiaside A alleviated oxidative stress in mice with heart failure by activating the Nrf2/heme oxygenase-1 (HO-1) signaling pathway (11). Forsythiaside B reduced the content of MDA in the serum

of myocardial ischemia-reperfusion rats, and reverse the decrease of SOD and GPx activities caused by myocardial ischemia (7).

Besides, forsythoside A showed the vasoprotective effect through relaxing the isolated rat aorta. Specifically, forsythiaside A dose-dependently inhibited norepinephrine-induced vasoconstriction by reducing the influx of extracellular calcium ions caused by norepinephrine (13). When low-density lipoprotein is oxidized and accumulated on the arterial wall for a long time, it will cause arteriosclerosis. Forsythoside B could reverse the cytotoxicity elicited by oxidized low-density lipoprotein, inhibit the *in vitro* oxidation of low-density lipoprotein to play a cytoprotective role (14).
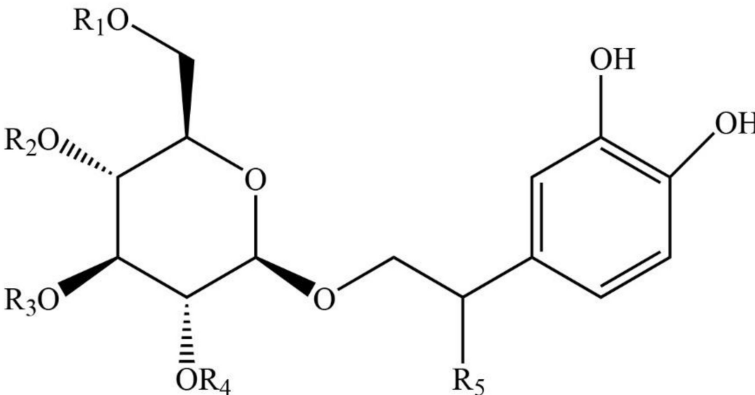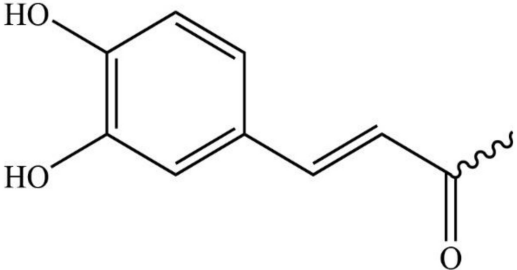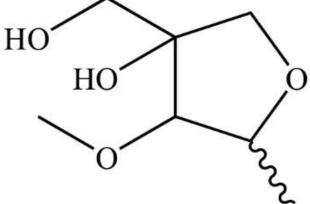
Anti-inflammation

Inflammation is a defense mechanism that occurs when tissues are stimulated by some damages such as trauma, infection by pathogens including bacteria, viruses, parasites, and other inflammatory agents. Inflammatory mediators released from activated mast cells, neutrophils, and macrophages serve as modulator to promote or inhibit the inflammation process (15–17). TLR4/NF-κB is a vital anti-inflammatory pathway, which has attracted much attention in numerous studies on the anti-inflammatory activity of forsythiasides.

Toll-like receptors are a family of pattern-recognition receptors mostly expressed on the surface of cells involved in innate immunity. As a Type I integral membrane protein, TLRs consist of two major parts: an ectodomain of leucine-rich repeats and a cytoplasmic domain of Toll/IL-1R homology domain (18). Among the ten different TLRs discovered in humans, TLR4 is well-known for its characteristic to detect lipopolysaccharide (LPS). LPS non-covalently associates with TLR4 to form an activated heterodimer (LPS/TLR4/myeloid differentiation-2) complex, assisted by membrane cluster differentiation-14 coreceptor (19). Then the complex dimerization recruits MyD88-adaptor-like protein and MyD88, which allows activation of several IL-1 receptor-associated kinases (IRAKs). These IRAKs lead to the ubiquitination of TNF-α receptor-associated factor 6 (TRAF-6), an adaptor molecule activating the transforming growth factor beta-activated kinase 1 (TAK1). Then TAK1 phosphorylates several kinases, resulting in NF-κB being released with other elements (20). However, unlike the above-mentioned TLR4/MyD88/NF-κB pathway, TLR4 can stimulate the production of type I interferons (IFN) as a result of acting on related proteins and phosphorylation of interferon regulatory factor 3 (IRF3) (20).

In dozens of studies on the anti-inflammatory effects of forsythosides A and B, LPS has been widely used to establish

TABLE 1 The chemical structures of forsythiasides.

Structure code/compound	Structure

Stem nucleus of forsythiasides

B

C

Forsythiaside A	R_1 = Rha, R_2 = B, R_3 = R_4 = R_5 = H
Forsythiaside B	R_1 = Api, R_2 = B, R_3 = Rha, R_4 = R_5 = H
Forsythiaside C	R_1 = Rha, R_2 = B, R_3 = R_4 = H, R_5 = OH
Forsythiaside D	R_1 = Rha, R_2 = R_3 = R_4 = H, R_5 = OH
Forsythiaside E	R_1 = Rha, R_2 = R_3 = R_4 = H, R_5 = OH
Forsythiaside F	R_1 = Xyl, R_2 = B, R_3 = Rha, R_4 = R_5 = H
Forsythiaside G	R_1 = C, R_2 = B, R_3 = Rha, R_4 = R_5 = H
Forsythiaside H	R_1 = Rha, R_2 = R_3 = R_5 = H, R_4 = B
Forsythiaside I	R_1 = Rha, R_2 = R_4 = R_5 = H, R_3 = B
Forsythiaside J	R_1 = Xyl, R_2 = R_3 = R_5 = H, R_4 = B
Forsythiaside K	R_1 = Rha, R_2 = B, R_3 = R_4 = H, R_5 = OCH$_3$

Rha, Rhamnose; Api, apiose; Xyl, Xylose.

inflammation models. Forsythiaside A could significantly reverse the increase of TLR4 and NF-κB protein expression induced by LPS (21), which was also observed in the inflammation of PC12 cells induced by hypoxia/reoxygenation (22). Not only that, forsythosides A and B also reduced the expression of NF-κB through other pathways such as JNK-interacting protein (JIP)/c-Jun N-terminal kinase (JNK)/NF-κB and Nrf2/HO-1/NF-κB, thereby affecting the process of inflammation (23, 24). It is worth mentioning that although Nrf2 and NF-κB are the two key transcription factors regulating cellular response to oxidative stress and inflammation, respectively, the absence of Nrf2 can exacerbate NF-κB activity, leading to the increase of cytokine production (25). Both forsythiasides A and B could inhibit the expression of NF-κB by activating the Nrf2/HO-1 pathway, thereby preventing LPS-induced inflammation in BV2 microglia cells
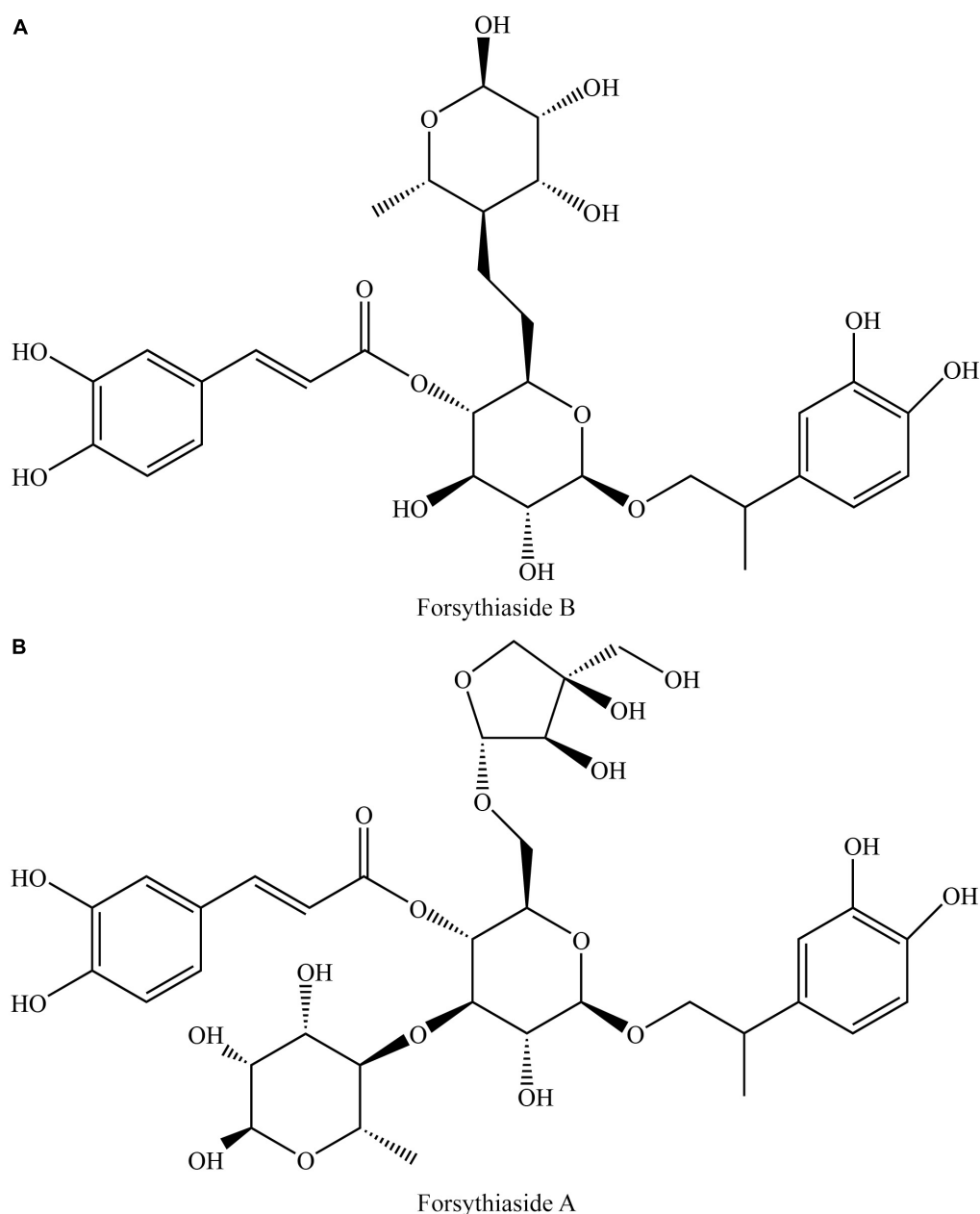
FIGURE 1
Structures of forsythiaside A **(A)** and forsythiaside B **(B)**.

and RAW 264.7 macrophages as well as ovalbumin (OVA)-induced allergic airway inflammation in mice (24, 26–28). As a result, inflammatory factors such as TNF-α and ILs were also regulated in the inflammation model treated by forsythiasides. Forsythiasides could protect against inflammation *via* the NF-κB pathway by regulating TLR4 and Nrf2. **Figure 2** shows how forsythiasides act on the TLR4/MyD88/NF-κB pathway to exert the anti-inflammatory effects. The anti-inflammation properties of forsythiasides A and B are presented in **Table 2**.

Neuroprotection

Alzheimer's disease (AD) is an age-related neurodegenerative disease, whose pathological features are the neurofibrillary tangles formed by the deposition of amyloid-β (Aβ), hyperphosphorylated tau protein, and neuron loss (29). Among them, Aβ is a 38-43 amino acid polypeptide processed from amyloid precursor protein (APP), which plays an important role in causing the imbalance of synaptic homeostasis and clearance dysfunction of lysosomal (30, 31). Recently, deposition was reported

FIGURE 2
Mechanism of anti-inflammation and anti-oxidation by forsythiasides.
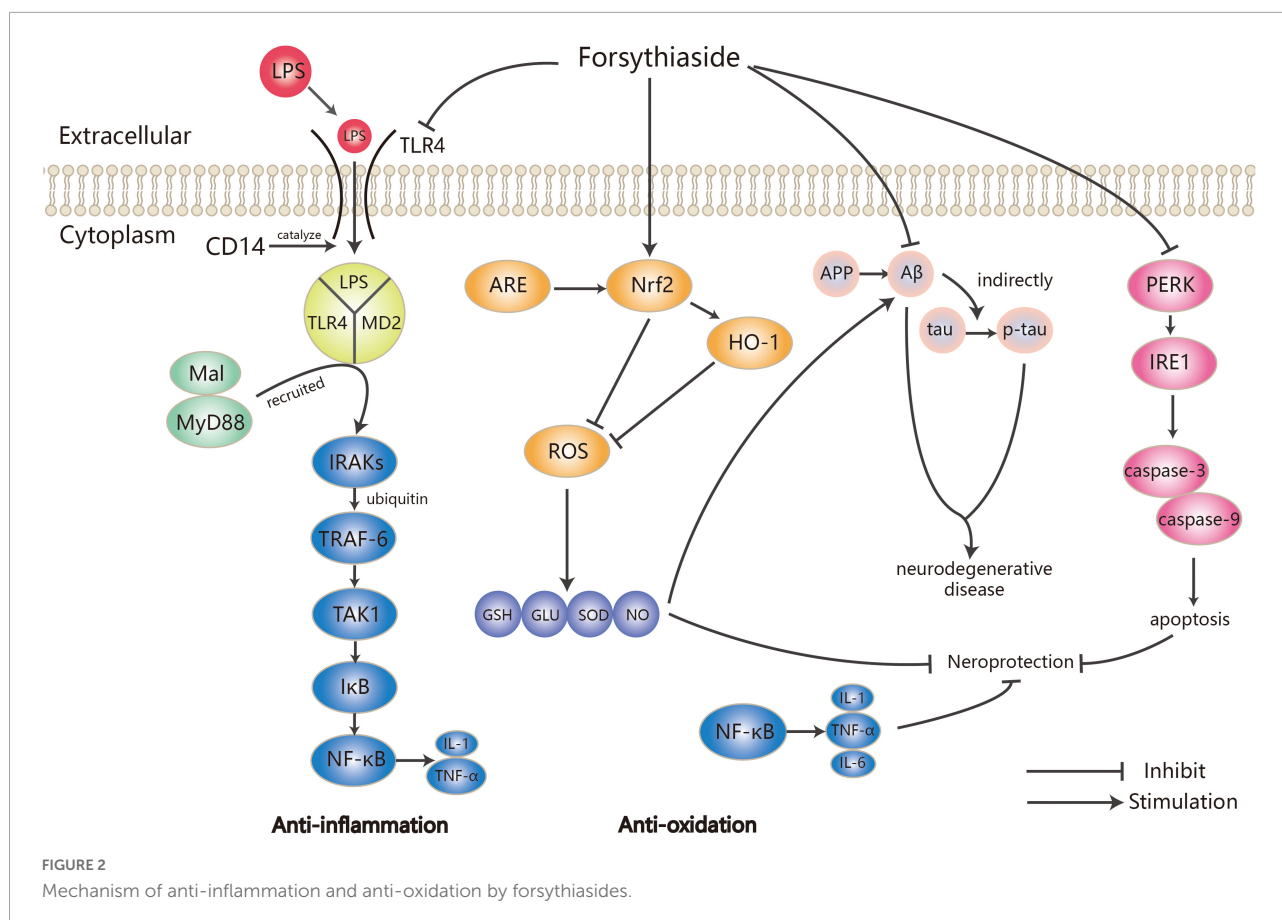
to be promoted by interferon-induced transmembrane protein 3, a γ-secretase modulatory protein induced by inflammatory cytokines.

The neuroprotective effect of forsythiasides is related to their anti-neuroinflammatory activity. Specifically, they could significantly down-regulate inflammatory factors such as interleukin and tumor necrosis factor. The levels of inflammatory factors TNF-α, IL-1β, and IL-6 in the brain tissue of APP/PS1 mice and SAMP8 mice were higher than those of wild-type mice. Interestingly, forsythiasides could reverse these enhanced inflammatory factors. Furthermore, forsythiaside B inhibited NF-κB to exert anti-neuroinflammatory effect by insulting the activation of JIP-3/JNK and reducing the expression of WDFY1/TLR3 (32). Besides, forsythiaside A inhibited the cannabinoid receptor 1 (CB1R)-dependent NF-κB signaling pathway to reduce the secretion of TNF-α and PEG$_2$ in organotypic hippocampal slices of mice (33).

In addition, forsythiasides increased the content of acetylcholine in Aβ-induced AD mouse, which is one of the important neurotransmitters in the central cholinergic system, indicating that forsythiasides have the potential to improve the function of acetylcholine (34).

Lung protection

Acute lung injury (ALI) is one of the earliest and highest morbidity complications after severe trauma or infection. Up-regulation of inflammatory factors serves as a sign of direct response and the development of sustained cell damage (35). A large number of studies have shown that forsythiasides A and B have protective effects on LPS-induced ALI. After the ALI mouse model was treated with forsythiasides, the pathological damage of the lung tissue was relieved in varying degrees (36, 37). At the same time, the gene and protein expression of TLR4, MyD88, and NF-κB were suppressed (36), and the levels of inflammatory factors such as TNF-α, IL-1β, and IL-6 were down-regulated (37). Furthermore, forsythiaside A could reduce the production of chemotactic protein CCL-2, inhibit the adhesion and migration of monocytes to type II lung epithelial cells, thereby decreasing the pathological symptoms of acute lung injury (38). In addition, forsythiaside A could reduce the inflammatory injury of H9N2 avian influenza virus-induced ALI mice by inhibiting MyD88 and NF-κB signaling pathways to down-regulate inflammatory factors such as TNF-α, IL-6, IL-1β (39, 40). Moreover, in mice with cigarette smoke-induced chronic obstructive pulmonary disease, forsythoside A not

only decreased inflammatory cytokines and NO production by inhibiting NF-κB signaling pathway, but also increased glutathione/glutathione ratio of peptide disulfides that prevent lung damage (41).

Kidney protection

Nephrotic syndrome (NS) is a common type of glomerular disease in children and adults and has many complications resulting in difficult prognosis. Forsythiaside A significantly reduced the levels of urine protein, blood creatinine and urea nitrogen in a nephropathy rat model induced by adriamycin, and decreased the number of apoptotic cells in the kidney tissue (42). Forsythiaside A also dose-dependently depressed the expression of NF-κB p65/Macrophage inflammatory protein-2 in the renal tissue and the levels of inflammatory factors such as IL-6, IL-1β, and TNF-α in serum, improving survival in rats with doxorubicin-induced nephropathy (42).

Diabetic nephropathy (DN) is a common cause of mortality in diabetic patients, and is generally caused by persistent high glucose (HG). Podocytes play an important role in maintaining glomerular structure and filtration. Due to the limited division ability, the damage and reduction of podocytes are the key factors to accelerate the progression of DN. It was found that forsythiaside A inhibited matrix metalloproteinase-12, down-regulated extracellular regulated protein kinases (ERK)/p38 mitogen-activated protein kinase (MAPK) signaling pathway, reduced the expression levels of p-ERK, p-p38, and p-JNP in cells, and inactivated MAPK signaling to alleviate the oxidative stress and inflammation caused by HG (43).

Liver protection

Galactosamine (GalN) is a hepatotoxic substance that can inhibit the synthesis of RNA and protein in liver cells, causing diffuse liver necrosis and inflammation. In a mouse model of acute liver injury induced by LPS/GalN, forsythiaside A inhibited NF-κB activation and reduced TNF-α levels in serum, protecting against liver damage (44).

Bone protection

Osteoclasts, one of the components of bone tissue, have the function of bone resorption. They cooperate with osteoblasts to play a key role in the development and formation of bone (45). Forsythiaside A suppressed LPS-induced skull osteolysis in mice by decreasing the differentiation and formation of osteoclasts to restrain bone resorption. Besides, forsythiaside A also inhibited osteoclast differentiation and reduce ovariectomy-elicited bone loss in mice (46).

Anti-oxidation

Nuclear factor-erythroid 2-related factor 2 plays a vital role in transcriptional activation of genes driven by the antioxidant

responsive element (ARE), which mediates transcriptional regulation of phase II detoxification enzyme and antioxidant proteins to clear reactive oxygen species (ROS) (12). HO-1, one of Nrf2-target genes, exerts protection against oxidative injury and modulation of inflammation as well as contribution to angiogenesis (47). In the LPS-induced RAW 264.7 macrophage model, oxidative stress was observed (28). Forsythiaside A inhibited the activation of phosphatidylinositol 3-kinase (PI3K)/protein kinase B (AKT) pathway. At the same time, it activated the Nrf2/HO-1 pathway and reduced the level of ROS. Forsythoside A also depressed the production of inflammatory mediators NO and PGE$_2$, and decreased the expression of pro-inflammatory cytokines TNF-α and IL-1β (28). Meanwhile, the regulatory effect of forsythiaside A on the Nrf2/HO-1 pathway was observed in the OVA-induced mouse asthma model (26). **Figure 1** displays how forsythiasides exerts the anti-oxidation effects by regulation of the Nrf2/HO-1 pathway.

Free radicals scavenging

Free radicals are the product of the body's oxidation process, and the appropriate number of free radicals helps maintain the body's normal physiological functions. The body can maintain the free radical level in a stable range by scavenging the excessive free radicals. Too high concentration of free radicals in the body acts on lipids to undergo peroxidation. The resulting peroxide product MDA denatures cross-link proteins, damages DNA, inactivates enzymes and hormones to damage cells, and finally accelerates aging (48). Forsythiaside A exerted neuroprotective and hepatoprotective effects by clearing MDA (44, 49). Moreover, it was found that forsythiaside A had a dose-dependent anti-oxidant effect on scavenging DPPH free radicals, hydroxyl free radicals, and superoxide anion free radicals, etc. (50–52).

Superoxide dismutase (SOD) is a free radical scavenger widely present in aerobic metabolizing cells, which plays a key role in the body's oxidation and antioxidant balance. Studies have shown that when inflammation occurs, the level of ROS in cells increases significantly (28). Forsythiaside A could strengthen the body's antioxidant capacity, and relieve oxidative stress caused by inflammation or ischemic damage through enhancing the activity of cell SOD and increasing the content of glutathione (GSH), glutathione peroxidase (GSH-Px) and catalase (53, 54). The mechanism of action was related to regulation of the PI3K/AKT/Nrf2/HO-1 signaling pathway (28, 55), indicating that forsythiaside A has a certain potential in alleviating inflammation and oxidative damage.

Neuroprotection

There is certain evidence that excessive oxidative stress factors can produce toxicity to nerve cells, which is related to degenerative memory impairment in AD patients. SOD and GSH-Px are endogenous antioxidant enzymes, which reflect the

TABLE 2 Anti-inflammatory effects of forsythiasides.

Forsythiaside Subtype	Dose	Inflammation model	Action	Mechanism	References
A	20, 80, 320 µg/ml	LPS-induced RAW264.7 cells and primary lymphocytes	Increase of cell viability	Inhibition of HMGB1/TLR4/NF-κB pathway and downregulation of Foxp3, IL-10 and TGF-β1	21
A	1.25, 2.5, 5 mol/L	Ischemia reperfusion-induced PC12 cells	Reduction of inflammatory response	Inhibition of TLR4/NF-κB pathway	22
B	10, 40 mg/kg	APP/PS1 mice	Decrease of Aβ deposition and tau phosphorylation, and reverse of cognitive decline	Attenuating the activation of JIP3/JNK and WDFY1/TLR3, inhibiting the NF-κB pathway	23
A	2.5, 5, 10 µg/ml	LPS-induced BV-2 cells	Reduction of inflammatory response	Regulating NF-κB and Nrf2/HO-1 pathways, reducing the release of TNF-α, IL-1β and PGE$_2$	24
A	15, 30, 60 mg/kg	OVA-induced asthma in mice	Attenuating lung histopathology and suppressing inflammatory responses in asthma	Activation of Nrf2/HO-1 pathway, and decrease of IL-4, IL-5, and IL-13 levels	26
A and B	5, 10, 20 and 12.5, 25, 50, 100 µmol/L	LPS-induced RAW264.7 cells	Alleviation of inflammatory response	Activation of KEAP1/Nrf2/HO-1 pathway, reduction of NO, IL-1β, IL-6 and TNF-α levels	27, 28
A	80 µmol/L	Aβ$_{25-35}$-treated hippocampal slices	Alleviation of learning and memory deficits	Suppressing the overexpression of COX-2 and MAGL proteins and upregulating the levels of 2-AG	33
A	60 mg/kg	LPS-induced acute lung injury in mice	Ameliorating pathological damage and macrophage infiltration of lung	Regulation of miR-124/CCL2 pathway	38
A	12.5, 25, 50 mg/kg	LPS-induced acute lung injury in mice	Attenuating inflammatory cell infiltration and pulmonary interstitial edema	Inhibiting TXNIP/NLRP3 pathway	90
A	20 mg/kg	Influenza A Virus-infected mice	Reducing lung inflammation and inflammatory cell infiltration	Regulation of RLRS-mediated pathways in lung immune cells	72
A	20, 40, 80 mg/kg	IBV-induced infectious bronchitis in avian	Ameliorating clinical signs and lung damage	Increasing CD3$^+$, CD4$^+$, CD8$^+$ T lymphocytes, regulating IL-2, IL-4, IFN-α	78
A	15, 30 mg/kg	OVA-induced asthma in mice	Attenuating airway inflammatory cell infiltration	Depression of p38 MAPK/NF-κB pathway	91
A and B	30, 60, 120 µmol/L	CuSO$_4$-induced Zebrafish	Relieving damage to the neuromasts in the lateral line	Reducing the expression of ROS, NO, Wdr3, and MRPs7	92
A	2.5, 5, 10 µg/ml	S. aureus-induced primary bovine mammary epithelial cells	Reduction of inflammatory response	Inhibition of MAPK/NF-κB pathways, down-regulation of the expression of TNF-α, IL-1β, IL-6	93
A	30 mg/kg	Chick type II collagen induced rheumatoid arthritis in mice	Relieving symptoms in rheumatoid arthritis	Decreasing the expression level of TNF-α protein in serum	94
A	30, 60 mg/kg	LPS-induced spleen of chicken	Reduction of inflammatory response	Suppressing the gene and protein levels of IL-17 and IL-6	95
A	40 mg/kg	Zymosan-induced peritonitis in mice	Alleviation of acute peritonitis	Deceasing the expression of NF-κB, the number of neutrophils and the release of TNF-α, IL-6 and MCP-1	96
A	25, 50, 100 µg/ml	LPS-induced human airway epithelial cells	Reduction of inflammatory response	Reduction of NO secretion and SOD level	97
A	5, 20, 80 mg/kg	2,4-dinitrochlorobenzene in ethanol induced ulcerative colitis in rats	Alleviation of colon lesions	Inhibiting the release of TNF-α and IL-2, increasing the expression of IL-4	98
A and B	6 mg/kg	Dimethylbenzene-induced ear swelling in mice	Alleviation of ear swelling and inflammatory response	Decreasing the production of TNF-α and IL-6	99
B	0.65, 1.30, 2.60 µmol/L	Caecal ligation and puncture -induced sepsis in rats	Reduction of lethality and counteraction of LPS activity	Reducing the levels of TNF-α, IL-6, HGMB1 and TREM-1	100

TABLE 3 Antibacterial effects of forsythiasides.

Forsythiaside subtype	Bacteria	References
A	Inhibiting the growth of *Escherichia coli, Staphylococcus aureus, Streptococcus pneumoniae, Bacillus subtilis, Streptococcus agalactiae, Pseudomonas aeruginosa*, and reversing the resistance of *Aeromonas hydrophila* to enrofloxacin	61–63, 65, 66, 101
B	Suppressing the growth of *Proteus mirabilis, Staphylococcus aureus*, multi-drug resistant *Staphylococcus aureus*	64, 67

body's ability to scavenge free radicals and play a key role in the antioxidant capacity of brain cells. Forsythoside A exerted neuroprotective effects by activating Nrf2 and endoplasmic reticulum stress pathway to reduce cerebral ischemic damage. Forsythiaside A increased the activities of SOD and GSH-Px in the Aβ-induced aging mouse model, and reduced the levels of peroxidation product MDA and important oxygen free radicals NO *in vivo* and *in vitro*, alleviating learning and memory deficits in aging mice (49). Forsythiaside A also had a certain effect on delaying the body's aging by increase of the antioxidant capacity.

Skin protection

Cell protective enzymes such as SOD and GPX can prevent excessive levels of active oxygen to maintain the body's stability. Forsythiaside B had strong antioxidant and free radical scavenging activities. It activated the expression of Nrf2, regulated the level of nuclear transcription factors of cell protective enzymes, and induced the protective ability of phase II cells to exert skin protection (56). Transient receptor potential vanilloid 3 (TRPV3) channel plays an important role in skin physiology, which is associated with genetic Olmsted syndrome characterized by palmoplantar keratoderma and severe pruritus. Forsythiaside B had the therapeutic potential for the treatment of chronic pruritus, skin allergies or inflammation-related skin diseases due to its specific inhibition of overactive TRPV3. It suppressed channel currents activated by TRPV3 agonists in a dose-dependent manner and significantly attenuated acute and chronic pruritus in a dry skin mouse model (57). Another report showed that forsythiaside B had a protective effect on free radical-induced functional endothelial injury (58).

Liver protection

In the acute liver injury mouse model induced by LPS/GalN, forsythiaside A significantly reduced the content of MDA and attenuated the pathological injury of the mouse liver by

activation of the Nrf2/HO-1 signaling pathway, indicating its liver protection effect related to anti-oxidation (44).

Anti-bacterial activity

Forsythiasides A, B, and I show a widely anti-bacterial activity in many investigations. For instance, enrofloxacin, one of the most used fluoroquinolones, has good therapeutic effect on many pathogens such as *Escherichia coli*, Pseudomonas and *Aeromonas hydrophila*. Owing to the widespread use of quinolones, the bacterial resistance has become more and more prominent (59). Studies have found that forsythiaside A could down-regulate the expression of key genes in the differentiation family of drug-resistant nodular cells, and significantly inhibit enrofloxacin resistance to *A. hydrophila* (60, 61). *Forsythia suspensa* affected the growth of drug-resistant bacteria of *A. hydrophila*, presumably mainly through amino acid metabolism, glycolysis, carbon, and nitrogen metabolism, as well as stress-related ABC transport and chemotaxis pathways. Bacterial drug resistance is closely related to its efflux pump system, which can be reduced through inhibiting the activity or reducing the expression for efflux pump.

In addition, forsythiaside A has an obvious antibacterial activity against *E. coli*, *Staphylococcus aureus*, and *Streptococcus pneumoniae*. The K-B paper disk method to measure the diameter of the inhibition zone showed its successive decrease effect on the three bacteria (62). *In vivo* and *in vitro* experiments suggested that forsythiaside A had certain inhibitory effect on *S. aureus*, *Streptococcus lactis*, and *Streptococcus agalactiae* (63). Similarly, forsythiaside B was also found to have antibacterial activity against *Proteus mirabilis* and *S. aureus* (64). There are also many reports that forsythiaside A had strong inhibitory effect on *E. coli*, *Pseudomonas aeruginosa*, and *Bacillus subtilis* [32](65, 66). Moreover, forsythoside B displayed strong antibacterial activity against multi-drug resistant *S. aureus* (67). Although forsythiasides have extensive antibacterial effects, the

TABLE 4 Pharmacological activities of forsythiasides.

Forsythiaside subtype	Pharmacological activity
A	Anti-inflammation, antivirus, antioxidation, immune regulation, antibacteria, abatement of fever, antitumor, neuroprotection, kidney tissue protection, lung tissue protection, liver tissue protection, hair loss protection, inhibition of osteoclast differentiation, inhibition of vasoconstriction
B	Anti-inflammation, antibacteria, cell protection, neuroprotection, lung tissue protection, skin protection, cardiomyocyte protection, anti-tumor
C	Antivirus
D	Antivirus
E	Antitumor
F	Still not clear
G	Still not clear
H	Still not clear
I	Abatement of fever, antibacteria
J	Still not clear
K	Still not clear

related mechanism needs to be further studied. The antibacterial properties of forsythiasides are summarized in Table 3.

Anti-viral activity

As a commonly used Chinese medicine, *F. suspensa* has strong antiviral activity. Studies have exhibited that forsythiaside has inhibitory effect on a variety of viruses. Forsythiaside A could directly kill chicken infectious bronchitis viruses *in vitro* and inhibit the infection of infectious bronchitis viruses in a dose-dependent manner, but no obvious effect was observed in the infected cells. When a large dose of forsythiaside A was used to pretreat chicken embryo kidney cells, the infectivity of infectious bronchitis virus was significantly inhibited (68). The mechanism was probably related to the induction of IFN-α by forsythiaside A, which up-regulated the relevant factors of the janus kinase–signal transducer and activator of transcription signaling pathway (68). Further research found that forsythiaside A significantly inhibited the replication of the viruses in the cells, and enhance the expression of mRNA related to receptors such as melanoma differentiation-associated gene-5 laboratory of genetics and physiology 2, nod-like receptor family caspase activation and recruitment domain containing 5 and antiviral proteins such as IRF7, IFN-α, and IFN-β (69). The above evidence shows that forsythiaside A has the effect of anti-infectious bronchitis.

Matrix protein 1 (M1 protein), the most abundant one in viruses, plays an important role in maintaining the virus structure and the process of virus replication assembly, and germination. Forsythiaside A could cause slow or abnormal germination of influenza A viruses and the mechanism may relate to decrease in the expression of M1 protein and interfere with the germination process of newly formed viruses (70). Forsythiaside A alleviated the symptoms of weight loss and lung tissue damage caused by influenza virus infection in mice by

attenuating the mRNA expression of TLR7, MyD88, IRAK4, TRAF6 in TLR7 signaling pathway and NF-κB p65, reducing the gene and protein expression of retinoicacidinduciblegene-1, mitochondrial antiviral signaling protein and NF-κB, and inhibiting the replication of influenza A viruses to control infection (71, 72). In addition, studies have found that forsythosides C and D were two main components against influenza viruses in the anti-influenza capsules of Forsythiae Fructus (73). It can be seen that forsythiasides have great potential in anti-virus.

Immunomodulation

Regulatory T cells (Tregs), a subgroup of T cells, are important immune cells with independent functions in the body. Tregs not only participate in cellular immunity, but also maintain the body's immune balance by suppressing effector T cells to avoid excessive immunity. Therefore, Tregs play a huge role in preventing autoimmune diseases, anti-graft rejection, and tumor immunity (74). The cell-specific nuclear transcription factor Foxp3 can characteristically mark Tregs and play a key role in the development and functional maintenance of Tregs (75).

Forsythiaside A was found to possess immunomodulatory effect by regulating Tregs (76). When the body is infected by endotoxin, endotoxemia will result. Bacterial endotoxin can increase the survival and proliferation ability of Tregs, and enhance their immunosuppressive function to inhibit the body's immune response. Forsythiaside A exerted the immunomodulatory effect by reducing the level of peripheral blood Tregs and the expression of foxp3 transcription factors in endotoxin mice (21). In addition, forsythiaside A inhibited the replication of bovine viral diarrhea viruses in peripheral blood mononuclear cells cultured *in vitro*. It plays an important role in immune regulation by promoting the transcription of

OX40, 4-1BB, and 4-1BBL which increase the regulation of the activation and proliferation of T cells (77). In addition, forsythiaside A significantly enhanced the number of CD3^{+}, CD4^{+}, CD8^{+} T lymphocytes in the blood of chickens infected with infectious bronchitis viruses (IBV), showing regulatory effect on the immune function of chickens (78).

Antipyretic activity

The hypothalamus is the advanced center of body temperature regulation, and some nerve nuclei play an important role in this process, such as the paraventricular nucleus (PVN) and supraoptic nucleus. Furthermore, there are abundant temperature-sensing neurons in the periphery such as the dorsal root ganglia (DRG), which also exert a key role in thermoregulation. The temperature-sensitive protein TRPA1 is abundantly expressed in the body temperature regulation center (79). Forsythiaside A effectively reduced the body temperature of fever mice induced by subcutaneous injection of yeast suspension through increasing the expression of TRPA1 in the PVN, supraoptic nucleus and DRG (80). Not only that, forsythiaside A also inhibited the secretion of inflammatory mediators such as PGE2 and IL-8, and mitigated symptoms of fever in mice injected with yeast suspension subcutaneously. The mechanism of action may be related to inhibiting the expression of TRPV1 and reducing calcium influx and MAPK phosphorylation (81). Forsythiaside I, the main component of Qingqiao, was also found to possess the function of clearing heat and removing toxicity (82).

Other activities

As active ingredients from a multifunctional medicinal plant, forsythiasides display an anticancer activity to a certain degree. Forsythia Fructus could prolong the survival time of melanoma mice, whose components forsythiasides A, E, and I significantly inhibited the cell viability of B16-F10 cells (83). In addition, forsythoside B suppressed the proliferative activity of cervical cancer cells by blocking the expression of NF-κB and up-regulating p21 binding to the cyclin E/CDK2 complex (84).

Besides, forsythiaside A significantly improved the survival rate of rats with cerebral ischemia and reduced neurological deficits by inhibiting neuronal apoptosis and attenuating the expression of caspase-3 and caspase-9 (85). Forsythiaside A obviously increased hair density and thickness in mice with androgenetic alopecia by 50 and 30%, respectively, and decreased the expression of caspase-9 and caspase-3 in the skin by 40 and 53%, respectively. It also inhibited DHT-induced apoptosis of human hair dermal papilla cells and human keratinocytes. Forsythiaside A is a natural product with the potential to treat androgenetic alopecia due to its protective effect on hair loss by inhibiting apoptosis and delaying hair

cells entering the degenerative phase (86). Forsythiaside A attenuated APAP-induced hepatocyte degeneration and necrosis by inhibiting the PI3K/AKT pathway associated with apoptosis and reversing the abnormal expression of caspase-3, caspase-8, caspase-9, bax, and bcl-2 (87).

Prospective and conclusion

As one of commonly used Chinese medicines, Forsythiae Fructus has extensive pharmacological effects, such as anti-inflammatory, clearing heat, removing toxicity, antibacterial, and antioxidant. Forsythiasides are abundant in *F. suspensa*. This article summarized the pharmacological activities of forsythiasides A-K (**Table 4**), which have a similar chemical structure. However, most of the current investigations focus on forsythiasides A and B. NF-κB is a DNA-binding transcription factor existing in eukaryotic cells, which participates in normal physiological processes such as immune and inflammatory response, and is seen as the convergence point of multiple signal pathways. The NF-κB immune signal pathway is closely related to the biological processes of development, proliferation, differentiation, and apoptosis in immune cells, and plays an important role in the regulation of inflammatory cytokine gene expression. In addition, studies have shown that the NF-κB signaling pathway is closely related to the occurrence of cancer (88). Forsythiasides exert anti-inflammatory, anti-tumor, neuroprotective and lung damage protective effects by inhibiting the activation of NF-κB signaling pathway. Furthermore, forsythiasides can also perform the pharmacological activity through activating the Nrf2 signaling pathway and down-regulated the expression of HMGB1 and TLR4. Many documents reported that the strong neuroprotective effect of forsythiasides is related to reduction of Aβ deposition, alleviation of inflammation and oxidative stress of nerve cells, and decrease of caspase-3 activation to inhibit cell apoptosis. Forsythiasides have potential to treat AD by reversing nerve damage and memory dysfunction.

Although forsythiasides possess many pharmacological activities, there exist some limitations. Forsythiasides A and B show strong antibacterial activity and the ability to scavenge free radicals *in vitro*. In addition to normal bacteria, forsythiasides also have inhibitory effect on drug-resistant bacteria. However, the current investigations on antibacterial and free radical scavenging effects of forsythiasides are mostly concentrated on *in vitro* experiments, failing to further validate these *in vivo*. Forsythiasides interfere with the replication process of the virus, exhibiting the evident antiviral activity. However, the current literature only reported their inhibitory effects on chicken infectious bronchitis viruses and influenza A viruses. In addition, forsythiasides A and B were considered to be closely related to the pseudo-allergic reaction caused by Shuanghuanglian injection (89). However, there are few toxicology investigations reported.

In summary, subsequent studies on forsythiasides should be carried out in view of the above limitations. The NF-κB signaling pathway is closely relevant to a variety of human diseases such as inflammation, tumor, and tissue damage. The other pharmacological effects should be explored further based on NF-κB signaling pathway. Forsythiasides have potential to be an adjuvant drug for the treatment of Alzheimer's disease owing to the significant neuroprotective effect, so their anti-AD mechanism should be explored further. The antibacterial and antioxidant activities of forsythiasides *in vivo* should also be investigated and relevant toxicological studies need to be carried out. Finally, it is hoped that the above-mentioned problems will be solved further and more evidence is provided for the clinical applications of forsythiasides.

Author contributions

HZ, MJ, and LZ: conceptualization. H-XY and Q-PL: writing-original. H-XY and HZ: writing-review and editing. HZ, MJ, LZ, Y-XZ, Y-YC, PA, and Y-ZX: verification and recommendation. All authors contributed to the article and approved the submitted version.

Funding

Conflict of interest

The authors declare that the research was conducted in the absence of any commercial or financial relationships that could be construed as a potential conflict of interest.

Publisher's note

All claims expressed in this article are solely those of the authors and do not necessarily represent those of their affiliated organizations, or those of the publisher, the editors and the reviewers. Any product that may be evaluated in this article, or claim that may be made by its manufacturer, is not guaranteed or endorsed by the publisher.

References

1. Hu J, Ma L, Zhang J, Xu C. Research progress of *Forsythia suspensa*. *Cent South Pharm.* (2012) 10:760–4.

2. Xia W, Dong C, Yang C, Chen H. Research progress on chemical constituents and pharmacology of *Forsythia suspensa. Mod Chin Med.* (2016) 18:1670–4. doi: 10.13313/j.issn.1673-4890.2016.12.031

3. Zhang T, Shi L, Liu W, Zhang M, Yang J, Li F. research progress on chemical constituents and pharmacological effects of *Forsythia. J Liaoning U Tradit Chinese Med.* (2016) 18:222–4. doi: 10.13194/j.issn.1673-842x.2016.12.067

4. Wang Z, Xia Q, Liu X, Liu W, Huang W, Mei X, et al. Phytochemistry, pharmacology, quality control and future research of *Forsythia suspensa* (Thunb.) Vahl: a review. *J Ethnopharmacol.* (2018) 210:318–39. doi: 10.1016/j.jep.2017.08. 040

5. Wei Q, Li P, Wu T, Li C, Zhang R. Progress in phenylethanoid glycosides from *Forsythia suspensa. Chin J Clin Pharmacol.* (2018) 34:2481–5. doi: 10.13699/j.cnki. 1001-6821.2018.20.024

6. Yan X, Xiang Z, Wen J, Zhang W, Yang B, Qu Z, et al. Phenylethanoid glycosides from fruits of *Forsythia Suspensa. Chin Tradit Herb Drugs.* (2016) 47:3362–5.

7. Jiang W, Fu F, Xu B, Tian J, Zhu H, Hou J. Cardioprotection with forsythoside B in rat myocardial ischemia-reperfusion injury: relation to inflammation response. *Phytomedicine.* (2010) 17:635–9. doi: 10.1016/j.phymed.2009. 10.017

8. Piccolo EB, Thorp EB, Sumagin R. Functional implications of neutrophil metabolism during ischemic tissue repair. *Curr Opin Pharmacol.* (2022) 63:102191. doi: 10.1016/j.coph.2022.102191

9. Maiocchi SL, Ku J, Thai T, Chan E, Rees MD, Thomas SR. Myeloperoxidase: a versatile mediator of endothelial dysfunction and therapeutic target during cardiovascular disease. *Pharmacol Ther.* (2021) 221:107711. doi: 10.1016/j. pharmthera.2020.107711

10. Andrassy M, Volz HC, Igwe JC, Funke B, Eichberger SN, Kaya Z, et al. High-mobility group box-1 in ischemia-reperfusion injury of the heart. *Circulation.* (2008) 117:3216–26. doi: 10.1161/circulationaha.108.769331

11. Fu Q, Ma D, Tong Y, Li H, Shen C. Protective effect and possible mechanism of forsythiaside A on pressure overload heart failure in mice. *Prog Anat Sci.* (2021) 27:65–7. doi: 10.16695/j.cnki.1006-2947.2021.01.017

12. Lee J, Calkins M, Chan K, Kan Y, Johnson J. Identification of the NF-E2-related factor-2-dependent genes conferring protection against oxidative stress in primary cortical astrocytes using oligonucleotide microarray analysis. *J Biol Chem.* (2003) 278:12029–38. doi: 10.1074/jbc.M211558200

13. Iizuka T, Nagai M. Vasorelaxant effects of forsythiaside from the fruits of *Forsythia suspensa. Yakugaku Zasshi.* (2005) 125:219–24. doi: 10.1248/yakushi. 125.219

14. Martin-Nizard F, Sahpaz S, Furman C, Fruchart J, Duriez P, Bailleul F. Natural phenylpropanoids protect endothelial cells against oxidized LDL-induced cytotoxicity. *Planta Med.* (2003) 69:207–11. doi: 10.1055/s-2003-38474

15. Metz M, Grimbaldeston M, Nakae S, Piliponsky A, Tsai M, Galli S. Mast cells in the promotion and limitation of chronic inflammation. *Immunol Rev.* (2007) 217:304–28. doi: 10.1111/j.1600-065X.2007.00520.x

16. Soehnlein O, Steffens S, Hidalgo A, Weber C. Neutrophils as protagonists and targets in chronic inflammation. *Nat Rev Immunol.* (2017) 17:248–61. doi: 10.1038/nri.2017.10

17. Hamidzadeh K, Christensen S, Dalby E, Chandrasekaran P, Mosser D. Macrophages and the recovery from acute and chronic inflammation. *Annu Rev Physiol.* (2017) 79:567–92. doi: 10.1146/annurev-physiol-022516-034348

18. Kashani B, Zandi Z, Pourbagheri-Sigaroodi A, Bashash D, Ghaffari S. The role of toll-like receptor 4 (TLR4) in cancer progression: a possible therapeutic target? *J Cell Physiol.* (2021) 236:4121–37. doi: 10.1002/jcp.30166

19. Jagtap P, Prasad P, Pateria A, Deshmukh S, Gupta SA. Single step in vitro bioassay mimicking TLR4-LPS pathway and the role of MD2 and CD14 coreceptors. *Front Immunol.* (2020) 11:5. doi: 10.3389/fimmu.2020.00005

20. Brooks D, Barr L, Wiscombe S, McAuley D, Simpson A, Rostron A. Human lipopolysaccharide models provide mechanistic and therapeutic insights into systemic and pulmonary inflammation. *Eur Respir J.* (2020) 56:1901298. doi: 10.1183/13993003.01298-2019

21. Zeng X, Yuan W, Zhou L, Wang S, Xie Y, Fu Y. Forsythoside A exerts an anti-endotoxin effect by blocking the LPS/TLR4 signaling pathway and inhibiting Tregs in vitro. *Int J Mol Med.* (2017) 40:243–50. doi: 10.3892/ijmm.2017.2990

22. Ma Z, Zhang D, Sun J, Niu J, Ren Q, Wu Q, et al. Forsythiaside A inhibits inflammation induced by cerebral ischemia through TLR4/NF-κB. *Acta U Med Anhui.* (2021) 56:730–4. doi: 10.19405/j.cnki.issn1000-1492.2021.05.011

23. Kong F, Jiang X, Wang R, Zhai S, Zhang Y, Wang D. Forsythoside B attenuates memory impairment and neuroinflammation via inhibition on NF-κB signaling in Alzheimer's disease. *J Neuroinflamm.* (2020) 17:305. doi: 10.1186/s12974-020-01967-2

24. Wang Y, Zhao H, Lin C, Ren J, Zhang S. Forsythiaside A exhibits anti-inflammatory effects in LPS-stimulated BV2 microglia cells through activation of NRF2/HO-1 signaling pathway. *Neurochem Res.* (2016) 41:659–65. doi: 10.1007/s11064-015-1731-x

25. Wardyn J, Ponsford A, Sanderson C. Dissecting molecular cross-talk between NRF2 and NF-κB response pathways. *Biochem Soc Trans.* (2015) 43:621–6. doi: 10.1042/bst20150014

26. Qian J, Ma X, Xun Y, Pan L. Protective effect of forsythiaside A on OVA-induced asthma in mice. *Eur J Pharmacol.* (2017) 812:250–5. doi: 10.1016/j.ejphar.2017.07.033

27. Wu A, Yang Z, Huang Y, Yuan H, Lin C, Wang T, et al. Natural phenylethanoid glycosides isolated from *Callicarpa kwangtungensis* suppressed lipopolysaccharide-mediated inflammatory response via activating Keap1/NRF2/HO-1 pathway in RAW 264.7 macrophages cell. *J Ethnopharmacol.* (2020) 258:112857. doi: 10.1016/j.jep.2020.112857

28. Tang H, Che N, Liu H, Ma X, Li J, Li L. Forsythiaside A suppresses LPS-induced inflammation and oxidative stress by inhibiting PI3K/Akt pathway and activating Nrf2/HO-1 pathway. *Immunol J.* (2021) 37:390–6. doi: 10.13431/j.cnki.immunol.j.20210054

29. Hyman BT, Phelps CH, Beach TG, Bigio EH, Cairns NJ, Carrillo MC, et al. National institute on aging-Alzheimer's association guidelines for the neuropathologic assessment of Alzheimer's disease. *Alzheimers Dement.* (2012) 8:1–13. doi: 10.1016/j.jalz.2011.10.007

30. Thinakaran G, Koo EH. Amyloid precursor protein trafficking. *Proc Funct J Biologic Chem.* (2008) 283:29615–9. doi: 10.1074/jbc.R800019200

31. Knopman D, Amieva H, Petersen R, Chételat G, Holtzman D, Hyman B, et al. Alzheimer disease. *Nat Rev Dis Primers.* (2021) 7:33. doi: 10.1038/s41572-021-00269-y

32. Kong F. *Study on the Protective effect of Forsythiaside B on Alzheimer's Disease and its undering mechanism* Master's thesis. Changchun: Jilin University (2020).

33. Chen L, Yan Y, Chen T, Zhang L, Gao X, Du C, et al. Forsythiaside prevents β-amyloid-induced hippocampal slice injury by upregulating 2-arachidonoylglycerol via cannabinoid receptor 1-dependent NF-κB pathway. *Neurochem Int.* (2019) 125:57–66. doi: 10.1016/j.neuint.2019.02.008

34. Yan X, Chen T, Zhang L, Du H. Protective effects of Forsythoside A on amyloid beta-induced apoptosis in PC12 cells by downregulating acetylcholinesterase. *Eur J Pharmacol.* (2017) 810:141–8. doi: 10.1016/j.ejphar.2017.07.009

35. Johnson E, Matthay M. Acute lung injury: epidemiology, pathogenesis, and treatment. *J Aerosol Med Pulm Drug Deliv.* (2010) 23:243–52. doi: 10.1089/jamp.2009.0775

36. Zhou L, Yang H, Ai Y, Xie Y, Fu Y. Protective effect of forsythiaside A on acute lung injure induced by lipopolysaccharide in mice. *Chin J Cell Mol Immunol.* (2014) 30:151–4. doi: 10.13423/j.cnki.cjcmi.007031

37. Liu J, Li X, Yan F, Pan Q, Yang C, Wu M, et al. Protective effect of forsythoside B against lipopolysaccharide-induced acute lung injury by attenuating the TLR4/NF-κB pathway. *Int Immunopharmacol.* (2019) 66:336–46. doi: 10.1016/j.intimp.2018.11.033

38. Lu Z, Liu S, Ou J, Cao H, Shi L, Liu D, et al. Forsythoside A inhibits adhesion and migration of monocytes to type II alveolar epithelial cells in lipopolysaccharide-induced acute lung injury through upregulating miR-124. *Toxicol Appl Pharmacol.* (2020) 407:115252. doi: 10.1016/j.taap.2020.115252

39. Sheng N, Lu G, Fu Y, Hu G. Effect of forsythoside A on the expression of inflammatory genes in H9N2-AIV Mice. *China Anim Health.* (2020) 22:49–50.

40. Sheng N, Lu G, Fu Y, Tian X, Hu G. Effect of forsythoside A on Toll-like receptor signal pathway in mice infected with H9N2 Avian influenza. *J Beijing U Agric.* (2020) 35:94–100. doi: 10.13473/j.cnki.issn.1002-3186.2020.0317

41. Cheng L, Li F, Ma R, Hu X. Forsythiaside inhibits cigarette smoke-induced lung inflammation by activation of NRF2 and inhibition of NF-κB. *Int Immunopharmacol.* (2015) 28:494–9. doi: 10.1016/j.intimp.2015.07.011

42. Lu C, Zheng S, Liu J. Forsythiaside A alleviates renal damage in adriamycin-induced nephropathy. *Front Biosci.* (2020) 25:526–35. doi: 10.2741/4818

43. Quan X, Liu H, Ye D, Ding X, Su X. Forsythoside A alleviates high glucose-induced oxidative stress and inflammation in podocytes by inactivating MAPK signaling via MMP12 inhibition. *Diabetes Metab Syndr.* (2021) 14:1885–95. doi: 10.2147/dmso.s305092

44. Pan C, Zhou G, Chen W, Zhuge L, Jin L, Zheng Y, et al. Protective effect of forsythiaside A on lipopolysaccharide/d-galactosamine-induced liver injury. *Int Immunopharmacol.* (2015) 26:80–5. doi: 10.1016/j.intimp.2015.03.009

45. Chen H, Wang Y. Function and regulation of the osteoclast in the pathological changes of bone destruction in rheumatoid arthritis. *Chin J Osteoporos.* (2016) 22:1168–73.

46. Sun X. *The Mechanism of Forsythiaside A Inhibiting Osteoclast Differentiation and Its Therapeutic Application* Master Thesis. Hangzhou: Zhejiang University (2018).

47. Loboda A, Damulewicz M, Pyza E, Jozkowicz A, Dulak J. Role of Nrf2/HO-1 system in development, oxidative stress response and diseases: an evolutionarily conserved mechanism. *Cell Mol Life Sci.* (2016) 73:3221–47. doi: 10.1007/s00018-016-2223-0

48. Liu J, Zhang L. Functions of forsythiaside on the damage of DNA induced by hydroxyl radical. *J Shanxi Coll Tradit Chin Med.* (2006) 7:23–4.

49. Wang H, Wang L, Liu X, Li C, Xu S, Farooq A. Neuroprotective effects of forsythiaside on learning and memory deficits in senescence-accelerated mouse prone (SAMP8) mice. *Pharmacol Biochem Be.* (2013) 105:134–41. doi: 10.1016/j.pbb.2012.12.016

50. Delazar A, Sabzevari A, Mojarrab M, Nazemiyeh H, Esnaashari S, Nahar L, et al. Free-radical-scavenging principles from *Phlomis caucasica. J Nat Med.* (2008) 62:464–6. doi: 10.1007/s11418-008-0255-y

51. Georgiev M, Alipieva K, Orhan I, Abrashev R, Denev P, Angelova M. Antioxidant and cholinesterases inhibitory activities of *Verbascum xanthophoeniceum* GRISEB. and its phenylethanoid glycosides. *Food Chem.* (2011) 128:100–5. doi: 10.1016/j.foodchem.2011.02.083

52. Piao X, Wu Q, Tian Y. Antioxidants from *Forsythia suspensa. Lishizhen Med Materia Med Res.* (2010) 21:1307–9.

53. Zhao Y. *Effect of Forsythaside on the Cytokine and Antionxidative Function in Bursa of Fabricius of Chickens.* Master Thesis Harbin: Northeast Agricultural University (2013).

54. Li H, Chen J, Zhao Y, Wu Y, Li X, Li Y. Effect of forsythiaside on antioxidation induced by LPS in liver of chickens. *China Poultry.* (2013) 35:20–2.

55. Ma Z, Zhang D, Sun J, Niu J, Ren Q, Wu Q, et al. Forsythiaside A inhibited cerebral ischemic induced oxidative damage through AKT/NRF2 signaling pathway. *Prog Mod Biomed.* (2021) 21:214–8. doi: 10.13241/j.cnki.pmb.2021.02.004

56. Sgarbossa A, Dal Bosco M, Pressi G, Cuzzocrea S, Dal Toso R, Menegazzi M. Phenylpropanoid glycosides from plant cell cultures induce heme oxygenase 1 gene expression in a human keratinocyte cell line by affecting the balance of NRF2 and BACH1 transcription factors. *Chem Biol Interact.* (2012) 199:87–95. doi: 10.1016/j.cbi.2012.06.006

57. Zhang H, Sun X, Qi H, Ma Q, Zhou Q, Wang W, et al. Pharmacological inhibition of the temperature-sensitive and ca-permeable transient receptor potential vanilloid TRPV3 Channel by natural forsythoside b attenuates pruritus and cytotoxicity of keratinocytes. *J Pharmacol Exp Ther.* (2019) 368:21–31. doi: 10.1124/jpet.118.254045

58. Ismailoglu U, Saracoglu I, Harput U, Sahin-Erdemli I. Effects of phenylpropanoid and iridoid glycosides on free radical-induced impairment of endothelium-dependent relaxation in rat aortic rings. *J Ethnopharmacol.* (2002) 79:193–7. doi: 10.1016/s0378-8741(01)00377-4

59. Nelson J, Chiller T, Powers J, Angulo F. Fluoroquinolone-resistant Campylobacter species and the withdrawal of fluoroquinolones from use in

poultry: a public health success story. *Clin Infect Dis.* (2007) 44:977–80. doi: 10.1086/512369

60. Ying X, Yang Y. New veterinary antibacterial drug—enrofloxacin. *Chin J Vet Drug.* (1995) 29:53–6.

61. Dong Y, Feng D, Sun J, Zhang X, Hu K, Yang X. Delaying effect of forsythiaside A *Aeromonas hydrophila* resistance to enrofloxacin and its exocytosis. *J Southern Agric.* (2019) 50:187–93.

62. Zhang Y, Han Y, Liang L, Shang C, Xue H. Preparation and antibacterial antioxidant activity of phillyrin, forsythiaside A on n-butanol part extract from qingqiao of *Forsythia* suspensa. *Chin J Exp Tradit Med.* (2014) 20:192–6. doi: 10.13422/j.cnki.syfjx.2014210192

63. Wang H, Jiang H, Wu G. Research on the antibacterial effect of forsythiaside in vitro and in vivo. *China Feed.* (2005) 26–7.

64. Didry N, Seidel V, Dubreuil L, Tillequin F, Bailleul F. Isolation and antibacterial activity of phenylpropanoid derivatives from *Ballota nigra*. *J Ethnopharmacol.* (1999) 67:197–202. doi: 10.1016/s0378-8741(99)00019-7

65. Qin Z, Xu J, Zhang L. Studies on the anti-bacteria effect of fructus forsythia and folium forsythia in vitro. *Food Eng.* (2013) 49–52.

66. Qu H, Zhang Y, Wang Y, Li B, Sun W. Antioxidant and antibacterial activity of two compounds (forsythiaside and forsythin) isolated from *Forsythia suspensa*. *J Pharma Pharmacol.* (2008) 60:261–6. doi: 10.1211/jpp.60.2.0016

67. Nazemiyeh H, Rahman M, Gibbons S, Nahar L, Delazar A, Ghahramani M, et al. Assessment of the antibacterial activity of phenylethanoid glycosides from *Phlomis lanceolata* against multiple-drug-resistant strains of *Staphylococcus aureus*. *J Nat Med.* (2008) 62:91–5. doi: 10.1007/s11418-007-0194-z

68. Li H, Wu J, Zhang Z, Ma Y, Liao F, Zhang Y, et al. Forsythoside a inhibits the avian infectious bronchitis virus in cell culture. *Phytother Res.* (2011) 25:338–42. doi: 10.1002/ptr.3260

69. Zhang T, Liu B, Yang X, Lv A, Zhang Z, Gong P, et al. Effect of forsythoside A on expression of intracellular receptors and antiviral gene in IBV-infected cells. *J Beijing U Agric.* (2017) 32:37–42. doi: 10.13473/j.cnki.issn1002-3186.2017.0118

70. Law A, Yang C, Lau A, Chan G. Antiviral effect of forsythoside A from *Forsythia suspensa* (Thunb.) Vahl fruit against influenza A virus through reduction of viral M1 protein. *J Ethnopharmacol.* (2017) 24:236–47. doi: 10.1016/j.jep.2017.07.015

71. Deng L, Pang P, Zheng K, Nie J, Xu H, Wu S, et al. Forsythoside A controls influenza A virus infection and improves the prognosis by inhibiting virus replication in mice. *Molecules.* (2016) 21:524. doi: 10.3390/molecules21050524

72. Zheng X, Fu Y, Shi S, Wu S, Yan Y, Xu L, et al. Effect of forsythiaside A on the RLRs signaling pathway in the lungs of mice infected with the influenza A virus FM1 strain. *Molecules.* (2019) 24:4219. doi: 10.3390/molecules24234219

73. Zhao W, Shi R, Liu B, Zhang J. Isolation and elucidation of antiviral substances from lianqiao bingduqing capsule on influenza virus. *Chin Tradit Pat Med.* (2005) 27:81–5.

74. Hall BT. Cells: soldiers and spies–the surveillance and control of effector T cells by regulatory T cells. *Clin J Am Soc Nephrol.* (2015) 10:2050–64. doi: 10.2215/cjn.06620714

75. Yuan W, Yang H, Fu Y. Research progress of traditional chinese medicine on the immune regulatory function of regulatory T cells. *Chin Tradit Pat Med.* (2014) 36:1041–4.

76. Zhang X. Effect of forsythiaside A on immune regulation in endotoxemia mice and mechanism of action. *Guid J Tradit Chin Med Pharm.* (2016) 22:57–60. doi: 10.13862/j.cnki.cn43-1446/r.2016.21.018

77. Song Q, Weng X, Cai D, Zhang W, Wang J. Forsythoside A inhibits BVDV Replication via TRAF2-Dependent CD28-4-1BB Signaling in Bovine PBMCs. *PLoS One.* (2016) 11:e0162791. doi: 10.1371/journal.pone.0162791

78. Wang X, Li X, Wang X, Chen L, Ning E, Fan Y, et al. Experimental study of forsythoside A on prevention and treatment of avian infectious bronchitis. *Res Vet Sci.* (2021) 135:523–31. doi: 10.1016/j.rvsc.2020.11.009

79. Ding Z, Gomez T, Werkheiser J, Cowan A, Rawls S. Icilin induces a hyperthermia in rats that is dependent on nitric oxide production and NMDA receptor activation. *Eur J Pharmacol.* (2008) 578:201–8. doi: 10.1016/j.ejphar.2007.09.030

80. Su H, Wan H, Liu C, Kong X, Lin N. Effect of forsythiaseide A on temperature and expression of TRPA1 in mice with yeast induced pyrexia. *Chin J Exp Tradit Med Formulae.* (2016) 22:134–8. doi: 10.13422/j.cnki.syfjx.2016010134

81. Liu C, Su H, Wan H, Qin Q, Wu X, Kong X, et al. Forsythoside A exerts antipyretic effect on yeast-induced pyrexia mice via inhibiting transient receptor

potential vanilloid 1 function. *Int J Biol Sci.* (2017) 13:65–75. doi: 10.7150/ijbs.18045

82. Ma L, Gao J, Zhang L. Screening for active components of heat-clearing and detoxifying from green fructus forsythiae. *Chem Res Appl.* (2019) 31:271–7.

83. Bao J, Ding R, Liang Y, Liu F, Wang K, Jia X, et al. Differences in chemical component and anticancer activity of green and ripe forsythiae fructus. *Am J Chin Med.* (2017) 45:1513–36. doi: 10.1142/s0192415x17500823

84. Zhang Z, Lv Y, Huang P. Forsythiaside B inhibits the proliferation activity of HeLa cells though transcription factor NF-κB. *Chin J Clin Pharmacol Ther.* (2020) 25:387–92.

85. Ma T, Shi Y, Wang Y. Forsythiaside A protects against focal cerebral ischemic injury by mediating the activation of the NRF2 and endoplasmic reticulum stress pathways. *Mol Med Rep.* (2019) 20:1313–20. doi: 10.3892/mmr.2019.10312

86. Shin HS, Park SY, Song HG, Hwang E, Lee DG, Yi TH. The androgenic alopecia protective effects of forsythiaside-A and the molecular regulation in a mouse model. *Phytother Res.* (2015) 29:870–6. doi: 10.1002/ptr.5324

87. Gong L, Zhou H, Wang C, He L, Guo C, Peng C, et al. Hepatoprotective effect of forsythiaside a against acetaminophen-induced liver injury in zebrafish: coupling network pharmacology with biochemical pharmacology. *J Ethnopharmacol.* (2021) 271:113890. doi: 10.1016/j.jep.2021.113890

88. Taniguchi K, Karin M. NF-κB, inflammation, immunity and cancer: coming of age. *Nat Rev Immunol.* (2018) 18:309–24. doi: 10.1038/nri.2017.142

89. Han J, Zhang Y, Pan C, Xian Z, Pan C, Zhao Y, et al. Forsythoside A and Forsythoside B contribute to shuanghuanglian injection-induced pseudoallergic reactions through the RHOA/ROCK Signaling Pathway. *Int J Mol Sci.* (2019) 20:6266. doi: 10.3390/ijms20246266

90. Liang H, Liu K, Zhuang Z, Sun H, Sun B, Jiao M, et al. Potential of Forsythoside I as a therapeutic approach for acute lung injury: involvement of TXNIP/NLRP3 inflammasome. *Mol Immunol.* (2021) 134:192–201. doi: 10.1016/j.molimm.2021.03.004

91. Lin X, Li J, Che N, Li L, Li L. Forsythiaside A suppresses airway inflammation of asthma through inhibition of p38 MAPK/NF-kappa B signaling pathway. *Chin J Immunol.* (2019) 35:2971–4.

92. Gong L, Yu L, Gong X, Wang C, Hu N, Dai X, et al. Exploration of anti-inflammatory mechanism of forsythiaside A and forsythiaside B in CuSO4-induced inflammation in zebrafish by metabolomic and proteomic analyses. *J Neuroinflamma.* (2020) 17:173. doi: 10.1186/s12974-020-01855-9

93. Zhang J, Zhang Y, Huang H, Zhang H, Lu W, Fu G, et al. Forsythoside A inhibited S. Aureus stimulated inflammatory response in primary bovine mammary epithelial cells. *Microb Pathog.* (2018) 116:158–63. doi: 10.1016/j.micpath.2018.01.002

94. Cheng G, Lv D, Liu L, Wang B, Wang W, Zhang W, et al. Study on the Inhibitory mechanism of forsythiaside A against rheumatoid arthritis of rats. *Animal Husbandry Feed Sci.* (2014) 35:1–3. doi: 10.16003/j.cnki.issn1672-5190.2014.05.062

95. Cheng G, Zhang Q, Yue L, Xu L, Zhu D, Liu H, et al. Effect of forsythiaside A on the Levels of IL-17 and IL-6 in spleen of chickens inflamed by endotoxin. *Heilongjiang Animal Sci Vet Med.* (2017) 149–52. doi: 10.13881/j.cnki.hljxmsy.2017.2096

96. Zhang X, Ding Y, Kang P, Zhang X, Zhang T. Forsythoside A modulates zymosan-induced peritonitis in mice. *Molecules.* (2018) 23:593. doi: 10.3390/molecules23030593

97. Liu J, Zhang L. Anti-inflammatory activity of *Forsythia suspensa* extract on human airway epithelial cells inflammation model. *Nat Product Res Dev.* (2015) 27:1248–53. doi: 10.16333/j.1001-6880.2015.07.023

98. Yu L, Jiang H, Liu H. Effect of forsythiaside A on immune function in rats with ulcerative colitis. *Chin J Pathophysiol.* (2020) 36:1128–32.

99. Quan Y, Yuan A, Gong X, Peng C, Li Y. Investigation on anti-inflammatory components of *Forsythia suspensa*. *Nat Product Res Dev.* (2017) 29:435–8. doi: 10.16333/j.1001-6880.2017.3.013

100. Jiang W, Xu Y, Zhang S, Zhu H, Hou J. Forsythoside B protects against experimental sepsis by modulating inflammatory factors. *Phytother Res.* (2012) 26:981–7. doi: 10.1002/ptr.3668

101. Zhang Y. *Studies on the Main Chemical Constituuents of Qingqiao and Laoqiao, And the activity of Phillyrin and Forsythiaside A* Master Thesis. Jinzhong: Shanxi University of Chinese Medicine (2015).

Hypertension as a risk factor for atherosclerosis: Cardiovascular risk assessment

Anastasia V. Poznyak[1]*, Nikolay K. Sadykhov[2], Andrey G. Kartuesov[3], Evgeny E. Borisov[2], Alexandra A. Melnichenko[3], Andrey V. Grechko[4] and Alexander N. Orekhov[1,2,3]

[1]Institute for Atherosclerosis Research, Moscow, Russia, [2]Petrovsky National Research Centre of Surgery, Moscow, Russia, [3]Laboratory of Angiopathology, Institute of General Pathology and Pathophysiology, Moscow, Russia, [4]Federal Research and Clinical Center of Intensive Care Medicine and Rehabilitology, Moscow, Russia

Atherosclerosis is a predecessor of numerous cardiovascular diseases (CVD), which often lead to morbidity and mortality. Despite the knowledge of the pathogenesis of atherosclerosis, an essential gap in our understanding is the exact trigger mechanism. A wide range of risk factors have been discovered; however, a majority of them are too general to clarify the launching mechanism of atherogenesis. Some risk factors are permanent (age, gender, genetic heritage) and others can be modified [tobacco smoking, physical inactivity, poor nutrition, high blood pressure, type 2 diabetes (T2D), dyslipidemia, and obesity]. All of them have to be taken into account. In the scope of this review, our attention is focused on hypertension, which is considered the most widespread among all modifiable risk factors for atherosclerosis development. Moreover, high blood pressure is the most investigated risk factor. The purpose of this review is to summarize the data on hypertension as a risk factor for atherosclerosis development and the risk assessment.

KEYWORDS

atherosclerosis, hypertension, cardiovascular disease, cardiovascular risk, vessels

Atherosclerosis is the main cause of cardiovascular disease

Atherosclerosis is the main cause of cardiovascular diseases (CVD). Intima of middle- and large-sized arteries is most vulnerable to atherosclerosis, especially the sites of vessel branching. It can be explained by the nature of the blood flow since areas exposed to normal shear stress seem to be protected. One of the initial events

in atherogenesis is the expression of adhesion molecules by activated endothelium. This allows mononuclear leukocytes, such as monocytes and T-cells, to attach to the endothelium and infiltrate the intima. Along with these cells, dendritic cells, mast cells, neutrophils, and B-cells may also be present in lesions. The essential type of cells present in the atherosclerotic lesion is the smooth muscle cells (SMCs). These cells change their phenotype to synthetic and migrate to the intima. The hallmark of atherosclerosis is the appearance of fatty streaks further evolving into atherosclerotic plaques. Atherosclerosis can induce CVD through stenosis and atherothrombosis, which are capable of decreasing blood flow. Atherothrombosis occurs when plaques are damaged by the effects of proinflammatory cytokines and chemokines on the fibrous cap. When plaques are damaged and ruptured, the prothrombotic material is exposed to the coagulation system, with the ensuing inhibition of blood flow and thus the induction of CVD (1).

For a very long time, CVD has been the leading global cause of premature mortality. According to statistics, by 2030, 23.6 million people will be dying from CVD every year. In northwestern and southern Europe, there is a moderate downward trend in mortality and morbidity due to CVD (2).

In Europe, CVD are the cause of 49% of deaths. It is the most important cause of premature mortality and Disability Adjusted Life Years ("DALYS") in Europe, which attaches great importance to this topic in the field of public health. The annual cost of medical care for CVD in the European Union is about 192 billion euros (3). CVD can be caused by a large number of factors. Some of them are permanent (age, gender, genetic heritage) and others are changeable, that is, they can be influenced [tobacco smoking, physical inactivity, poor nutrition, high blood pressure, type 2 diabetes (T2d), dyslipidemia, obesity] (4). Risk factor control (45–75%) and proper treatment of CVD (25–55%) are responsible for reducing CVD mortality in highly developed countries (5).

Cardiovascular risk factors

The main risk factors for atherosclerosis and, subsequently, CVD, are high blood pressure (BP), cigarette smoking, diabetes mellitus, and lipid metabolism disorders. Among them, high blood pressure is linked with the most convincing evidence of a causal relationship and has a high prevalence of exposure (6). In **Figure 1** we provided the simplified scheme of various risk factors' impact. However, there is concrete evidence that the biologically normal blood pressure level in humans is significantly lower than the level that is usually used both in clinical practice and research, which leads to an underrepresentation of the role of blood pressure as a risk factor for CVD (7). We put forward an integrated theory of the cause-effect relationship of CVD, which is confirmed by a reliable set

of consistent evidence: CVD in humans are primarily caused by a right-sided shift in the distribution of blood pressure.

Due to the dominance of social networks, there are plenty of theories, but only a few satisfy the basic requirements of causality. Scientific theories are the most reliable because they are structured and can be refuted by systematic observation and experimental verification of the hypothesis testing. Our theory meets almost all the criteria of causality proposed by Bradford Hill. The changes that have arisen since the period of the post-industrial revolution have entailed consequences for the morbidity profile of the world's population. As a result of technological progress, society is increasingly inclined to a sedentary lifestyle. This fact has led to an increase in the number of chronic diseases, such as obesity, T2D, and systemic hypertension, conditions known to be associated with increased cardiovascular risk (8).

As mortality and morbidity of CVD inexorably increased, the Framingham Study was launched to study risk factors and physiopathology associated with CVD. This prospective, long-term study made it possible to stratify cardiovascular risk as to the probability of a coronary event in the next 10 years. Since then, the Framingham score has been a practical method for assessing cardiovascular risk in various population groups (9).

This indicator makes it possible to assess the risk of coronary heart disease (CHD) for 10 years based on such parameters as blood pressure, systolic blood pressure (SBP), total cholesterol, HDL cholesterol, smoking, and antihypertensive treatment. Based on the calculated risk, an individual can be classified as having a low, medium, or high risk of developing CAD, including fatal coronary death or non-fatal myocardial infarction (MI) (10).

The risk factors for CAD include modifiable lifestyle factors, such as smoking, dyslipidemias, obesity, sedentariness, diabetes, and alcohol intake, as well as non-modifiable characteristics like age, sex, and family history. Among the modifiable risk factors, arterial hypertension is recognized as the key to ischemic diseases and disorders of cerebral circulation (11). A randomized study involved 3,845 participants with an average age of 83 years; this study revealed that lowering BP from 161/84 to 144/78 mmHg reduces the risk of cerebral circulatory disorders by 30% and cardiovascular events by 23% (12).

Smoking

Another significant modifiable risk factor is smoking. It is known that smokers over the age of 60 have doubled risk of atherosclerosis and subsequent CVD compared to non-smokers. For people under the age of 60, the risk is five times higher (4). In addition to CV risk, smoking is linked with a higher prevalence of chronic kidney disease (CKD). In an observational study of 65,589 people who were observed for 10.3 years, it was shown that the risk of developing CKD is 4 and 3.3 times

FIGURE 1
Risk factors for atherosclerosis development.
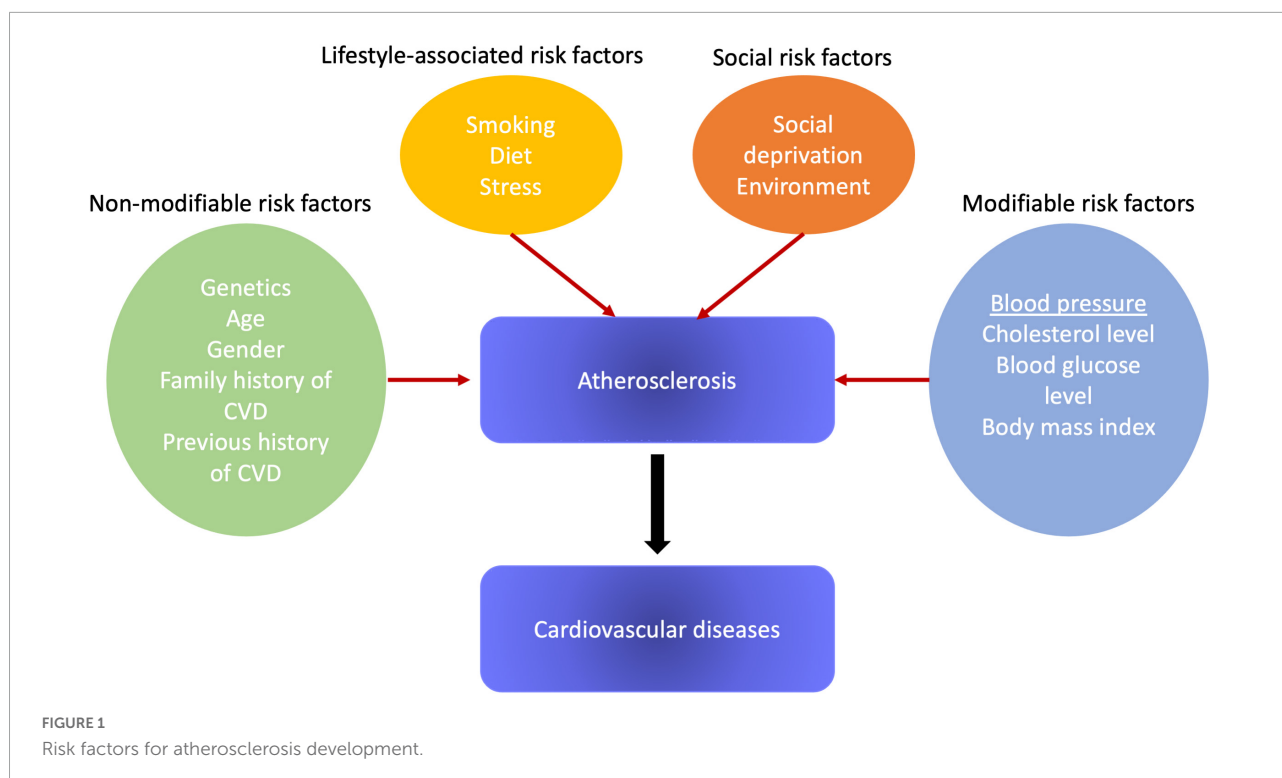
higher in current and former smokers, respectively, compared with non-smokers (13).

Diet-associated risk factors

Controlling lifestyle-related factors, including diet and exercise, is fundamental to preventing atherosclerosis. Atherogenic and hypocaloric diets lead to hypertension, diabetes, dyslipidemia, overweight, and other disorders. Compared with those patients who do not suffer from diabetes, patients with diabetes have hypertension twice as often (14). Diabetes is also one of the most crucial risk factors for determining CAD, so the presence of this pathology is considered a risk factor equivalent to a heart attack, that is, despite the absence of any CV signs, diabetics are classified as "high cardiovascular risk" (15).

The Framingham study reports that high triglyceride levels and low HDL cholesterol lead to an elevated risk of CV. Based on data from the same Framingham study, it was found that obesity is the cause of 26% of cases of hypertension in men and 28% in women, and approximately 23% of cases of CHD in men and 15% in women (16).

However, it should be noted that the traditional Framingham indicator was developed in the 1950s and confirmed in the 1960s and 1970s when the prevalence of overweight and obesity in the United States was 1/3 of the current figure and acute MI was more common among men

(17). Since the 1980s, heart attacks have become increasingly common among women, and obesity has become a key global problem. Therefore, this indicator may underestimate the CV risk in the modern population (18).

Thus, to elevate the positive prognostic value of CAD in the traditional Framingham risk scale, it was proposed to add factors that suggest subclinical atherosclerotic disease, called emerging factors, which include peripheral vascular diseases, thickening of the intima-media wall of the carotid artery, and calcium content in the coronary arteries, which contribute to an elevation in CV levels since they are markers of endothelial damage (19).

Combination of risk factors

Moreover, to assess cardiovascular risk, other factors, such as C-reactive protein and the presence of metabolic syndrome, and traditional risk factors, such as a family history of premature CHD, should be taken into account (20). Also, other risk factors, namely aggravating factors, were also added to the traditional Framingham scale: left ventricular hypertrophy (LVH) *via* electrocardiography, microalbuminuria (30–300 mg/24 h), and CKD (plasma creatinine levels higher than 1.5 mg/dL or creatinine filtration below 60 mL/min) (21). According to this, the presence of one of these factors elevates the risk score to a higher level in contrast to the results that were obtained as a result of applying the traditional Framingham score.

In this regard, there is a question of whether the assessment of CV risk in patients with arterial hypertension will increase the probability of coronary events for 10 years by taking into account aggravating risk factors. Since CVD entails social and economic losses, the study of the alleged coronary risks gives the prospect of applying more appropriate therapeutic measures, thus preventing these events (22). The objective of this study was to assess cardiovascular risk in patients with arterial hypertension using the traditional Framingham risk assessment in comparison with the assessment modified by the inclusion of new risk factors.

Hypertension

In the course of epidemiological studies, arterial hypertension was found to be the most significant modifiable CV risk factor, accounting for 48% of all strokes and 18% of all coronary events. Thus, antihypertensive treatment is still the cornerstone of primary and secondary prevention of CVD. Despite these statistics, only about 40% of patients with arterial hypertension receive medication (antihypertensive agents) and only 1/3 of them are successfully treated for normotension (23). To analyze the effect of antihypertensive drugs on cardiovascular risk, various research schemes were used, the outcomes of which were ambiguous. Population studies have revealed a positive association of antihypertensive agents with coronary artery calcification (CAC) and the progression of CAC. Associations with clinical CV events were less consistent; some studies demonstrated a markedly elevated risk, while in others the risk when taking antihypertensive drugs was not noticed (24). The results of randomized placebo-controlled trials (RCTs) were also ambiguous and depended on the specific outcome under consideration and the characteristics of the patient: gender, race, and the presence of additional CV risk factors (25).

When analyzing the relationship between antihypertensive and cardiovascular risk, it is extremely important to determine whether blood pressure is effectively controlled. Several RCTs have demonstrated that a more active, compared with a less active decrease in blood pressure, leads to a lower risk of stroke and CV events; however, this does not apply to coronary events (26, 27). In the REGARDS (Reasons for Geographic and Racial Differences in Stroke) trial (28), participants with blood pressure lowered to the ideal level still had a higher risk of stroke in contrast to those participants who reached the ideal blood pressure level without resorting to treatment. The same was also observed in Multi-Ethnic Study of Atherosclerosis (MESA) trial (29) for coronary and cardiovascular events. The key difficulty with such drug epidemiology is the indication since the distribution of treatment in epidemiological studies is not randomized, and indications for antihypertensive treatment may be linked with the risk of CVD.

Hypertension in atherosclerosis

Hypertension is likely to affect the arterial tree by thickening artery walls, the development of atherosclerotic plaques, and their vulnerability to rupture. However, there are almost no data on the difference in the impact of a wide range of BP values (normal, high-normal, pre-hypertension, and overt hypertension) on atherosclerosis development. Since 2017, the American Heart Association/American College of Cardiology (AHA/ACC) (30, 31) and the European Society of Cardiology (ESC) (32) have diverged in the definition of hypertension. ESC maintained the previous definition (SBP 140–149 mmHg, DBP 90–99 mmHg) (32) and the AHA/ACC adopted a lower threshold to define hypertension (SBP 130–139 mmHg, DBP 80–89 mmHg) (30). Despite these criteria being inconsistent, both guidelines give advice to control elevated BP by non-pharmacological interventions in the first instance and to start treating with antihypertensive drugs only in case the risk becomes high. The association between BP and cardiovascular events is linear (33), cut-offs are used to categorize BP as optimal, normal, high-normal, or hypertension. Recent studies revealed that the risk associated with high-normal BP is also in charge. Thus, Whelton et al. demonstrated a positive association of a rise in BP with coronary artery calcium prevalence, as well as the incidence of atherosclerosis-linked cardiovascular events using data from the MESA. In those who do not have classical risk factors and whose systolic BP (SBP) < 130 mmHg, the occurrence of atherosclerotic lesions, as well as the risk of incident adverse events increase in step with SBP increases above 90 mmHg (34–36).

The Framingham Heart study demonstrated that high normal blood pressure and hypertension (stage 1, stage 2, and higher) elevate the risk of CHD in both men and women (37). The Japanese urban cohort study (Suita Study) revealed that high normal BP and hypertension of the 1st and 2nd stages or higher lead to an increased risk of MI in men, and that hypertension of stage 2 or higher increases the risk of MI in women (38). We have summarized the data on the effects of blood pressure elevation on cardiovascular outcomes in **Table 1**.

Meta-analysis of individual data for 1 million adults examined in 61 prospective studies revealed that over the entire range of values of normal SBP decreasing to 115 mmHg, the slope of the relationship between mortality from CHD (plotted on a double scale) and normal levels of SBP was approximately constant in each age range, although the relative strength of the association was weaker for CHD than for stroke mortality in middle ages (39). Moreover, for the relationship between mortality from CHD and the usual values of diastolic blood pressure (DBP) decreasing to 75 mmHg, the age-related HRs associated with differences of 10 mmHg in the usual DBP are equivalent to those associated with differences of 20 mmHg in the usual values of SBP (40).

TABLE 1 Effects of various rates of hypertension on cardiovascular outcomes.

Study	Subjects	Hypertension	Effect	References
Framingham heart study	Women	High normal blood pressure	Increased risk of CHD	Garcia et al. (37)
Framingham heart study	Women	Hypertension stage 1	Increased risk of CHD	Garcia et al. (37)
Framingham heart study	Women	Hypertension stage 2	Increased risk of CHD	Garcia et al. (37)
Framingham heart study	Men	High normal blood pressure	Increased risk of CHD	Garcia et al. (37)
Framingham heart study	Men	Hypertension stage 1	Increased risk of CHD	Garcia et al. (37)
Framingham heart study	Men	Hypertension stage 2	Increased risk of CHD	Garcia et al. (37)
Japanese urban cohort study (Suita study)	Men	High normal blood pressure	Increased risk of MI	Park (38)
Japanese urban cohort study (Suita study)	Men	Hypertension stage 1	Increased risk of MI	Park (38)
Japanese urban cohort study (Suita study)	Men	Hypertension stage 2	Increased risk of MI	Park (38)
Japanese urban cohort study (Suita study)	Women	Hypertension stage 2	Increased risk of MI	Park (38)
Meta-analysis by the Japan arteriosclerosis longitudinal study group	Men	Higher SBP, pulse pressure and average blood pressure	Increased risk of MI (1.2 per 1,000 person-years)	Hussain et al. (41), Sobenin et al. (42), Andersson et al. (43)
Meta-analysis by the Japan arteriosclerosis longitudinal study group	Women	Higher SBP, pulse pressure and average blood pressure	Not increased risk of MI (0.5 per 1,000 person-years)	Hussain et al. (41), Sobenin et al. (42), Andersson et al. (43)

The Japan Arteriosclerosis Longitudinal Study Group conducted a meta-analysis of 16 cohort studies, numbering 48,224 Japanese men and women (40–89 years old) at the initial stage and an average of 8.4 years of follow-up (41, 42). A higher SBP, pulse pressure, and average blood pressure led to an increase in the risk of MI in men, but not in women. The incidence of MI was 1.2 and 0.5 per 1,000 person-years in men and women, respectively. Due to the small sample size of women, the relationship between higher blood pressure values and incident MI may not be observed in women (43).

A recent study by Gonzalez-Guerra et al. showed that in the preclinical model of atherosclerosis, the mechanical effect of mild BP increase directly stimulates the progression of atherosclerotic lesions independent of the RAAS pathway activation. This finding is consistent with the hypothesis that not only hypertension, but even non-optimal BP is a risk factor for the progress of atherosclerosis (44).

Several compound classes appeared to have antihypertensive effect. Among such drugs, there are ACE (angiotensin-converting enzyme) inhibitors, calcium-channel blockers, ARB (angiotensin receptor blockers) inhibitors, beta-adrenergic blockers, diuretics (thiazides/thiazide-like diuretics/loop diuretics/potassium-sparing diuretics), vasodilators (hydralazine/minoxidil), and others. However, the use of antihypertensive drugs was sown to improve only blood pressure, but not the CVD risk (45).

Hypertension and total cardiovascular risk

The concept is based on the fact that only a small part of the population with hypertension has an isolated increase in BP,

while the majority have additional cardiovascular risk factors. In addition, the combination of BP and other risk factors can reinforce each other, which results in a total cardiovascular risk that exceeds the sum of its individual components (46). After all, in high-risk individuals, antihypertensive treatment strategies, such as initiation and intensity of treatment, the use of drug combinations, etc., as well as other treatment methods, may differ from those used in lower-risk individuals (47).

In people at high risk, blood pressure control is difficult and requires a more frequent combination of antihypertensive drugs together with other therapy, primarily statin treatment. The therapeutic approach should consider the total CV risk in addition to BP levels to increase the cost-effectiveness of hypertension treatment (48).

Assessment of total cardiovascular risk

It is not difficult to assess the total cardiovascular risk in certain subgroups of patients, for example, in patients with previous CVD, diabetes, CHD, or with highly elevated single risk factors. With all these conditions, the total CV risk is high or extremely high, so there is a need for intensive treatment, which reduces the CV risk (49). Nevertheless, quite a lot of patients with arterial hypertension do not belong to any of these categories, and the identification of patients with low, moderate, high, or very high risk requires the use of models to assess the total cardiovascular risk, which will allow the therapeutic approach to be properly adjusted (50).

To assess the total cardiovascular risk, several computerized methods have been developed. Their meanings and limitations were also considered. The SCORE model was developed

based on large European cohort studies. This model evaluates the risk of death from CV and not only coronary diseases for 10 years, depending on age, gender, smoking habits, total cholesterol, and SBP (51, 52). The SCORE model makes it possible to calibrate graphs for individual countries, which has been done for many European countries. At the international level, two sets of charts are set: one for high-risk countries and one for low-risk countries (53). An electronic interactive version of SCORE—Heart Score[1] also takes into account the effect of LDL cholesterol on total CV risk. The charts and their electronic versions can help in risk assessment and management, but must be interpreted in the light of the clinician's knowledge and experience, especially about local conditions. In addition, the conclusion that the assessment of total cardiovascular risk is associated with improved clinical outcomes compared to other strategies was not sufficiently studied in a randomized trial (54, 55).

The cardiovascular risk may be higher than indicated in the tables in people who have a sedentary lifestyle and in people with central obesity; the high relative risk linked with being overweight is higher in young people than in older people. Socially disadvantaged people and members of certain ethnic minorities may also have a higher risk of CVDs. Individuals with elevated fasting glucose levels and/or an abnormal glucose tolerance test who do not meet the diagnostic criteria for T2D belong to the same category. The same applies to patients with elevated levels of triglycerides, fibrinogen, apolipoprotein B, lipoprotein A, and highly sensitive C-reactive protein. Also, people with a family history of premature CVD under the age of about 60 years may have a high CV risk (56).

In the SCORE model, the total CV risk is expressed as the absolute risk of death from CVD within 10 years. Due to the strong age dependence in young patients, the absolute total CV risk may be low even in the presence of high BP with additional risk factors (57). But with insufficient treatment, this condition can result in an irreversible high-risk condition years later. In younger patients, when choosing a treatment, it is better to follow a quantitative assessment of relative risk or an assessment of the age of the heart. The table of relative risk is available in the Joint European Societies' Guidelines for the prevention of CVD in clinical practice, which is convenient when consulting young people (58, 59).

Additional attention was paid to the detection of asymptomatic organ damage since asymptomatic changes in several organs associated with hypertension indicate a steady development in the continuum of CVD, which significantly increases the risk exceeding the risk caused by the mere presence

of risk factors. Thus, the search for asymptomatic organ damage can be significant whenever evidence of additional risk is discussed (60).

Additional emphasis was placed on the detection of asymptomatic organ damage since hypertension-related asymptomatic changes in the continuum of CVD greatly elevate the risk exceeding the risk caused by the mere presence of risk factors (50).

International guidelines for the management of hypertension like the 1999 and 2003 World Health Organization/International Society of Hypertension guidelines, 2003, 2007, and 2013 European Society of Hypertension/European Society of Cardiology guidelines, and the 2012 European Society of Cardiology prevention guidelines have stratified CV risk in different categories based on BP category, CV risk factors, asymptomatic organ damage, and the presence of diabetes or symptomatic CVD or CKD (61). The classification by low, moderate, high, and very high risk refers to a 10-year increase in mortality from CVD, as defined in the prevention guidelines of the European Society of Cardiology 2012.

Conclusion

Numerous investigations proclaim the association between increased blood pressure and atherosclerosis. The results of these studies are reflected in guidelines and risk assessment scores. However, there is still no definitive data on the effects of various levels of increased BP (mild increase, severe increase, etc.), as well as the causal relationship. Of course, all these factors affect the efficiency of models for assessing cardiovascular risk and thus alter the detection and prevention success (62, 63).

To date, all existing models for assessing cardiovascular risk have limitations that need to be taken into account. The importance of damage to target organs in determining the total risk depends on how scrupulously the damage is assessed based on available facilities. For example, the rationale for assessing total CV risk is to make optimal use of limited resources for the prevention of atherosclerosis and CVD or to evaluate preventive measures in accordance with the elevated risk (64). However, absolute risk stratification is commonly used by private or public health care providers to determine the barrier below which treatment is not recommended. Any threshold for determining a high total CV risk is arbitrary, as is the use of limit values resulting in intensive interventions above this threshold and no actions below. Hypertension is one of the strongest risk factors for almost atherosclerosis, subsequent CVDs, as well as for cardiac events. The difference between high normal BP and hypertension is based on arbitrary limit values, and hypertension is the level at which intervention to lower BP

has preventive benefits, which is confirmed by a number of documents. Atherosclerosis prevention and guidelines for the treatment of moderately elevated BP should be associated with a quantitative assessment of the total CV risk (65–67).

Author contributions

AP: writing—original draft preparation. NS, AK, EB, AM, AG, and AO: writing—review and editing. All authors contributed to the article and approved the submitted version.

Funding

Conflict of interest

The authors declare that the research was conducted in the absence of any commercial or financial relationships that could be construed as a potential conflict of interest.

The reviewer AM declared a shared affiliation with the authors EB and AG to the handling editor at the time of review.

Publisher's note

All claims expressed in this article are solely those of the authors and do not necessarily represent those of their affiliated organizations, or those of the publisher, the editors and the reviewers. Any product that may be evaluated in this article, or claim that may be made by its manufacturer, is not guaranteed or endorsed by the publisher.

References

1. Libby P. The changing landscape of atherosclerosis. *Nature.* (2021) 592:524–33. doi: 10.1038/s41586-021-03392-8

2. Virani SS, Alonso A, Aparicio HJ, Benjamin EJ, Bittencourt MS, Callaway CW, et al. American heart association council on epidemiology and prevention statistics committee and stroke statistics subcommittee. heart disease and stroke statistics-2021 update: a report from the american heart association. *Circulation.* (2021) 23:e254–743. doi: 10.1161/CIR.0000000000000950

3. Mc Namara K, Alzubaidi H, Jackson JK. Cardiovascular disease as a leading cause of death: how are pharmacists getting involved? *Integr Pharm Res Pract.* (2019) 8:1–11. doi: 10.2147/IPRP.S133088

4. Gallucci G, Tartarone A, Lerose R, Lalinga AV, Capobianco AM. Cardiovascular risk of smoking and benefits of smoking cessation. *J Thoracic Dis.* (2020) 12:3866–76. doi: 10.21037/jtd.2020.02.47

5. Francula-Zaninovic S, Nola IA. Management of measurable variable cardiovascular disease' risk factors. *Curr Cardiol Rev.* (2018) 14:153–63. doi: 10.2174/1573403X14666180222102312

6. Stewart J, Manmathan G, Wilkinson P. Primary prevention of cardiovascular disease: a review of contemporary guidance and literature. *JRSM Cardiovasc Dis.* (2017) 6:2048004016687211. doi: 10.1177/2048004016687211

7. Bhatnagar A. Environmental determinants of cardiovascular disease. *Circ Res.* (2017) 121:162–80. doi: 10.1161/CIRCRESAHA.117.306458

8. Babu RB, Alam M, Helis E, Fodor JG. Population-based versus high-risk strategies for the prevention of cardiovascular diseases in low- and middle-income countries. *Indian Heart J.* (2012) 64:439–43. doi: 10.1016/j.ihj.2012.08.001

9. Karunathilake SP, Ganegoda GU. Secondary prevention of cardiovascular diseases and application of technology for early diagnosis. *BioMed Res Int.* (2018) 2018:5767864. doi: 10.1155/2018/5767864

10. Institute of Medicine (Us) Committee on Assuring the Health of the Public in the 21st Century. *The Future of the Public's Health in the 21st Century*. Washington (DC): National Academies Press (2002).

11. Feigin VL, Brainin M, Norrving B, Gorelick PB, Dichgans M, Wang W, et al. What Is the best mix of population-wide and high-risk targeted strategies of primary stroke and cardiovascular disease prevention? *J Am Heart Assoc.* (2020) 9:e014494. doi: 10.1161/JAHA.119.014494

12. Visseren F, Mach F, Smulders YM, Carballo D, Koskinas KC, Bäck M, et al. 2021 ESC Guidelines on cardiovascular disease prevention in clinical practice. *Eur Heart J.* (2021) 42:3227–337. doi: 10.1093/eurheartj/ehab484

13. Fuchs FD, Whelton PK. High Blood Pressure and Cardiovascular Disease. *Hypertension.* (2020) 75:285–92. doi: 10.1161/HYPERTENSIONAHA.119.14240

14. Saiz LC, Gorricho J, Garjón J, Celaya MC, Erviti J, Leache L. Blood pressure targets for the treatment of people with hypertension and cardiovascular disease. *Cochrane Database Syst Rev.* (2018) 7:CD010315. doi: 10.1002/14651858.CD010315.pub3

15. Park JH, Moon JH, Kim HJ, Kong MH, Oh YH. Sedentary lifestyle: overview of updated evidence of potential health risks. *Korean J Fam Med.* (2020) 41:365–73. doi: 10.4082/kjfm.20.0165

16. Mansur A, Favarato D. Trends in mortality rate from cardiovascular disease in brazil, 1980-2012. *Arquivos Bras cardiol.* (2016) 107:20–5. doi: 10.5935/abc.20160077

17. Martins SM. Death from cancer and cardiovascular disease between two Brazils. *Arquivos Bras Cardiol.* (2020) 114:207–8. doi: 10.36660/abc.20200017

18. Mahmood SS, Levy D, Vasan RS, Wang TJ. The framingham heart study and the epidemiology of cardiovascular disease: a historical perspective. *Lancet.* (2014) 383:999–1008. doi: 10.1016/S0140-6736(13)61752-3

19. Nilsen A, Hanssen TA, Lappegård KT, Eggen AE, Løchen ML, Selmer RM, et al. Change in cardiovascular risk assessment tool and updated Norwegian guidelines for cardiovascular disease in primary prevention increase the population proportion at risk: the Tromsø Study 2015-2016. *Open Heart* (2021) 8:e001777. doi: 10.1136/openhrt-2021-001777

20. Brown JC, Gerhardt TE, Kwon E. *Risk Factors For Coronary Artery Disease*. Treasure Island,FL: StatPearls Publishing (2022).

21. Blood Pressure Lowering Treatment Trialists' Collaboration. Age-stratified and blood-pressure-stratified effects of blood-pressure-lowering pharmacotherapy for the prevention of cardiovascular disease and death: an individual participant-level data meta-analysis. *Lancet.* (2021) 398:1053–64. doi: 10.1016/S0140-6736(21)01921-8

22. Jo W, Lee S, Joo YS, Nam KH, Yun HR, Chang TI, et al. Association of smoking with incident CKD risk in the general population: A community-based cohort study. *PLoS One.* (2020) 15:e0238111. doi: 10.1371/journal.pone.0238111

23. Newman JD, Schwartzbard AZ, Weintraub HS, Goldberg IJ, Berger JS. Primary prevention of cardiovascular disease in diabetes mellitus. *J Am College Cardiol.* (2017) 70:883–93. doi: 10.1016/j.jacc.2017.07.001

24. Gulsin GS, Athithan L, McCann GP. Diabetic cardiomyopathy: prevalence, determinants and potential treatments. *Therapeut Adv Endocrinol Metab.* (2019) 10:2042018819834869. doi: 10.1177/2042018819834869

25. Félix-Redondo FJ, Grau M, Fernández-Bergés D. Cholesterol and cardiovascular disease in the elderly. Facts and gaps. *Aging Dis.* (2013) 4:154–69.

26. Powell-Wiley TM, Poirier P, Burke LE, Després JP, Gordon-Larsen P, Lavie CJ, et al. Obesity and cardiovascular disease: a scientific statement from the

american heart association. *Circulation.* (2021) 143:e984–1010. doi: 10.1161/CIR. 0000000000000973

27. Sobenin IA, Sazonova MA, Postnov AY, Bobryshev YV, Orekhov AN. Changes of mitochondria in atherosclerosis: possible determinant in the pathogenesis of the disease. *Atherosclerosis.* (2013) 227:283–8. doi: 10.1016/j. atherosclerosis.2013.01.006

28. Woodward M. Cardiovascular disease and the female disadvantage. *Int J Environ Res Public Health.* (2019) 16:1165. doi: 10.3390/ijerph16071165

29. Perez HA, Garcia NH, Spence JD, Armando LJ. Adding carotid total plaque area to the Framingham risk score improves cardiovascular risk classification. *Arch Med Sci AMS.* (2016) 12:513–20. doi: 10.5114/aoms.2016.59924

30. Wong ND. Cardiovascular risk assessment: the foundation of preventive cardiology. *Am J Prev Cardiol.* (2020) 1:100008. doi: 10.1016/j.ajpc.2020.100008

31. Sobenin IA, Sazonova MA, Postnov AY, Bobryshev YV, Orekhov AN. Mitochondrial mutations are associated with atherosclerotic lesions in the human aorta. *Clin Dev Immunol.* (2012) 2012:832464. doi: 10.1155/2012/832464

32. Tanaka F, Komi R, Nakamura M, Tanno K, Onoda T, Ohsawa M, et al. Additional prognostic value of electrocardiographic left ventricular hypertrophy in traditional cardiovascular risk assessments in chronic kidney disease. *J Hypertension.* (2020) 38:1149–57. doi: 10.1097/HJH.0000000000002394

33. Mensah GA, Roth GA, Fuster V. The global burden of cardiovascular diseases and risk factors: 2020 and beyond. *J Am College Cardiol.* (2019) 74:2529–32. doi: 10.1016/j.jacc.2019.10.009

34. Guerrero-García C, Rubio-Guerra AF. Combination therapy in the treatment of hypertension. *Drugs Context.* (2018) 7:212531. doi: 10.7573/dic.212531

35. Chistiakov DA, Orekhov AN, Sobenin IA, Bobryshev YV. Plasmacytoid dendritic cells: development, functions, and role in atherosclerotic inflammation. *Front Physiol.* (2014) 5:279. doi: 10.3389/fphys.2014.00279

36. Gronewold J, Kropp R, Lehmann N, Stang A, Mahabadi AA, Kälsch H, et al. Cardiovascular risk and atherosclerosis progression in hypertensive persons treated to blood pressure targets. *Hypertension.* (2019) 74:1436–47. doi: 10.1161/ HYPERTENSIONAHA.119.13827

37. Garcia M, Mulvagh SL, Merz CN, Buring JE, Manson JE. Cardiovascular disease in women: clinical perspectives. *Circ Res.* (2016) 118:1273–93. doi: 10.1161/ CIRCRESAHA.116.307547

38. Park S. Ideal Target Blood Pressure in Hypertension. *Korean Circ J.* (2019) 49:1002–9. doi: 10.4070/kcj.2019.0261

39. Akinyelure OP, Jaeger BC, Moore TL, Hubbard D, Oparil S, Howard VJ, et al. Racial differences in blood pressure control following stroke: the regards study. *Stroke.* (2021) 52:3944–52. doi: 10.1161/STROKEAHA.120.033108

40. Blaha MJ, DeFilippis AP. Multi-Ethnic Study of Atherosclerosis (MESA): JACC Focus Seminar 5/8. *J Am College Cardiol.* (2021) 77:3195–216. doi: 10.1016/j. jacc.2021.05.006

41. Hussain MA, Al Mamun A, Peters SA, Woodward M, Huxley RR. The burden of cardiovascular disease attributable to major modifiable risk factors in Indonesia. *J Epidemiol.* (2016) 26:515–21. doi: 10.2188/jea.JE20150178

42. Sobenin IA, Salonen JT, Zhelankin AV, Melnichenko AA, Kaikkonen J, Bobryshev YV, et al. Low density lipoprotein-containing circulating immune complexes: role in atherosclerosis and diagnostic value. *Biomed Res Int.* (2014) 2014:205697. doi: 10.1155/2014/205697

43. Andersson C, Nayor M, Tsao CW, Levy D, Vasan RS. Framingham Heart Study: JACC focus seminar, 1/8. *J Am College Cardiol.* (2021) 77:2680–92. doi: 10.1016/j.jacc.2021.01.059

44. Ogata S, Watanabe M, Kokubo Y, Higashiyama A, Nakao YM, Takegami M, et al. Longitudinal trajectories of fasting plasma glucose and risks of cardiovascular diseases in middle age to elderly people within the general japanese population: the suita study. *J Am Heart Assoc.* (2019) 8:e010628. doi: 10.1161/JAHA.118.010628

45. Liu K, Colangelo LA, Daviglus ML, Goff DC, Pletcher M, Schreiner PJ, et al. Can antihypertensive treatment restore the risk of cardiovascular disease to ideal levels?: the coronary artery risk development in young adults (CARDIA) study and the multi-ethnic study of atherosclerosis (MESA). *J Am Heart Assoc.* (2015) 4:e002275. doi: 10.1161/JAHA.115.002275

46. Bundy JD, Li C, Stuchlik P, Bu X, Kelly TN, Mills KT, et al. Systolic blood pressure reduction and risk of cardiovascular disease and mortality: a systematic review and network meta-analysis. *JAMA Cardiol.* (2017) 2:775–81. doi: 10.1001/ jamacardio.2017.1421

47. Rapsomaniki E, Timmis A, George J, Pujades-Rodriguez M, Shah AD, Denaxas S, et al. Blood pressure and incidence of twelve cardiovascular diseases: lifetime risks, healthy life-years lost, and age-specific associations in 125 million people. *Lancet.* (2014) 383:1899–911. doi: 10.1016/S0140-6736(14) 60685-1

48. Harada A, Ueshima H, Kinoshita Y, Miura K, Ohkubo T, Asayama K, et al. Absolute risk score for stroke, myocardial infarction, and all cardiovascular disease: Japan Arteriosclerosis Longitudinal Study. *Hypertension Res.* (2019) 42:567–79. doi: 10.1038/s41440-019-0220-z

49. Al-Shamsi S, Regmi D, Govender RD. Incidence of cardiovascular disease and its associated risk factors in at-risk men and women in the United Arab Emirates: a 9-year retrospective cohort study. *BMC Cardiovasc Disord.* (2019) 19:148. doi: 10.1186/s12872-019-1131-2

50. Piepoli MF, Hoes AW, Agewall S, Albus C, Brotons C, Catapano AL, et al. 2016 European guidelines on cardiovascular disease prevention in clinical practice: the sixth joint task force of the european society of cardiology and other societies on cardiovascular disease prevention in clinical practice (constituted by representatives of 10 societies and by invited experts) developed with the special contribution of the european association for cardiovascular prevention & rehabilitation (EACPR). *Eur Heart J.* (2016) 37:2315–81. doi: 10.1093/eurheartj/ ehw106

51. Muntner P, Whelton PK. Using predicted cardiovascular disease risk in conjunction with blood pressure to guide antihypertensive medication treatment. *J Am College Cardiol.* (2017) 69:2446–56. doi: 10.1016/j.jacc.2017.02.066

52. Chistiakov DA, Sobenin IA, Orekhov AN, Bobryshev YV. Myeloid dendritic cells: development, functions, and role in atherosclerotic inflammation. *Immunobiology.* (2015) 220:833–44. doi: 10.1016/j.imbio.2014.12.010

53. Marinier K, Macouillard P, de Champvallins M, Deltour N, Poulter N, Mancia G. Effectiveness of two-drug therapy versus monotherapy as initial regimen in hypertension: A propensity score-matched cohort study in the UK Clinical Practice Research Datalink. *Pharmacoepidemiol Drug Safe.* (2019) 28:1572–82. doi: 10.1002/ pds.4884

54. Williams B, Masi S, Wolf J, Schmieder RE. Facing the challenge of lowering blood pressure and cholesterol in the same patient: report of a symposium at the european society of hypertension. *Cardiol Therapy.* (2020) 9:19–34. doi: 10.1007/ s40119-019-00159-1

55. Chistiakov DA, Revin VV, Sobenin IA, Orekhov AN, Bobryshev YV. Vascular endothelium: functioning in norm, changes in atherosclerosis and current dietary approaches to improve endothelial function. *Mini Rev Med Chem.* (2015) 15:338– 50. doi: 10.2174/1389557515666150226114031

56. Leon BM, Maddox TM. Diabetes and cardiovascular disease: Epidemiology, biological mechanisms, treatment recommendations and future research. *World J Diabetes.* (2015) 6:1246–58. doi: 10.4239/wjd.v6.i13.1246

57. Lloyd-Jones DM, Braun LT, Ndumele CE, Smith SC Jr, Sperling LS, Virani SS, et al. Use of risk assessment tools to guide decision-making in the primary prevention of atherosclerotic cardiovascular disease: A special report from the american heart association and american college of cardiology. *J Am Coll Cardiol.* (2019) 73:3153–67. doi: 10.1016/j.jacc.2018.11.005

58. Payne RA. Cardiovascular risk. *Br J Clin Pharmacol.* (2012) 74:396–410. doi: 10.1111/j.1365-2125.2012.04219.x

59. Myasoedova VA, Kirichenko TV, Melnichenko AA, Orekhova VA, Ravani A, Poggio P, et al. Anti-atherosclerotic effects of a phytoestrogen-rich herbal preparation in postmenopausal women. *Int J Mol Sci.* (2016) 17:1318. doi: 10.3390/ ijms17081318

60. Puddu PE, Piras P, Kromhout D, Tolonen H, Kafatos A, Menotti A. Re-calibration of coronary risk prediction: an example of the Seven Countries Study. *Sci Rep.* (2017) 7:17552. doi: 10.1038/s41598-017-17784-2

61. Boateng GO, Adams EA, Odei Boateng M, Luginaah IN, Taabazuing MM. Obesity and the burden of health risks among the elderly in Ghana: a population study. *PLoS One.* (2017) 12:e0186947. doi: 10.1371/journal.pone.0186947

62. Lloyd-Jones DM. Cardiovascular risk prediction: basic concepts, current status, and future directions. *Circulation.* (2010) 121:1768–77. doi: 10.1161/ CIRCULATIONAHA.109.849166

63. Summerhill VI, Grechko AV, Yet SF, Sobenin IA, Orekhov AN. The atherogenic role of circulating modified lipids in atherosclerosis. *Int J Mol Sci.* (2019) 20:3561. doi: 10.3390/ijms20143561

64. Greenland P, Blaha MJ, Budoff MJ, Erbel R, Watson KE. Coronary calcium score and cardiovascular risk. *J Am College Cardiol.* (2018) 72:434–47. doi: 10.1016/ j.jacc.2018.05.027

65. Prakash D. Target organ damage in newly detected hypertensive patients. *J Fam Med Primary Care.* (2019) 8:2042–6. doi: 10.4103/jfmpc.jfmpc_231_19

66. Haan YC, Diemer FS, Van Der Woude L, Van Montfrans GA, Oehlers GP, Brewster LM. The risk of hypertension and cardiovascular disease in women with uterine fibroids. *J Clin Hypertension.* (2018) 20:718–26. doi: 10.1111/jch.13253

67. Unger T, Borghi C, Charchar F, Khan NA, Poulter NR, Prabhakaran D, et al. 2020 International society of hypertension global hypertension practice guidelines. *Hypertension.* (2020) 75:1334–57. doi: 10.1161/HYPERTENSIONAHA.120.15026

frontiers | Frontiers in Cardiovascular Medicine

Relevance of lipoproteins, membranes, and extracellular vesicles in understanding C-reactive protein biochemical structure and biological activities

Lawrence A. Potempa[1]*, Wei Qiao Qiu[2,3,4], Ashley Stefanski[1] and Ibraheem M. Rajab[1]

[1]College of Science, Health and Pharmacy, Roosevelt University Schaumburg, Schaumburg, IL, United States, [2]Department of Pharmacology and Experimental Therapeutics, Boston University School of Medicine, Boston, MA, United States, [3]Alzheimer's Disease Center, Boston University School of Medicine, Boston, MA, United States, [4]Department of Psychiatry, Boston University School of Medicine, Boston, MA, United States

Early purification protocols for C-reactive protein (CRP) often involved co-isolation of lipoproteins, primarily very low-density lipoproteins (VLDLs). The interaction with lipid particles was initially attributed to CRP's calcium-dependent binding affinity for its primary ligand—phosphocholine—the predominant hydrophilic head group expressed on phospholipids of most lipoprotein particles. Later, CRP was shown to additionally express binding affinity for apolipoprotein B (apo B), a predominant apolipoprotein of both VLDL and LDL particles. Apo B interaction with CRP was shown to be mediated by a cationic peptide sequence in apo B. Optimal apo B binding required CRP to be surface immobilized or aggregated, treatments now known to structurally change CRP from its serum soluble pentamer isoform (i.e., pCRP) into its poorly soluble, modified, monomeric isoform (i.e., mCRP). Other cationic ligands have been described for CRP which affect complement activation, histone bioactivities, and interactions with membranes. mCRP, but not pCRP, binds cholesterol and activates signaling pathways that activate pro-inflammatory bioactivities long associated with CRP as a biomarker. Hence, a key step to express CRP's biofunctions is its conversion into its mCRP isoform. Conversion occurs when (1) pCRP binds to a membrane surface expressed ligand (often phosphocholine); (2) biochemical forces associated with binding cause relaxation/partial dissociation of secondary and tertiary structures into a swollen membrane bound intermediate (described as $mCRP_m$ or pCRP*); (3) further structural relaxation which leads to total, irreversible dissociation of the pentamer into mCRP and expression of a cholesterol/multi-ligand binding sequence that extends into the subunit core; (4) reduction of the CRP subunit intrachain disulfide bond which enhances CRP's binding accessibility for various ligands and activates

acute phase proinflammatory responses. Taken together, the biofunctions of CRP involve both lipid and protein interactions and a conformational rearrangement of higher order structure that affects its role as a mediator of inflammatory responses.

Discovery and isolation protocols for C-reactive protein from body fluids

This review is focused on the relevance of lipids and lipoproteins to the structures, functions, and bioactivities of C-reactive protein (CRP). From its discovery eighty years ago, CRP has been described as existing in serum in more than one form, with at least one such form having some association with apo B-containing lipoproteins. While more recent studies have primarily focused only on the lipid-free, highly defined serum soluble pentameric protein, the role of lipids in affecting CRP biochemical and immunological characteristics need renewed and updated consideration.

Purification focused on precipitation methods

A detailed compendium of CRP purification methods and procedures from its discovery in 1941 to current times is presented in the **Supplementary material** and is summarized in this manuscript as **Supplementary Table 1**. Of key relevance, apo B containing lipoproteins often co-isolate with CRP, which appears in serum in multiple forms with different electrophoretic mobilities. As described, lipids were often removed from source fluids to facilitate affinity isolation procedures and remove contaminating proteins. The biophysical attributes of highly purified CRP described it as a non-glycosylated, non-covalently associated, homo-pentameric

---

Abbreviations: pCRP, pentameric C-reactive protein; mCRP, monomeric, modified C-reactive protein; VLDL, very low density lipoproteins; LDL, low density lipoproteins; LDL-R, LDL receptor; apo B, apolipoprotein B; apo E, apolipoprotein E; CPS, C-polysaccharide fraction of pneumococcal cell walls; PC, phosphocholine; PtC, phosphatidyl choline; PtS, phosphatidyl serine; DEAE, diethylaminoethyl; GuHCl, guanidinium hydrochloride; mCRP$_m$, membrane-associated modified CRP (an intermediate structure retaining pentameric orientation while also expressing mCRP-antigenicity); pCRP*, a partially changed pentameric CRP structure that expresses some mCRP-specific properties; CBP, cholesterol binding peptide sequence of CRP.

globular protein with each subunit having a calcium-regulated primary binding affinity for phosphocholine (PC) ligand.

Elaborating on C-reactive protein binding interaction for lipid-associated phosphocholine ligand

Using PC groups immobilized on agarose resin and celite-delipidated ascites fluids spiked with 2 mM calcium and adjusted to pH 8.5, Volanakis et al. (1) found complement proteins C3, C4, C1-INH and C1s co-eluting with CRP, as well as IgG and plasminogen. In studying how isolated CRP could bind membrane-associated phosphocholine, Volanakis and Wirtz (2) proved that only PC groups exposed away from the planar membrane surface were suitable ligands. A natural mechanism to expose such groups occurs when membrane lipids are de-esterified into mono-acyl structures (i.e., lysolecithin) by the action of Phospholipase A2 (PLA2). Lysolecithin adds to membrane curvature and has detergent-like properties, exposing not only PC groups, but apolar regions associated with fatty acyl chain packing. The PLA2 hydrolyzed fatty acid is often arachidonic acid, which enters eicosanoid activation pathways. By exposing PC groups, increasing membrane curvature, and releasing arachidonic acid, PLA2 is a known activator of acute-phase inflammatory processes. The biological responses activated by PLA2 include binding and activating CRP. Quantification of PLA2 in serum has diagnostic value. Compounds that selectively inhibit this enzyme are targets of anti-inflammatory drug development (3, 4).

Besides enzymatic removal of a fatty acyl chain on a phospholipid, PC group exposure and increased membrane surface curvature occur when fatty acyl chains are shortened by oxidative processes as might occur by the action of reactive oxygen species. CRP does bind to oxidatively shortened acyl chain-modified lipid structures (5).

Deacylated or acyl-chain shortened lipids result in increased membrane curvature which plays a role in CRP binding. This concept affects CRP binding not only to plasma membranes, but

to its interactions with lipoproteins, which can vary greatly in size and curvature. While each CRP subunit binds a PC ligand as a function of calcium with a weak to modest dissociation value (K_d = 2–18 μM) (6–9), redundant and simultaneous binding of connected binding sites in the pentameric protein provide additional avidity to elicit biological activation energies sufficient to regulate certain CRP bioactivities. The primary force affecting zwitterionic PC group binding to CRP is the negatively charged phosphate group. This realization led to identifying other structures containing phosphate monoesters (i.e., nucleotides, DNA, RNA, and chromatin) as alternative binding ligands for CRP (10, 11). The positively charged choline group of PC does contribute ∼10-fold increased binding affinity for CRP. A closer examination of cationic molecules as ligands for CRP is included below.

How apolar lipid regions interact with and affect C-reactive protein structure

When pCRP binds to the surface of an activated plasma membrane, different biochemical forces loosen both electrostatic and hydrophobic interactions holding the pentamer together. Initially, the pentamer swells into an intermediate conformation referred to as $mCRP_m$ (membrane-associated mCRP), or pCRP*. When sufficient external bonding energy is added, pCRP subunits "flip" to assume a new protein structural energy equilibrium which includes enhanced interactions with apolar lipids zones and lipid raft-directed cholesterol binding (4, 12–14). The membrane-bound form of mCRP has strong pro-inflammatory activation bioactivities which include leukocyte activation and cellular damage (15, 16).

The cholesterol-binding peptide of the CRP subunit is localized to residues 35–47 of the 206 amino acid subunit primary sequence (i.e., the CBP). Exposure of this cholesterol binding cleft extends from the periphery of the subunit surface deep into the subunit interior involving the sole disulfide-linked bond found in the interior of each globular CRP subunit (linking residues C_{36} and C_{97}). Of relevance, optimal cholesterol binding to the exposed cleft occurs after reduction of this intrachain disulfide bond, suggesting an added level of regulation is needed to release the full potential of CRP's pro-inflammatory activities (17). A synthetic peptide of CBP (i.e., V_{35}CLHFYTELSSTR$_{47}$) not only inhibited mCRP binding to cholesterol, but its binding to C1q, fibronectin, collagen IV, fibrinogen, apolipoprotein B, and lipoprotein particles (18). The CBP is not associated with the PC binding pocket of each CRP subunit but includes residues ($_{40}$YTE$_{42}$) which contribute to the non-covalent inter-subunit stabilization of the pentamer (19). Exposure of CBP to allow CRP to bind cholesterol and its other defined ligands would require subunit dissociation. In addition to residues

$_{40}$YTE$_{42}$, Li et al. (18) identified the $_{36}$CLH$_{38}$ tripeptide as the most important in regulating diverse CRP binding activities. The fact that this reactive sequence includes cysteine, which forms an intra-chain disulfide bond with C_{97} located deep within the globular subunit in the compacted structure, also underscores the importance of subunit dissociation and conformational change to express the bioactivities inherent in the CRP molecule. The fact that reducing the disulfide bond, which relaxes protein tertiary constraints manifest by covalent bonding, will maximally elicit CRP activities, is consistent with significant conformational change as a driving factor for expressing CRP biofunction(s).

Mackiewicz et al. (20), using transmission electron microscopy, showed CRP causes a structural clustering of lipids in nanoparticles and could aggregate LDLs. The initial CRP interaction with lipid particles was calcium-dependent and reversible, but over time, the interaction became permanent and correlated with lipid reorganization. These observations are consistent with a lipid-mediated conversion of pCRP into mCRP.

The nature of CRP's interaction with lipid was examined using surface tension techniques and various lipid monolayer constructs. While PC-containing lipids could bind pCRP, only mCRP directly inserted into physiologically relevant monolayers that included cholesterol-rich lipid rafts (12, 14). Insertion was dependent on cholesterol content and was mediated by two peptide sequences in CRP, one defined by the CBP described above (i.e., residues 35–47), and one defined by the C-terminal octapeptide (i.e., residues 199–206). This latter sequence localizes to the inter-subunit contact areas that stabilize pentameric CRP and only becomes exposed when pCRP dissociates into mCRP. The octapeptide maps to the unique antigenic epitope expressed on mCRP and the partially dissociated $mCRP_m$, but not on pCRP (21) (**Figures 1**, **2**).

Lipoproteins and C-reactive protein

The relevance of lipids to CRP synthesis pathways was described by Kushner and Feldman (22) when liver was identified as the main site of synthesis. Prior to release from hepatocytes into circulation, synthesized CRP was found sequestered in intracellular vesicles that also contained apo B-containing Very Low-Density Lipoproteins (VLDLs), underscoring CRP's association with lipids begins with post-translational processing and secretion during the early moments of a stimulated acute phase response.

The direct interaction of CRP with lipoprotein particles was described by Saxena et al. (23) using an affinity adsorbent with immobilized rat CRP. Lipoprotein fractions prepared by ultracentrifugation from outdated human blood were passed across this resin and VLDLs carrying apolipoprotein B and
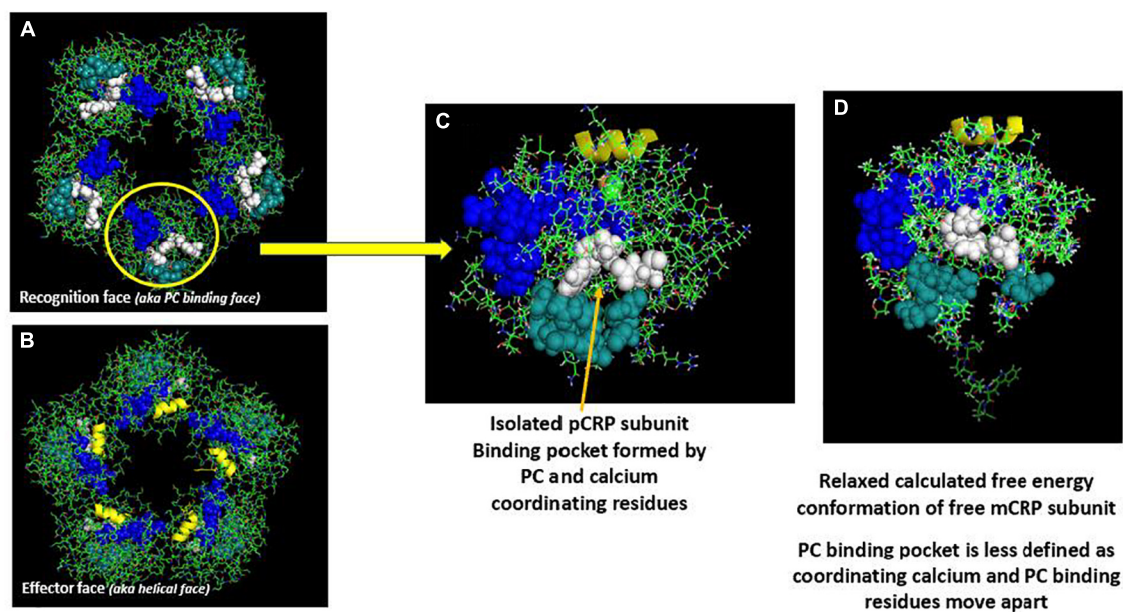
FIGURE 1

Orientation of calcium-dependent—phosphocholine binding sites and the multi-reactive cholesterol binding peptide (CBP) on serum soluble pentameric CRP (pCRP) and a calculated low energy predictive free CRP subunit (mCRP). **(A)** pCRP (PDB: B109) Recognition face (aka: PC-binding face). **(B)** pCRP flipped 180° to show the Effector face (aka: helical face; helix shown in yellow). Key residues involved in PC binding to CRP subunits: F66, S74, E81, Q150 (Shown in white); Key residues involved in Calcium binding to CRP subunits (2/subunit): D60, N61, E138, Q139, D140, E147, Q150 (shown in dark teal); Defined Cholesterol binding peptide sequence (CBP) on CRP subunits (Residues 35–47: V35CLHFYTELSSTR47 (shown in blue). Note all Calcium and PC binding sites orient on the same face of pCRP such that, when pCRP binds PC, it sits flat on the PC-presenting surface. Key residues in CRP identified in Ji et al. and Pathak and Agrawal (14, 106). **(C)** Isolated pCRP subunit looking down on the PC binding recognition face. Depicted residues are the same as defined in panels **(A,B)**. **(D)** Predicted low free energy structure of the free CRP subunit based solely on its primary protein sequence as described in Xu (42). Note both PC and calcium binding residues rotate away such that the defined binding pocket is altered. Also note the extended peptide sequence shown below the core globular structure. This peptide corresponds to C-terminal residues of CRP (i.e., residues 198–206) that contribute to inter-subunit stabilization in pentameric CRP. A major shift in the orientation of these residues occurs when pCRP subunits dissociate. Of relevance, these residues map to a unique mCRP epitope not expressed in pCRP (21, 107).

apolipoprotein E, and LDLs carrying apolipoprotein B bound the immobilized protein. When unfractionated plasma was used as the source of lipoproteins, similar binding of apo E and apo B lipoproteins were observed, albeit binding of LDLs was much reduced. Binding required calcium and lipoproteins could be eluted using phosphocholine hapten suggesting lipoprotein binding to (rat) CRP involves exposed PC groups. Unlike human CRP, rat CRP is a glycoprotein. Removing sialic acid residues did not affect lipoprotein binding (24). Rat CRP was later shown to also bind apo A1 (HDL) lipoproteins containing cholesterol (25).

In direct LDL binding studies using human CRP, mCRP but not pCRP bound LDL in a calcium independent manner. Binding occurred not only with normal LDLs, but with LDLs oxidized with copper sulfate, and to LDLs both directly adsorbed to, or captured onto a solid phase surface. When purified apo B was used as the binding ligand, both mCRP and pCRP bound, with mCRP exhibiting stronger binding. Binding was inhibited by fluid phase apo B, and by a pentadeca peptide fragment (15-mer) derived from apo B and containing the cationic nonapeptide sequence mediating apo B binding to the LDL-receptor (i.e., apo B sequence #3358-3372 T$_{3358}$**RLT**R**KR**G**LK**LATAL$_{3372}$) (26). The calculated inhibition constant of the pentadecameric peptide was more than 800-fold stronger than that of intact apo B protein and was not influenced by calcium (12). These data show both pCRP and mCRP bind cationic ligands in a way distinct from how calcium regulates CRP binding to phosphocholine ligands.

As the cationic sequence in apo B effecting both CRP and LDL-R binding contains both arginine residues (3) and lysine residues (2), site-directed group modification studies were performed to examine which cationic groups were primarily responsible for interactions with CRP. Modifying apo B lysine residues using aceto-acetylation had no effect, but modifying apo B arginine residues with 1,2, cyclohexanedione reduced binding to rat CRP by ~70% (25). These data, along with studies of human CRP and rabbit CRP (27–31), indicate CRP has a selectively stronger binding affinity for arginine-containing ligands than lysine-containing ligands (32, 33).
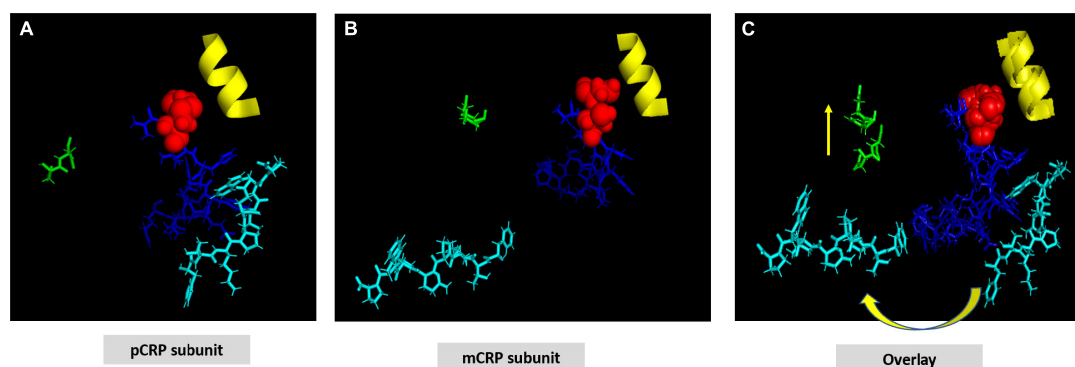
FIGURE 2

Structural shift of selected residues comparing pCRP subunit and mCRP subunit. **(A)** Shows a pCRP subunit with disulfide bond (C36-C97) shown as red spheres; CRP effector face helix (residues P168-L176) shown in yellow; the cholesterol/multi-ligand binding sequence (CBP: V35-R47) shown in blue; calcium binding residues (D60-N61) shown in green; and the C-terminal octapeptide (F198-P206), which contains residues involved in the inter-subunit contact zone of pCRP pentameric structure shown in cyan. All other residues on the pCRP subunit are hidden to facilitate visualization of the orientation of these described residues. **(B)** Shows these same residues oriented in an mCRP subunit model calculated using low free energy structural algorithms of the CRP primary sequence. **(C)** Overlay of pCRP and mCRP oriented to best overlap the disulfide bond and effector face helix. Note the reorientation of highlighted calcium binding residues and the significant rotation of the inter-subunit contact residues away from the CPB peptide. Shifting the calcium binding residues would affect its stabilizing role in maintaining pCRP's quaternary structure and in regulating CRP's binding to phosphocholine ligand. These changes lead to the large rotation of the inter-subunit contact residues allowing ligand access to CPB. Note that the C-terminal octapeptide maps to a unique epitope expressed on mCRP and not pCRP. The structural changes shown here are consistent with increased aqueous exposure of these residues allowing for specific antibody binding.

Other binding interactions of C-reactive protein with cationic ligands

The complement protein C1q, cationic protein with a pI of 9.3, often co-isolates with CRP. It directly binds CRP on the effector face of the pentameric disc (i.e., the opposite face from the PC-binding recognition face) (16) and mediates activation of the classical complement pathway. CRP also binds polycations such as poly-arginine, poly-lysine, and protamine, and positively charged liposomes (33–37) in a way that affects CRP's effects on both classical and alternative complement pathways (35, 36, 38). While initial CRP-complement studies interpreted CRP's activities as a protein of rigid structure forming immune-complex-like aggregates that regulate its bioactivities, the more recent awareness and understanding of its distinctive structural isoforms has led to the understanding that the capacity of CRP to bind cationic ligands and complement proteins is enhanced when CRP is in its modified conformation (mCRP) (12, 15, 39, 40).

Salt bridges and peptide sequences involved in C-reactive protein structural packing

The CRP pentamer associates non-covalently into its discoid structure using electrostatic, apolar and hydrogen bonding forces. External ligand affecting any of these bonds may influence CRP packing and, by extension, bioactivity. Key electrostatic interactions defined by high-resolution structural analyses identified various salt bridges that contribute to inter-subunit contact stabilization of the pentameric conformation (19, 41). Specific <u>sequences</u> at the five inter-subunit contact sites involve residues in the 114–123 loop ($K_{114}PRVRKSLKK_{123}$) (containing six closely spaced cationic amino acids (shown in bold type), sequence 187–202 ($W_{187}RALKYEVQGEVFTKP_{202}$) near the C-terminal end of each subunit, and residues 40–42 ($Y_{40}TE_{42}$) which localize to the middle of the CBP. Specific <u>residues</u> involved in electrostatic stabilization include R_{118} binding to D_{155} on juxtaposed subunits, E_{101} binding to K_{201}, and E_{197} binding to K_{123}. Arginine 118 is also localized near the carboxyl group of Proline 202 of the inter-subunit stabilizing sequence described above. The $R_{118} \rightarrow D_{155}$ interaction is sequestered deep in the interaction zone with the carboxyl oxygen of D_{155} approximately 3.4 Å from the guanidino nitrogen in R_{118} (**Figure 3**). Using iterative programs to predict thermodynamically predicted structures for the relaxed mCRP isoform (42–47), there is a large rotation of these sequence when a pCRP subunit converts into mCRP, substantially increasing the distance between these residues. Any external force that can compete with this intramolecular salt bridge and weaken it (such as a ligand expressing an arginine cationic charge) can promoting ligand-induced conversion of pCRP into mCRP. In appreciation of the significantly different bioactivities of each CRP isoform, this pathway has relevance to how CRP is altered to

control its pro- and anti-inflammatory activities (40, 48). The application of expressed arginine residues in both apolipoprotein B (and apolipoprotein E) to CRP binding are discussed below.

Electrostatic binding residues have also been implicated in controlling CRP binding to the C1q component and to CRP-mediacted complement activation (49). Using mutational analyses, the C1q binding site on CRP involves a binding pocket lined with charged residues H_{38}, E_{88}, and D_{112} (50); CRP residue Y_{175} also provides hydrogen bonding energy in the CRP-C1q interaction (51). D_{112} and Y_{175} directly contact C1q, and, along with H_{38}, are critical for complement activation. Li et al. (18) showed CRP's CBP was predominantly involved in CRP-C1q interactions, with peptides $L_{83}FEVPEVT_{90}$ and $A_{92}PVHICTSWESASGI_{106}$ contributing energy to the binding reaction. Of note, peptide 92–106 involves the intrachain disulfide bond which is localized two residues removed from H_{38}. Access to each of these sites would require conformational rearrangement of CRP. Braig et al. (16) discussed in the CRP-C1q interaction in greater detail, showing how C1q globular head groups could interact on the effector face side of the central void of a partially relaxed CRP pentamer, described as pCRP*. Residues D_{112} and Y_{175} are juxtaposed and are aligned around the central core of pCRP, being most accessible for interaction with the C1q globular head group when CRP is in its compacted pentameric configuration. The CBP peptide is localized on each subunit around the central void nearer the recognition face of pCRP. Exposing these residues for C1q binding would require a structural change in CRP. Using size measurements, the C1q head group is too large to fit inside the void but could provide binding energies to push the loosely associated CRP subunits in pCRP* into the irreversible mCRP conformation, releasing its pro-inflammatory effects (summarized in **Figure 4**).

Cationic arginine residues on C1q are reported as critical for its interaction with immunoglobulin (52) and CRP (51). Hence, anionic aspartate (D) and glutamate (E) residues on CRP are particularly relevant for arginine-based salt bridges.

Comparison of apolipoprotein B and apolipoprotein E structures affecting binding reactivities

While apolipoprotein E and apolipoprotein B are distinctive proteins, apo E is known to have binding affinity for the same LDL receptor that binds apo B. Its cationic binding sequence resembles the cationic nonapeptide sequence defined for apo B binding to LDL-R (**Table 1**).

Apolipoprotein E biofunction involves coordinating the binding of lipoproteins of various sizes and shapes (e.g., LDL, VLDL and HDL) to lipoprotein receptors, especially to

LDL-receptor (LDL-R). Comprised of 299 amino acids, the ∼34 kD apo E contains two major functional domains linked by a protease-sensitive hinge peptide. Its N-terminal domain comprises ∼63% of its primary sequence (i.e., residues 1–191) and contains the cationic peptide sequence known to bind LDL receptor. Its C-terminal domain comprises ∼30% of its sequence (i.e., residues 210–299) and contains phospholipid binding residues that anchor apo E to lipoprotein surfaces.

There is a high percentage of basic amino acids in repeated clusters throughout apo E, with arginine accounting for 11% of the amino acid content of the protein. Its N-terminal sequence is divided into hydrophilic 4 helical domains, the fourth of which contains the cationic receptor binding sequence. Its C-terminal domain contains binding residues for polar head groups of phospholipids and for apolar residues to better anchor apo E to the hydrophobic/hydrophilic interface of a lipoprotein particle. Apo E binds to the polar head groups of lipid molecules and extends over the lipoprotein surface rather than inserting into the hydrophobic lipid core of the particle. This orientation facilitates HDL core expansion with cholesterol esters, in a way that is not limited by a requirement for apolar molecular interactions and surface curvature issues inherent in differed sized and shaped HDL particles. De-lipidated apo E does self-aggregate into oligomers. However, mutating selective residues in the C-terminal domain can abrogate self-aggregation allowing for the detailed study of monomeric apo E proteins (53–59).

The strongly cationic nonapeptide sequence mediating apo E's binding to the LDL-receptor ($R_{142}KLRKRLLR_{150}$) is buried and inaccessible in delipidated apo E. In the absence of lipids, apo E collapses upon itself forming a globular tertiary structure in which its N-terminal and C-terminal domains are stabilized by five salt bridges, hydrogen bonds and apolar interactions. The cationic LDL-R binding sequence is hidden in this compacted structural orientation. Exposing this binding sequence follows a two-step process involving a marked conformational change in the tertiary structure of apo E. Step 1 is rapid and involves phospholipid binding or the C-terminal domain to exposed phospholipid head groups on lipoprotein particles. Apo E sits on the polar head groups (e.g., phosphocholine) of these phospholipids, being juxtaposed to but not inserted into the apolar membrane region. As apo E associates with lipids, the salt bridges holding its two domains together weaken, relaxing the tertiary structure of the apoprotein. Step 2 is a slower, reversible process involving relaxing the N-terminal domain into an open conformation with increased exposure of the LDL-R binding peptide (53, 60). To provide perspective on the major conformational rearrangement of apo E in the absence and presence of lipids, Chen noted the distance between residues N-terminal domain residue C_{112} and C-terminal domain residue W_{264} (specifically for apo E3) was ∼28Å in the absence of lipid, but > 80 Å in
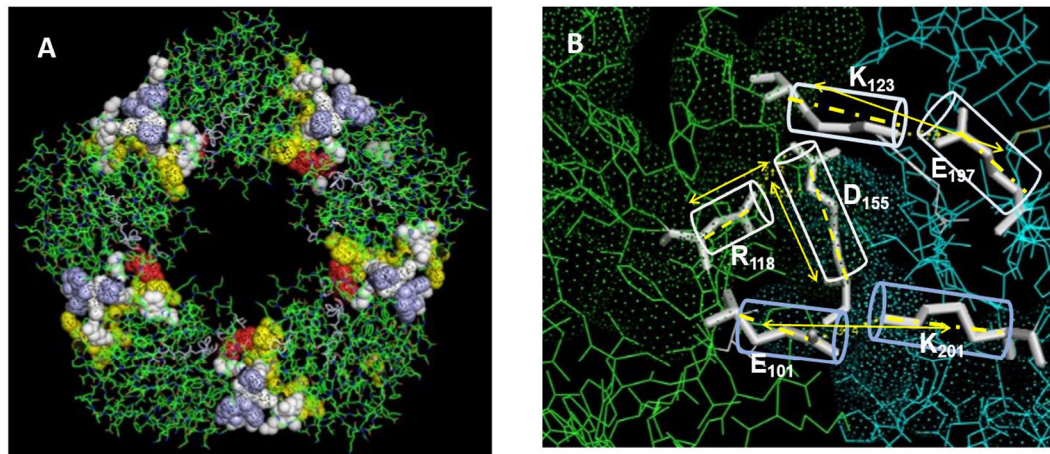
FIGURE 3
Residues stabilizing pCRP non-covalent inter-subunit contact zones. **(A)** Oriented to show the PC binding recognition face of CRP. Residues Y40TE42 shown as red spheres; Residues P115RVRKSLKK123 shown as yellow spheres; Residues E197VFTKP202 shown as light blue spheres. Residues contributing dominant salt bridges R118-D155; E101-K201; K123-E197 shown at white spheres. **(B)** Displays stick figures and bond distances of stabilizing salt bridges E101-K201: 3.3 Å; K123-E197: 3.4. Å; R118-D155: 3.2 Å. Note the E101-K201 and -K123-E197 salt bridges are linear while the R118-D155 salt bridge occurs at an acute angle. Lv et al. (108) identified the R118-D155 salt bridge as an absolute requirement for the assembly of CRP into its pentameric configuration. Ligands affecting the integrity of this salt bridge would affect the stability of the pentamer, and by extension, the expression of the mCRP, biologically active mCRP conformer.
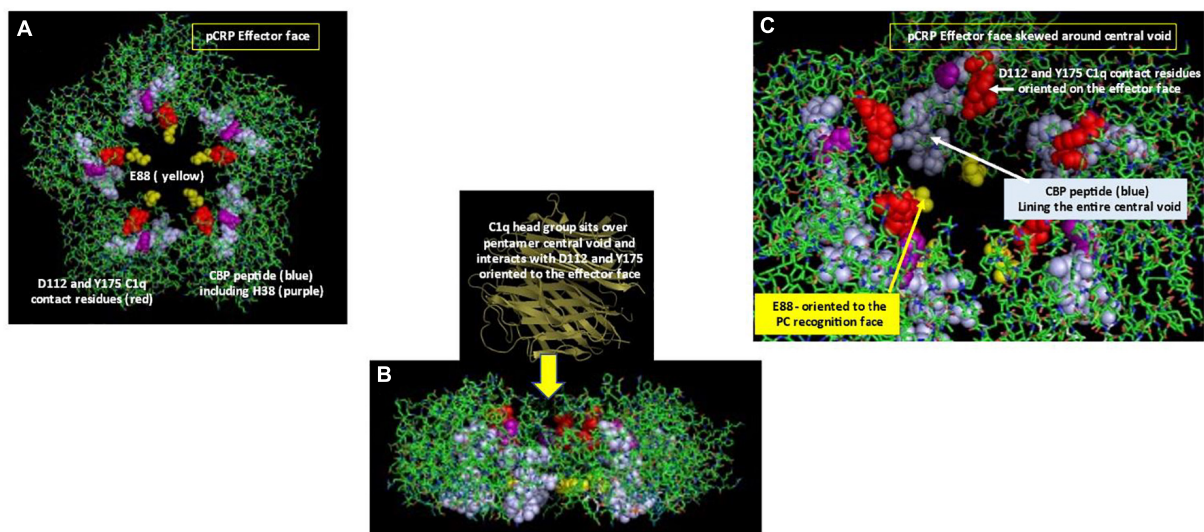
FIGURE 4
Orientation of C1q head group and Cholesterol Binding Peptide (CBP) residues in pCRP. **(A)** Depicts the Effector (helical) face of the pCRP pentameric disc with a top-down look of pCRP bound to membrane PC ligands. Residues D112 and Y175, which directly react with the C1q globular head group (50) shown in red. The Cholesterol binding peptide is shown in blue. Included within CBP is C1q binding reside H38 (shown in purple). C1q binding residue E88 shown in yellow points into the central void but orients to the PC-recognition face, far removed from the effector face in intact pCRP. **(B)** Depicts a side-view of pCRP shown in panel **(A)**. Initial C1q head group binding occurs symmetrically over all five subunits over the central void on the effector face (16). Note the CBP and E88 residues orient toward the recognition face. To fully expose C1q binding and CBP residues, a conformational change in CRP is required. Binding interactions of CRP with activated membranes including PC groups and apolar regions at the membrane hydrophobic/hydrophilic interface, coupled with forces provided by the large C1q head group contribute energies needed for pCRP conformational change into mCRP. Furthermore, membrane bound cationic groups (e.g., choline, stearyl amine) could provide electrostatic binding to recognition face oriented E88 to help the non-covalently associated CRP subunits to dissociate and structurally rearrange into mCRP. **(C)** Depicts a portion of pCRP as shown in panel **(A)**, skewed to show how direct contact residues D112 And Y175 (red) for C1q binding orient to the effector face, near the central void, being more accessible for initial C1q head group binding. Note the CBP residues (blue) line the entire central void from the effector face to the recognition face. Also, note the orientation of C1q binding residue E88 oriented on the opposite face of the pCRP pentameric disc.

TABLE 1 Comparison of cationic sequences of apo B and apo E involved in interaction with the LDL-receptor.

	Comparison of Cationic Sequences binding LDL Receptors									
	3359	3360	3361	3362	3363	3364	3365	3366	3367	apo E3 and E4
Apo B	R	L	T	R	K	R	G	L	K	
Apo E	R	K	L	R	K	R	L	L	R	C- > R
	142	143	144	145	146	147	148	149	150	158

The yellow shading is meant to highlight all cationic residues in these comparable sequences (i.e., R (arginines) and K (lysines).
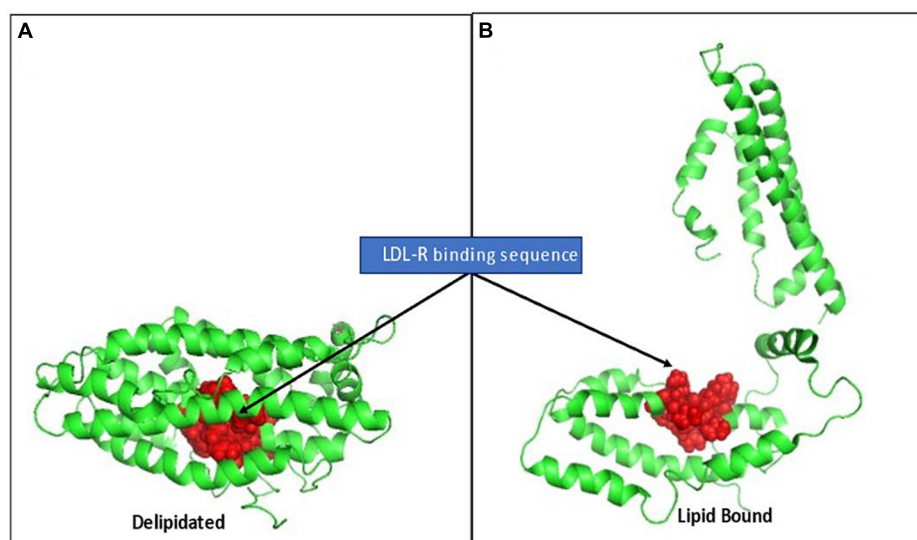
FIGURE 5
Rendition of the structural change in apo E elicited by lipid binding, exposing the LDL-R binding sequence. **(A)** Depicts full length apo E3 (PBD: 2L7b) structural packing as a delipidated protein. The cationic nonapeptide mediating apo E binding to LDL-receptors (R142KLRKRLLR150) shown as red spheres, being inaccessible in the interior of the compacted lipid-free tertiary structure. **(B)** Based on Chen et al. (53), who described a two-step conformational change in apo E on lipid binding, this rendition is provided to visualize how lipid binding can contribute to apo E conformational changes that alter access to its receptor binding sequence and, in turn, its biofunction in mobilizing lipoprotein/membrane associated cholesterol.

its presence (see **Figure 5** for perspective of these structural changes).

Apo E is known to exist in three allelic forms which involve specific cysteine to arginine mutations at 2 sites in its 299 amino acid sequence, one of which is C_{112} mentioned above. Apo E2 contains cysteine residues at both position 112 and 158 (i.e., C_{112}, C_{158}). Apo E3 contains a cysteine residue at position 112, but an arginine residue at position 158 (i.e., C_{112}, R_{158}). Apo E4 contains arginine residues at both positions 112 and 158 (i.e., R_{112}, R_{158}). In apo E4, the arginine residue expressed at position 112 adds an additional salt bridge to residue E_{109} within the N-terminal domain, which also causes a structural rotation that increases exposure of R_{61}. R_{61} becomes accessible to form the additional salt bridge with C-terminal domain residue E_{255} (54). Mahley went on to report (56) that the additional salt bridge in apo E4 is of importance in the increased neuro-degenerative pathologies associated with this isoform.

Each expressed protein differentially binds lipids and apo E receptors, including the LDL receptor. The binding affinity of apo E4 to LDL-R was stronger than apo E3, which in turn was stronger than apo E2 (61). As the mutated residues are in the N-terminal aqueous, receptor binding domains of apo E and not the C-terminal lipid-binding domain, apo E4 shows stronger binding to the LDL-R but less capacity to process cholesterol than other apo E alleles (57, 59). As the brain contains 23% of total body cholesterol (62), processes that affect cholesterol transport in the brain can have pathophysiological consequences.

Apo E also binds (anionic) heparin sulfate proteoglycans and amyloid-beta (Aβ) peptides. Heparin binding, presumably by competing for intramolecular salt bridges, can open up apo E structure to allow for LDL-R binding. Different apo E isotypes can affect how αβ peptides are generated from the transmembrane amyloid precursor protein (APP) and how they are aggregated and cleared (63). The toxicity associated with αβ peptide deposition is associated with hyperphosphorylation of the microtubular protein tau which can lead to neurofibrillary tangles in the brains of Alzheimer's patients (53, 54, 58).

Bioeffects of C-reactive protein-lipid/apolipoprotein complexes

CRP admixed with liposomes or Large Unilamellar Vesicles (LUVETs) has anti-cancer activity both *in vitro* and *in vivo* [summarized in Potempa et al. (48)].

Bian et al. (64) reported that the interaction of CRP could increase movement of apo B-containing LDLs across endothelial cells and promote development of atherosclerotic plaques. The effect of CRP required NAPDH oxidase to generate ROS and was blocked when sulfhydryl groups were reduced.

Li et al. (65) investigated how CRP could affect LDL directional transport across endothelial cell barriers. Transport occurred both into and out of tissues with a preference for movement from blood into tissues. The directional movement was regulated by the basement membrane matrix such that, when the basement membrane was altered, CRP was redirected back into the blood.

In rat studies, peritoneal macrophages differentially processed CRP-LDL complexes compared to CRP-acetylated-LDL (i.e., altered) complexes (66). Altered LDL particles bound a scavenger receptor as opposed to normal LDL binding to LDL receptors. Shih et al. (67) later reported CRP mediated altered LDL binding more specifically to the LOX-1 scavenger receptor on endothelial cells, and that arginine residues on the receptor were involved in this interaction. In direct macrophage binding and uptake studies of pCRP and mCRP isoforms with both normal LDL and oxidized LDL particles, the mCRP isoform and not the pCRP isoform enhanced binding and uptake of normal LDLs to macrophage LDL receptors but reduced binding and uptake of oxidized LDL (12, 68).

In mouse models of atherosclerosis using both transgenic models expressing human CRP, or knockout models of endogenous CRP, CRP has been differently reported to (1) accelerate progression of atherosclerosis in apo E-deficient mice (69); (2) slow the development of atherosclerosis (70, 71); and (3) have no effect (72). These reports were completed before there was substantial literature describing distinctive CRP isoforms and did not consider how each of pCRP and mCRP may have influenced results generated. As studies evolved, it is now clearly apparent that different CRP isoform do have different pro- and anti-atherogenic effects. Schwedler et al. (73) used an apo E knockout mouse model showed pCRP injections increased aortic plaque size while modified CRP decreased plaque formation. The observed effects of mCRP were related to regulation of reactive oxygen and peroxynitrite formation (i.e., pro-inflammatory stimulation) but in ways that impaired vascular relaxation responses (74). Ji et al. (12) and Schwedler et al. (75) showed mCRP but not pCRP preferentially associated with oxidized LDL. As mentioned above, mCRP inhibited altered LDL uptake by macrophages in a way that

reduced formation of atherogenic plaques. The mCRP effect did not involve Fcγ receptors CD16 (which binds mCRP) nor CD32 (which binds pCRP) [summarized in Wu et al. (15)] nor the LOX-1 scavenger receptor on macrophages (as opposed to endothelial cells).

Liposome-bound CRP activates complement. Effects require liposomes to contain either phosphatidylcholine (PtC) or sphingomyelin (both PC containing lipids). CRP-mediated complement effects were influenced by liposome lipid acyl chain length, degree of unsaturation, and cholesterol content (76). The addition of a positive charge either as stearyl amine or cetyltrimethylammonium bromide, or addition of galactosyl ceramide to certain liposomes, improved CRP binding and complement activation activities.

CRP complexed with lipoproteins can also activate complement (77, 78). Binding to lipoproteins requires CRP's primary binding ligand, phosphocholine, be made accessible by either enzymatically treating or oxidizing LDLs (79, 80). Wang et al. (81) showed how lipoprotein oxidation affects surface curvature and promotes CRP binding. The average diameter of LDL particles is 25–26 nm, but oxidation decreases particle size and increases surface curvature. CRP preferentially bound to highly curved, smaller lipoprotein mimetic particles. When bound by these smaller, highly curved particles, pCRP not only binds but is structurally altered into the mCRP isoform, which stays associated with the lipoprotein particle (resisting dissociation with chelators or disruptive washing treatments). To specifically look at how each of the pCRP and mCRP isoforms affected complement activation pathways, Ji et al. (12) showed mCRP rather than pCRP could bind the C1q component of the classical C system through its collagen-like stem. Lipoprotein bound mCRP activated the classical C pathway, but also recruited the alternative pathway regulating protein Factor H to the CRP-activated surface. Factor H functions to limit the production of the membrane attack complex (MAC) suggesting conformationally altered CRP, after insertion into lipid membranes, can promote Complement-mediated opsonization but inhibit C-mediated cell lysis pathways.

In addition to complement, CRP-lipoprotein particles regulate coagulation pathways involving tissue factor and thrombin activation. Using Phosphatidyl serine/Phosphatidyl choline (PtS: PtC) liposomal vesicles as an anchor for tissue factor, CRP inhibited factor VIIa mediated tissue factor activation of Factor X and the initiation of fibrin formation (82, 83). The capacity of CRP to combine with VLDL was also linked to processes that contribute to disseminated intravascular coagulation (DIC) (83, 84). Also, CRP has been implicated in fat embolism pathologies associated with therapeutic infusions of lipid emulsions (i.e., "Intralipid") (85, 86). Even without intralipid infusion, extremely high CRP blood levels (>200 μg/ml) appear to complex with VLDLs in blood and reduced normal phagocytic cell function, which in

turn affects the clearance of bacteria in models of sepsis (87). Very high blood CRP levels are known to be associated with poor outcomes to any disease (48, 88). Its association with VLDLs suggests a mechanism by which CRP can contribute to morbidity. **Table 2** summarizes distinctive bioactivities of pCRP and mCRP with a focus on lipid and lipoprotein.

C-reactive protein and extracellular vesicles/microparticles

Extracellular lipid vesicles released from cell membranes or synthesized to carry various biochemical molecules (e.g., mRNA-based vaccines) represent an emerging field of diagnostic and therapeutic medicine (89). Of relevance to this review, the mCRP isoform has been shown to associate with small, lipid microparticles found in circulation.

mCRP forms on and inserts into membranes to as a regulatory step in eliciting the biofunction of CRP as an acute phase reactant. As a strong pro-inflammatory mediator, mCRP will activate leukocytes to stimulate and amplify the inflammatory response, producing ROS and secreting enzymes that affect the tissue environment, including the membrane into which mCRP inserted. The destructive power of leukocyte activation creates bits of sloughed membranes, which can carry mCRP and enter circulation as extracellular lipidic vesicles. Crawford et al. (90) showed patients with peripheral artery disease (PAD) did express mCRP-associated microparticles in blood. These particles, ranging in size from 0.1 to 1 μm [compared to platelets (3 μm), RBCs (7 μm) lymphocytes (7–10 μm) and polymorphonuclear leukocytes (PMNs) (15–25 μm)], and were primarily derived from activated endothelial cells (verified using co-marker FACS analyses). While these microparticles are derived from plasma membrane lipids, their small size and high curvature results in PS and PE lipids, normally found on the inner leaflet of an intact plasma membrane, found in high concentration on the surface of microparticles.

Habersberger et al. (91) showed mCRP-lipid microparticles were elevated in blood of patients after a myocardial infarction. These microparticles were enriched in lyso-PC (monoacyl phosphatidyl choline) and were shown to enhance the conversion of pCRP into mCRP. Isolated mCRP-associated microparticles did have pro-inflammatory bioactivity when added to endothelial cells in culture.

Habersberger's group also showed that formation of mCRP from pCRP on a membrane surface could be prevented if pCRP was first neutralized by a bivalent bis-PC compound that links two juxtaposed pentamers (92). This compound binds two PC binding sites in a way that forms a recognition face-to-recognition face soluble decamers which can no longer bind

membrane exposed PC groups. As pCRP is not localized to an apolar membranous zone, insufficient biochemical energy is available to loosen the pentameric structure and lead to expression of the mCRP isoform.

Trial et al. (5) discussed how lipid microparticles can bind both pCRP and mCRP. Adding pCRP to freshly isolated microparticles from cardiac patient blood resulted in conversion of pCRP to mCRP within 20 minutes. Of note, lipid-associated CRP antigens could not be quantified using standard CRP nephelometric measurement assays. Furthermore, the level of FACS-quantified mCRP-lipid complexes did not correlate with lipid-free pCRP concentration in blood, even at high sensitivity levels (i.e., 1–10 μg/ml).

Taken together, while highly soluble pCRP can exist as a lipid-free protein in blood, binding to an activated membrane surface through PC or cationic ligands, can localize CRP to apolar biochemical energies that contribute to its dissociation and structural change into mCRP. Structurally altered mCRP expresses a cholesterol binding domain and enters lipid rafts which activate and amplify pro-inflammatory signaling pathways of the acute phase of an inflammatory response. Activated leukocyte effector responses at involved tissue sites will enzymatically degrade mCRP or cause it to be sloughed away from activated cell surface as a lipid microparticle complex, resulting in down-regulation of the acute inflammatory response. Serum soluble pCRP thus circulates as a pro-activator of inflammation, requiring interaction with lipids to release its important bioactivities in host defense responses.

Clinical relevance of C-reactive protein-lipoprotein interactions

CRP-lipid interaction in atherosclerotic disease has been a focus topic of many studies. Before the understanding that CRP exists in at least two distinctive isoforms, diametrically opposite conclusions were reached for directly comparable experimental model systems. When reagents were developed to differentially study pCRP from mCRP, results consistently showed pCRP prevented, while mCRP promoted monocyte processing of potentially atherogenic LDL particles (68). Even though mCRP is a strong pro-inflammatory mediator, it lessened atherogenesis of modified LDLs in animal models of disease (93). Further, the CRP effect on atherosclerosis did not depend on PC binding as, when mutant proteins were constructed to lose PC binding activity (i.e., $F_{66}A/T_{76}Y/E_{81}A$), "CRP" still bound atherogenic LDLs and, when injected into atherogenic-prone mice, slowed disease progression, and reduced the size of aortic lesions (94). Recently, Cheng et al. (95) showed the dose level of injected mCRP was an important factor in protecting from induced liver disease. At lower doses, mCRP conferred protection from disease, but at higher doses, this protection was lost,

attributed to mCRP ability to over-stimulate the *in situ* inflammatory response.

In the Schwedler et al. (73) study using an apo E knockout mouse model, pCRP injections increased aortic plaque size while modified CRP decreased plaque formation. Histologically, the mCRP antigen co-localized with deposits of apolipoprotein B and macrophages. The observed effects of mCRP were related to regulation of ROS and RNS formation and vascular relaxation responses, underscoring that mCRP's effects in stimulating acute inflammatory responses may have positive therapeutic benefits (48, 74, 75).

Other studies suggest a pathological role for mCRP in atherosclerosis, thrombosis, angiogenesis, and cerebrovascular pathologies (96, 97). mCRP antigen has been found in brain tissues associated with damaged micro vessels and in human and mouse brains involved with neuroinflammation (98–100). Since mCRP forms from pCRP, drugs that inhibit the *in situ* formation of mCRP from pCRP could have therapeutic value in treating both systemic and cerebral inflammatory diseases (3, 101).

Alzheimer's disease involves neuroinflammation and dysfunction in biochemical processing of cholesterol in the brain (102, 103). Over the past decade, individuals expressing the apo E4 allele have been shown to have increased risk for developing early onset Alzheimer's disease and appear to have poorer outcomes following any type of severe brain injury. A better understanding of the relevance of apo E proteins to inflammatory processes and to cholesterol balance will contribute to medical advances in the prevention and

TABLE 2 Key observations of pCRP and mCRP interactions with lipids and lipoproteins.

	Pentameric CRP (pCRP)	Monomeric, modified CRP (mCRP)
Binding to lipids	● pCRP binds exposed phosphocholine (PC) groups of the phospholipids of membranes, liposomes, and lipoproteins as a function of calcium ● Key factors promoting pCRP binding include lipid acyl chain length (shorter chains), degree of unsaturation and cholesterol content ● Also, including of a positive charge as either as stearyl amine or cetyltrimethylammonium bromide improved binding ● pCRP calcium-dependent binding was also seen when Phosphoethanolamine (PE) was used instead of phosphocholine (PC)	● mCRP does not express calcium dependent PC binding specificity ● Monolayer technique experiments established mCRP interacts with the hydrophobic tail of LDL lipids through membrane insertion ● In the presence of calcium, mCRP induced substantial increase in monolayer membrane pressure formed by LDL lipid extracts; indicates membrane insertion ● mCRP interacts with RBC ghost membranes and is highly resistant to alkaline carbonate and high salt extraction; indicates it inserts into bilayers like an integral protein ● The majority of RBC ghost-associated mCRP remained insoluble with Triton X-100; this is consistent with the behavior of lipid raft-resident proteins
Complement activation	● The positive charge or presence of galactosyl ceramide to certain liposomes improves pCRP binding and complement activation activities ● CRP binds C1q of the classical pathway on the opposite face of the pentameric disc from the PC-binding face	● mCRP binds C4bp and enhances degradation of C4b and C3b ● C1q and C4bp compete for mCRP binding ● mCRP binds factor H and factor H-like protein 1 (FHL1) and modulates the alternative complement pathway
Binding to Apolipoproteins	● pCRP binds apo B; binding does not require calcium	● mCRP binds apo B at a greater affinity that pCRP ● mCRP binds both isolated apo B and LDL-associated apoB through its cationic peptide sequence ● mCRP binding to native LDL can be inhibited by competitors that interfere with electrostatic interactions and apolar interactions; indicates mCRP interacts with lipoproteins using electrostatic binding and apolar binding
Effect of modification of lipoproteins	● pCRP did not bind native LDLs either in the presence of Calcium or EDTA ● Lipoproteins oxidized to alter fatty acyl chain length and unsaturation do bind pCRP through calcium-dependent interactions with exposed PC groups ● Lipoproteins enzymatically treated to cleave apolipoproteins bound pCRP as a function of calcium	● Once bound to native LDL, mCRP is not eluted by high salt indicating a binding is primarily apolar ● mCRP interacted with lipid extracts from each of native, oxidized and enzymatically treated lipoproteins
Observations relevant to unrecognized pCRP conversion to mCRP	● Binding of "CRP" to apo B/lipoproteins best when CRP was aggregate and immobilized. ● Aggregated CRP immobilized on a surface (conditions shown to from the mCRP isoform) bound LDL and VLDL from normal human serum (i.e., apoB-containing lipids). ● Various experimental results with strongly chelated pCRP are more like results generated with mCRP than pCRP in calcium ● pCRP in calcium will bind to exposed PC groups in membrane surfaces but initially, will not insert into the apolar lipid zone. With prolonged incubation times (e.g., 2–4 h) membrane associated CRP will insert into hydrophobic zones	

Relevant references: (4, 37–40, 107, 109–112).

treatment of this disease. A relationship between apo E4 and plasma CRP levels relevant to the development of Alzheimer's disease has been reported (104). Furthermore, the mCRP isoform bound to endothelial cell CD31 (a receptor mediating platelet and leukocyte binding and transcytosis), influencing apo E4-related responses in the development of Alzheimer's disease (100).

Summary

CRP has been known since the 1940s as a diagnostic marker for inflammation. Its blood levels change rapidly and pronouncedly with any tissue damaging process that involves non-memory, innate immune defense system activation, leading to its designation as the "prototypic acute phase reactant" of host defense responses. Its exact biological role as a key protein in this process has been an area of uncertainty and confusion covering decades of detailed study.

While most detailed studies of CRP structure/function relationships have focused on the lipid-free, highly aqueously soluble, non-covalently linked, non-glycosylated pentameric protein, substantial literature exists that describes CRP as a blood protein that also associates with apolipoprotein B-expressing lipoproteins. While a primary binding reactivity with lipoproteins involves calcium-regulated binding affinity with exposed phosphocholine groups, CRP also directly binds to a cationic peptide sequence as expressed on the apolipoprotein. In either case, bound CRP is localized to and interacts with lipid surfaces (i.e., lipoproteins or membranes). Little attention has been given to the role and influence of amphipathic lipid molecules as regulators of CRP structures and bioactivities.

A key evolution in understanding CRP's role as a biological response modifier was the recognition that when dissociated, CRP subunits undergo a rapid, irreversible conformational rearrangement into an isoform with strong affinity for apolar regions of lipid surfaces. When CRP is brought into juxtaposition with an apolar zone, the localized non-polar biochemical energies not only help dissociate the pentamer and contribute to the conversion of CRP into the mCRP isoform, but a novel binding site for membrane-bound cholesterol is expressed. As mCRP is formed, it is drawn into a membrane where it stimulates activation and signaling pathways that contribute to a strong pro-inflammatory host defense responses (which more accurately describes "CRP" as the prototypic acute phase reactant) (105). Conformational rearrangement of CRP from the pentamer to the modified monomer results in significate loss of aqueous solubility, loss of antigenicity associated with the pentamer, and expression of new (neo) epitopes associated with the conformational isomer. Once formed, mCRP sequesters into lipid zones which masks its detection using assays and reagents developed for the non-lipid-associated highly aqueously soluble protein found in blood and body fluids.

Lipid-associated mCRP can be sloughed off activate membrane surfaces into body fluids, being found associated with micro-particles. The strong lipid association is of relevance to reassessing all prior studies describing CRP lipoprotein associations in blood. As lipid-soluble mCRP can be formed from pCRP, which initially binds to the aqueous surface of lipoproteins using its calcium-regulated affinity for PC groups, any CRP that is not readily dissociated from the lipoprotein particle by simple chelation, must be evaluated as the lipid bound mCRP isoform rather than the pCRP isoform. As pCRP and mCRP are now known to have distinctive anti- and pro-inflammatory bioactivities, respectively, it is possible to reassess the role(s) CRP may play in different lipoprotein-involved pathophysiologies such as cardiovascular diseases and neurodegenerative diseases.

Conflict of interest

Publisher's note

Supplementary material

The Supplementary Material for this article can be found online at: https://www.frontiersin.org/articles/10.3389/fcvm.2022.979461/full#supplementary-material

References

1. Volanakis JE, Clements WL, Schrohenloher RE. C-reactive protein: purification by affinity chromatography and physicochemical characterization. *J Immuno Meth.* (1978) 23:285–95. doi: 10.1016/0022-1759(78)90203-X

2. Volanakis JE, Wirtz KW. Interaction of C-reactive protein with artificial phosphatidylcholine bilayers. *Nature.* (1979) 281:155–7. doi: 10.1038/281155a0

3. Caprio V, Badimon L, Di Napoli M, Fang WH, Ferris GR, Guo B, et al. pCRP-mCRP dissociation mechanisms as potential targets for the development of small-molecule anti-inflammatory chemotherapeutics. *Front Immunol.* (2018) 9:1089–96. doi: 10.3389/fimmu.2018.01089

4. Rajab IM, Majerczyk D, Olson ME, Addams JMB, Choe ML, Nelson MS, et al. C-reactive protein in gallbladder diseases – diagnostic and therapeutic insights. *Biophys Rep.* (2020) 6:49–67. doi: 10.1007/s41048-020-00108-9

5. Trial J, Potempa LA, Entman ML. The role of C-reactive protein in innate and acquired inflammation: new perspectives. *Inflammation Cell Signal.* (2016) 3:e1409–18. doi: 10.14800/ics.1409

6. Heegaard NH, Robey FA. A capillary electrophoresis-based assay for the binding of Ca2+ and phosphorylcholine to human C-reactive protein. *J Immunol Methods.* (1993) 166:103–10. doi: 10.1016/0022-1759(93)90333-3

7. Christopeit T, Gossas T, Danielson UH. Characterization of Ca2+ and phosphocholine interactions with C-reactive protein using a surface plasmon resonance biosensor. *Anal Biochem.* (2009) 391:39–44. doi: 10.1016/j.ab.2009.04.037

8. Mikolajek H, Kolstoe SE, Pye VE, Mangione P, Pepys MB, Wood SP. Structural basis of ligand specificity in the human pentraxins, C-reactive protein and serum amyloid P component. *J Mol Recognit.* (2011) 24:371–7. doi: 10.1002/jmr.1090

9. Zeller J, Shing KC, Nero T, Krippner G, McFadyen J, Bogner B, Kreuzaler S, et al. *Discovery, in-vitro, and in-vivo efficacy of an anti-inflammatory small molecule inhibitor of C-reactive protein. Research Square preliminary report.* (2021) Available online at: doi: 10.21203/rs.3.rs-944388/v1

10. Gotschlich EC, Edelman GM. Binding properties and specificity of C-reactive protein. *Proc Natl Acad Sci USA.* (1967) 57:706–12. doi: 10.1073/pnas.57.3.706

11. Robey FA, Jones KD, Tanaka T, Liu T-Y. Binding of C-reactive protein to chromatin and nucleosome core particles. *J Biol Chem.* (1984) 259:7311–6.

12. Ji SR, Wu Y, Potempa LA, Qiu Q, Zhao J. The interactions of low-density lipoprotein with different forms of C-reactive protein: implication of an active role of modified C-reactive protein in the pathogenesis of atherosclerosis. *Int J Biochem Cell Biol.* (2006) 38:648–61. doi: 10.1016/j.biocel.2005.11.004

13. Ji SR, Wu Y, Zhu L, Potempa LA, Sheng FL, Wei L, et al. Cell membranes and liposomes dissociate C-reactive protein (CRP) to form a new, biologically active structural intermediate: mCRPm. *FASEB J.* (2007) 21:284–94. doi: 10.1096/fj.06-6722com

14. Ji S-R, Bai L, Shi J-M, Li H-Y, Potempa LA, Filep JG, et al. Monomeric C-reactive protein activates endothelial cells via interaction with lipid raft membrane microdomains. *FASEB J.* (2009) 23:1806–16. doi: 10.1096/fj.08-116962

15. Wu Y, Potempa LA, El Kebir D, Filep JG. C-reactive protein and inflammation: conformational changes affect function. *Biol Chem.* (2015) 396:1181–97. doi: 10.1515/hsz-2015-0149

16. Braig D, Nero TL, Koch H-G, Kaiser B, Wang X, Thiele JR, et al. Characterization of transitional changes in the CRP structure leading to the exposure of pro-inflammatory binding sites. *Nat Commun.* (2017) 23:14188–207. doi: 10.1038/ncomms14188

17. Wang M-Y, Ji S-R, Bai C-J, El Kebir D, Li H-Y, Shi J-M, et al. A redox switch in C-reactive protein modulates activation of endothelial cells. *FASEB J.* (2011) 25:3186–96. doi: 10.1096/fj.11-182741

18. Li HY, Wang J, Meng F, Jia ZK, Su Y, Bai QF, et al. An intrinsically disordered motif mediates diverse actions of monomeric C-reactive protein. *J Biol Chem.* (2016) 291:8795–804. doi: 10.1074/jbc.M115.695023

19. Shrive AK, Cheetham GM, Holden D, Myles DA, Turnell WG, Volanakis JE, et al. Three dimensional structure of human C-reactive protein. *Nat Struct Biol.* (1996) 3:346–54. doi: 10.1038/nsb0496-346

20. Mackiewicz MR, Hodges HL, Reed SM. C-reactive protein induced rearrangement of phosphatidylcholine on nanoparticle mimics of lipoprotein particles. *J Phys Chem B.* (2010) 114:5556–62. doi: 10.1021/jp911617q

21. Ying S-C, Shephard E, deBeer FC, Siegel JN, Harris D, Gewurz BE, et al. Localization of sequence-determined neo-epitopes and neutrophil digestion fragments of C-reactive protein utilizing monoclonal antibodies and synthetic peptides. *Mol Immunol.* (1992) 29:677–87. doi: 10.1016/0161-5890(92)90205-c

22. Kushner I, Feldman G. Control of the acute phase response. Demonstration of C-reactive protein synthesis and secretion by during acute inflammation in the rabbit. *J Exp Med.* (1978) 148:466–77. doi: 10.1084/jem.148.2.466

23. Saxena U, Nagpurkar A, Dolphin PJ, Mookerjea S. A study on the selective binding of apoprotein B- and E-containing human plasma lipoproteins to immobilized rat serum phosphorylcholine-binding protein. *J Biol Chem.* (1987) 262:3011–6.

24. Saxena U, Francis-Collins J, Hall J, Legal Y, Barrowman J, Nagpurkar A, et al. Removal of apoprotein-B-containing lipoproteins by plasmapheresis using immobilized phosphorylcholine-binding protein affinity adsorbent. *Biochem Cell Biol.* (1990) 68:255–9. doi: 10.1139/o90-035

25. Schwalbe RA, Coe JE, Nelsestuen GL. Association of rat C-reactive protein and other pentraxins with rat lipoproteins containing apolipoproteins E and A1. *Biochemistry.* (1995) 34:10432–9. doi: 10.1021/bi00033a015

26. Cladaras C, Hadzopoulou-Cladaras M, Nolte RT, Atkinson D, Zannis VI. The complete sequence and structural analysis of human apolipoprotein B-100: relationship between apoB-100 and apoB-48 forms. *EMBO J.* (1986) 5:3495–507. doi: 10.1002/j.1460-2075.1986.tb04675.x

27. Cabana VG, Gewurz H, Siegel JN. Interaction of very low-density lipoproteins (VLDLs with rabbit CRP. *J Immunol.* (1982) 128:2342–8.

28. Cabana VG, Siegel JN, Sabesin SM. Effects of the acute phase response on the concentration and density distribution of plasma lipids and apolipoproteins. *J Lipid Res.* (1989) 30:39–49.

29. de Beer FC, Soutar AK, Baltz ML, Trayner IM, Feinstein A, Pepys MB. Low density lipoprotein and very low-density lipoprotein are selectively bound by aggregated C-reactive protein. *J Exp Med.* (1982) 156:230–42. doi: 10.1084/jem.156.1.230

30. Rowe IF, Soutar AK, Trayner IM, Baltz ML, de Beer FC, Walker L, et al. Rabbit and rat C-reactive proteins bind apolipoprotein B-containing lipoproteins. *J Exp Med.* (1984) 159:604–16. doi: 10.1084/jem.159.2.604

31. Rowe IF, Soutar AK, Trayner IM, Thompson GR, Pepys MB. Circulating human C-reactive protein binds very low-density lipoproteins. *Clin Exp Immunol.* (1984) 58:237–44.

32. Dougherty TJ, Gewurz H, Siegel JN. Preferential binding and aggregation of rabbit C-reactive protein with arginine-rich proteins. *Mol Immunol.* (1991) 28:1113–20. doi: 10.1016/0161-5890(91)90026-g

33. Dicamelli R, Potempa LA, Siegel J, Suyehira L, Petras K, Gewurz H. Binding reactivity of C-reactive protein for polycations. *J Immunol.* (1980) 125:1933–8.

34. Potempa LA, Siegel J, Gewurz H. Binding reactivity of C-reactive protein for polycations. II Modulatory effects of calcium and phosphocholine. *J Immunol.* (1981) 127:1509–14.

35. Siegel J, Rent R, Gewurz H. Interactions of C-reactive protein with the complement system I. Protamine-induced consumption of complement in acute phase sera. *J Exp Med.* (1974) 140:631–47. doi: 10.1084/jem.140.3.631

36. Siegel J, Osmand AP, Wilson MF, Gewurz H. Interactions of C-reactive protein with the complement system II. C-reactive protein-mediated consumption of complement by poly-L-lysine polymers and other polycations. *J Exp Med.* (1975) 142:709–21. doi: 10.1084/jem.142.3.709

37. Mold C, Rodgers CP, Richards RL, Alving CR, Gewurz H. Interaction of C-reactive protein with liposomes. III. Membrane requirements for binding. *J Immunol.* (1981) 126:856–60.

38. Richards RL, Gewurz H, Siegel J, Alving CR. Interactions of C-reactive protein and complement with liposomes. II. Influence of membrane composition. *J Immunol.* (1979) 122:1185–9.

39. Mihlan M, Blom AM, Kupreishvili K, Lauer N, Stelzner K, Bergstrom F, et al. Monomeric C-reactive protein modulates classic complement activation on necrotic cells. *FASEB J.* (2011) 25:4198–210. doi: 10.1096/fj.11-186460

40. Rajab IM, Hart PC, Potempa LA. How C-reactive protein structural isoforms with distinctive bioactivities affect disease progression. *Front Immunol.* (2020) 112:2126. doi: 10.3389/fimmu.2020.02126

41. Thompson D, Pepys MB, Wood SP. The physiological structure of human C-reactive protein and its complex with phosphorylcholine. *Structure.* (1999) 7:169–77. doi: 10.1016/S0969-2126(99)80023-9

42. Xu J. Distance-based protein folding powered by deep learning. *Proc Natl Acad Sci USA.* (2019) 116:16856–65. doi: 10.1073/pnas.1821309116

43. Xu J, Mcpartlon M, Li J. Improved protein structure prediction by deep learning irrespective of co-evolution information. *BioRxiv* [Preprint] (2020):doi: 10.1101/2020.10.12.336859

44. Xu J, Wang S. Analysis of distance-based protein structure prediction by deep learning in CASP13. *Proteins.* (2019) 87:1069–81. doi: 10.1002/prot.25810

45. Wang S, Li Z, Yu Y, Xu J. Folding membrane proteins by deep transfer learning. *Cell Syst.* (2017) 5: 202–211.e3. doi: 10.1016/j.cels.2017.09.001

46. Wang S, Sun S, Li Z, Zhang R, Xu J. Accurate de novo prediction of protein tact map by ultra-deep learning model. *PLoS Comput Biol.* (2017) 13: e1005324. doi: 10.1371/journal.pcbi.1005324

47. Wang S, Sun S, Xu J. Analysis of deep learning methods for blind protein contact prediction in CASP12. *Proteins.* (2018) 86 Suppl 1:67–77. doi: 10.1002/prot.25377

48. Potempa LA, Rajab IM, Olson ME, Hart PC. C-reactive protein and cancer. Interpreting the differential bioactivities of its pentameric (pCRP) and monomeric, modified (mCRP) isoforms. *Front Immunol.* (2021) 12:744129. doi: 10.3389/fimmu.2021.744129

49. Singh SK, Ngwa DN, Agrawal A. Complement activation by C-reactive protein is critical for protection of mice against pneumococcal infection. *Front Immunol.* (2020) 11:1812. doi: 10.3389/fimmu.2020.01812

50. Agrawal A, Shrive AK, Greenhough TJ, Volanakis JE. Topology and structure of the C1q-binding site on C-reactive Protein. *J Immunol.* (2001) 166:3998–4004.

51. Roumenina LT, Ruseva MM, Zlatarova A, Ghai R, Kolev M, Olova N, et al. Interaction of C1q with IgG1, C-reactive protein and pentraxin 3: mutational studies using recombinant globular head modules of human C1q A, B, and C chains. *Biochemistry.* (2006) 45:4093–104. doi: 10.1021/bi052646f

52. Kojouharova MS, Gadjeva MG, Tsacheva IG, Zlatarova A, Roumenina LT, Tchorbadjieva MI, et al. Mutational analyses of the recombinant globular regions of human C1q A, B, and C chains suggest an essential role for arginine and histidine residues in the C1q-IgG interaction. *J Immunol.* (2004) 172:4351–8. doi: 10.4049/jimmunol.172.7.4351

53. Chen J, Li Q, Wang J. Topology of human apolipoprotein E3 uniquely regulates its diverse biological functions. *PNAS.* (2011) 108:14813–18. doi: 10.1073/pnas.1106420108

54. Mahley RW, Rall SC Jr. Apolipoprotein E: far more than a lipid transport protein. *Annu Rev Genomics Hum Genet.* (2000) 1:507–37. doi: 10.1146/annurev.genom.1.1.507

55. Mahley RW, Weisgraber KH, Huang Y. Apolipoprotein E4: a causative factor and therapeutic target in neuropathology, including Alzheimer's disease. *Proc Natl Acad Sci USA.* (2006) 103:5644–51. doi: 10.1073/pnas.0600549103

56. Mahley RW, Weisgraber KH, Huang Y. Apolipoprotein E: structure determines function, from atherosclerosis to Alzheimer's disease to AIDS. *J Lipid Res.* (2009) 50:S183–8. doi: 10.1194/jlr.R800069-JLR200

57. Bu G. Apolipoprotein E and its receptors in Alzheimer's disease: pathways, pathogenesis, and therapy. *Nat Rev Neurosci.* (2009) 10:333–44. doi: 10.1038/nrn2620

58. Liu CC, Liu CC, Kanekiyo T, Xu H, Bu G. Apolipoprotein E and Alzheimer disease: risk, mechanisms, and therapy. *Nat Rev Neurol.* (2013) 9:106–18. doi: 10.1038/nrneurol.2012.263

59. Phillips MC. Apolipoprotein E isoforms and lipoprotein metabolism. *IUBMB Life.* (2014) 66:616–23. doi: 10.1002/iub.1314

60. Prakashchand DD, Mondal J. Conformational reorganization of apolipoprotein E triggered by phospholipid assembly. *J Phys Chem.* (2021) 125:5285–95. doi: 10.1021/acs.jpcb.1c03011

61. Johnson LA, Olsen RH, Merkens LS, DeBarber A, Steiner RD, Sullivan PM, et al. Apolipoprotein E-low density lipoprotein receptor interaction affects spatial memory retention and brain ApoE levels in an isoform-dependent manner. *Neurobiol Dis.* (2014) 64:150–62. doi: 10.1016/j.nbd.2013.12.016

62. Dietschy JM, Turley SD. Thematic review series: brain lipids. Cholesterol metabolism in the central nervous system during early development and in the mature animal. *J Lipid Res.* (2004) 45:1375–97. doi: 10.1194/jlr.R400004-JLR200

63. Chang TY, Yamauchi Y, Hasan MT, Chang C. Cellular cholesterol homeostasis and Alzheimer's disease. *J Lipid Res.* (2017) 58:2239–54. doi: 10.1194/jlr.R075630

64. Bian F, Yang X, Zhou F, Wu PH, Xing S, Xu G, et al. C-reactive protein promotes atherosclerosis by increasing LDL transcytosis across endothelial cells. *Br J Pharmacol.* (2014) 171:2671–84. doi: 10.1111/bph.12616

65. Li HY, Liu XL, Liu YT, Jia ZK, Filep JG, Potempa LA, et al. Matrix sieving-enforced retrograde transcytosis regulates tissue accumulation of C-reactive protein. *Cardiovasc Res.* (2019) 115:440–52. doi: 10.1093/cvr/cvy181

66. Mookerjea S, Francis J, Hunt D, Yang CY, Nagpurkar A. Rat C-reactive protein causes a charge modification of LDL and stimulates its degradation by macrophages. *Arterioscler Thromb.* (1994) 14:282–7. doi: 10.1161/01.atv.14.2.282

67. Shih HH, Zhang S, Cao W, Hahn A, Wang J, Paulsen JE, et al. CRP is a novel ligand for the oxidized LDL receptor LOX-1. *Am J Physiol Heart Circ Physiol.* (2009) 296:H1643–50. doi: 10.1152/ajpheart.00938.2008

68. Eisenhardt SU, Starke J, Thiele JR, Murphy A, Björn Stark G, Bassler N, et al. Pentameric CRP attenuates inflammatory effects of mmLDL by inhibiting mmLDL–monocyte interactions. *Atherosclerosis.* (2012) 224:384–93. doi: 10.1016/j.atherosclerosis.2012.07.039

69. Paul A, Ko KW, Li L, Yechoor V, McCrory MA, Szalai AJ, et al. C-reactive protein accelerates the progression of atherosclerosis in apolipoprotein E-deficient mice. *Circulation.* (2004) 109:647–55. doi: 10.1161/01.CIR.0000114526.50618.24

70. Kovacs A, Tornvall P, Nilsson R, Tegnér J, Hamsten A, Björkegren J. Human C-reactive protein slows atherosclerosis development in a mouse model with human-like hypercholesterolemia. *Proc Natl Acad Sci USA.* (2007) 104:13768–73. doi: 10.1073/pnas.0706027104

71. Teupser D, Weber O, Rao NT, Sass K, Thiery J, Fehling HJ. No reduction of atherosclerosis in C-reactive protein (CRP)-deficient mice. *J Biol Chem.* (2011) 286:6272–9. doi: 10.1074/jbc.M110.161414

72. Hirschfield GM, Gallimore JR, Kahan MC, Hutchinson WL, Sabin CA, Benson GM, et al. Transgenic human C-reactive protein is not proatherogenic in apolipoprotein E-deficient mice. *Proc Natl Acad Sci USA.* (2005) 102:8309–14. doi: 10.1073/pnas.0503202102

73. Schwedler SB, Amann K, Wernicke K, Krebs A, Nauck M, Wanner C, et al. Native C-reactive protein (CRP) increases, whereas modified CRP reduces atherosclerosis in ApoE-knockout-mice. *Circulation.* (2005) 112:1016–23. doi: 10.1161/CIRCULATIONAHA.105.556530

74. Schwedler SB, Kuhlencordt PJ, Ponnuswamy PP, Hatiboglu G, Quaschning T, Widder J, et al. Native C-reactive protein induces endothelial cell dysfunction in ApoE-/- mice: implications for iNOS and reactive oxygen species. *Atherosclerosis.* (2007) 195:e76–84. doi: 10.1016/j.atherosclerosis.2007.06.013

75. Schwedler SB, Hansen-Hagge T, Reichert M, Schmiedeke D, Schneider R, Galle J, et al. Monomeric C-reactive protein decreases acetylated LDL uptake in human endothelial cells. *Clin Chem.* (2009) 55:1728–31. doi: 10.1373/clinchem.2009.125732

76. Narkates AJ, Volanakis JE. C-reactive protein binding specificities: artificial and natural phospholipid bilayers. *Ann N Y Acad Sci.* (1982) 389:172–82. doi: 10.1111/j.1749-6632

77. Tsujimoto M, Inoue K, Nojima S. Reactivity of human C-reactive protein with positively charged liposomes. *J Biochem.* (1981) 90:1507–14. doi: 10.1093/oxfordjournals.jbchem.a133617

78. Bhakdi S, Torzewski M, Klouche M, Hemmes M. Complement and atherogenesis: binding of CRP to degraded, nonoxidized LDL enhances complement activation. *Arterioscler Thromb Vasc Biol.* (1999) 19:2348–54. doi: 10.1161/01.atv.19.10.2348

79. Chang MK, Binder CJ, Torzewski M, Witztum JL. C-reactive protein binds to both oxidized LDL and apoptotic cells through recognition of a common ligand: phosphorylcholine of oxidized phospholipids. *Proc Natl Acad Sci USA.* (2002) 99:13043–8. doi: 10.1073/pnas.192399699

80. Bhakdi S, Torzewski M, Paprotka K, Schmitt S, Barsoom H, Suriyaphol P, et al. Possible protective role for C-reactive protein in atherogenesis: complement activation by modified lipoproteins halts before detrimental terminal sequence. *Circulation.* (2004) 109:1870–6. doi: 10.1161/01.CIR.0000124228.08972.26

81. Wang MS, Messersmith RE, Reed SM. Membrane curvature recognition by C-reactive protein using lipoprotein mimics. *Soft Matter.* (2012) 8:7909–18. doi: 10.1039/C2SM25779C

82. Carson SD, Ross SE. Effects of lipid-binding proteins apo A-I, apo A-IL, beta 2-glycoprotein I, and C-reactive protein on activation of factor X by tissue factor–factor VIIa. *Thromb Res.* (1988) 50:669–78. doi: 10.1016/0049-3848(88)90325-8

83. Dennis MW, Downey C, Brufatto N, Nesheim ME, Stevenson K, Toh CH. Prothrombinase enhancement through quantitative and qualitative changes affecting very low-density lipoprotein in complex with C-reactive protein. *Thromb Haemost.* (2004) 91:522–30. doi: 10.1160/TH03-08-0548

84. Nesheim M, Samis J, Walker J, Becker L, Brufatto N, Fischer T, et al. Lipoprotein-complexed C-reactive protein and the biphasic transmittance waveform in critically ill patients. *Blood Rev.* (2002) 16 Suppl 1:S15–22.

85. Hulman G. The pathogenesis of fat embolism. *J Pathol.* (1995) 176:3–9. doi: 10.1002/path.1711760103

86. Rowe IR, Soutar AK, Pepys MB. Agglutination of intravenous lipid emulsion ('Intralipid') and plasma lipoproteins by C-reactive protein. *Clin Exp Immunol.* (1986) 66:241–7.

87. Cheng Z, Abrams ST, Toh J, Wang SS, Downey C, Ge X, et al. Complexes between C-reactive protein and very low-density lipoprotein delay bacterial

clearance in sepsis. *J Immunol.* (2020) 204:2712–21. doi: 10.4049/jimmunol. 1900962

88. Potempa LA, Rajab IM, Hart PC, Bordon J, Fernandez-Botran R. Insights into the use of C-reactive protein (CRP) as a diagnostic index of disease severity in COVID-19 infections. *Am J Trop Med Hyg.* (2020) 103:561–3. doi: 10.4269/ajtmh. 20-0473

89. Skotland T, Sagini K, Sandvig K, Llorente A. An emerging focus on lipids in extracellular vesicles. *Adv Drug Deliv Rev.* (2020) 159:308–21. doi: 10.1016/j.addr. 2020.03.002

90. Crawford JR, Trial J, Nambi V, Hoogeveen RC, Taffet GE, Entman ML. Plasma levels of endothelial microparticles bearing monomeric c-reactive protein are increased in peripheral artery disease. *J Cardiovasc Transl Res.* (2016) 9:184–93. doi: 10.1007/s12265-016-9678-0

91. Habersberger J, Strang F, Scheichl A, Htun N, Bassler N, Merivirta RM, et al. Circulating microparticles generate and transport monomeric C-reactive protein in patients with myocardial infarction. *Cardiovasc Res.* (2012) 96:64–72. doi: 10.1093/cvr/cvs237

92. Pepys MB, Hirschfield GM, Tennent GA, Gallimore JR, Kahan MC, Bellotti V, et al. Targeting C-reactive protein for the treatment of cardiovascular disease. *Nature.* (2006) 440:1217–21. doi: 10.1038/nature04672

93. Singh SK, Agrawal A. Functionality of C-reactive protein for atheroprotection. *Front Immunol.* (2019) 10:1655. doi: 10.3389/fimmu.2019. 01655

94. Pathak A, Singh SK, Thewke DP, Agrawal A. Conformationally altered C-reactive protein capable of binding to atherogenic lipoproteins reduces atherosclerosis. *Front Immunol.* (2020) 11:1780. doi: 10.3389/fimmu.2020.0 1780

95. Cheng B, Lv J-M, Liang Y-L, Zhu L, Huang X-P, Li H-Y, et al. Secretory quality control constrains functional selection-associated protein structure innovation. *Comm Biol.* (2022) 5:268–78. doi: 10.1038/s42003-022-03220-3

96. Badimon L, Peña E, Arderiu G, Padró T, Slevin M, Vilahur G, et al. C-reactive protein in atherothrombosis and angiogenesis. *Front Immunol.* (2018) 9:430. doi: 10.3389/fimmu.2018.00430

97. Slevin M, Krupinski J. A role for monomeric C-reactive protein in regulation of angiogenesis, endothelial cell inflammation and thrombus formation in cardiovascular/cerebrovascular disease? *Histol Histopathol.* (2009) 24:1473–8. doi: 10.14670/HH-24.1473

98. Strang F, Scheichl A, Chen YC, Wang X, Htun NM, Bassler N, et al. Amyloid plaques dissociate pentameric to monomeric C-reactive protein: a novel pathomechanism driving cortical inflammation in Alzheimer's disease? *Brain Pathol.* (2012) 22:337–46. doi: 10.1111/j.1750-3639.2011. 00539.x

99. Slevin M, Matou-Nasri S, Turu MM, Luque A, Rovira N, Badimon L, et al. Modified C-reactive protein is expressed by stroke neo-vessels and is a potent activator of angiogenesis in vitro. *Brain Pathol.* (2010) 20:151–65. doi: 10.1111/ j.1750-3639.2008.00256.x

100. Zhang Z, Na H, Gan Q, Tao Q, Alekseyev Y, Hu J, et al. Monomeric C-reactive protein via endothelial CD31 for neurovascular inflammation in an ApoE genotype-dependent pattern: a risk factor for Alzheimer's disease? *Aging Cell.* (2021) 20:e13501–23. doi: 10.1111/acel.13501

101. Slevin M, Heidari N, Azamfirei L. Monomeric C-reactive protein: current perspectives for utilization and inclusion as a prognostic indicator and therapeutic target. *Front Immunol.* (2022) 13:866379. doi: 10.3389/fimmu.2022.866379

102. Heneka MT, Carson MJ, El Khoury J, Landreth GE, Brosseron F, Feinstein DL, et al. Neuroinflammation in Alzheimer's disease. *Lancet Neurol.* (2015) 14:388–405. doi: 10.1016/S1474-4422(15)70016-5

103. Feringa FM, van der Kant R. Cholesterol and Alzheimer's disease; from risk genes to pathological effects. *Front Aging Neurosci.* (2021) 13:690372. doi: 10.3389/fnagi.2021.690372

104. Tao Q, Alvin Ang TF, Akhter-Khan SC, Itchapurapu IS, Killiany R, Zhang X, et al. Alzheimer's disease neuroimaging initiative. impact of C-reactive protein on cognition and alzheimer disease biomarkers in homozygous apolipoprotein e ε4 carriers. *Neurology.* (2021) 97:e1243–52. doi: 10.1212/WNL.0000000000012512

105. Gewurz H, Mold C, Siegel J, Fiedel B. C-reactive protein and the acute phase response. *Adv Intern Med.* (1982) 27:345–72.

106. Pathak A, Agrawal A. Evolution of C-reactive protein. *Front Immunol.* (2019) 10:943. doi: 10.3389/fimmu.2019.00943

107. Potempa LA, Yao Z-Y, Ji S-R, Filep JG, Wu Y. Solubilization and purification of recombinant modified C-reactive protein from inclusion bodies using reversible anhydride modification. *Biophys Rep.* (2015) 1:18–33. doi: 10. 1007/s41048-015-0003-2

108. Lv JM, Chen JY, Liu ZP, Yao ZY, Wu YX, Tong CS, et al. mCellular folding determinants and conformational plasticity of native c-reactive protein. *Front Immunol.* (2020) 11:583–90. doi: 10.3389/fimmu.2020.00583

109. Narkates AJ, Volanakis JE. C-Reactive protein binding specificities: artificial and natural phospholipid bilayers. *Ann N Y Acad Sci.* (1982) 389:172–82. doi: 10.1111/j.1749-6632

110. Volanakis JE, Narkates AJ. Binding of human C4 to C-reactive protein-pneumococcal C-polysaccharide complexes during activation of the classical complement pathway. *Mol Immunol.* (1983) 20:1201–7. doi: 10.1016/0161-5890(83)90143-8

111. Richards RL, Gewurz H, Osmand AP, Alving CR. Interactions of C-reactive protein and complement with liposomes. *Proc Natl Acad Sci USA.* (1977) 74:5672–6. doi: 10.1073/pnas.74.12.5672

112. McFadyen JD, Zeller J, Potempa LA, Pietersz GA, Eisenhardt SU, Peter K. C-reactive protein and its structural isoforms: an evolutionary conserved marker and central player in inflammatory diseases and beyond. *Subcell Biochem.* (2020) 94:499–520. doi: 10.1007/978-3-030-41769-7_20

Multi-omics of *in vitro* aortic valve calcification

Daria Semenova[1,2†], Arsenii Zabirnyk[3,4†], Arseniy Lobov[1†],
Nadezda Boyarskaya[2], Olga Kachanova[2], Vladimir Uspensky[2],
Bozhana Zainullina[5], Evgeny Denisov[6],
Tatiana Gerashchenko[6], John-Peder Escobar Kvitting[3,4],
Mari-Liis Kaljusto[4], Bernd Thiede[3], Anna Kostareva[2],
Kåre-Olav Stensløkken[3], Jarle Vaage[3,4*†] and
Anna Malashicheva[1*†]

[1]Institute of Cytology Russian Academy of Science, St. Petersburg, Russia, [2]Almazov National
Medical Research Center Russia, St. Petersburg, Russia, [3]Heart Physiology Research Group, Division
of Physiology, Institute of Basic Medical Sciences, University of Oslo, Oslo, Norway, [4]Oslo University
Hospital, Oslo, Norway, [5]Centre for Molecular and Cell Technologies, St. Petersburg State
University, St. Petersburg, Russia, [6]Laboratory of Cancer Progression Biology, Cancer Research
Institute, Tomsk National Research Medical Center, Russian Academy of Sciences, Tomsk, Russia

Heart valve calcification is an active cellular and molecular process that partly remains unknown. Osteogenic differentiation of valve interstitial cells (VIC) is a central mechanism in calcific aortic valve disease (CAVD). Studying mechanisms in CAVD progression is clearly needed. In this study, we compared molecular mechanisms of osteogenic differentiation of human VIC isolated from healthy donors or patients with CAVD by RNA-seq transcriptomics in early timepoint (48 h) and by shotgun proteomics at later timepoint (10th day). Bioinformatic analysis revealed genes and pathways involved in the regulation of VIC osteogenic differentiation. We found a high amount of stage-specific differentially expressed genes and good accordance between transcriptomic and proteomic data. Functional annotation of differentially expressed proteins revealed that osteogenic differentiation of VIC involved many signaling cascades such as: PI3K-Akt, MAPK, Ras, TNF signaling pathways. Wnt, FoxO, and HIF-1 signaling pathways were modulated only at the early timepoint and thus probably involved in the commitment of VIC to osteogenic differentiation. We also observed a significant shift of some metabolic pathways in the early stage of VIC osteogenic differentiation. Lentiviral overexpression of one of the most upregulated genes (ZBTB16, PLZF) increased calcification of VIC after osteogenic stimulation. Analysis with qPCR and shotgun proteomics suggested a proosteogenic role of ZBTB16 in the early stages of osteogenic differentiation.

KEYWORDS

multi-omics, transcriptomics, proteomics, valve interstitial cells, calcification, aortic valve

Introduction

Heart valve calcification is an active cellular and molecular process that mostly remains unknown (1). Calcification of the aortic valve causing aortic stenosis is the most common pathology of heart valves in the Western world. Its occurrence increases exponentially with age (2). The only available treatment for calcific aortic valve disease (CAVD) is open-heart surgery or transcatheter aortic valve replacement (3). Thus, there is an urgent clinical need to develop pharmacological inhibition of calcification. Understanding the cellular and molecular mechanisms of calcification is essential for development of pharmacological inhibition.

Valve interstitial cells (VIC) are located between components of the extracellular matrix inside the valve leaflet (4). This heterogeneous group of cells is considered to play a key role in the pathogenesis of aortic valve stenosis and calcification (5). Under the influence of pathological biochemical and biomechanical stimuli, VIC can differentiate in an osteogenic direction, which eventually leads to aortic valve calcification (6).

One of the emerging approaches to unravel insight into the mechanisms of various diseases is a comprehensive and unbiased assessment of the whole set of proteins or transcripts by specific omics technologies such as proteomics and RNA sequencing (RNAseq). Our study aimed to investigate the differences of proteins, genes, and signaling of human VIC obtained from healthy donors and patients with aortic valve stenosis. Furthermore, to compare the molecular mechanisms of osteogenic differentiation in these groups using a paired multi-omics approach. Another aim was to identify novel players of calcification and identify perspective target(s) for anti-CAVD pharmacotherapy.

Materials and methods

Cell cultures

The study protocols were approved by the local Ethics Committee of the Almazov Federal Medical Research Centre and the Regional Ethics Committee South East Norway and performed in accordance with principles of the Declaration of Helsinki. In this study only valves from male donors were included in order to eliminate possible gender differences. All patients gave written informed consent. Human VIC were isolated from tricuspid aortic valves ($n = 12$) explanted during aortic valve replacement due to calcific aortic valve disease (CAVD) at the National Almazov Research Centre, Saint Petersburg, Russia and the Department of Cardiothoracic Surgery, Oslo University Hospital, Oslo, Norway. Patients with known infective endocarditis and rheumatic disease were excluded from the study. VIC from normal aortic valves which

were used as a control group were isolated from healthy tricuspid aortic valves obtained from explanted hearts from recipients of heart transplantation ($n = 12$).

To isolate VIC, valve leaflets were washed in PBS and incubated with 0.2% collagenase type 4 solution for 24 h at 37°C. Then the tissue was pipetted repeatedly to break up the tissue mass and centrifuged at 300 g for 5 min. The pellet containing VIC were resuspended in basic culture medium consisted of DMEM (Gibco) supplemented with 15% FBS (HyClone, GE Healthcare), 2 mM L-glutamine (Gibco), and 100 units/ml penicillin/streptomycin (Gibco), and plated on T75 flask.

VIC were cultured in standard growth medium (DMEM supplemented with 15% FBS and 100 units/ml penicillin/streptomycin at 37°C in 5% CO_2 until confluence of 70–80% before passaging. Cells from passages 3–5 were used for all experiments.

Induction of osteogenic differentiation

To induce osteogenic differentiation of VIC, we used classic osteogenic medium: DMEM supplemented with 10% FBS, 2 mM L-glutamine, 100 units/ml penicillin/streptomycin, 50 mg/ml ascorbic acid, 0.1 mM dexamethasone and 10 mM b–glycerophosphate.

The cells were plated: in 24-well tissue culture plates (33×10^3 cells per well) for Alizarin red staining; in 6-well tissue culture plates (220×10^3 cells per well) for RNA isolation; in 100-mm tissue culture dishes (750×10^3 cells per dish) for lysates obtaining. The cells were seeded in basic culture medium for 24 h at 37°C, 5% CO_2. The next day osteogenic differentiation was induced. The medium was changed twice a week over a 21-day differentiation period.

Alizarin red staining

Calcium deposits were visualized by Alizarin Red staining. Cells were washed with PBS, fixed in 70% ethanol for 60 min, washed twice with distilled water and stained using Alizarin Red solution (Sigma).

qPCR

RNA from cultured cells was isolated using ExtractRNA (Eurogene, Russia) by standard phenol/chloroform extraction procedure in accordance with the manufacturer's instructions. For RNA isolation, VIC were cultured for 48 h in the presence of osteogenic medium and in standard cultivation conditions. Total RNA (1 µg) was reverse transcribed with MMLV RT kit (Eurogen, Russia). Real-time PCR was performed with 1 µL cDNA and SYBRGreen PCRMastermix (Eurogen, Russia) in

the Light Cycler system using specific forward and reverse primers for target genes. Corresponding gene expression level was normalized to GAPDH from the same samples. Changes in target genes expression levels were calculated as fold differences using the comparative $\Delta\Delta CT$ method. All primers sequences can be presented at request.

RNA-seq transcriptomics

RNA quality was assessed by capillary electrophoresis using an Agilent Bioanalyzer 2100 (Agilent Technologies).

RNA-sequencing was carried out on the equipment of the Core Facility "Medical Genomics" (Tomsk NRMC) and the Tomsk Regional Common Use Center. The technology of highly processive sequencing of libraries prepared from total RNA was used to determine the transcriptomic profile of VIC cultures and evaluate differentially expressed genes, as well as analyze the involved signaling pathways. RNA was isolated from cell cultures from healthy aortic valves ($n = 6$) and from CAVD patients ($n = 6$) using standard phenol-chloroform procedure. Library preparation was performed using the Illumina TruSeq Stranded mRNA kit according to the manufacturer instructions. In brief, on the first library preparation stage, total RNA was incubated with oligo(dT) magnetic particles, while the particle hybridizes the fraction poly-adenylated RNA. After purification of the poly-adenylated fraction, a reverse transcription reaction was performed using a six-membered random primer. On the next step, the second DNA strand was synthesized. The acquired 3' pre-library DNA was adenylated and a paired end adapter ligation reaction was performed. After ligating the adapter, libraries were amplified using indexed primers. On the next step, the libraries were checked using the instrument Agilent Bioanalizer 2100. Libraries were sequenced on the Illumina NextSeq550 platform using single-ended reagents. All samples were run simultaneously. The raw data obtained by the sequencer was analyzed using software packages STAR, Rsem, DEseq2. For assembly were used GRCH38 reference using Gencode coding region annotation v28. The obtained data on differential expression was visualized by software packages included in the R programming environment and Phantasus program. Involved paths were explored using the base GSEA path data and the corresponding R environment package.

Shotgun proteomics of VIC under osteogenic differentiation

Mass spectrometry-based proteomic analyses were performed by the Proteomics Core Facility, Department of Biosciences, University of Oslo. This facility is a member of the National Network of Advanced Proteomics Infrastructure (NAPI), which is funded by the Research Council of Norway INFRASTRUKTUR-program (project number: 295910).

Material obtained from patients with aortic valve stenosis ($n = 8$) and healthy donors ($n = 8$) was used for proteomic analysis.

On the 10th day after induction of osteogenic differentiation, the cells were lysed in RIPA buffer (ThermoFisher Scientific) supplemented with protease inhibitors Roche cOmplete^{TM} Protease Inhibitor Cocktail (Sigma-Aldrich, United States). After isolation, the protein concentration was measured, and its quality was checked using PAGE electrophoresis.

The cell slurry was homogenized with a pestle (20x) for mechanical breakage of the cells followed by sonication using an Ultrasonic processor (Vibra-Cell, Sonics and Materials Inc., Newtown, CT, United States). Samples were centrifuged at 16,000 g for 20 min at 4°C. To 40 µl, four volumes of ice-cold acetone was added, vortexed and precipitated at $-20°C$ overnight. Samples were centrifuged at 16,000 $\times$ g for 20 min at 4°C and the supernatant was discarded. Proteins were re-dissolved in 50 µl 6 M urea and 100 mM ammonium bicarbonate, pH 7.8. For reduction and alkylation of cysteines, 2.5 µl of 200 mM DTT in 100 mM Tris–HCl, pH 8 was added and the samples were incubated at 37°C for 1 h followed by addition of 7.5 µl 200 mM iodoacetamide for 1 h at room temperature in the dark. The alkylation reaction was quenched by adding 10 µl 200 mM DTT at 37°C for 1 h. Subsequently, the proteins were digested with 10 µg trypsin for 16 h at 37°C. The digestion was stopped by adding 5 µl 50% formic acid and the generated peptides were purified using an OMIX C18-SPE, 10 µl (Agilent, Santa Clara, CA, United States), and dried using a Speed Vac concentrator (Concentrator Plus, Eppendorf, Hamburg, Germany).

The tryptic peptides were dissolved in 10 µl 0.1% formic acid/2% acetonitrile and 5 µl analyzed using an Ultimate 3000 RSLCnano-UHPLC system connected to a Q Exactive mass spectrometer (Thermo Fisher Scientific, Bremen, Germany) equipped with a nano electrospray ion source. For liquid chromatography separation, an Acclaim PepMap 100 column (C18, 2 µm beads, 100 Å, 75 µm inner diameter, 50 cm length) (Dionex, Sunnyvale CA, United States) was used. A flow rate of 300 nL/min was employed with a solvent gradient of 4–35% B in 100 min, to 50% B in 20 min and then to 80% B in 3 min. Solvent A was 0.1% formic acid and solvent B was 0.1% formic acid/90% acetonitrile. The mass spectrometer was operated in the data-dependent mode to automatically switch between MS and MS/MS acquisition. Survey full scan MS spectra (from m/z 400 to 2,000) were acquired with the resolution $R = 70,000$ at m/z 200, after accumulation to a target of 1e5. The maximum allowed ion accumulation times were 60 ms. The method used allowed sequential isolation of up to the ten most intense ions, depending on signal intensity (intensity threshold 1.7e4), for fragmentation using higher-energy collisional induced dissociation (HCD) at a target value of 1e5 charges, NCE 28, and a resolution $R = 17,500$. Target ions

already selected for MS/MS were dynamically excluded for 30 s. The isolation window was m/z = 2 without offset. For accurate mass measurements, the lock mass option was enabled in MS mode. Data were acquired using Xcalibur v2.5.5 and raw files were processed using ProteoWizard release version 3.0.331.

The identification and quantification of proteins from mass spectrometric data was carried out in the MaxQuant software in the "Label-free" quantification mode by default settings. MaxQuant output was analyzed in R by sparse partial least squares discriminant analysis (sPLS-DA) and differential expression analysis by "Limma" package. There were two groups of donors collected in the 2018 and 2019 years which were analyzed independently, but by the same method, in the 2018 and 2019 subsequently. Thus, we excluded batch effect associated with the year according to "Limma" package recommendations.

Functional annotation was performed by the DAVID— Database for Annotation, Visualization and Integrated Discovery (v6.8[1], accessed on 07/02/2022; and by SIGNAL— Selection by Iterative pathway Group and Network Analysis Looping [v1.0[2]; accessed 07/02/2022; (7)].

The mass spectrometry proteomics data and protein identification results have been deposited to the ProteomeXchange Consortium *via* the PRIDE partner repository.

Overexpression of ZBTB16 by lentiviral transduction

For overexpression we constructed plasmid for ZBTB16 overexpression by restriction cloning of full sequence of ZBTB16 to pCIG3 (pCMV-IRES-GFP version 3) plasmid purchased from Adgene (Plasmid #78264[3]; accessed 07/02/2022). Full-sized fragment of ZBTB16 mRNA was amplified from TetO-FUW (Addegene[4]) with the targeted insert (ZBTB16) using the primers with extinctions for restriction cloning: F: ATTCTGTAGAATTCGGCCACCATGGATCTGACAAAAT GGGCAT; R: ATTCTGTAGGATCCTCACACATAGCACAGG TAGAGGT.

Lentiviral production was performed as described previously by three plasmid system. In brief, 100-mm dishes of subconfluent 293T cells were co-transfected with 15 μg pCIG3-ZBTB16, 5.27 μg pMD2.G and 9.73 μg pCMV-dR8.74psPAX2 packaging by polyethylenimine (PEI). The following day, the medium was changed to the fresh one and the cells were incubated for 24 h to obtain high-titer virus production. Produced lentivirus was concentrated from the supernatant

---

1 https://david.ncifcrf.gov/

2 https://signal.niaid.nih.gov/

3 https://addgene.org/

4 https://www.addgene.org/61543/

by ultracentrifugation, resuspended in 1% BSA/PBS and frozen in aliquots at −80°C. The virus titer was defined by GFP-expressing virus; the efficiency of VIC transduction was 85–90% by GFP.

Lentiviral packaging plasmids were a generous gift from Prof. Didier Trono (École Polytechnique Fédérale de Lausanne, Switzerland). pGa981-6 plasmid was a gift from Prof. Urban Lendahl (Karolinska Institutet, Stockholm, Sweden).

Physiological effect of ZBTB16 overexpression was evaluated by Alizarine red staining and qPCR on *Runx2*, *Col1A1* and *Zbtb16* as described above.

Proteomics analysis of physiological effect of ZBTB16 overexpression

To evaluate physiological effect of ZBTB16 overexpression, we performed proteomics analysis of VIC in control (transduction with empty vector) and VIC with overexpression of ZBTB16 during osteogenic differentiation. Proteomic analysis was performed by "shotgun" approach, but analysis was performed by tandem mass spectrometry with trapped ion mobility at St. Petersburg State University core facility center "Molecular and Cell technologies."

On the 10th day after the induction of osteogenic differentiation, the cells were lysed in RIPA buffer (ThermoFisher, United States) supplemented with protease inhibitors Roche cOmplete[TM] Protease Inhibitor Cocktail (Sigma-Aldrich, United States). The cell slurry was sonicated on Ultrasonic bath with ice for 20 min. Samples were centrifuged at 16,000 *g* for 20 min at 4°C. To 100 μl, four volumes of ice-cold acetone was added, vortexed and precipitated at −20°C overnight. Samples were centrifuged at 16,000 × *g* for 20 min at 4°C and the supernatant was discarded. Protein pellet was washed by acetone, air-dried and re-dissolved in 8M Urea/50 mM ammonium bicarbonate (Sigma Aldrich, United States). Then the protein concentration was measured by QuDye Protein Quantification Kit (Lumiprobe, Russia) in Qubit 4.0 fluorometer (Thermo Fisher, United States).

20 μg of each sample were incubated for 1 h at 37°C with 5 mM DTT (Sigma Aldrich, United States) with subsequent incubation in 15 mM iodoacetamide for 30 min in the dark at RT (Sigma Aldrich, United States). Next, the samples were diluted with seven volumes of 50 mM ammonium bicarbonate and incubated for 16 h at 37°C with 400 ng of Trypsin Gold (ratio 1:50; Promega, United States). The sample was mixed with formic acid (Sigma Aldrich, United States) to 1% final concentration, evaporated in Labconco Centrivap Centrifugal Concentrator and desalted with C18 ZipTip (MilliporeSigma, United States) according to manufacturer recommendations. Desalted peptides were evaporated and dissolved in water/0.1% formic acid for further LC-MS/MS analysis.

Approximate 500 ng of peptides were used for shotgun proteomics analysis by nanoHPLC-MS/MS with trapped ion mobility in TimsToF Pro mass spectrometer (Bruker Daltonics, Germany). HPLC was performed in two-column separation mode with Acclaim PepMap 5 mm Trap Cartridge (Thermo Fisher, United States) and Bruker Fifteen separation column (C18 ReproSil AQ, 150 mm × 0.75 mm, 1.9 μm, 120 A; Bruker Daltonics, Germany) in gradient mode with 400 nL/min flow rate. Phase A was water/0.1% formic acid, phase B was acetonitrile/0.1% formic acid. The gradient was from 2% to 30% phase B for 42 min, then to 95% of phase B for 6 min with subsequent wash with 95% phase B for 6 min. CaptiveSpray ion source was used for electrospray ionization with 1,600 V of capillary voltage, 3 L/min N_2 flow, and 180°C source temperature. MS/MS acquisition was performed in automatic DDA PASEF mode with 0.5 s cycle in positive polarity with the fragmentation of ions with at least two charges in m/z range from 100 to 1,700 and ion mobility range from 0.85 to 1.30 1/K0.

Protein identification was performed in Peaks Xpro software (Bioinformatics Solutions Inc., Canada) using human protein SwissProt database[5] (accessed on 07/02/2022; organism: Human [9606]; uploaded on 2 March 2021; 20,394 sequences) and protein contaminants database CRAP[6] (version of 4 March 2019; accessed on 07/02/2022). The search parameters were: parent mass error tolerance 10 ppm and fragment mass error tolerance 0.05 Da, protein and peptide FDR less than 1%, two possible missed cleavage sites, proteins with at least two unique peptides were included for further analysis. Cysteine carbamidomethylation was set as fixed modification. Methionine oxidation, acetylation of protein N-term, asparagine, and glutamine deamidation were set as variable modifications.

The mass spectrometry proteomics data and protein identification results have been deposited to the ProteomeXchange Consortium *via* the PRIDE partner repository with the dataset identifier PXD031572.

Reviewer account details:

Username: reviewer_pxd031572@ebi.ac.uk

Password: X4dvODZ9

For statistical analysis we used the proteins with NA in less than 85% of samples, then performed imputation of missed values by k-nearest neighbors with subsequent $\log_2$-transformation and quantile normalization. Finally, we performed analysis of differential expression by "limma" package. Functional annotation was performed by the Database for Annotation, Visualization and Integrated Discovery (DAVID) v6.8[7] (accessed on 07/02/2022).

---

[5] https://www.uniprot.org/

[6] https://www.thegpm.org/crap/

[7] https://david.ncifcrf.gov/

Results

Global transcriptomic and proteomic signatures differ in VIC from patients with or without CAVD before and after osteogenic differentiation

VIC from healthy ($n = 6$) and calcified aortic valves ($n = 6$) were compared after cultivation in standard conditions and after osteogenic differentiation by transcriptomics (after 48 h) and by proteomics after 10 days.

After bioinformatics processing, we identified 17,850 transcripts and 1,594 proteins. Despite different time points, most of the transcripts corresponding to proteins found by proteomics were also identified in RNA-seq (**Figure 1A**).

We performed analysis on the obtained data by Partial Least Squares discriminant analysis (PLS-DA; **Figures 1B,C**). Control and differentiated cells formed distinct clusters, while VIC from healthy donors and patients with CAVD demonstrated partly overlapping groups on both proteomics and transcriptomics data. Nevertheless, proteomics data show that VIC from healthy and diseased donors represent distinct clusters on the 10th day after induction of osteogenic differentiation (**Figure 1C**). Totally four predicted clusters were formed. Furthermore, VIC from patients with CAVD have physiological differences which influence osteogenic differentiation *in vitro*.

However, we were unable to identify transcripts or proteins which were different between VIC from diseased and healthy donors. The only exception was protein arginine *N*-methyltransferase 5 (PRMT5, O14744) which was downregulated in control VIC from patients with CAVD by proteomics data compared to VIC from healthy aortic valves ($\log_2 FC = -20.16$; adjusted *P*-value < 0.001).

Molecular mechanisms of osteogenic differentiation in VIC

We performed an analysis of differentially expressed genes (DEGs) between control and differentiated VIC. While we quantified products of the same genes on different levels (transcripts and proteins) we translated transcript and protein names to corresponding gene names. Therefore, further we will use DEGs abbreviation for both RNA-seq and shotgun proteomics with specific clarification in which level expression was quantified. Two hundred-and-fourteen and 27 DEGs were up-regulated and 66 and 31 DEGs were down-regulated in transcriptomics and proteomics data, respectively, with at least fourfold difference in the cells after induction of osteogenic differentiation (**Figures 2A,B**).

These two datasets were from the same donors, but at different timepoints. Therefore, the overall Pearson correlation
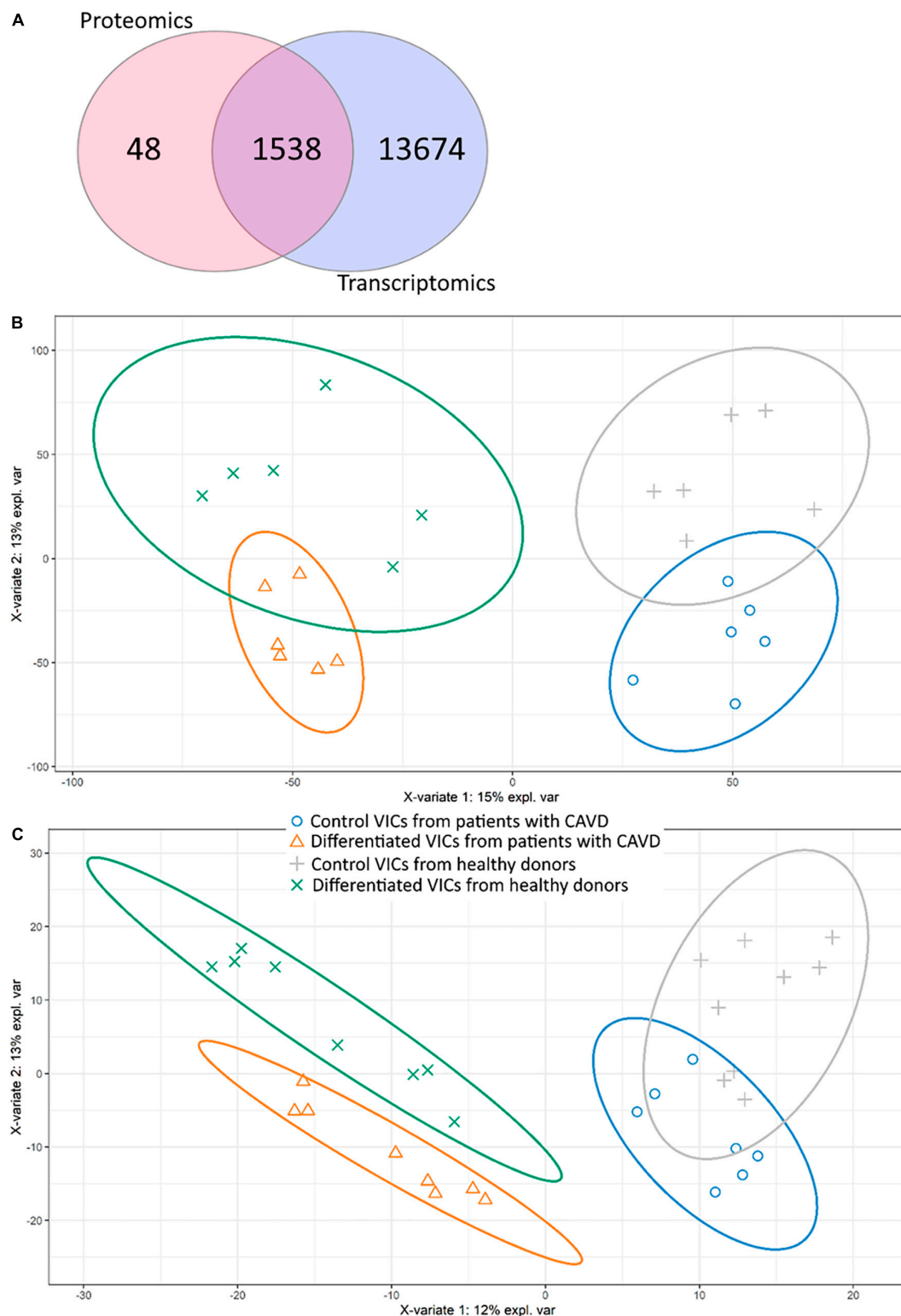
FIGURE 1
Comparison of proteomic and transcriptomic profiles of human valve interstitial cells (VIC) from patients with or without calcific aortic valve disease (CAVD) in standard cultivation (control) and in osteogenic medium (differentiated). **(A)** Venn diagram shows the number of unique gene products identified by shotgun proteomics and RNA-seq transcriptomics. (b-c) Partial least squares-discriminant analysis (PLS-DA) score plots based on transcriptomic **(B)** and proteomic **(C)** data. Yellow triangles—differentiated VIC from patients with CAVD, green crosses—differentiated VIC from healthy donors, gray pluses—control VIC from healthy donors, blue circles—control VIC from patients with CAVD.
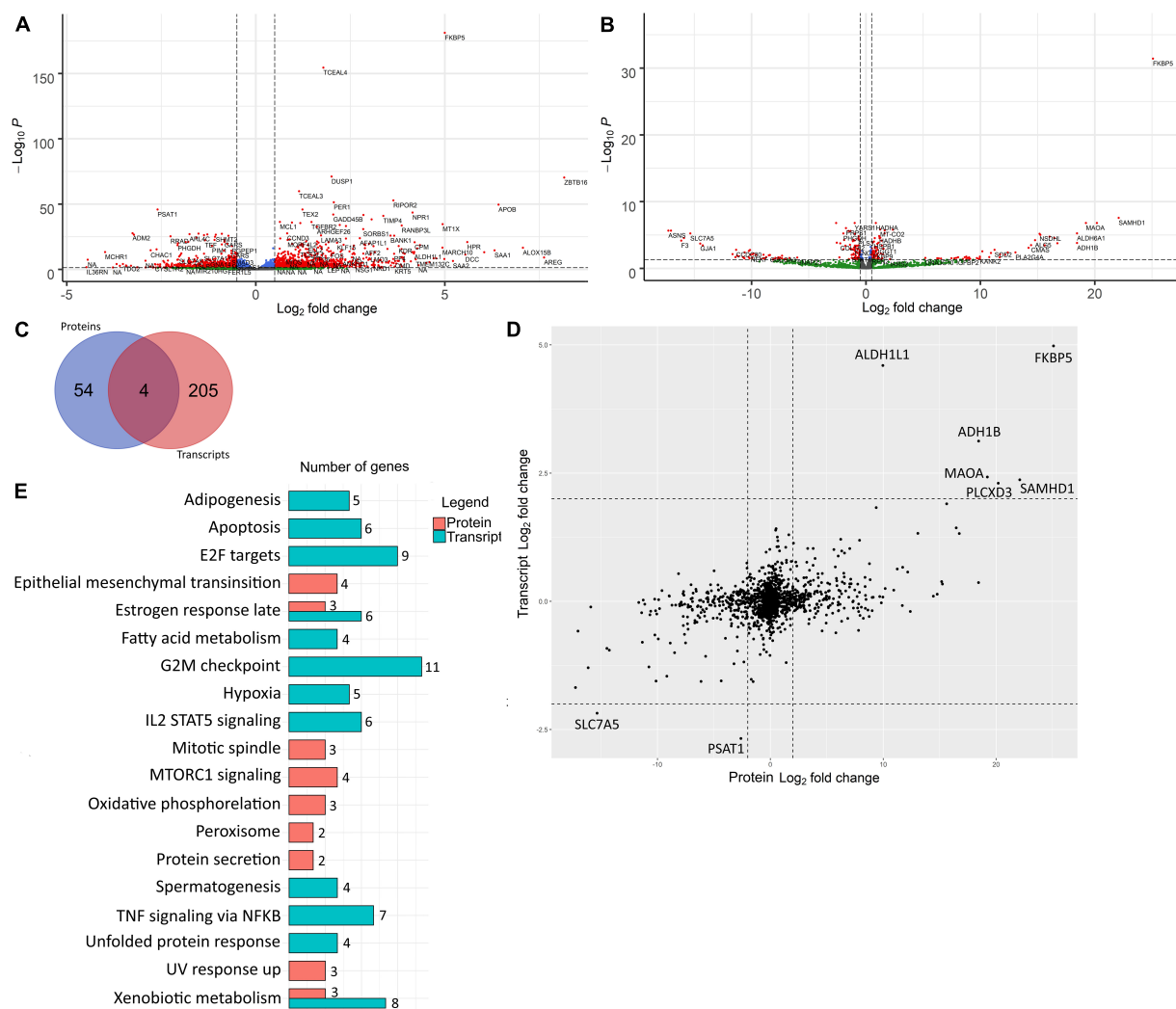
FIGURE 2

Differentially expressed genes involved in osteogenic differentiation of human valve interstitial cells (VIC) from healthy and calcified valves were identified by transcriptomics and proteomics analysis at early and late time points respectively. **(A)** Volcano plot of RNA-seq analysis of control VIC and 48 h after induction of osteogenic differentiation. Log$_2$ fold change—level of change in expression-Log10P—logarithm of P-value. Dotted lines cut off transcripts with P-value < 0.05 and Log$_2$ fold change > |1|. **(B)** Volcano plot of proteomics analysis of control VIC and 10 days after induction of osteogenic differentiation Log$_2$ fold change—level of change in expression-Log$_{10}$P—logarithm of P-value. Dotted lines cut off transcripts with P-value < 0.05 and Log$_2$ fold change > |1|. **(C)** Venn diagram representing overlapping of DEGs with Log$_2$ fold change > |2| between control and differentiated VIC founded in proteomic and transcriptomic data. **(D)** Scatter plot of comparison of Log$_2$Fold Change of genes identified in both proteomic and transcriptomic data. The dotted line separates the border of Log$_2$ fold change > |1|. **(E)** Bar chart representing the number of DEGs with Log$_2$ fold change > |2| found in proteomic and transcriptomic involved in biological processes based on their overlapping with information in Hallmark gene sets in MSigDB database. All represented overlaps have FDR q-values less than 0.05.

between proteomic and transcriptomic data was only 0.39. Accordingly, most of the major DEGs were unique for each time point (**Figure 2C**). Nevertheless, there were no DEGs with opposite expression levels in proteomic and transcriptomic data (**Figure 2D**). DEGs in early and later time points were involved in different biological processes except for estrogen response and xenobiotic metabolism which were enriched in both proteomic and transcriptomic DEGs (**Figure 2E**). After 48 h, most of the unique DEGs were associated with the cell cycle

("Apoptosis," "E2F targets," "G2M checkpoint"), differentiation ("Adipogenesis"), and signaling cascades ("Il2 stat5 signaling," "TNF signaling *via* NFKB"). At the later stage, there are DEGs associated with another signaling cascade ("mTORc1 signaling") and with metabolic changes ("Peroxisome," "Oxidative phosphorylation," "Epithelial mesenchymal transition," "UV response up," "Protein secretion").

Similar results were obtained by the enrichment analysis against KEGG database. The transcriptomics data at 48 h

showed that the DEGs were involved in the "Cell cycle" (8 DEGs, q-value 2.86 e^{-5}), "Drug metabolism cytochrome P450" (7 DEGs, q-value 1.81 e^{-5}) "neuroactive ligand receptor interaction" (7 DEGs, q-value 1.74 e^{-2}) "Tyrosine metabolism" (4 DEGs, q-value 4.1 e^{-3}) "Metabolism of xenobiotics by cytochrome P450" (4 DEGs, q-value 1.74 e^{-3}), "Glycine, serine and threonine metabolism" (3 DEGs, q-value 1.74 e^{-2}) and "Fatty acid metabolism" (3 DEGs, q-value 3.56 e^{-2}). While DEGs found based on proteomics data on the later stage are involved in "Huntington's disease" (4 DEGs, q-value 1.64 e^{-2}) and "Cardiac muscle contraction" (3 DEGs, q-value 1.64 e^{-2}).

For a more detailed analysis of enriched biological processes, we performed enrichment analysis of our transcriptomics and proteomics data sets against KEGG: biological processes database *via* signal-net analysis without additional fold change filtration (see footnote 2) [accessed 01.02.2022; (7); **Figures 3**, **4**]. We found a significant shift in VIC physiology in the early stages of osteogenic differentiation associated with the upregulation of many metabolic pathways. Good accordance was observed of proteomics and transcriptomics data at two different time points. Downregulated biological processes were more similar between time points while most of the upregulated biological processes were specific for either early or later timepoint (**Figures 3**, **4**).

For a more detailed study of inducers and participants of osteogenic differentiation, we present the top 24 up- or downregulated DEGs ranked according to statistical parameters and *Runx2* as one of the central regulators of osteogenic differentiation (log2Fold Change, *p*-value; **Figure 5**). The RNA-seq data for all 24 genes were all confirmed by the results of qPCR analysis (**Figure 5**).

The top upregulated genes included cell cycle regulators and transcriptional factors involved in metabolism (ALDH1L1, DUSP1, ITIH3, MARCH10, PDK4, MARCH10, PDK4, RGS2, SAA1, SAMHD1, TIMP4, TSC22; **Figure 5**); genes that regulate the processes of differentiation and cell adhesion (FKBP5, ITGA10, KLF15, MAOA, SORBS1, TIMP4; **Figure 5**). Some of genes associated with Notch and BMP signaling pathways were activated (RANBP3L, TMEM100; **Figure 5**), while others were suppressed (CHAC1, GREM2; **Figure 5**) upon induction of VIC osteogenic differentiation. Finally, we noted some genes that mediate cell proliferation and metabolic processes in the regulation of cardiovascular homeostasis (ADM2, PSAT1, RRAD).

ZBTB16 as an enhancer of osteogenic differentiation

One of the most upregulated early proteins involved in osteogenic differentiation of VIC was ZBTB16 (PLZF; **Figure 2**). To investigate its possible role in osteogenic differentiation, we performed lentiviral transduction by a genetic construction bearing full-length ZBTB16 gene. Overexpression of ZBTB16 (confirmed by qPCR and proteomics data; **Figures 6B,D**) increased mineralization measured by Alizarin red (**Figure 6A**) as well as the expression level of *Runx2* (master gene of osteogenic differentiation) and *Col1a* (**Figure 6B**).

To reveal possible molecular mechanisms by which ZBTB16 enhances osteogenic differentiation of VIC, we compared VIC in osteogenic conditions with and without ZBTB16 overexpression by lentiviral transduction using shotgun proteomics with ion mobility. Overall, 3,865 protein groups were identified, 2,293 of which were used for further analysis by sparse partial least square discriminant analysis (sPLS-DA) and differentially expressed genes (DEGs) analysis. We revealed two distinct clusters of VIC with or without overexpression of ZBTB16 (**Figure 6C**). Only nine upregulated and four downregulated DEGs had at least a twofold difference (**Figure 6D** and **Table 1**). Due to its overexpression, ZBTB16 (Q05516) was the mostly upregulated protein (**Figures 6B,D**).

Discussion

To investigate molecular mechanisms of experimentally induced aortic valve calcification *in vitro*, we performed proteotranscriptomic analysis of human VIC isolated from healthy and calcified aortic valves. VIC from healthy and diseased patients formed partially overlapping clusters of genes before and after osteogenic differentiation. These clusters demonstrated four distinct biological groups which are associated with molecular mechanisms of osteogenic differentiation. Overexpressing ZBTB16, one of the most upregulated genes from the transcriptomic analysis, increased calcification in VIC after osteogenic stimulation.

Omic studies represent an important tool for assessment of molecular mechanisms underlying biological processes. It is not clear, however, which material is best to use. We used primary VIC *in vitro* culture. This has some obvious disadvantages as the cells *in vitro* may be different from the cells inside the living valve leaflet. Several studies have identified changes in transcripts (8) or proteins (9–13) in the blood of CAVD patients. This approach benefits from the availability of the material and can also identify biomarkers for CAVD. An obvious drawback of this approach is a non-specific footprint of the blood transcriptome with minimal aortic valve transcriptome/proteome contribution.

This problem might be solved by a target analysis of aortic leaflets secretome (14, 15), proteomics (16–24), or transcriptomics (25–27) investigations on the whole human leaflets extracted during surgery. Such data give *in vivo* insight into disease pathogenesis. Nevertheless, it has an important drawback providing the mixed data from all cell subtypes present in the calcified valve leaflet. A recent study by Kossar et al. (28) combined both blood and whole aortic leaflets
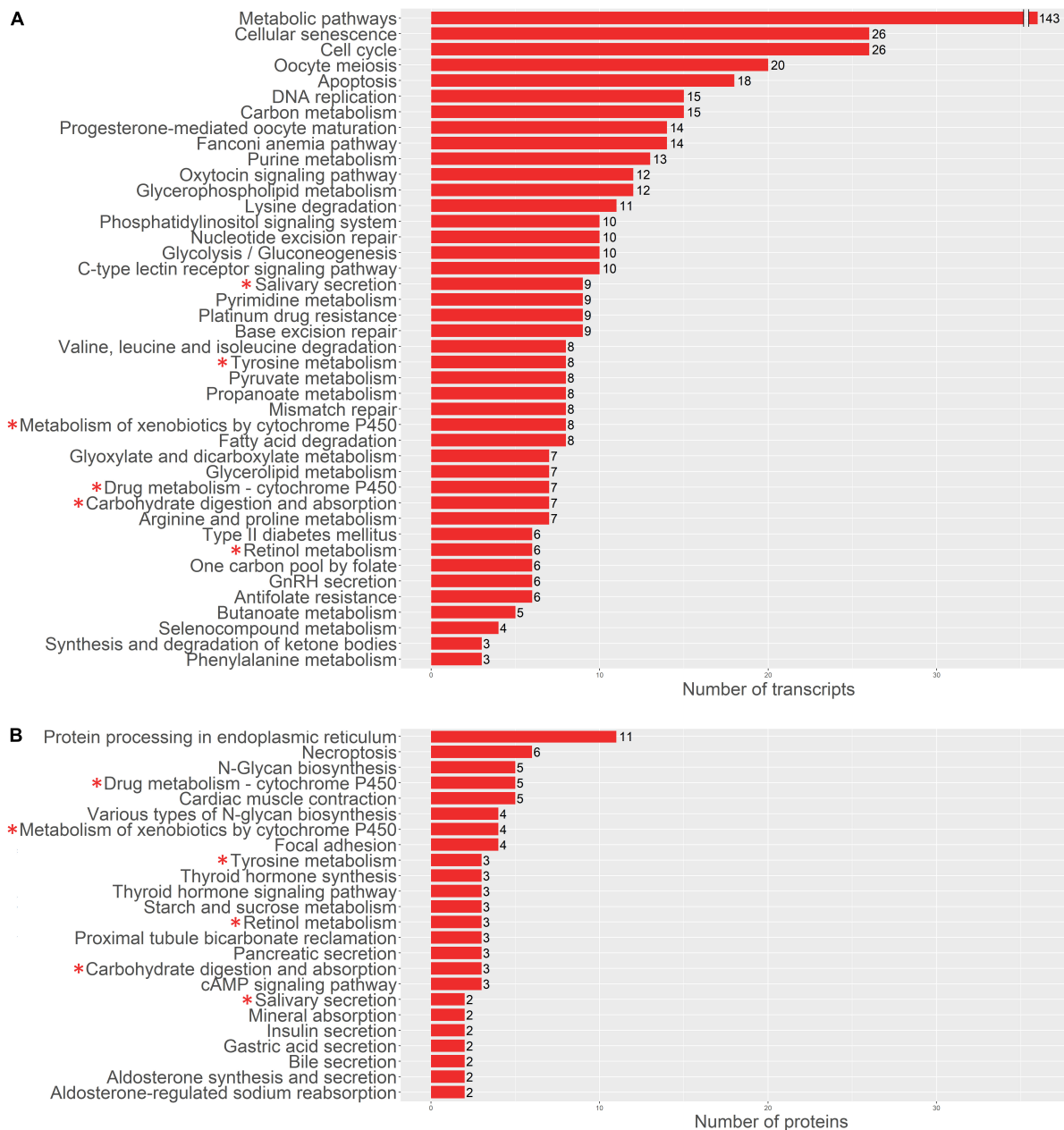
FIGURE 3

Pathway enrichment analysis of upregulated genes involved in osteogenic differentiation of human aortic valve interstitial cells (VIC) by KEGG: biological processes database. Abscissa axis represents biological processes associated with VIC osteogenic differentiation in early timepoint by RNA-seq transcriptomics data **(A)** or later timepoint by shotgun proteomics data **(B)**; ordinate axis represents number of identified differentially expressed transcripts **(A)** or proteins **(B)** enriched in corresponding biological process. Asterisk marked KEGG (*): biological processes enriched in both proteomics and transcriptomics data.

RNA-sequencing and identified extracellular matrix regulators as possible CAVD markers and targets for therapy. Using several sources (whole leaflet, its secretome, and plasma) for omics analysis in CAVD combined with transcriptomics (29) or proteomics (30) have been reported. Finally, to obtain omics data from the cells responsible for valve calcification (namely VIC), proteomics have been performed on primary

rat (31), bovine (30, 32), and human (33–35) VIC cultures from both healthy or calcified valves. Unlike investigations in blood and valve leaflets, employment of primary cell cultures provides possibilities for functional analysis in the naïve and osteoblast-like state leading to calcification. By analyzing human VIC populations transcriptome, Xu et al. (36) identified novel functional interactions among resident VIC subpopulations.
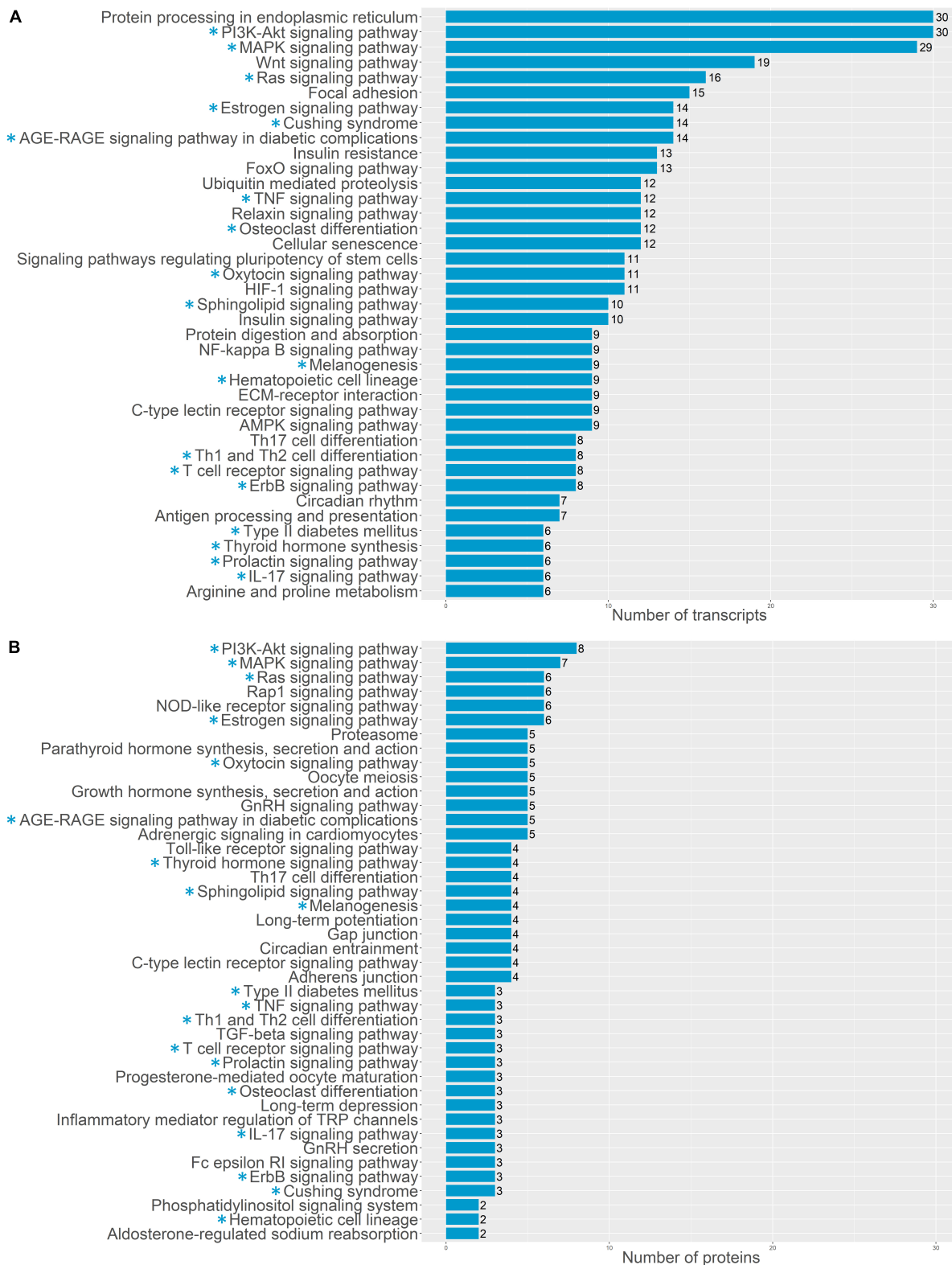
FIGURE 4

Pathway enrichment analysis of upregulated genes involved in osteogenic differentiation of human aortic valve interstitial cells (VIC) by KEGG: biological processes database. Abscissa axis represents biological processes associated with VIC osteogenic differentiation in early timepoint by RNA-seq transcriptomics data **(A)** or later timepoint by shotgun proteomics data **(B)**; ordinate axis represents number of identified differentially expressed transcripts **(A)** or proteins **(B)** enriched in corresponding biological process. Asterisk marked KEGG (*): biological processes enriched in both proteomics and transcriptomics data.
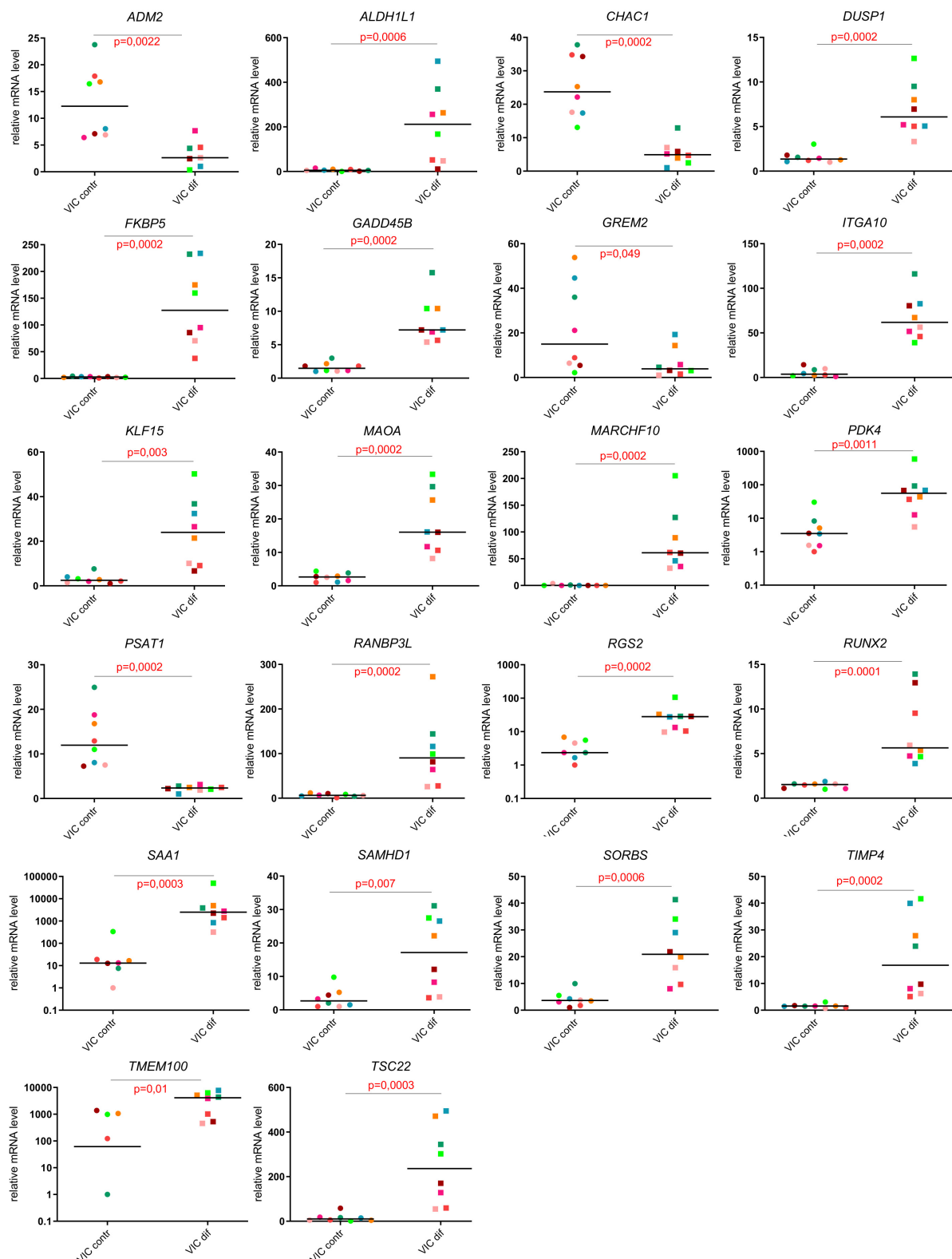
FIGURE 5

Evaluation of the expression levels of the most responsive genes in comparison of undifferentiated and differentiated human valve interstitial cells (VIC) from healthy donors and patients with CAVD using qPCR.
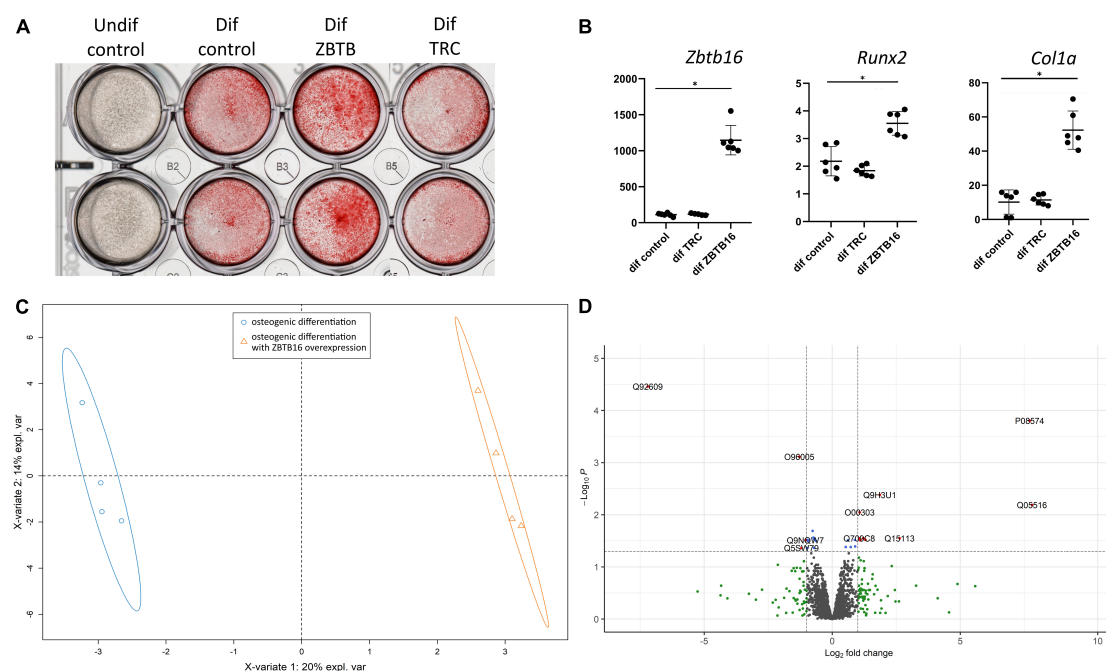
FIGURE 6

Effect of ZBTB16 (PLZF) on human valve interstitial cells (VIC) osteogenic differentiation. **(A)** Results of Alizarine red stain of VIC cultured in standard medium (undif control), osteogenic medium (dif control), osteogenic medium with transduction by an empty vector (dif TRC), osteogenic medium with transduction by construction for ZBTB16 overexpression (dif ZBTB). **(B)** Results of qPCR of *Zbtb16*, *Runx2*, and *Col1a* in VIC cultured in standard medium (undif control), osteogenic medium (dif control), osteogenic medium with transduction by construction for ZBTB16 overexpression (dif ZBTB). **p*-value < 0.05. **(C)** Clusterization by sparse partial least square discriminant analysis (sPLS-DA). **(D)** Volcano plot demonstrating results of analysis of differential expression by limma between VIC in osteogenic conditions and VIC in osteogenic conditions with ZBTB16 overexpression. Log$_2$ fold change—level of change in expression -Log$_{10}$P—logarithm of adjusted p–value. Dotted lines cut off transcripts with adjusted *p*-value < 0.05 and Log$_2$ fold change > |1|.

Recently, studies combining proteomics and transcriptomics, called multi-omics, have emerged. In a pioneer study, a comprehensive investigation in whole human valve tissue and cell culture was performed. However, this study only employed VIC from calcified valves (37). The present investigation using VIC from both healthy donors and patients with CAVD might fill some gaps of knowledge.

Valve interstitial cells from patients with CAVD have properties leading to epigenomic changes

As seen in sPLS-DA plots (**Figure 1**) and in qPCR verification of omics data (**Figure 4**), there were high biological variation between the individual donors of VIC. Human cell donor-to-donor heterogeneity is known to be high and should be taken into account (38). Thus, observed high variation is assumed to have biological nature. Such high intragroup variation reduces sensitivity of differential expression analysis. Nonetheless, we identified Protein arginine *N*-methyltransferase 5 (PRMT5, O14744) as markedly downregulated in VIC isolated from patients with CAVD. Protein arginine methyltransferases

(PRMTs) are enzymes that catalyze methylation on protein arginine residues. Histones are the main PRMTs target, but they also demethylate many other proteins (39). PRMT5 has been suggested to define an osteogenic context. Kota et al. (40) demonstrated that selective inhibition of PRMT5 in murine bone marrow stromal cells led to increased osteoblast differentiation through blockage of symmetric dimethylation of H3R8 and H4R3 (40). Other epigenetic mechanisms were also previously revealed to be involved in CAVD progression. Theodoris et al. (41) demonstrated that Notch1 haploinsufficiency led to differential H3K27ac at Notch1-bound enhancers (41). The epigenetic changes in VIC may form their osteogenic phenotype and promote calcification (42). Targeted comparison of the epigenome of VIC from patients with CAVD and healthy donors needs to be studied in future studies.

Mesenchymal stem cells (MSC) are often used in studies of osteodifferentiation. Molecular mechanisms of osteogenic differentiation of VIC are assumed to be similar, but not the same as osteogenic differentiation of MSCs and osteoblasts (43, 44). Unique molecular mechanisms of VIC osteogenic differentiation may be possible targets for anti-CAVD therapy. We found that molecular mechanisms of VIC osteogenic differentiation

TABLE 1 Differentially expressed proteins between human valve interstitial cells (VIC) in osteogenic conditions and VIC in osteogenic conditions with ZBTB16 overexpression.

Uniprot Accession	Gene name	Log$_2$FC	adj.P.Val
Upregulated proteins			
Q05516	ZBTB16	7.8	0.00647
P08574	CYC1	7.7	0.00016
Q15113	PCOLCE	2.6	0.02827
Q9H3U1	UNC45A	1.85	0.00415
P50281	MMP14	1.3	0.03024
Q9BVM4	GGACT	1.2	0.02827
Q92504	SLC39A7	1.1	0.03077
O00303	EIF3F	1.1	0.00897
Q709C8	VPS13C	1.05	0.02827
Downregulated proteins			
Q92609	TBC1D5	−7.2	3.46e-05
O96005	CLPTM1	−1.3	0.00077
Q5SW79	CEP170	−1.2	0.04325
Q9NQW7	XPNPEP1	−1	0.03077

Log$_2$FC — Log$_2$ of fold change in expression, adj.P.Val—adjusted *P*-value.

described by us differ from mechanisms of MSC osteogenic differentiation described previously. Comparison of MSC and VIC ostedifferentiation is presented in supplementary data.

ZBTB16 increased *in vitro* aortic valve calcification

Based on proteomics and transcriptomics data, we detected several proteins which have been less studied in cardiovascular calcification, including ZBTB16 (PLZF). ZBTB16 is a highly conservative zinc-finger transcription factor that might be found in a wide range of species from Nematoda to mammals. It has 9 DNA binding zinc finger domains in C-term. In N-term it has POZ domain involved in protein-protein interactions involved in transcription repression, e.g., by recruiting a histone deacetylase (45, 46). ZBTB16 has a vital role in spermatogenesis (47) and is involved in maintaining cell stemness through regulation of self-renewal and differentiation balance (45). In humans, ZBTB16 has no tissue specificity and might be identified in various tissues from the brain to the pancreas [by the data of Human Protein Atlas[8], accessed 18.01.2022; (48)].

This transcriptional factor is less studied in osteogenic differentiation, but it might be associated with skeletal development and osteoblast differentiation. ZBTB16 is not normally expressed in MSCs, but starts to express at

the early stages of osteoblast differentiation of MSCs (the second day from the start of osteogenic differentiation) (45). ZBTB16 expression in MSCs is controlled by epigenetic mechanisms—loss of H3K27me3 was accompanied by a strong gain of H3K27ac across the whole ZBTB16 locus. Moreover, ZBTB16 targets epigenome by itself—ZBTB16 influencing H3K27 acetylation at osteogenic genes and stimulating their expression (49). Therefore, ZBTB16 siRNA knockdown significantly reduced the expression of genes that were normally induced osteoblast committed of BM-MSCs (49).

In our study, ZBTB16 was one of the most upregulated genes during osteogenic differentiation of VIC. Overexpression of ZBTB16 significantly enhanced both matrix mineralization and RUNX2 and Col1A1 expression in VIC. Overexpression of ZBTB16 caused a relatively small number of DEGs. We did not find any described interactions in STRING database[9] (accessed 30.01.2022) between ZBTB16 and the DEGs induced by ZBTB16 overexpression.

One of the proteins upregulated by ZBTB16 is UNC45A. There is no systematic evaluation of its role in osteogenic differentiation. It is known that loss-of-function in UNC45A causes bone fragility (50). In the United States patent, US20110263675A1 authors provide UNC45A as one of the targets of miR-27a which has an important role in the shift of MSCs from adipogenic to osteogenic differentiation (51, 52).

eIF-3 is also upregulated by ZBTB16 overexpression. eIF-3 is associated with ribosomes where it recruits other eIF-proteins and forms pre-initiation complex. It was demonstrated that eIF-3 binds to specific mRNA 5' untranslated region and enhances translation of some mRNA involved in cell cycling, differentiation, and apoptosis (53). ZBTB16 has 5' untranslated exon (54), so we might assume that eIF-3 is involved in ZBTB16 translation.

Conclusion

We revealed physiological differences between valve interstitial cells (VIC) isolated from healthy donors before and after osteogenic differentiation which confirm pathological changes in VIC associated with CAVD progression. Signaling pathways might provide targets for anti-CAVD therapy. Finally, upregulation of ZBTB16 (PLZF) in VIC enhanced osteodifferentiation of VIC. This protein may be a target to inhibit soft tissue calcification.

---

8   https://proteinatlas.org/

9   https://string-db.org/

Data availability statement

Ethics statement

The studies involving human participants were reviewed and approved by Ethics Committee of Almazov National Medical Research Center, ethical permit 12.26/2014. The patients/participants provided their written informed consent to participate in this study.

Author contributions

Funding

Conflict of interest

The authors declare that the research was conducted in the absence of any commercial or financial relationships that could be construed as a potential conflict of interest.

Publisher's note

All claims expressed in this article are solely those of the authors and do not necessarily represent those of their affiliated organizations, or those of the publisher, the editors and the reviewers. Any product that may be evaluated in this article, or claim that may be made by its manufacturer, is not guaranteed or endorsed by the publisher.

References

1. Zebhi B, Lazkani M, Bark D Jr. Calcific aortic stenosis-a review on acquired mechanisms of the disease and treatments. *Front Cardiovasc Med.* (2021) 8:734175. doi: 10.3389/fcvm.2021.734175

2. Lamprea-Montealegre JA, Otto CM. Health behaviors and calcific aortic valve disease. *J Am Heart Assoc.* (2018) 7:e008385. doi: 10.1161/JAHA.117.008385

3. Head SJ, Çelik M, Kappetein AP. Mechanical versus bioprosthetic aortic valve replacement. *Eur Heart J.* (2017) 38:2183–91. doi: 10.1093/eurheartj/ehx141

4. Butcher JT, Mahler GJ, Hockaday LA. Aortic valve disease and treatment: the need for naturally engineered solutions. *Adv Drug Deliv Rev.* (2011) 63:242–68. doi: 10.1016/j.addr.2011.01.008

5. Rutkovskiy A, Malashicheva A, Sullivan G, Bogdanova M, Kostareva A, Stensløkken K-O, et al. Valve interstitial cells: the key to understanding the pathophysiology of heart valve calcification. *J Am Heart Assoc.* (2017) 6:e006339. doi: 10.1161/JAHA.117.006339

6. Dweck MR, Boon NA, Newby DE. Calcific aortic stenosis: a disease of the valve and the myocardium. *J Am College Cardiol.* (2012) 60:1854–63. doi: 10.1016/j.jacc. 2012.02.093

7. Katz S, Song J, Webb KP, Lounsbury NW, Bryant CE, Fraser IDC. Signal: a web-based iterative analysis platform integrating pathway and network approaches optimizes hit selection from genome-scale assays. *Cell Syst.* (2021) 12:338–52.e5. doi: 10.1016/j.cels.2021.03.001

8. Thériault S, Gaudreault N, Lamontagne M, Rosa M, Boulanger M-C, Messika-Zeitoun D, et al. A transcriptome-wide association study identifies PALMD as a susceptibility gene for calcific aortic valve stenosis. *Nat Commun.* (2018) 9:988. doi: 10.1038/s41467-018-03260-6

9. Gil-Dones F, Darde VM, Alonso-Orgaz S, Lopez-Almodovar LF, Mourino-Alvarez L, Padial LR, et al. Inside human aortic stenosis: a proteomic analysis of plasma. *J Proteomics.* (2012) 75:1639–53. doi: 10.1016/j.jprot.2011.11.036

10. Satoh K, Yamada K, Maniwa T, Oda T, Matsumoto K. Monitoring of serial presurgical and postsurgical changes in the serum proteome in a series of patients with calcific aortic stenosis. *Dis Mark.* (2015) 2015:694120. doi: 10.1155/2015/ 694120

11. Mourino-Alvarez L, Baldan-Martin M, Gonzalez-Calero L, Martinez-Laborde C, Sastre-Oliva T, Moreno-Luna R, et al. Patients with calcific aortic stenosis exhibit systemic molecular evidence of ischemia, enhanced coagulation, oxidative stress and impaired cholesterol transport. *Int J Cardiol.* (2016) 225:99–106. doi: 10.1016/j.ijcard.2016.09.089

12. Olkowicz M, Debski J, Jablonska P, Dadlez M, Smolenski RT. Application of a new procedure for liquid chromatography/mass spectrometry profiling of plasma amino acid-related metabolites and untargeted shotgun proteomics to identify mechanisms and biomarkers of calcific aortic stenosis. *J Chromatogr A.* (2017) 1517:66–78. doi: 10.1016/j.chroma.2017.08.024

13. Ljungberg J, Janiec M, Bergdahl IA, Holmgren A, Hultdin J, Johansson B, et al. Proteomic biomarkers for incident aortic stenosis requiring valvular replacement. *Circulation.* (2018) 138:590–9. doi: 10.1161/CIRCULATIONAHA.117.03 0414

14. de la Cuesta F, Alvarez-Llamas G, Gil-Dones F, Darde VM, Calvo E, Lopez JA, et al. Secretome of human aortic valves. Methods. *Mol Biol.* (2013) 1005:237–43. doi: 10.1007/978-1-62703-386-2_19

15. Alvarez-Llamas G, Martin-Rojas T, de la Cuesta F, Calvo E, Gil-Dones F, Darde VM, et al. Modification of the secretion pattern of proteases, inflammatory mediators, and extracellular matrix proteins by human aortic valve is key in severe aortic stenosis. *Mol Cell Proteomics.* (2013) 12:2426–39. doi: 10.1074/mcp.M113. 027425

16. Weisell J, Ohukainen P, Napankangas J, Ohlmeier S, Bergmann U, Peltonen T, et al. Heat shock protein 90 is downregulated in calcific aortic valve disease. *BMC Cardiovasc Disord.* (2019) 19:306. doi: 10.1186/s12872-019-01294-2

17. Martin-Rojas T, Mourino-Alvarez L, Alonso-Orgaz S, Rosello-Lleti E, Calvo E, Lopez-Almodovar LF, et al. iTRAQ proteomic analysis of extracellular matrix remodeling in aortic valve disease. *Sci Rep.* (2015) 5:17290. doi: 10.1038/srep17290

18. Gil-Dones F, Martin-Rojas T, Lopez-Almodovar LF, de la Cuesta F, Darde VM, Alvarez-Llamas G, et al. Valvular aortic stenosis: a proteomic insight. *Clin Med Insights Cardiol.* (2010) 4:1–7. doi: 10.4137/CMC.S3884

19. Matsumoto K, Satoh K, Maniwa T, Araki A, Maruyama R, Oda T. Noticeable decreased expression of tenascin-X in calcific aortic valves. *Connect Tissue Res.* (2012) 53:460–8. doi: 10.3109/03008207.2012.702818

20. Suzuki H, Chikada M, Yokoyama MK, Kurokawa MS, Ando T, Furukawa H, et al. Aberrant glycosylation of lumican in aortic valve stenosis revealed by proteomic analysis. *Int Heart J.* (2016) 57:104–11. doi: 10.1536/ihj.15-252

21. Bouchareb R, Guauque-Olarte S, Snider J, Zaminski D, Anyanwu A, Stelzer P, et al. Proteomic architecture of valvular extracellular matrix: FNDC1 and MXRA5 are new biomarkers of aortic stenosis. *JACC Basic Transl Sci.* (2021) 6:25–39. doi: 10.1016/j.jacbts.2020.11.008

22. Lim J, Aguilan JT, Sellers RS, Nagajyothi F, Weiss LM, Angeletti RH, et al. Lipid mass spectrometry imaging and proteomic analysis of severe aortic stenosis. *J Mol Histol.* (2020) 51:559–71. doi: 10.1007/s10735-020-09905-5

23. Schlotter F, de Freitas RCC, Rogers MA, Blaser MC, Wu PJ, Higashi H, et al. ApoC-III is a novel inducer of calcification in human aortic valves. *J Biol Chem.* (2021) 296:100193. doi: 10.1074/jbc.RA120.015700

24. Han RI, Hu CW, Loose DS, Yang L, Li L, Connell JP, et al. Differential proteome profile, biological pathways, and network relationships of osteogenic proteins in calcified human aortic valves. *Heart Vessels.* (2021) 37:347–58. doi: 10.1007/s00380-021-01975-z

25. Padang R, Bagnall RD, Tsoutsman T, Bannon PG, Semsarian C. Comparative transcriptome profiling in human bicuspid aortic valve disease using RNA sequencing. *Physiol Genom.* (2015) 47:75–87. doi: 10.1152/physiolgenomics.00115.2014

26. Wang J, Wang Y, Gu W, Ni B, Sun H, Yu T, et al. Comparative transcriptome analysis reveals substantial tissue specificity in human aortic valve. *Evol Bioinform Online.* (2016) 12:175–84. doi: 10.4137/EBO.S37594

27. Guauque-Olarte S, Droit A, Tremblay-Marchand J, Gaudreault N, Kalavrouziotis D, Dagenais F, et al. RNA expression profile of calcified bicuspid, tricuspid, and normal human aortic valves by RNA sequencing. *Physiol Genom.* (2016) 48:749–61. doi: 10.1152/physiolgenomics.00041.2016

28. Kossar AP, Anselmo W, Grau JB, Liu Y, Small A, Carter SL, et al. Circulating and tissue matricellular RNA and protein expression in calcific aortic valve disease. *Physiol Genom.* (2020) 52:191–9. doi: 10.1152/physiolgenomics.00104.2019

29. MacGrogan D, Martínez-Poveda B, Desvignes JP, Fernandez-Friera L, Gomez MJ, Gil Vilariño E, et al. Identification of a peripheral blood gene signature predicting aortic valve calcification. *Physiol Genom.* (2020) 52:563–74. doi: 10.1152/physiolgenomics.00034.2020

30. Renato M, Bertacco E, Franchin C, Arrigoni G, Rattazzi M. Proteomic analysis of interstitial aortic valve cells acquiring a pro-calcific profile. *Methods Mol Biol.* (2013) 1005:95–107. doi: 10.1007/978-1-62703-386-2_8

31. Cui L, Rashdan NA, Zhu D, Milne EM, Ajuh P, Milne G, et al. End stage renal disease-induced hypercalcemia may promote aortic valve calcification *via* annexin VI enrichment of valve interstitial cell derived-matrix vesicles. *J Cell Physiol.* (2017) 232:2985–95. doi: 10.1002/jcp.25935

32. Bertacco E, Millioni R, Arrigoni G, Faggin E, Iop L, Puato M, et al. Proteomic analysis of clonal interstitial aortic valve cells acquiring a pro-calcific profile. *J Proteome Res.* (2010) 9:5913–21. doi: 10.1021/pr100682g

33. Goto S, Rogers MA, Blaser MC, Higashi H, Lee LH, Schlotter F, et al. Standardization of human calcific aortic valve disease *in vitro* modeling reveals passage-dependent calcification. *Front Cardiovasc Med.* (2019) 6:49. doi: 10.3389/fcvm.2019.00049

34. Yu B, Khan K, Hamid Q, Mardini A, Siddique A, Aguilar-Gonzalez LP, et al. Pathological significance of lipoprotein(a) in aortic valve stenosis. *Atherosclerosis.* (2018) 272:168–74. doi: 10.1016/j.atherosclerosis.2018.03.025

35. Khan K, Yu B, Kiwan C, Shalal Y, Filimon S, Cipro M, et al. The role of Wnt/β-catenin pathway mediators in aortic valve stenosis. *Front Cell Dev Biol.* (2020) 8:862. doi: 10.3389/fcell.2020.00862

36. Xu K, Xie S, Huang Y, Zhou T, Liu M, Zhu P, et al. Cell-type transcriptome atlas of human aortic valves reveal cell heterogeneity and endothelial to mesenchymal transition involved in calcific aortic valve disease. *Arterioscler Thromb Vasc Biol.* (2020) 40:2910–21. doi: 10.1161/ATVBAHA.120.314789

37. Schlotter F, Halu A, Goto S, Blaser MC, Body SC, Lee LH, et al. Spatiotemporal multi-omics mapping generates a molecular atlas of the aortic valve and reveals networks driving disease. *Circulation.* (2018) 138:377–93. doi: 10.1161/CIRCULATIONAHA.117.032291

38. Phinney DG. Functional heterogeneity of mesenchymal stem cells: implications for cell therapy. *J Cell Biochem.* (2012) 113:2806–12. doi: 10.1002/jcb.24166

39. Couto ESA, Wu CY, Citadin CT, Clemons GA, Possoit HE, Grames MS, et al. Protein arginine methyltransferases in cardiovascular and neuronal function. *Mol Neurobiol.* (2020) 57:1716–32. doi: 10.1007/s12035-019-01850-z

40. Kota SK, Roening C, Patel N, Kota SB, Baron R. PRMT5 inhibition promotes osteogenic differentiation of mesenchymal stromal cells and represses basal interferon stimulated gene expression. *Bone.* (2018) 117:37–46. doi: 10.1016/j.bone.2018.08.025

41. Theodoris CV, Li M, White MP, Liu L, He D, Pollard KS, et al. Human disease modeling reveals integrated transcriptional and epigenetic mechanisms of NOTCH1 haploinsufficiency. *Cell.* (2015) 160:1072–86. doi: 10.1016/j.cell.2015.02.035

42. Bogdanova M, Zabirnyk A, Malashicheva A, Enayati KZ, Karlsen TA, Kaljusto ML, et al. Interstitial cells in calcified aortic valves have reduced differentiation potential and stem cell-like properties. *Sci Rep.* (2019) 9:12934. doi: 10.1038/s41598-019-49016-0

43. Kostina A, Lobov A, Semenova D, Kiselev A, Klausen P, Malashicheva A. Context-specific osteogenic potential of mesenchymal stem cells. *Biomedicines.* (2021) 9:673. doi: 10.3390/biomedicines9060673

44. Monzack EL, Masters KS. Can valvular interstitial cells become true osteoblasts? A side-by-side comparison. *J Heart Valve Dis.* (2011) 20:449–63.

45. Liu TM, Lee EH, Lim B, Shyh-Chang N. Concise review: balancing stem cell self-renewal and differentiation with PLZF. *Stem Cells.* (2016) 34:277–87. doi: 10.1002/stem.2270

46. David G, Alland L, Hong SH, Wong CW, DePinho RA, Dejean A. Histone deacetylase associated with mSin3A mediates repression by the acute promyelocytic leukemia-associated PLZF protein. *Oncogene.* (1998) 16:2549–56. doi: 10.1038/sj.onc.1202043

47. Costoya JA, Hobbs RM, Barna M, Cattoretti G, Manova K, Sukhwani M, et al. Essential role of Plzf in maintenance of spermatogonial stem cells. *Nat Genet.* (2004) 36:653–9. doi: 10.1038/ng1367

48. Uhlén M, Fagerberg L, Hallström BM, Lindskog C, Oksvold P, Mardinoglu A, et al. Proteomics. Tissue-based map of the human proteome. *Science.* (2015) 347:1260419. doi: 10.1126/science.1260419

49. Agrawal Singh S, Lerdrup M, Gomes AR, van de Werken HJ, Vilstrup Johansen J, Andersson R, et al. Plzf targets developmental enhancers for activation during osteogenic differentiation of human mesenchymal stem cells. *Elife.* (2019) 8:e40364. doi: 10.7554/eLife.40364

50. Esteve C, Francescatto L, Tan PL, Bourchany A, De Leusse C, Marinier E, et al. Loss-of-function mutations in UNC45A cause a syndrome associating cholestasis, diarrhea, impaired hearing, and bone fragility. *Am J Hum Genet.* (2018) 102:364–74. doi: 10.1016/j.ajhg.2018.01.009

51. Federov, Y, Leake D. Methods of modulating mesenchymal stem cell differentiation. Patent United States US20110263675A1. (2011).

52. You L, Pan L, Chen L, Gu W, Chen J. MiR-27a is essential for the shift from osteogenic differentiation to adipogenic differentiation of mesenchymal stem cells in postmenopausal osteoporosis. *Cell Physiol Biochem.* (2016) 39:253–65. doi: 10.1159/000445621

53. Lee AS, Kranzusch PJ, Cate JH. eIF3 targets cell-proliferation messenger RNAs for translational activation or repression. *Nature.* (2015) 522:111–4. doi: 10.1038/nature14267

54. van Schothorst EM, Prins DE, Baysal BE, Beekman M, Licht JD, Waxman S, et al. Genomic structure of the human Plzf gene. *Gene.* (1999) 236:21–4. doi: 10.1016/S0378-1119(99)00277-2

Check for updates

The critical issue linking lipids and inflammation: Clinical utility of stopping oxidative stress

Bradley Field Bale[1]*, Amy Lynn Doneen[1],
Pierre P. Leimgruber[1,2] and David John Vigerust[3]

[1]Department of Medical Education and Clinical Sciences, Washington State University College of Medicine, Spokane, WA, United States, [2]Department of Medical Education and Clinical Sciences, University of Washington School of Medicine, Seattle, WA, United States, [3]Department of Neurological Surgery, Vanderbilt University School of Medicine, Nashville, TN, United States

The formation of an atheroma begins when lipoproteins become trapped in the intima. Entrapped lipoproteins become oxidized and activate the innate immune system. This immunity represents the primary association between lipids and inflammation. When the trapping continues, the link between lipids and inflammation becomes chronic and detrimental, resulting in atherosclerosis. When entrapment ceases, the association between lipids and inflammation is temporary and healthy, and the atherogenic process halts. Therefore, the link between lipids and inflammation depends upon lipoprotein retention in the intima. The entrapment is due to electrostatic forces uniting apolipoprotein B to polysaccharide chains on intimal proteoglycans. The genetic transformation of contractile smooth muscle cells in the media into migratory secretory smooth muscle cells produces the intimal proteoglycans. The protein, platelet-derived growth factor produced by activated platelets, is the primary stimulus for this genetic change. Oxidative stress is the main stimulus to activate platelets. Therefore, minimizing oxidative stress would significantly reduce the retention of lipoproteins. Less entrapment decreases the association between lipids and inflammation. More importantly, it would halt atherogenesis. This review will analyze oxidative stress as the critical link between lipids, inflammation, and the pathogenesis of atherosclerosis. Through this perspective, we will discuss stopping oxidative stress to disrupt a harmful association between lipids and inflammation. Numerous therapeutic options will be discussed to mitigate oxidative stress. This paper will add a new meaning to the Morse code distress signal SOS-stopping oxidative stress.

KEYWORDS

oxidative stress, platelet-derived growth factor, smooth muscle cell transformation, proteoglycans, remnant cholesterol, lipoprotein retention

Introduction

The two special issues of Frontiers in Cardiovascular Medicine devoted to the association of lipids and inflammation are significant collections in consideration of atherosclerosis. Arterial diseases, both macro and micro, represent the most prevalent health issues related to morbidity and mortality. Macrovascular disease leads to the most common cause of death and sustained disability. Heart attacks have remained the

number one cause of mortality in the United States for over a century. Ischemic strokes are the fifth leading cause of death and the most common cause of severe long-term disability (1). Microvascular disease is prevalent and emerging as the primary etiology of chronic diseases of aging, including dementia (2). Such disease is responsible for Americans outliving their health by 13 years (3). The underlying pathology for both types of vascular disease is atherosclerosis (4). Pathogenesis of arterial disease depends on the development of chronic inflammation created by sustained activation of immunity from lipids (5). This review will discuss reducing oxidative stress as a measure to make this chronic situation addressable and surmountable.

———

Abbreviations: ACL, ATP citrate lyase; ADMA, Asymmetrical dimethylarginine; AHI, Apneas or hypopneas per hour; AMPK, Adenosine monophosphate-activated protein kinase; AngII, Angiotensin II; Angpt1, Angiopoietin—1; Angpt2, Angiopoietin 2; apoB, Apolipoprotein B; AQG, Air quality guidelines; ATP, Adenosine triphosphate; BA, Bempedoic acid; BB, Beta blockers; BMI, Body mass index; CAD, Coronary artery disease; CAT, Catalase; CCB, Calcium channel blockers; CKD, Chronic kidney disease; cIMT, Carotid intima-medial thickness; circMAP3K5, Circular mitogen-activated protein kinase—5; COX-2, Cyclooxygenase—2; CPAP, Continuous positive airway pressure; cSMC, Contractile smooth muscle cells; CV, Cardiovascular; CVD, Cardiovascular disease; EC-SOD, Extracellular superoxide dismutase; ED, Endothelial dysfunction; eNOS, endothelial nitric oxide synthase; ET-1, Endothelin-1; FA, Fatty acids; FRAP, Ferric-reducing ability of plasma; GGPP, geranyl-geranyl-pyrophosphate; GLP-1, Glucagon-like peptide-1; GLUT4, Glucose transporter—4; GPx, Glutathione peroxidase; GSH, Glutathione; HCV, Hepatitis C virus; HIV, Human immunodeficiency virus; HMG-CoA, 3-hydroxy-3-methylglutaryl coenzyme A; HTN, Hypertension; IDL, Intermediate-density lipoprotein; IR, Insulin resistance; LDL, Low-density lipoprotein; LDL-C, Low-density-lipoprotein cholesterol; MDA, Malondialdehyde; miR-22-3, MicroRNA 22-3; MPO, Myeloperoxidase; MRI, Magnetic resonance imaging; msSMC, Migratory secretory smooth muscle cells; mtDNA, Mitochondrial Deoxynucleic acid; NADPH, Nicotinamide adenine dinucleotide phosphate; NF-κB, Nuclear factor kappa B; NLRP3, (NOD)-like receptor protein-3; NO, Nitric oxide; Nrf2, Nuclear factor erythroid 2-related factor 2; OA, Oral appliance; OS, Oxidative stress; OSA, Obstructive sleep apnea; PCSK-9, Proprotein convertase subtilisin/kexin type 9; PDGF, Platelet-derived growth factor; PKC, Protein Kinase C; PLAC2, Lipoprotein-associated phospholipase A-2; RA, Rheumatoid arthritis; RAAS, Renin-angiotensin-aldosterone system; RCT, Randomized clinical trials; RNS, Reactive nitrogen species; ROS, Reactive oxygen species; RWE, Real world evidence; SGLT-2, Sodium-glucose cotransporter 2; SIRT3, Mitochondrial deacetylase sirtuin 3; SLE, Systemic lupus erythematosus; SOD, Superoxide dismutase; SOS, Stopping oxidative stress; T2DM, Type II diabetes Meletus; TBARS, Thiobarbituric acid-reactive substances; TET2, ten-eleven translocation-2; TG, Triglyceride; TGFβ, Tumor growth factor β; TLR, Toll-like receptors; TNFα, Tumor necrosis factor α; TXA2, Thromboxane A2; TXB2, Thromboxane B2; TZD, Thiazolidinediones; VLDL, Very-low-density lipoprotein.

Background

The pathogenesis of atherosclerosis begins with trapping lipoproteins in the intima during extravasation from the arterial lumen (6). Lipoproteins up to 70 nm can pass through endothelial cells *via* transcytosis. Therefore, all lipoproteins except the largest very-low-density lipoproteins (VLDL) and chylomicrons can enter the arterial wall from the lumen in a healthy state. These particles diffuse through the wall and efflux on the adventitial side. The critical factor in forming an atheroma is the retention of migrating lipoproteins in the intima. This entrapment occurs *via* electrostatic forces between apolipoprotein B (apoB) and polysaccharide chains in proteoglycans (7). The captured lipoproteins become aggregated and oxidized.

The resulting ox-LDL activates the immune system stimulating endothelial dysfunction (ED). A critical component of the pathogenesis of atherosclerosis is ED (8). The ox-LDL stimulates innate immunity in endothelial cells through toll-like receptors (TLRs). Stimulation of TLRs results in intracellular chemical reactions which activate nuclear factor-kappa B (NF-kB). As a result, the cell nucleus produces inflammatory cytokines such as interleukin 1 beta, interleukin 6, interleukin 18, and tumor necrosis factor alpha. In addition, NF-kB increases the inflammasome nucleotide-binding oligomerization domain (NOD)-like receptor protein 3 (NLRP3). One crucial function of NLRP3 is the assembly of caspase 1. The cytokines IL-1 beta and IL-18 require cleavage by caspase-1 to become functional. There is an accompanying increase in mitochondrial reactive oxygen species (ROS) which has a bidirectional relationship with NLRP3. The mitochondrial and inflammasome activity increases and preserves the OS. These multiple reactions of inflammation contribute significantly to ED (9). Lectin-like receptors for ox-LDL in the endothelium upregulate the production of intercellular cell adhesion molecule-1 and vascular cell adhesion molecule, which recruit monocytes into the intima. The lipid-proteoglycan complexes get phagocytized *via* scavenger receptors, leading to foam cell formation (10). The foam cells will coalesce into fatty streaks and subsequent atheroma. Accumulating evidence indicates endothelial shear stress and autophagy also play a critical role in the endothelial dysfunction of atherosclerosis (11). Regardless of the evolving science about the mechanisms of ED, continued retention of lipoproteins will perpetuate ED leading to chronic inflammation and ongoing pathogenesis of atherosclerosis (12).

Preventing and halting atherosclerosis requires eliminating apoB and its associated LDL-C from getting trapped in the intima. The retention would cease if proteoglycans were absent within the intima. Proteoglycans originate from contractile smooth muscle cells (cSMCs) in the media, which get genetically transformed into migratory secretory smooth muscle cells (msSMCs). The msSMCs then move into the deep layer of the

intima and produce proteoglycans (13). There are numerous triggers for the formation of msSMCs, but the most prominent is platelet-derived growth factor (PDGF). Therefore, inhibiting PDGF could significantly reduce atherogenesis (14). Oxidative stress (OS) is the primary stimulus to activate platelets (15). Activated platelets produce PDGF (16). Therefore, minimizing OS would significantly reduce the trapping of apolipoprotein B in the intima. Decreasing this first step in forming an atheroma would mitigate the association between lipids and chronic inflammation and impair the pathogenesis of atherosclerosis.

OS occurs when reactive oxygen species (ROS) are abundant relative to antioxidants. Mild OS can be beneficial. However, moderately or severely elevated levels of oxidants damage cellular components such as proteins, lipids, and nucleic acids. Such injury impairs cellular function and may cause apoptosis (17). Adenosine triphosphate (ATP), the primary cellular energy source, is formed from oxidant reactions. Mitochondria produce the majority of ATP and ∼90% of ROS. Other cellular elements, including cytoplasm, cell membrane, endoplasmic reticulum, and peroxisome, generate a minor amount of ROS. To maintain homeostasis, all of these cellular elements generate antioxidants (18). The mechanisms responsible for ROS production are complex, as are the mechanisms for antioxidant formation, and the explanatory science is still evolving (19, 20). Despite this, the science is definitive that OS is a significant facilitator of chronic degenerative pathologies (21). Mitochondrial therapy is being investigated for many chronic disease pathologies, including atherosclerosis, due to the pivotal role of mitochondria in OS (22, 23).

This review will analyze OS as the critical link between lipids, inflammation, and atherosclerosis. CV risk factors, both known and emerging, will be examined through the lens of OS. The discussion will be about managing these conditions and the judicial use of therapeutic options to stop OS. Reducing OS would result in sustainable prevention and halting of arterial disease. This paper will examine results from a real-world clinic using such a comprehensive approach. Stopping OS (SOS) is paramount in breaking the association between lipids and chronic inflammation. SOS is vital in achieving arterial wellness.

Traditional and emerging CV risks

In this section, known and evolving CV risk factors will be addressed through the lens of causing OS prior to the OS generated by lipoproteins retained in the intima. Any risk factor that produces such OS will enhance the trapping of lipoproteins and increase the chance of a chronic association between lipids and inflammation. This chronicity is due to an ongoing atherogenic process. Adequate management of CV risk factors will assuage OS, decreasing PDGF. As a result, msSMCs production will decrease, yielding the opportunity to halt atherogenesis (24).

Lipoproteins

Lipoproteins are a well-known traditional CV risk factor. Low-density-lipoprotein -cholesterol (LDL-C) has garnered the most attention as a risk for arterial disease. However, decades of evidence indicate that apoB is more predictive than LDL-C (25). This review focuses on OS generation prior to lipoprotein trapping in the intima. Some lipoproteins can generate OS in the plasma natively before intimal oxidation. Very low-density lipoprotein (VLDL), intermediate-density lipoprotein (IDL), and chylomicrons are inflammatory in their indigenous state. In contrast, low-density lipoprotein (LDL) is not inflammatory until it becomes trapped and oxidized in the intima (26).

The explanation involves capturing VLDL, IDL, and chylomicrons on the endothelium. After attaching to the endothelium, lipoprotein lipase (LPL) hydrolyses them, releasing free fatty acids into the circulation (27). Free fatty acids activate systemic OS (28, 29). In addition, Shin et al. have shown that VLDL, IDL, and chylomicrons in the plasma generate OS *via* stimulating nicotinamide adenine dinucleotide phosphate (NADPH) oxidase-dependent superoxide formation (30). Therefore, decreasing remnant cholesterol (VLDL, IDL, chylomicrons) should mitigate the formation of PDGF, reducing the genetic transformation of cSMCs. Thus, decreasing the first step in the pathogenesis of atherosclerosis. Supporting evidence for this is accumulating. In 2020, Castañer et al. demonstrated that remnant cholesterol, but not LDL-C, was associated with major adverse cardiovascular events independent of other risk factors (31). A review paper argues that remnant cholesterol promotes atherosclerosis beyond LDL-C (32). A cohort-based study found that elevated remnant cholesterol significantly increased the risk of myocardial infarction, ischemic stroke, and peripheral artery disease (33). Remnant cholesterol rises significantly postprandially. Not surprisingly, postprandial lipidemia is associated with the development of atherosclerosis and a heightened risk for CV events. OS increases with this type of lipidemia (34, 35). Fortunately, the severity of remnant cholesterol can be reduced in numerous ways, from lifestyle to altering the gut microbiome to nutraceutical and pharmacological interventions (36, 37). Current evidence indicates a need to take a clinical focus on reducing remnant cholesterol.

Hypertension

Hypertension is a significant risk factor for CVD. It is prevalent in approximately half of all Americans and at least a third of the world population (1). Hypertension was the number one risk factor for stroke (38). OS is central in hypertension. Factors involved in hypertension, such as angiotensin II, aldosterone, and endothelin 1, activate NADPH. This activity causes an increase in ROS, leading to systemic OS (39). As

demonstrated in hypertension, the ensuing OS will stimulate cSMCs to transform into msSMCs (40). Managing hypertension can disrupt this detrimental situation and reduce CV risk (41). More intensive control can potentially lower CV risk further (42). Numerous interventions to treat hypertension include lifestyle, behavioral therapies, over-the-counter supplements, and pharmaceutical agents (43, 44). Globally, ∼90% of patients with hypertension can be controlled (45). Achieving effective blood pressure management is a vital measure to prevent a chronic association between lipids and inflammation and the pathogenesis of atherosclerosis.

Direct or indirect smoking

Direct or indirect smoking is the most documented modifiable risk factor for arterial disease. Smoking now includes hookahs, e-cigarettes, and cigarettes. The extracts from the smoke generate the CV risk. These particles generate OS by reducing mitochondrial deacetylase sirtuin 3 (SIRT3), which increases the hyperacetylation of superoxide dismutase (SOD). This reduces the clearance of reactive oxygen species (ROS), generating systemic OS. In addition, nicotine is a ligand for alpha1 nicotinic acetylcholine receptors, which also induces cSMCs to transform into msSMCs (46). Therefore, exposure to nicotine in any form, including patches, chewing, and passive or active smoking, initiates atherosclerosis's pathogenesis. Smoking cessation and nicotine exposure avoidance are critical in disrupting the pathogenesis of atherosclerosis and a chronic association between lipids and inflammation.

As expected, decreasing smoking reduces CV mortality in CVD patients (35). Many studies have evaluated interventions to assist in the discontinuation of smoking. One of the early ones showed the benefit of the "5A's": ask, advise, assess, assist and arrange (47). Graphic pictures of the severe health issues from smoking can be a practical, motivational tool for smoking cessation (48). Evaluation of other factors to stimulate cessation have been published (49). More recently, a telemedicine approach using holistic counseling effectively enrolled non-motivated patients into treatment for cessation (50). Preventing atherosclerosis and a chronic association between lipids and inflammation demands smoking cessation.

Type 2 diabetes

Type 2 diabetes (T2DM) is an undisputable CV risk factor and is generally considered a coronary artery disease equivalent (51). Insulin resistance (IR) is the main underlying issue that drives individuals to T2DM (52). IR is prevalent globally in all social and ethnic demographics (53). Approximately one-third of Americans are prediabetic with underlying IR (54). There is a decrease in peripheral tissue cellular response to insulin with IR. Understanding the mechanism causing the blunted response relates to the pathogenesis of arterial disease. OS is the critical mechanism for the pathogenesis of IR. Individuals at risk for new-onset diabetes and, thus, who are prediabetic, have underlying conditions that cause OS. Individuals may have one or many of these issues. They include the following: inadequate sleep (55), low vitamin D (56), autoimmune disease (57), periodontal disease (58), elevated remnant cholesterol (59), hypertension (60), psychosocial issues (61), chronic infectious disease (62), air pollution (63), nicotine exposure (64), gut dysbiosis (65), elevated myeloperoxidase (66), poor diet (67), and a sedentary lifestyle (68). The increased ROS produced by these conditions blocks the skeletal muscle and adipose cells' insulin receptor ability to phosphorylate insulin receptor substrate-1 (IRS-1). The non-phosphorylation of IRS-1 results in the failure of glucose transporter 4 (GLUT4) migration to the cell membrane. GLUT4 is critical for glucose uptake by the cell; without it, hyperglycemia ensues (69). If the IR continues, the pancreatic beta cells become fatigued, leading to hypoinsulinemia and diabetic hyperglycemia (70). As the core reason for IR, OS explains the strong association between T2DM and CV risk. With comprehensive care managing all the modifiable conditions mentioned above, IR is preventable. Avoiding IR is a monumental step toward reducing CV risk.

Diet

Diet is well established as a factor influencing CV risk. Multiple healthy eating patterns are available (71). When evaluating various diets from an oxidative stress perspective, it is reasonable to expect a benefit from many diet patterns so long as the diet contains healthy choices. Foods that reduce CV risk contain significant amounts of antioxidants such as ascorbic acid, tocopherols, beta-carotene, flavonoids, polyphenols, and lycopene. Such natural antioxidant products include fruits, vegetables, grains, legumes, tea, and some fish. Consumption of these foods prevents or reverses systemic OS (72). This effect decreases PDGF production, reducing cSMCs transformation into msSMCs. Healthy foods decrease SMC transformation, which explains some of their anti-atherosclerosis effects (14). The amount of food eaten, even with healthy choices, is important. Overconsumption can lead to obesity and OS. Restricting calories by as little as 15% decreases OS (73). Remnant cholesterol surges postprandially. Therefore, it is no surprise that restricting consumption to a time frame of 10 h or less each day reduces systemic OS (74). The personalizing of the diet based on genetics

is gaining traction as a clinical tool to influence circulating lipoprotein levels. Pérez-Beltrán et al. published an extensive review regarding various gene variants that influence diets and the resultant circulating lipid levels. Their publication summarizes dietary recommendations related to numerous genetic polymorphisms (75). A nutrigenetic panel can provide individualized dietary advice to lower triglycerides, which represent the inflammatory remnant cholesterol lipoproteins. Dietary compliance would reduce OS. Books will continue to be written on one size fits all panacea CV risk-reducing diets. Knowledge does not support such a diet. Science does support food can reduce CV risk. The choices need to be healthy antioxidant foods, quantities that do not increase weight, consumption during a daily 10-h or less time frame, and personalized with genetics.

Physical activity

Physical activity is an irrefutable CV risk factor. Papers are continually published demonstrating either increased CV risk from being sedentary or decreased CV risk from being active (76). This finding is congruent with the effect of activity on OS. Chronic ROS overproduction in skeletal muscle cells induced by physical inactivity leads to systemic OS (77). Aerobic exercise reduces mitochondrial ROS production by suppressing NADPH oxidase expression. In addition, with aerobic exercise, there is increased catalase antioxidant activity. Damaged mitochondrial DNA (mtDNA) causes an increase in ROS. Exercise prevents the deterioration of mtDNA by increasing mtDNA content, enhancing ATP formation, and reducing mitochondrial swelling. It is important to note that resistive exercise reduces endothelin-1 (ET-1), an additional trigger for transforming cSMCs into msSMCs (78). Resistive exercise also significantly reduces OS. Elderly individuals who enrolled in a 12-week program demonstrated this effect.

The degree of physical activity is directly related to CV risk at any age (79, 80). As a critical initiator of atherogenesis, OS is fundamental in the relationship between activity and CV risk. Addressing physical activity with patients is a core element of management to reduce the risk of atherosclerosis. In the United States, guidelines recommend for adults 150 min a week of moderate-intensity or 75 min a week of vigorous-intensity. Only two-thirds of Americans are achieving those goals. In addition, the sedentary time has increased to 6.4 h a day (81). Latin Americans have similar guidelines recommending 150 min a week of moderate activity and $\leq$8 h/d of sedentary behavior. Only 48 and 22% achieved those goals, respectively (82). The Secretary of Health and Human Services issued a scientific report in 2018 on the vital importance of physical activity. The document contains a wealth of suggestions to assist in attaining higher compliance with physical activity (https://health. gov/our-work/nutrition-physical-activity/physical-activity-guidelines/current-guidelines/scientific-report). Educating people about the significance of avoiding OS to achieve arterial wellness could enhance conformity to guidelines. Physical activity is a powerful force to mitigate the pathogenesis of atherosclerosis.

Weight

Weight, as indicated by BMI, is considered one of the eight essentials for heart health (83). Khan et al. demonstrated that female individuals with BMI >25 have increased CVD risk (84). All obese (BMI $\geq$ 30) people, regardless of metabolic health, have elevated CV risk (85). Obesity is a substantial issue in America, where ~40% of adults are obese [National Center for Health Statistics, 2018. National Health and Nutrition Examination Survey. 2012. URL: http://www.CDC.gov/nchs/nhanes.htm (accessed 2014-09-08) (WebCite Cache)]. The CV risk involves OS. There are multiple mechanisms generating the OS. Fat accumulation increases NADPH oxidase activity and endoplasmic reticulum stress in adipocytes leading to increased production of ROS. Obesity also decreased the activity of superoxide dismutase (SOD), which is a powerful antioxidant. Obesity is associated with increased leptin, remnant cholesterol, and blood glucose, all of which drive OS (86). Weight is modifiable through numerous measures, including counseling, exercise, diet, medications, and surgery (87, 88). Eliminating excess weight is an effective tool to subdue the pathogenesis of arterial disease and a chronic association between lipids and inflammation.

Hyperuricemia

Hyperuricemia has been associated with CVD for decades. Numerous known CV risk factors, such as hypertension, abdominal obesity, insulin resistance, metabolic syndrome, and chronic kidney disease, are also associated with elevated uric acid. After adjusting for these known risk factors, some studies indicate hyperuricemia is not an independent CV risk factor (89). However, evolving evidence supports elevated uric acid as an independent CV risk factor (90). Hyperuricemia is associated with OS, which could provide the mechanism for an independent relationship with CVD. Impaired excretion of uric acid is the cause of ~90% of hyperuricemia. Elevated uric acid levels stimulate nicotinamide adenine dinucleotide phosphate (NADPH) oxidase, which leads to increased ROS. The resulting OS upregulates xanthine oxidoreductase activity which generates additional OS. This subject is complicated since uric acid can also perform as an antioxidant. Uric acid scavenges for carbon-centered radicals and peroxyl radicals which reduces OS. Uric acid

provides approximately half of the antioxidant activity in serum (91). Hyperuricemia also can inhibit PDGF- induced cSMC transformation to msSMCs (92). The ALL-HEART study presented by Dr. Isla Shelagh Mackenzie at the European Society of Cardiology Congress, Barcelona, Spain, on August 27, 2022, failed to show benefits in reducing CV risk with the xanthine oxidase inhibitor allopurinol in patients with ischemic heart disease. Due to the above conflicting information, it appears premature to consider hyperuricemia an independent CV risk factor.

Periodontal disease

Periodontal disease is an emerging CV risk factor (93). The high-risk periodontal pathogens are causal to atherosclerosis (94). One of the mechanisms involved is increasing the transformation of cSMCs to msSMCs (95). Periodontal disease, in general, also increases OS. Sharma and colleagues demonstrated the importance of OS generated by periodontal disease in chronic kidney disease (96). Therapy for periodontal disease reduces the levels of OS biomarkers (97). Therefore, the treatment of periodontal disease would reduce the pathogenesis of atherosclerosis by decreasing the trapping of lipoproteins in the intima. Approximately 65 million adults in the United States (US) have periodontitis, and in over 6 million, it is severe periodontal disease (98). Chronic periodontitis occurs in 68% of US adults $\geq$ 65 years of age (99). Globally periodontitis is the sixth most prevalent disease. Worldwide ~11% of adults have severe periodontitis (100). Managing periodontal disease represents a substantial opportunity to mitigate the chronic association between lipids and inflammation and reduce arterial disease.

In addition to periodontitis, other chronic infections are considered CV risk factors. Hepatitis C viral infection (HCV) is associated with a higher incidence of carotid atherosclerosis than non-HCV individuals. After adjusting for known CV risk factors, HCV independently predicts coronary and cerebral atherosclerosis risk (101). Human immunodeficiency virus (HIV) also appears to increase the risk of atherosclerosis independently. This finding suggests HIV should be considered a CV risk factor (102). Many chronic viral and bacterial infections are associated with heightened CV risk. Numerous mechanisms are involved in the overproduction of ROS by chronic infections. Studies have established that chronic infections increase oxidative stress (103). One consequence is the enrichment of proteoglycans in the intima to trap lipoproteins. Evidence is evolving that effective treatment of the pathogen causing the chronic infection will reduce CV risk (104, 105). Chronic infection will continue to evolve as a CV risk factor. Effective treatment of the causal pathogens would be expected to reduce the chronic

association between lipids and inflammation and reduce the risk of atherosclerosis.

Obstructive sleep apnea

Obstructive Sleep Apnea (OSA) is a well-established risk factor for strokes, heart attacks (106), obesity, metabolic syndrome, insulin resistance (107), hypertension (108), atrial fibrillation (109), and heart failure (110). The incidence of OSA is significant, affecting nearly one billion people worldwide (111), and represents a significant public health concern (112). A formal diagnosis of OSA utilizes a sleep study called polysomnography which monitors heart rate and rhythm, lung, and brain activity, breathing patterns, arm, and leg movements, and blood oxygen levels while asleep. The Diagnostic and Statistical Manual of Mental Disorders' five criteria for diagnosing OSA must record at least five obstructive apneas or hypopneas per hour of sleep (AHI). The apnea severity index includes mild apnea AHI 5–15, moderate AHI 15–30, and severe AHI > 30 (113). Airway obstructions predispose airways to collapse during inspiration, leading to alveolar hypoventilation, which induces sleep fragmentation through central nervous system activations (arousals). This intermittent hypoxia causes alterations in metabolic and immune system changes (114). OSA (at all levels of severity) results in recurrent periods of hypoxemia followed by reoxygenation, leading to ROS overproduction and increasing the inflammatory response. Chronic episodes of hypoxia followed by subsequent reoxygenation lead to the impairment of mitochondrial oxidative phosphorylation and induce the production of ROS, causing OS. In response to the OS due to OSA, the cSMCs become msSMCs (115). Many emerging and well-established therapies are available to treat OSA. These include the traditional continuous positive airway pressure therapy (CPAP), oral appliance (OA), and even upper airway stimulation devices. Depending on the severity of the OSA, each of these treatments can lead to amelioration of OSA (116). Data continues to emerge regarding the effectiveness of these treatments on the milieu of oxidative stress caused by untreated OSA (117). Diagnosis and management of OSA is critical in decreasing the chronic association of lipids and inflammation as well as atherosclerosis.

Psychosocial

Psychosocial is an established risk factor for cardiovascular risk. Epidemiological studies have confirmed the high co-morbidity between heart disease and psychosocial illnesses such as depression and anxiety. Immune system imbalance due to depression leads to platelet activation (118). Anxiety and depressive syndromes are associated with serotonin disruption.

Serotonin is involved with the homeostasis of platelet activity, vascular tone, thrombosis, and vasoconstriction resulting in negative CV consequences (119). Depression changes oxidative stress-related enzymes' activity leading to oxidative stress (120). Chronic stress response activates the nervous and sympathetic nervous system, ultimately stimulating cortisol secretion, leading to the onset of inflammation and OS (121). Severe anxiety is associated with OS in major depressive disorders (122). Evidence suggests a bidirectional association between psychosocial disorders and OS (123). Anti-depressive therapy reduces biomarkers of oxidative stress (124). Educational stress management reduces OS (125). Clinically, diagnosing and managing psychosocial impairments is essential to reduce the chronic association between lipids and inflammation by mitigating atherosclerosis's pathogenesis.

Vitamin D deficiency

Vitamin D deficiency is the most common nutrient deficiency worldwide. Low vitamin D levels are independently associated with coronary and carotid artery disease (126, 127). The inactive vitamin D precursors undergo 25-hydroxylation in the liver to form 25-hydroxyvitamin D [25(OH)D] (128). 25(OH)D is the primary circulating form of vitamin D and is therefore considered a circulating biomarker for vitamin D status. The definition of vitamin D insufficiency is serum 25(OH)D concentrations lower than 50 nmol/l (20 ng/ml) (129). Vitamin D is a potent antioxidant that facilitates healthy mitochondrial activity. Low levels of vitamin D impair mitochondrial functions, which causes OS. Adequate levels of vitamin D downregulate intracellular oxidative stress-related activities (130). Vitamin D has also been demonstrated to play a role in intracellular nuclear factor erythroid 2–related factor 2 (Nrf2) levels which are inversely related to the buildup of mitochondrial ROS, further leading to oxidative stress (131).

The knowledge about vitamin D and OS is congruent with the fact that vitamin D deficiency stimulates platelet activation (132). The activated platelets increase PDGF, increasing cSMCs to transform into msSMCs. A murine model showed that vitamin D supplementation inhibited the proliferation and transformation of vascular SMCs (133).

As expected, the increase in msSMCs will lead to retention of lipoproteins in the intima resulting in endothelial dysfunction through upregulation of NF-kB. Vitamin D decreases the signaling of NF-kB, which decreases the production of inflammatory cytokines (134). The cytokine IL-6 has a pro-atherothrombotic effect which vitamin D inhibits (135). Generally, vitamin D mitigates the harmful OS effects on the endothelium (136). Given the wealth of evidence that vitamin D deficiency is associated with numerous CV risk factors and the incidence of CVD, it is surprising that randomized trials have failed to show the benefit of vitamin D supplementation

for CVD (137). However, these trails have numerous limitations. One of the most significant is that no trials selected participants based on being deficient in vitamin D. Other issues to include are lack of power to demonstrate CVD benefits, significant variations in dosage of the supplement, inadequate length of follow-up, inability to analyze individual subject data and lack of standardization of 25(OH)D assay (138). Considering the overwhelming evidence that vitamin D deficiency is a CV risk factor, it seems prudent to assess a patient's 25(OH)D level clinically. If the level is inadequate, it seems reasonable to recommend management that would create an adequate level. Such action may impede the pathogenesis of atherosclerosis and the chronic association between lipids and inflammation.

The gut microbiome

The gut microbiome is considered the largest endocrine organ due to its immense production of biologically active metabolites. Adverse changes in the microbial composition are known as gut dysbiosis, which is associated with numerous CV risk factors, including hypertension, hyperlipidemia, and insulin resistance (139). Compared to individuals without atherosclerosis, patients with atherosclerosis have increased levels of *Streptococcus* and *Enterobacteriaceae* species (140). The gut microbiome signature represented by stool was significantly different in patients with coronary artery disease compared to healthy subjects. CAD patients had an abundance of *Escherichia-Shigella* and *Enterococcus* with a paucity of *Faecalibacterium*, *Subdoligranulum*, *Roseburia*, and *Eubacterium rectale* (141). Evidence continues to accumulate that gut dysbiosis is associated with the pathogenesis of atherosclerosis (142).

The gut microbiota metabolites influence mitochondrial ROS production, the production of antioxidants like glutathione, and Cyclooxygenase- 2 (COX-2) activity. These mechanisms allow commensal bacteria such as Lactobacilli and *Bifidobacteria* to lower OS and pathogenic bacteria like *Salmonella* and *E. coli* to increase OS (143–145). The relationship between systemic OS and gut dysbiosis is multidirectional. An increase in systemic OS increases the *E. coli* and *enterococcus* populations while lower the levels of *lactobacilli* (146). Mitigation of systemic OS with an antioxidant influenced the gut microbiome by increasing the quantity of commensal *Lactobacillus* and Bifidobacterium while decreasing the amount of pathogenic *E. coli* (147). The study of the gut microbiome is in its infancy. Scientists need to continue investigating the vastness of the role of gut microbial metabolites on health and OS. Therapies such as fecal transplants and probiotics need more formal research (148). The gut microbiome plays a critical role in CV health. There is a paucity of human data elucidating mechanistic insights. Future investigations are needed to improve clinical assessment and management of this novel CV risk factor (149).

Autoimmune diseases

Autoimmune diseases are well established as associated with heightened CV risk. Rheumatoid arthritis (RA), systemic lupus erythematosus (SLE), psoriasis, Sjogren's syndrome, and Crohn's disease show an increased risk of CV disease (150). RA increases the risk of a heart attack 7-fold, making it on par with T2DM for CVD risk (151). SLE triples the risk of heart disease (152). A hallmark feature of autoimmune disease is the increased production of ROS and reactive nitrogen species (RNS), leading to OS. An essential source of elevated ROS is mitochondrial dysfunction. Patients with RA compared to healthy subjects have a five-fold increase in mitochondrial ROS production. In addition, autoimmune disease patients generally have depleted levels of the antioxidant glutathione (153).

Rheumatoid arthritis (RA) as a prototype for autoimmune disease has been studied extensively in terms of OS. Mitochondria generate most of the ROS, creating the OS, which has a central role in the pathogenesis of RA. The relationship between OS and mitochondria is bidirectional. ROS attacks mitochondria causing destabilization and mutations of mtDNA. The damaged mitochondria create increased levels of ROS, resulting in a vicious cycle of OS. This knowledge helps explain why tumor necrosis factor (TNF) blocking agents reduce CV in RA patients. These agents suppress mitochondrial-generated OS. It also reinforces the need to study natural antioxidant agents known to reduce OS due to mitochondria, such as omega-3 and resveratrol (154). Clinically, it is reasonable to believe that management of autoimmune diseases focused on reducing OS will retard the pathogenesis of atherosclerosis and decrease the chronic association between lipids and inflammation.

Air pollution

Air pollution, a non-traditional CV risk factor, is exposure to fine particulate matter with a median aerodynamic diameter of <2.5 micrometers (μm) (PM2.5). Long-term exposure below the Environmental Protection Agency standard of <12 μg/m^3/annually increases CV risk (155). A study done in the European Union concluded that the risk from air pollution was higher than expected and significantly increased CV mortality (156). PM2.5 contains ROS and generates ROS from redox-active components. The current science unequivocally indicates that air pollution increases OS (157). OS is the central pathophysiological mechanism by which PM2.5 induces CV risk (158). This mechanism is supported by Abohashem et al.'s paper discussing animal studies that demonstrate PM2.5 activates the immune system resulting in increased production of monocytes from bone marrow and spleen. These monocytes then enter the atheroma. Using 18F-fluorodeoxyglucose positron emission tomography/computed tomography (18F-FDG-PET/CT) in humans, they found a direct

relationship between the degree of PM2.5 exposure and the degree of activity in the bone marrow and spleen. In addition, there was a direct relationship between the amount of PM2.5 exposure and inflammation in the ascending aorta. These results are expected consequences of trapping lipoproteins in the intima. The conclusion was that chronic PM2.5 exposure independently increases CV risk. They also mention that over 90% of the world population is exposed to levels of air pollution exceeding the WHO Air Quality Guidelines (AQG) of annual PM2.5 exposure of 10 μg/m^3, or 25 μg/m^3 24-h mean (159). Clinically, altering a patient's habitat is challenging, but patients deserve education about the CV risk of air pollution (160). Government policies to reduce PM2.5 should be a high priority (161). Individuals can check daily reports on the current level of air pollution. If the levels are unsafe, they should do their best to breathe filtered air. Reducing exposure to PM2.5 would positively decrease the chronic association between lipids and inflammation and reduce the risk of arterial disease.

Chronic kidney disease

Chronic kidney disease (CKD) is defined as two glomerular filtration rates (GFR) < 60 ml/min/1.73m² during 3 months or more or confirmed kidney damage for at least 3 months. CKD is considered an independent risk factor for CVD (162). CVD mortality doubles in stage 3 CKD and triples in stage 4 CKD (163, 164). A hallmark of CKD is OS which is present in the initial stages of the disease. CKD is strongly associated with age, hypertension, insulin resistance, dyslipidemia, nicotine use, OSA, vitamin D deficiency, air pollution, gut dysbiosis, neuropsychiatric disorders, poor lifestyle, obesity, autoimmune disease, periodontal disease, chronic infection, and hyperuricemia (96, 165–176). It seems reasonable that one or more of these conditions that increase OS may initiate the onset of CKD.

The increase in ROS injures the glomeruli. The OS generates structural injury to the very susceptible podocytes leading to glomerulosclerosis. A critical factor in the progression of CKD is the activation of transforming growth factor beta (TGF-β) in the podocytes. TGF-β suppresses mitochondrial function leading to additional OS and subsequent damage to mitochondrial DNA. The mechanisms through which mitochondrial damage and cellular dysfunction promote progression to renal failure are still under investigation. The increased albumin resulting in the urine can enter cells in the proximal tubules. As a result, protein kinase C (PKC) is activated, which further increases OS *via* ROS produced by NADPH oxidase. As explained earlier in the paper, hyperuricemia due to CKD can also heighten the OS level. Asymmetrical dimethylarginine (ADMA) levels are elevated in CKD. ADMA inhibits nitric oxide (NO) synthesis. Less NO results in an increase in ROS (177).

CKD is associated with decreased levels of cSMCs with an increase in msSMCs. Initially, hyperuricemia was felt to be the stimulus (92). However, more recent evidence indicates that caspase-1 is essential in CKD to induce the phenotypic change in cSMCs. CKD produces danger signal-associated molecular patterns such as hyperuricemia which can stimulate the innate immune system through TLRs generating caspase-1. CKD initiates a switch in SMCs from cSMCs to msSMCs. The mechanisms for this remain to be fully elucidated (178). It is apparent that mitigating the chronic association between lipids and inflammation requires curtailing the incidence of CKD (see Figure 1).

Treatment

Stopping oxidative stress (SOS) requires clinical management of all the discussed modifiable traditional and non-traditional CV risk factors. Those issues are remnant lipoproteins, hypertension, smoking, weight, diet, physical activity, insulin resistance, sleep, psychosocial, periodontal disease, other chronic infections, autoimmune disease, gut dysbiosis, vitamin D, and air pollution. This type of healthcare requires a holistic approach along with interdisciplinary collaboration. OS is the common denominator of the risk factors, making them interrelated (see Figure 1). For example, OS is at the root of insulin resistance pathogenesis which leads to T2DM. Therefore, it is no surprise that the above risk factors are associated with an increased risk of new-onset diabetes (55–64, 179–182). Accomplishing SOS demands comprehensive, integrated healthcare. Numerous frequently used drugs impact OS either directly or indirectly (183). This review analyzes many of these agents used to help manage CV risk through the lens of directly mitigating OS.
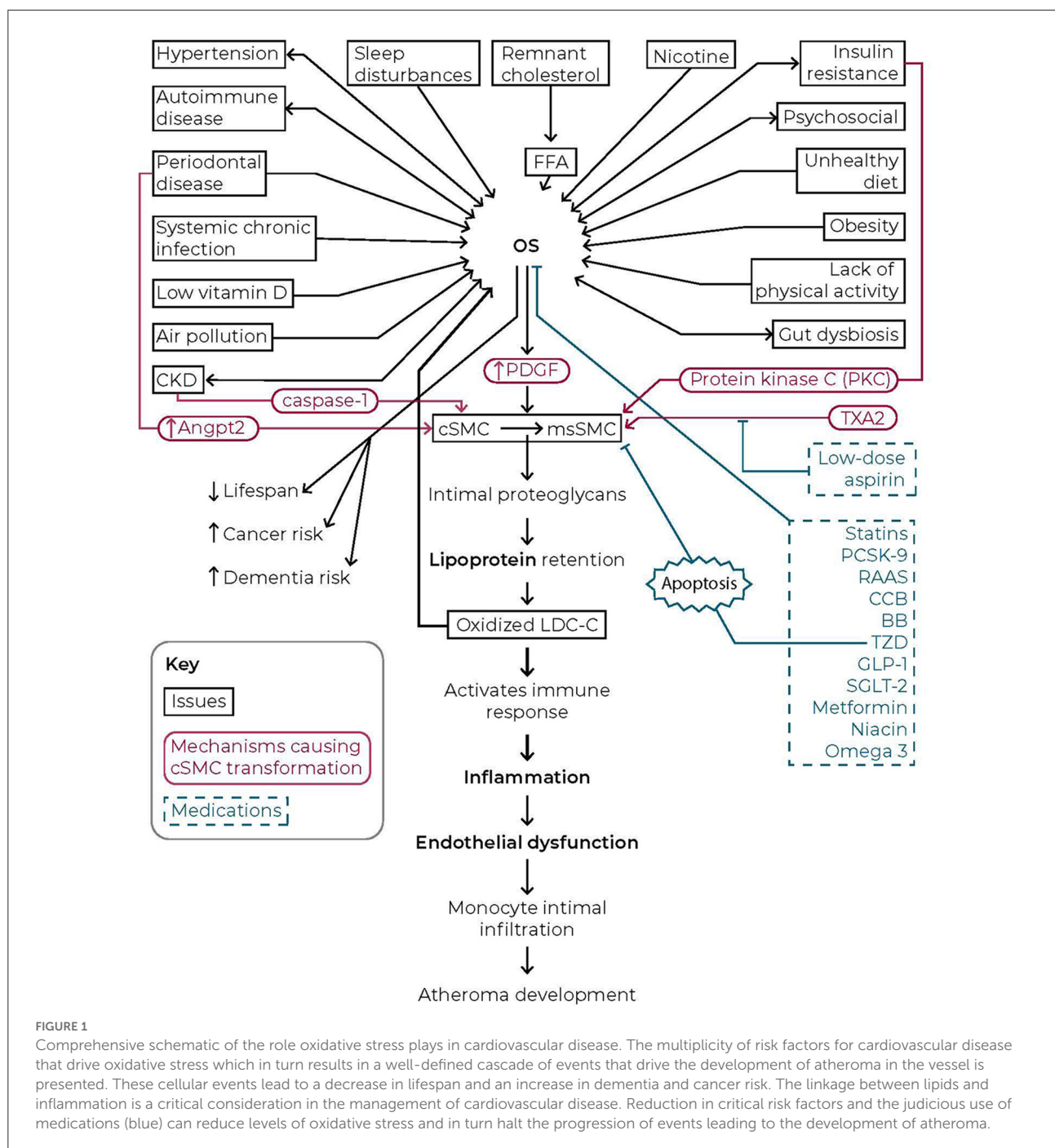
3-hydroxy-3-methylglutaryl coenzyme A (HMG-CoA) reductase inhibitors have evolved as a cornerstone medication to reduce CV risk. These drugs, better known as statins, are recommended in guidelines with benefits greatly outweighing harm (184). When examined through the perspective of OS, these agents excel. Within hours statins progressively reduce OS (185). Elevated NADPH-oxidase expression and activity create OS. A critical substance in the assembly and activity of NADPH-oxidase is Rac1, a guanosine triphosphatase. Stains decrease mevalonate, which results in a reduction in Rac1. The reduction in mevalonate causes a decrease in geranyl-geranyl-pyrophosphate (GGPP). Less GGPP causes increased expression of endothelial nitric oxide synthetase (eNOS). Statins help activate eNOS *via* phosphorylation. ENOS enhances the restoration of oxidative balance (186). As a significant bonus, statins increase the concentration of two powerful antioxidants, glutathione peroxidase and superoxide dismutase (187). This SOS effect of statins would reduce the PDGR-driven cSMC transformation. Chen and colleagues demonstrated this effect of statins (188). The biomarker

lipoprotein-associated phospholipase A-2 (PLAC2) increases during the pathogenesis of atherosclerosis (189). The reduction in PLAC2 in the statin trail LIPID accounted for most of the statin benefit (190). It is conceivable that statins primarily mitigate CV risk *via* directly reducing OS.

Bempedoic acid (BA) lowers cholesterol in a similar manner to statins. It inhibits ATP-citrate lyase (ACL), a catalyst necessary to form acetyl-CoA. Less production of acetyl-CoA causes decreased formation of HMG-CoA. Thus, it acts upstream from statins to inhibit HMG-CoA production. Just like statins, this will decrease mevalonate formation, which should result in the activation of eNOS, helping to restore oxidative balance. BA theoretically has the potential to lower remnant cholesterol since acetyl-CoA activity can lead to increased TG (191). However, studies have shown no significant decrease in TG levels to date (192–195). BA has not been investigated for its ability to increase antioxidants. No data is available evaluating BA's effect on PLAC2. BA does carry a warning of increasing uric acid. There currently is no CV outcome data, albeit some is expected later this year with the CLEAR trial (Evaluation of Major Cardiovascular Events in Patients With, or at High Risk for, Cardiovascular Disease Who Are Statin Intolerant Treated with Bempedoic Acid). The medication requires prior authorization, and the cost is a concern (196). It remains to be determined if BA is an effective agent to reduce OS.

Because triglyceride (TG) reduction independent of LDL-C lowers CV risk, lipid-lowering agents beyond statins are frequently required (197). TGs are a surrogate representation of remnant cholesterol, which natively creates OS. Therefore, any therapy that lowers TG will directly lower OS. The question is; do any of these therapies directly reduce OS by other mechanisms? Fibrates decrease the progression of atherosclerosis and reduce CV risk (198). However, the evidence does not support that fibrates reduce OS beyond what would be expected from lowering TG (199). Numerous studies confirm that proprotein convertase subtilisin/kexin type 9 (PCSK9) inhibitors significantly lower TG and CV risk (200–202). In addition to PCSK9 inducing LDL receptor degradation, it activates NADPH oxidase promoting OS. Therefore, PSCK9-inhibitors (PCSK9-I) may reduce OS beyond reducing TG. Accumulating evidence suggests PCSK9-I may reduce CV risk *via* SOS (203).

Niacin, the water-soluble vitamin B3, is the oldest and one of the most effective agents to affect all lipoproteins favorably (204). In an *in vitro* study utilizing human aortic endothelial cells, niacin inhibited ROS production by angiotensin II (205). Seventeen subjects with an insulin resistance type dyslipidemia demonstrated that 2 grams of niacin a day for 3 months significantly reduced TG and OS (206). However, the degree of reduction in OS in that study may have been due to the lowering of TG. Niacin is a precursor for nicotinamide adenine dinucleotide (NAD^+). Recently it was discovered that NAD^+ is a co-substrate for the sirtuin family of deacetylases which help maintain mitochondrial homeostasis. The benefits of niacin

FIGURE 1
Comprehensive schematic of the role oxidative stress plays in cardiovascular disease. The multiplicity of risk factors for cardiovascular disease that drive oxidative stress which in turn results in a well-defined cascade of events that drive the development of atheroma in the vessel is presented. These cellular events lead to a decrease in lifespan and an increase in dementia and cancer risk. The linkage between lipids and inflammation is a critical consideration in the management of cardiovascular disease. Reduction in critical risk factors and the judicious use of medications (blue) can reduce levels of oxidative stress and in turn halt the progression of events leading to the development of atheroma.

may primarily be related to its influence on the NAD^+/sirtuin-axis (207). *In vitro* and *in vivo* trials have confirmed that niacin reduces OS (208). Whether or not the mechanism for this reaches beyond its effect on TG is not established.

Omega 3 fatty acids (FAs) are an effective therapy for TG (209). A meta-analysis evaluating the effect of omega 3 FAs vs. placebo on the oxidative stress biomarker malondialdehyde (MDA) concluded a significant decrease in MDA with omega 3 FAs. The analysis also showed significantly increased activity

of the antioxidant enzyme glutathione peroxidase (GPx). The conclusion was that omega 3 FAs reduce OS. It was noted in the analysis that the change in MDA seemed to be due to the improvement in the lipid profile (210). The evidence indicates that the benefit of SOS with omega 3 FAs is due to a reduction in TG. In summary, all TG-lowering agents SOS, but the only one that does so beyond the lipid effect, maybe PCSK9 inhibitors.

Evidence indicates that blood pressure medications reduce CV risk regardless of a hypertensive diagnosis. Healthcare

providers should focus communication on the benefit of these agents on CV risk rather than the blood pressure benefit (211). Renin-angiotensin-aldosterone system (RAAS) medications have been considered a cornerstone for individuals with CVD (212). RAAS agents have pleiotropic effects beyond blood pressure reduction (213). RAAS therapy can double the antioxidant extracellular superoxide dismutase (EC-SOD) concentration. The change in EC-SOD partially explains the reduction in OS by RAAS medications (214). The main feature of RAAS agents is to reduce the effects on angiotensin II (AngII) either by reducing the production of AngII or blocking the receptor to activate AngII. AngII activates NADPH oxidase, which leads to increased ROS and OS (215). Amlodipine is a frequently used agent in individuals with CV risk. Amlodipine is known to reduce the progression of atherosclerosis. One mechanism by which it accomplishes this is inhibition of cSMC transformation and migration (216). Utilizing nitrotyrosine as a marker of OS, Kim and colleagues demonstrated therapy with amlodipine and a RAAS agent, and each significantly lowered the level after 24 weeks. The authors concluded that amlodipine reduces OS (217). Beta-blockers have a prominent role in managing CV risk. Carvedilol significantly reduced OS as measured by thiobarbituric acid-reactive substances (TBARS) (218). *In vitro* data have shown that carvedilol reduces ROS production by mitochondria (219). In a study of 44 patients with essential hypertension, multiple biomarkers, including the ferric-reducing ability of plasma (FRAP), glutathione/oxidized glutathione, malondialdehyde, and plasma 8-isoprostane, were used to assess OS. Twenty-three patients received carvedilol 12.5 mg/d, and twenty-one received nebivolol 5 mg/d for 12 weeks. All four biomarkers of OS improved significantly with carvedilol. There were no significant changes with nebivolol (220). These beneficial effects on the pathogenesis of atherosclerosis of the above three major classes of blood pressure medications were assessed in a comprehensive review of multiple strategies to manage hypertension (221). A significant reason the hypertensive medications amlodipine, carvedilol, and RAAS agents reduce CV risk is related to directly reducing OS.

Insulin resistance (IR), a CV risk factor, frequently requires medication therapy regardless of T2DM status. Hyperglycemia which results from IR, generates OS by multiple mechanisms (222). Therefore, any medication utilized to reduce IR and hyperglycemia will reduce OS. The question is, do any of them directly reduce OS by mechanisms other than reducing hyperglycemia. The alpha-glucosidase, dipeptidyl peptidase-4 inhibitors, and sulfonylurea agents have shown that they reduce OS (223–225). However, there is no evidence that the mechanism responsible reaches beyond reducing hyperglycemia. Metformin activates adenosine monophosphate-activated protein kinase (AMPK) (226). This activation leads to the expression of the antioxidant genes for the production of catalase (CAT), glutathione (GSH), and superoxide dismutase (SOD) (227). The increase in these

agents enhances the antioxidant system, reducing ROS (228). Activation of AMPK also maintains the cSMC phenotype (229). The mechanism of activating AMPK will reduce the initial step in the pathogenesis of atherosclerosis and is a mechanism separate from reducing hyperglycemia. Thiazolidinediones (TZD), glucagon-like peptide-1s (GLP-1), and sodium-glucose cotransporter 2 inhibitors (SGLT-2) also activate AMPK (230–232). The TZD pioglitazone also destroys SMCs, which have transformed into msSMCs (233). These actions are a significant benefit in shutting down the pathogenesis of atherosclerosis. Indeed, pioglitazone has excellent studies showing it has a positive effect on mitigating the progression of atherosclerosis in IR patients regardless of diabetic status (234–237). In summary, all antidiabetic drugs SOS. Metformin, GLP-1, SGLT-2, and TZD agents do so by effects outside of mitigating hyperglycemia. The best medication for SOS appears to be pioglitazone with its unique ability to cause apoptosis of msSMCs.

Discussion

A chronic association between lipids and inflammation develops with active pathogenesis of atherosclerosis. The first step in the pathogenesis involves trapping apolipoprotein B (apo B), which contains all the vascularly harmful cholesterol, in the intima. The contained cholesterol particles become oxidized and generate inflammation. The inflammation comes from activating the immune system to remove the oxidized particles from the arterial wall. The innate immune system initially responds by generating inflammatory cytokines and monocyte chemoattractant proteins affecting the endothelium. Subsequently, monocytes are captured on the endothelium and penetrate the intima. Macrophages are formed from those monocytes to digest the oxidized lipids. The adaptive immune system responds with effector T cells stimulated by antigens such as oxidized lipoproteins (238). If the trapping continues, the macrophages become engorged, becoming foam cells. In addition, SMCs may also become engorged with oxidized lipoproteins contributing to the mass of foam cells (239). If the process continues, the foam cells coalesce into fatty streaks and form atheroma. Active pathogenesis of atherosclerosis produces substances such as oxidized LDL and matrix metalloproteinase-2, which also contribute to the transformation of cSMCs (240). The three essential elements involved in the pathogenesis of atherosclerosis are apoB, endothelial permeability, and binding of lipoproteins in the intima (241). Individual analysis of these three components is helpful when attempting to end the chronic association between lipids and inflammation.

Would solely focusing on apoB stop the chronic association between lipids and inflammation? Excellent health requires cholesterol and fat. Cholesterol is a vital hormone ingredient,

now recognized as an essential regulator of innate immunity (242). Fat is also an essential ingredient for health (243). Their transport to cells depends on apoB. Therefore, extreme reduction or elimination of this component is not feasible. It is only harmful when it gets trapped in the intima or if it contains high levels of remnant cholesterol. If there is no retention of apoB in the intima, an individual could have high levels with low CV risk. The converse would also be true. If there is the retention of apoB in the intima, an individual could have low levels with high CV risk. There is evidence congruent with retention being the critical determinant for arterial disease. One study found that about half of the 231,986 people with coronary artery disease had low levels of apoB (244). Studies also demonstrate that the absolute risk for atherosclerosis in many people with high apoB is low, albeit the relative risk might be twice that of subjects with low apoB (245). The main factor determining the number of lipoproteins retained in the intima is the number of proteoglycans available to bind apoB. The quantity of apoB diffusing through the arterial wall far exceeds the quantity trapped in the intima (7). Thus, reducing the plasma apo B concentration will decrease the intimal retention to some degree, but it will not prevent it. As long as there is the intimal binding of apoB regardless of apoB concentration, there will be a persistent association between lipids and inflammation.

Would focus on endothelial permeability and the responsible immune milieu end the chronic lipid inflammatory association? The immune activation and subsequent endothelial response are mechanisms to maintain arterial wellness. Interfering with this process might reduce inflammation enough to lower the risk of an underlying atheroma creating a thrombus from endothelial rupture or erosion. CV event risk in patients with known arterial disease was lowered with the medication canakinumab, which inhibits the proinflammatory cytokine interleukin-1β. Such action, however, does not halt the intimal binding of apoB. Continuation of the pathogenesis of atherosclerosis was evident, with a significant number of patients receiving canakinumab requiring hospitalization for unstable angina (246). The immune reaction and resultant inflammation are designed to restore wellness. Should the unhealthy retention of apoB continue, the chronic association between lipoproteins and inflammation will remain.

Stopping the binding of apoB in the intima would end the chronic association between lipids and inflammation. Proteoglycans have a protein core with negatively charged glycosaminoglycan chains. ApoB carries a positive charge. This electrostatic force traps the lipoproteins (247). These binding proteoglycans are produced by msSMCS which originate from cSMCs. The change occurs in the medial layer, and the msSMCs move into the deep layer of the intima. Proteoglycans are then secreted into the intima. SMCs are the first cells seen in the intima in locations destined to develop atherosclerosis (13). Prevention of the cSMC transformation would halt the binding.

The chronic lipid inflammatory association would stop, as would the pathogenesis of atherosclerosis.

Vascular SMCs are subject to phenotypic change. The mechanisms resulting in transformation are complex. The plasticity of a SMC depends on its anatomic location, embryonic origin, maturity, and subtype. Most research has focused on the contractile phenotype and the synthetic phenotype. The genetic transformation involves the activation and suppression of SMC genes. PDGF can induce transformation, which is mediated by multiple mechanisms (248). One of those mechanisms was elucidated recently. A DNA-modifying enzyme ten-eleven translocation-2 (TET2) is a master epigenetic regulator of cSMC transformation (249). MicroRNA-22-3p (miR-22-3p) activates TET2 to transform cSMCs. Circular mitogen-activated protein kinase 5 (circMAP3K5) acts like a sponge for miR-22-3p. This reduction in the availability of miR-22-3p decreases the genetic transformation of cSMCs. In an *in vivo* mouse model, circMAP3K5 inhibited SMC-induced intimal hyperplasia. PDGF significantly reduces the expression of circMAP3K5 in human coronary artery SMCs (250). This reduction would lead to an increase in cSMC transformation to msSMCs. We have discussed numerous ways in which to minimize PDGF. The purpose of reducing PDGF is to reduce the creation of msSMCs.

Transformation of cSMCs into msSMCs can occur by other mechanisms. Angiopoietins are present in SMCs. They can influence genetic transformation. An increase in angiopoietin 2 (Angpt2) relative to angiopoietin 1 (Angpt1) in human aortic SMCs caused a transformation to migratory SMCs. The high-risk periodontal pathogen *Porphyromonas gingivalis* stimulated the Angpt2/Angpt1 ratio shift. The authors concluded that this mechanism links periodontal disease to atherosclerosis (95). Periodontal disease should be addressed as a CV risk factor. Protein kinase C (PKC) enhances the conversion of cSMCs to msSMCs. Insulin resistance activates PKC. Activated PKC also reduces nitric oxide and increases endothelial-1, increasing cSMC transformation (251). The solution is to minimize insulin resistance. Thromboxane A2 (TXA2) activates yes associated protein 1 (YAP)/WW-domain-containing transcription regulator 1 (TAZ), which causes more transformation of cSMCs to msSMCs (252). TXA2 is mainly synthesized *via* cyclooxygenase (COX)-1 in activated platelets. Urinary thromboxane B2 (TXB2) is a surrogate biomarker for TXA2 production. TXB2 is an independent risk factor for CV mortality. The authors suggest that TXB2 measurement could help guide the use of low-dose aspirin (253). Despite aspirin use, TXB2 levels can be elevated. Numerous health conditions can cause this. They include cigarette smoking, T2DM, HTN, obesity, and systemic lupus erythematosus. Any issue which causes OS activates platelets which increases the levels of TXA2, leading to higher TXB2 (254). To accomplish minimization of TXA2 requires managing all the CV risk factors causing OS and judicial use of low-dose aspirin.

Translation to clinical practice

Atherosclerosis and the accompanying chronic association of lipids and inflammation is arguably the most common and devastating human ailment. Researchers have noted preventing the seeding of msSMCs into the intima as a potential solution to halt the pathogenesis of atherosclerosis (13, 255, 256). Utilization of the science presented in this paper provides a clinical path to reduce the production of msSMCs by SOS. That achievement in an individual could eliminate chronic inflammation associated with lipids. More importantly, it could establish arterial health minimizing the risk for end-stage macrovascular diseases such as myocardial infarction and ischemic stroke. Most importantly, it would minimize the risk of developing chronic microvascular diseases of aging such as dementia, heart failure, renal failure, erectile dysfunction, peripheral arterial disease, and eye conditions like macular degeneration.

Numerous health issues are known to create arterial inflammation. These conditions included physical inactivity, lipids, smoking, hypertension, poor diet, obesity, insulin resistance, periodontal disease, other chronic infections, obstructive sleep apnea, psychosocial, vitamin D deficiency, gut dysbiosis, autoimmune diseases, and air pollution. Optimal clinical management of these health conditions has been proposed to halt atherosclerosis (257). In 2015, a retrospective analysis of data from a clinic utilizing the above approach was published. The study found that such individualized care positively affected the atherosclerotic disease process. The study evaluated the change in carotid intima-media thickness (cIMT) and carotid plaque during 8 years of clinical management of 576 patients. Baseline demographics revealed a mean age of 55.5 years, mean BMI of 27.5 kg/m^2, 39% female, 36% current or former smokers, 73% insulin resistant, 89% hyperlipidemia, 58% hypertensive, 34% Framingham Risk Score of $\geq$10% and 100% White. Carotid plaque was present in 85% of the patients. Coronary artery disease, as defined by coronary calcification or history of coronary event or intervention, was present in 25% of subjects. Eight years of therapy to improve all non-optimal health issues that created arterial inflammation resulted in a significant regression of cIMT and quantity of carotid plaque. There was also a significant reduction in Lp-PLA2, a biomarker that indicates active pathogenesis of atherosclerosis, as mentioned earlier in this paper. These results indicated not only halting arterial disease but also regressing the disease. In addition, no CV events occurred in any 576 patients (258). This information supports that knowledge regarding the causes of arterial inflammation can be translated into actual practice to stop the arterial disease.

Halting and regressing atherosclerosis theoretically should be beneficial. However, three prospective studies utilizing sophisticated imaging of arterial disease with MRI of carotids, near-infrared spectroscopy, and optical coherence tomography of the coronaries demonstrated that the lipid-richness of the plaque is the significant predictor of CV events (259–261). A retrospective study examined carotid plaque morphology changes in patients receiving multifactorial CV risk reduction treatment in the prevention clinic referenced in the above paragraph. The cohort consisted of 324 patients treated for 5 years with baseline characteristics very similar to the population of 576 patients mentioned above. At baseline, 53% of subjects had at least one lipid-rich plaque. At the end of 5 years, no patients had any lipid-rich plaque. The authors concluded that comprehensive, evidence-based management in a community-based prevention clinic benefits vulnerable plaque (262). These results indicate that clinicians can shut down and stabilize atherosclerosis with comprehensive management of health conditions causing OS and inflammation.

There are strengths in the above real-world evidence (RWE). Such evidence is increasing in importance. RWE can better mimic a patient's actual clinical situation. This reflection would include compliance with advice, number of illnesses, and magnitude of multiple treatments in an individual patient. RWE has obvious financial benefits compared to randomized clinical trials (RCT). Many unanswered questions in medicine which involve multiple variable interventions in an individual patient are not feasible to answer in RCT. RWE can also potentially generate answers faster than RCT. The expediency is especially true if the therapies are approved, making recruitment for an RCT more difficult (263). RWE is not limited to initiation by an investigator or dependent upon corporate sponsorship, which can introduce bias (264). It is now recognized that RWE is seriously needed to bolster the knowledge deficiency between RCTs and evidence-based, innovative management of complex diseases (265).

Let us examine some strengths of the RWE presented above, indicating halting and stabilizing of arterial disease. The outcome measurement of cIMT is robust. The same company performed all of the cIMT tests. Their sonographers and readers undergo routine testing for accuracy. There is a strong correlation between cIMT and atherosclerosis histology. The systemic presence of arterial disease is also correlated with cIMT. CV event risk is correlated with the change in cIMT. CV event risk decreases 12% for each 0.010 mm yearly reduction in cIMT progression (266). The RWE showed regression of cIMT instead of simply slowing progression. Identifying subclinical atherosclerosis with carotid plaque was clinically valuable in determining comprehensiveness and management goals. The presence of atherosclerosis is *conditio sine qua non* for risk of having a CV event (267). Finding atheroma in "healthy" subjects enhances patient management decisions (268). Subclinical carotid plaque is strongly associated with heart attack and stroke risk. Such identification should reclassify an individual's risk for a CV event (269). Identifying subclinical arterial disease is a cornerstone of the prevention clinic. This investigation allowed the migration to a ternary classification of CV prevention.

Primary prevention care was provided to patients without any arterial disease. Secondary prevention was delivered to individuals with subclinical arterial disease. Tertiary prevention was given to subjects who proved they had arterial disease with interventions or events. This classification aided therapy decisions such as low-dose aspirin (270). The high degree of management compliance is partially attributed to the patient's visualization of the plaque (271). The cIMT testing enhanced care, and the follow-up results proved that atherosclerosis's pathogenesis could be halted in an actual healthcare clinic.

Another strength of the RWE involves the monitoring of arterial inflammation. The prevention clinic assessed the adequacy of management of all the causes of arterial inflammation with these biomarkers. The endothelium was judged for the amount of inflammation by the hsCRP and wellness by the microalbumin-creatinine ratio (272, 273). Intimal inflammation and atherogenic activity were checked with lipoprotein-associated phospholipase A2 (Lp-PLA2) (189). Myeloperoxidase (MPO) was monitored since elevations are associated with an increased risk of endothelial rupture and erosion (274). Urinary F2-isoprostane was followed as a marker of oxidative stress (275). Clinically, the patient was judged to have a quiescent atherosclerotic process and low risk for an atherothrombotic event when all the inflammatory biomarkers were in an acceptable range. This approach was successful, albeit without a complete understanding of the reasons. As explained throughout this paper, we know that all the root causes of inflammation being managed in the clinic generate OS, leading to lipoprotein retention in the intima. The trapped lipoproteins then turn on the immune system, which causes the monitored biomarkers of inflammation to increase. With mitigation of OS, the first step in atherosclerosis's pathogenesis is prevented, ending the chronic association of lipids and inflammation. Once the atherosclerotic disease process stops, any existing atheroma has an opportunity to delipidate and shrink. The RWE showing a significant reduction in Lp-PLA2 supports this concept.

One glaring weakness of the RWE is that there was a lack of ethnic diversity. The good news is that from a biological standpoint, the principle of SOS should halt and stabilize arterial disease regardless of ethnicity. Humans are 99.99% identical from a genetic standpoint. There are different frequencies of genetic variants in ethnic groups, but humans are arguably the same race. Discrete human ethnic groups are based on social constructs such as language, neighborhoods, education, income, preferred foods, and physical activity (276). Biological responses to these social differences will affect the degree of OS. Therefore, any study evaluating the RWE in other ethnic populations must accurately assess the environmental and sociocultural issues affecting the risk factors that generate OS (277). Given this, arterial disease can be halted and stabilized in humans.

The RWE presented supports that the chronic association of lipids and inflammation can be interrupted. SOS can halt the pathogenesis of atherosclerosis. Clinically this requires individual patient management of the myriad of conditions that cause OS. Such management necessitates a time-consuming individualized interdisciplinary healthcare approach. An excellent term for such care is arteriology. There is a vast need for arteriologists. The RWE should be bolstered in additional clinics and populations. It would be challenging to design RCTs to strengthen the data due to the need for personalized care manipulating numerous variations in management. The current RWE is logical and anchored in evidence-based therapies. There is a new meaning for the distress code- SOS, which could enhance the lives of millions.

For interested individuals, the prevention clinic with the RWE has a nomenclature for the system of care delivered. It is called the BaleDoneen Method. Instruction in the method is delivered to other healthcare providers in an approved 17-h CME and CE course. The public can learn about the method from two books [Bale, Bradley F., Doneen, Amy L., & Cool, Lisa Collier (2014). Beat the Heart Attack Gene: The Revolutionary Plan to Prevent Heart Disease, Stroke, and Diabetes. Nashville, TN: John Wiley & Sons.; Bale, Bradley F., Doneen, Amy L., & Cool, Lisa Collier (2022). Healthy Heart Healthy Brain: The Personalized Path to Protect Your Memory, Prevent Heart Attacks and Strokes and Avoid Chronic Illness. New York, NY: Little, Brown Spark].

Author contributions

All authors listed have made a substantial, direct, and intellectual contribution to the work and approved it for publication.

Conflict of interest

The authors declare that the research was conducted in the absence of any commercial or financial relationships that could be construed as a potential conflict of interest.

Publisher's note

All claims expressed in this article are solely those of the authors and do not necessarily represent those of their affiliated organizations, or those of the publisher, the editors and the reviewers. Any product that may be evaluated in this article, or claim that may be made by its manufacturer, is not guaranteed or endorsed by the publisher.

References

1. Tsao CW, Aday AW, Almarzooq ZI, Alonso A, Beaton AZ, Bittencourt MS, et al. Heart disease and stroke statistics-2022 update: a report from the American Heart Association. *Circulation.* (2022) 145:e153–639. doi: 10.1161/CIR.0000000000001052

2. Hakim AM. Small vessel disease. *Front Neurol.* (2019) 10:1020. doi: 10.3389/fneur.2019.01020

3. Virani SS, Alonso A, Benjamin EJ, Bittencourt MS, Callaway CW, Carson AP, et al. Heart disease and stroke statistics-2020 update: a report from the American Heart Association. *Circulation.* (2020) 141:e139–596. doi: 10.1161/CIR.0000000000000757

4. Schwartz RS, Burke A, Farb A, Kaye D, Lesser JR, Henry TD, et al. Microemboli and microvascular obstruction in acute coronary thrombosis and sudden coronary death: relation to epicardial plaque histopathology. *J Am Coll Cardiol.* (2009) 54:2167–73. doi: 10.1016/j.jacc.2009.07.042

5. Bezsonov E, Sukhorukov V, Bukrinsky M, Orekhov A. Editorial: lipids and inflammation in health and disease. *Front Cardiovasc Med.* (2022) 9:864429. doi: 10.3389/fcvm.2022.864429

6. Nakashima Y, Fujii H, Sumiyoshi S, Wight TN, Sueishi K. Early human atherosclerosis: accumulation of lipid and proteoglycans in intimal thickenings followed by macrophage infiltration. *Arterioscler Thromb Vasc Biol.* (2007) 27:1159–65. doi: 10.1161/ATVBAHA.106.134080

7. Fogelstrand P, Borén J. Retention of atherogenic lipoproteins in the artery wall and its role in atherogenesis. *Nutr Metab Cardiovasc Dis.* (2012) 22:1–7. doi: 10.1016/j.numecd.2011.09.007

8. Davignon J, Ganz P. Role of endothelial dysfunction in atherosclerosis. *Circulation.* (2004) 109:III-27–32. doi: 10.1161/01.CIR.0000131515.03336.f8

9. He D, Xu L, Wu Y, Yuan Y, Wang Y, Liu Z, et al. Rac3, but not Rac1, promotes ox-LDL induced endothelial dysfunction by downregulating autophagy. *J Cell Physiol.* (2020) 235:1531–42. doi: 10.1002/jcp.29072

10. Li D, Mehta JL. Antisense to LOX-1 inhibits oxidized LDL–mediated upregulation of monocyte chemoattractant protein-1 and monocyte adhesion to human coronary artery endothelial cells. *Circulation.* (2000) 101:2889–95. doi: 10.1161/01.CIR.101.25.2889

11. Hua Y, Zhang J, Liu Q, Su J, Zhao Y, Zheng G, et al. The induction of endothelial autophagy and its role in the development of atherosclerosis. *Front Cardiovasc Med.* (2022) 9:831847. doi: 10.3389/fcvm.2022.831847

12. Nakashima Y, Wight TN, Sueishi K. Early atherosclerosis in humans: role of diffuse intimal thickening and extracellular matrix proteoglycans. *Cardiovasc Res.* (2008) 79:14–23. doi: 10.1093/cvr/cvn099

13. Doran AC, Meller N, McNamara CA. Role of smooth muscle cells in the initiation and early progression of atherosclerosis. *Arteriosc Thromb Vasc Biol.* (2008) 28:812–9. doi: 10.1161/ATVBAHA.107.159327

14. Ricci C, Ferri N. Naturally occurring PDGF receptor inhibitors with potential anti-atherosclerotic properties. *Vascul Pharmacol.* (2015) 70:1–7. doi: 10.1016/j.vph.2015.02.002

15. Freedman JE. Oxidative stress and platelets. *Arteriosc Thromb Vasc Biol.* (2008) 28:s11–6. doi: 10.1161/ATVBAHA.107.159178

16. Rossi E, Casali B, Regolisti G, Davoli S, Perazzoli F, Negro A, et al. Increased plasma levels of platelet-derived growth factor (PDGF-BB + PDGF-AB) in patients with never-treated mild essential hypertension. *Am J Hypertens.* (1998) 11:1239–43. doi: 10.1016/S0895-7061(98)00124-1

17. Lichtenberg D, Pinchuk I. Oxidative stress, the term and the concept. *Biochem Biophys Res Commun.* (2015) 461:441–4. doi: 10.1016/j.bbrc.2015.04.062

18. Tirichen H, Yaigoub H, Xu W, Wu C, Li R, Li Y. Mitochondrial reactive oxygen species and their contribution in chronic kidney disease progression through oxidative stress. *Front Physiol.* (2021) 12:627837. doi: 10.3389/fphys.2021.627837

19. Mailloux RJ. An update on mitochondrial reactive oxygen species production. *Antioxidants.* (2020) 9:472. doi: 10.3390/antiox9060472

20. Ježek J, Engstová H, Ježek P. Antioxidant mechanism of mitochondria-targeted plastoquinone SkQ1 is suppressed in aglycemic HepG2 cells dependent on oxidative phosphorylation. *Biochimica et Biophysica Acta Bioenergetics.* (2017) 1858:750–762. doi: 10.1016/j.bbabio.2017.05.005

21. Leyane TS, Jere SW, Houreld NN. Oxidative stress in ageing and chronic degenerative pathologies: molecular mechanisms involved in counteracting oxidative stress and chronic inflammation. *Int J Mol Sci.* (2022) 23:7273. doi: 10.3390/ijms23137273

22. Jiang Q, Yin J, Chen J, Ma X, Wu M, Liu G, et al. Mitochondria-targeted antioxidants: a step towards disease treatment. *Oxid Med Cell Longev.* (2020) 2020:1–18. doi: 10.1155/2020/8837893

23. Shemiakova T, Ivanova E, Wu WK, Kirichenko TV, Starodubova AV, Orekhov AN. Atherosclerosis as mitochondriopathy: repositioning the disease to help finding new therapies. *Front Cardiovasc Med.* (2021) 8:660473. doi: 10.3389/fcvm.2021.660473

24. Zhang M-J, Zhou Y, Chen L, Wang Y-Q, Wang X, Pi Y, et al. An overview of potential molecular mechanisms involved in VSMC phenotypic modulation. *Histochem Cell Biol.* (2016) 145:119–30. doi: 10.1007/s00418-015-1386-3

25. Sniderman AD, Navar AM, Thanassoulis G. Apolipoprotein B vs low-density lipoprotein cholesterol and non–high-density lipoprotein cholesterol as the primary measure of apolipoprotein B lipoprotein-related risk. *JAMA Cardiology.* (2022) 7:257. doi: 10.1001/jamacardio.2021.5080

26. Varbo A, Benn M, Tybjaerg-Hansen A, Nordestgaard BG. Elevated remnant cholesterol causes both low-grade inflammation and ischemic heart disease, while elevated low-density lipoprotein cholesterol causes ischemic heart disease without inflammation. *Circulation.* (2013) 128:1298–309. doi: 10.1161/CIRCULATIONAHA.113.003008

27. Le NA. Lipoprotein-associated oxidative stress: a new twist to the postprandial hypothesis. *Int J Mol Sci.* (2014) 16:401–19. doi: 10.3390/ijms16010401

28. Paolisso G, Gambardella A, Tagliamonte MR, Saccomanno F, Salvatore T, Gualdiero P, et al. Does free fatty acid infusion impair insulin action also through an increase in oxidative stress? *J Clin Endocrinol Metab.* (1996) 81:4244–8. doi: 10.1210/jcem.81.12.8954022

29. Soardo G, Donnini D, Domenis L, Catena C, De Silvestri D, Cappello D, et al. Oxidative stress is activated by free fatty acids in cultured human hepatocytes. *Metab Syndr Relat Disord.* (2011) 9:397–401. doi: 10.1089/met.2010.0140

30. Shin HK, Kim YK, Kim KY, Lee JH, Hong KW. Remnant lipoprotein particles induce apoptosis in endothelial cells by NAD(P)H oxidase-mediated production of superoxide and cytokines via lectin-like oxidized low-density lipoprotein receptor-1 activation: prevention by cilostazol. *Circulation.* (2004) 109:1022–8. doi: 10.1161/01.CIR.0000117403.64398.53

31. Castañer O, Pintó X, Subirana I, Amor AJ, Ros E, Hernáez Á, et al. Remnant cholesterol, not LDL cholesterol, is associated with incident cardiovascular disease. *J Am Coll Cardiol.* (2020) 76:2712–24. doi: 10.1016/j.jacc.2020.10.008

32. Sascău R, Clement A, Radu R, Prisacariu C, Stătescu C. Triglyceride-rich lipoproteins and their remnants as silent promoters of atherosclerotic cardiovascular disease and other metabolic disorders: a review. *Nutrients.* (2021) 13:1774. doi: 10.3390/nu13061774

33. Wadström BN, Wulff AB, Pedersen KM, Jensen GB, Nordestgaard BG. Elevated remnant cholesterol increases the risk of peripheral artery disease, myocardial infarction, and ischaemic stroke: a cohort-based study. *Eur Heart J.* (2021) 43:3258–3269. doi: 10.1093/eurheartj/ehab705

34. Zhao Y, Liu L, Yang S, Liu G, Pan L, Gu C, et al. Mechanisms of atherosclerosis induced by postprandial lipemia. *Front Cardiovasc Med.* (2021) 8:636947. doi: 10.3389/fcvm.2021.636947

35. Wang JL, Yin WJ, Zhou LY, Wang YF, Zuo XC. Association between initiation, intensity, and cessation of smoking and mortality risk in patients with cardiovascular disease: a cohort study. *Front Cardiovasc Med.* (2021) 8:728217. doi: 10.3389/fcvm.2021.728217

36. Hernandez P, Passi N, Modarressi T, Kulkarni V, Soni M, Burke F, et al. Clinical management of hypertriglyceridemia in the prevention of cardiovascular disease and pancreatitis. *Curr Atheros Rep.* (2021) 23:72. doi: 10.1007/s11883-021-00962-z

37. Fu J, Bonder MJ, Cenit MC, Tigchelaar EF, Maatman A, Dekens JAM, et al. The gut microbiome contributes to a substantial proportion of the variation in blood lipids. *Circ Res.* (2015) 117:817–24. doi: 10.1161/CIRCRESAHA.115.306807

38. O'Donnell MJ, Xavier D, Liu L, Zhang H, Chin SL, Rao-Melacini P, et al. Risk factors for ischaemic and intracerebral haemorrhagic stroke in 22 countries (the INTERSTROKE study): a case-control study. *Lancet.* (2010) 376:112–23. doi: 10.1016/S0140-6736(10)60834-3

39. Touyz RM, Rios FJ, Alves-Lopes R, Neves KB, Camargo LL, Montezano AC. Oxidative stress: a unifying paradigm in hypertension. *Canadian J Cardiol.* (2020) 36:659–70. doi: 10.1016/j.cjca.2020.02.081

40. Li FJ, Zhang CL, Luo XJ, Peng J, Yang TL. Involvement of the MiR-181b-5p/HMGB1 pathway in ang ii-induced phenotypic

transformation of smooth muscle cells in hypertension. *Aging Dis.* (2019) 10:231–48. doi: 10.14336/AD.2018.0510

41. Wright JT Jr, Williamson JD, Whelton PK, Snyder JK, Sink KM, Rocco MV, et al. A randomized trial of intensive versus standard blood-pressure control. *N Engl J Med.* (2015) 373:2103–16. doi: 10.1056/NEJMoa1511939

42. Zhang W, Zhang S, Deng Y, Wu S, Ren J, Sun G, et al. Trial of intensive blood-pressure control in older patients with hypertension. *New Engl J Med.* (2021) 385:1268–79. doi: 10.1056/NEJMoa2111437

43. Verma N, Rastogi S, Chia YC, Siddique S, Turana Y, Cheng HM, et al. Non-pharmacological management of hypertension. *J Clin Hypertens.* (2021) 23:1275–83. doi: 10.1111/jch.14236

44. Jones NR, McCormack T, Constanti M, McManus RJ. Diagnosis and management of hypertension in adults: NICE guideline update 2019. *Br J General Pract.* (2020) 70:90–1. doi: 10.3399/bjgp20X708053

45. Noubiap JJ, Nansseu JR, Nyaga UF, Sime PS, Francis I, Bigna JJ. Global prevalence of resistant hypertension: a meta-analysis of data from 3.2 million patients. *Heart.* (2019) 105:98–105. doi: 10.1136/heartjnl-2018-313599

46. Yoshiyama S, Chen Z, Okagaki T, Kohama K, Nasu-Kawaharada R, Izumi T, et al. Nicotine exposure alters human vascular smooth muscle cell phenotype from a contractile to a synthetic type. *Atherosclerosis.* (2014) 237:464–70. doi: 10.1016/j.atherosclerosis.2014.10.019

47. Schroeder SA. What to do with a patient who smokes. *JAMA.* (2005) 294:482–7. doi: 10.1001/jama.294.4.482

48. Brewer NT, Hall MG, Noar SM, Parada H, Stein-Seroussi A, Bach LE, et al. Effect of pictorial cigarette pack warnings on changes in smoking behavior: a randomized clinical trial. *JAMA Intern Med.* (2016) 176:905–12. doi: 10.1001/jamainternmed.2016.2621

49. Martins RS, Junaid MU, Khan MS, Aziz N, Fazal ZZ, Umoodi M, et al. Factors motivating smoking cessation: a cross-sectional study in a lower-middle-income country. *BMC Public Health.* (2021) 21:1419. doi: 10.1186/s12889-021-11477-2

50. Vinci C, Lam C, Schlechter CR, Shono Y, Vidrine JI, Wetter DW. Increasing treatment enrollment among smokers who are not motivated to quit: a randomized clinical trial. *Transl Behav Med.* (2022) 12: ibab114. doi: 10.1093/tbm/ibab114

51. Haffner SM, Lehto S, Rönnemaa T, Pyörälä K, Laakso M. Mortality from coronary heart disease in subjects with type 2 diabetes and in nondiabetic subjects with and without prior myocardial infarction. *New Engl J Med.* (1998) 339:229–34. doi: 10.1056/NEJM199807233390404

52. Goldstein BJ. Insulin resistance as the core defect in type 2 diabetes mellitus. *Am J Cardiol.* (2002) 90:3–10. doi: 10.1016/S0002-9149(02)02553-5

53. World Health Organization. *Global Report on Diabetes.* Geneva: World Health Organization (2016).

54. Centers for Disease Control and Prevention. *National Diabetes Statistics Report: Estimates of Diabetes and Its Burden in the United States, 2014.* Atlanta, GA: US Department of Health and Human Services (2014).

55. Yu Z, Cheng J-X, Zhang D, Yi F, Ji Q. Association between obstructive sleep apnea and type 2 diabetes mellitus: a dose-response meta-analysis. *Evid Based Complement Alternat Med.* (2021) 2021:1–14. doi: 10.1155/2021/1337118

56. Choi HS, Kim K-A, Lim C-Y, Rhee SY, Hwang Y-C, Kim KM, et al. Low serum vitamin D is associated with high risk of diabetes in korean adults. *J Nutr.* (2011) 141:1524–8. doi: 10.3945/jn.111.139121

57. Brauchli YB, Jick SS, Meier CR. Psoriasis and the risk of incident diabetes mellitus: a population-based study. *Br J Dermatol.* (2008) 159:1331–7. doi: 10.1111/j.1365-2133.2008.08814.x

58. Holmlund A, Lind L. Periodontal disease and a poor response to periodontal treatment were associated with an increased risk of incident diabetes: a longitudinal cohort study in Sweden. *J Clin Periodontol.* (2021) 48:1605–12. doi: 10.1111/jcpe.13558

59. Zhao J, Zhang Y, Wei F, Song J, Cao Z, Chen C, et al. Triglyceride is an independent predictor of type 2 diabetes among middle-aged and older adults: a prospective study with 8-year follow-ups in two cohorts. *J Transl Med.* (2019) 17:403. doi: 10.1186/s12967-019-02156-3

60. Tsimihodimos V, Gonzalez-Villalpando C, Meigs JB, Ferrannini E. Hypertension and diabetes mellitus. *Hypertension.* (2018) 71:422–28. doi: 10.1161/HYPERTENSIONAHA.117.10546

61. Harris ML, Oldmeadow C, Hure A, Luu J, Loxton D, Attia J. Stress increases the risk of type 2 diabetes onset in women: a 12-year longitudinal study using causal modelling. *PLoS ONE.* (2017) 12:e0172126. doi: 10.1371/journal.pone.0172126

62. Jeong D, Karim ME, Wong S, Wilton J, Butt ZA, Binka M, et al. Impact of HCV infection and ethnicity on incident type 2 diabetes: findings from a large population-based cohort in British Columbia. *BMJ Open Diabetes Res Care.* (2021) 9:e002145. doi: 10.1136/bmjdrc-2021-002145

63. Chen H, Burnett RT, Kwong JC, Villeneuve PJ, Goldberg MS, Brook RD, et al. Risk of incident diabetes in relation to long-term exposure to fine particulate matter in Ontario, Canada. *Environ Health Perspect.* (2013) 121:804–810. doi: 10.1289/ehp.1205958

64. Atuegwu NC, Perez MF, Oncken C, Mead EL, Maheshwari N, Mortensen EM. E-cigarette use is associated with a self-reported diagnosis of prediabetes in never cigarette smokers: results from the behavioral risk factor surveillance system survey. *Drug Alcohol Depend.* (2019) 205:107692. doi: 10.1016/j.drugalcdep.2019.107692

65. Luca M, Di Mauro M, Di Mauro M, Luca A. Gut microbiota in Alzheimer's disease, depression, and type 2 diabetes mellitus: the role of oxidative stress. *Oxid Med Cell Longev.* (2019) 2019:1–10. doi: 10.1155/2019/4730539

66. Heinecke JW, Goldberg IJ. Myeloperoxidase: a therapeutic target for preventing insulin resistance and the metabolic sequelae of obesity? *Diabetes.* (2014) 63:4001–3. doi: 10.2337/db14-1273

67. Bondonno NP, Davey RJ, Murray K, Radavelli-Bagatini S, Bondonno CP, Blekkenhorst LC, et al. Associations between fruit intake and risk of diabetes in the AusDiab cohort. *J Clin Endocrinol Metab.* (2021) 106:e4097–108. doi: 10.1210/clinem/dgab335

68. Sawada SS, Lee I-M, Naito H, Noguchi J, Tsukamoto K, Muto T, et al. Long-term trends in cardiorespiratory fitness and the incidence of type 2 diabetes. *Diabetes Care.* (2010) 33:1353–7. doi: 10.2337/dc09-1654

69. Hurrle S, Hsu WH. The etiology of oxidative stress in insulin resistance. *Biomed J.* (2017) 40:257–62. doi: 10.1016/j.bj.2017.06.007

70. Defronzo RA. Banting Lecture. From the triumvirate to the ominous octet: a new paradigm for the treatment of type 2 diabetes mellitus. *Diabetes.* (2009) 58:773–95. doi: 10.2337/db09-9028

71. Shan Z, Li Y, Baden MY, Bhupathiraju SN, Wang DD, Sun Q, et al. Association between healthy eating patterns and risk of cardiovascular disease. *JAMA Intern Med.* (2020) doi: 10.1001/jamainternmed.2020.2176

72. Venkatesh R, Sood D. *A Review of the Physiological Implications of Antioxidants in Food.* Bachelor of Science Interactive Qualifying Project. Worcester, Massachusetts, US: Worcester Polytechnic Institute (2011).

73. Redman LM, Smith SR, Burton JH, Martin CK, Il'Yasova D, Ravussin E. Metabolic slowing and reduced oxidative damage with sustained caloric restriction support the rate of living and oxidative damage theories of aging. *Cell Metab.* (2018) 27:805–15.e4. doi: 10.1016/j.cmet.2018.02.019

74. Gabel K, Cienfuegos S, Kalam F, Ezpeleta M, Varady KA. Time-restricted eating to improve cardiovascular health. *Curr Atheroscler Rep.* (2021) 23:22. doi: 10.1007/s11883-021-00922-7

75. Pérez-Beltrán YE, Rivera-Iñiguez I, Gonzalez-Becerra K, Pérez-Naitoh N, Tovar J, Sáyago-Ayerdi SG, et al. Personalized dietary recommendations based on lipid-related genetic variants: a systematic review. *Front Nutr.* (2022) 9:830283. doi: 10.3389/fnut.2022.830283

76. Hooker SP, Diaz KM, Blair SN, Colabianchi N, Hutto B, McDonnell MN, et al. Association of accelerometer-measured sedentary time and physical activity with risk of stroke among US adults. *JAMA Network Open.* (2022) 5:e2215385. doi: 10.1001/jamanetworkopen.2022.15385

77. Derbré F, Gratas-Delamarche A, Gómez-Cabrera MC, Viña J. Inactivity-induced oxidative stress: a central role in age-related sarcopenia? *Eur J Sport Sci.* (2014) 14:S98–108. doi: 10.1080/17461391.2011.654268

78. Kozakova M, Palombo C. Vascular ageing and aerobic exercise. *Int J Environ Res Public Health.* (2021) 18:10666. doi: 10.3390/ijerph182010666

79. Hogstrom G, Nordstrom A, Nordstrom P. High aerobic fitness in late adolescence is associated with a reduced risk of myocardial infarction later in life: a nationwide cohort study in men. *Eur Heart J.* (2014) 35:3133–40. doi: 10.1093/eurheartj/eht527

80. Fabris E, Sinagra G. Physical activity in older people: better late than never, but better early than late. *Heart.* (2022) 108:328–9. doi: 10.1136/heartjnl-2021-320462

81. Du Y, Liu B, Sun Y, Snetselaar LG, Wallace RB, Bao W. Trends in adherence to the physical activity guidelines for americans for aerobic activity and time spent on sedentary behavior among US adults, 2007 to 2016. *JAMA Network Open.* (2019) 2:e197597. doi: 10.1001/jamanetworkopen.2019.7597

82. Ferrari G, Cristi-Montero C, Drenowatz C, Kovalskys I, Gómez G, Rigotti A, et al. Meeting 24-h movement guidelines and markers of adiposity in adults from eight Latin America countries: the ELANS study. *Sci Rep.* (2022) 12:11382. doi: 10.1038/s41598-022-15504-z

83. Lloyd-Jones DM, Allen NB, Anderson CAM, Black T, Brewer LC, Foraker RE, et al. Life's essential 8: updating and enhancing the American Heart Association's construct of cardiovascular health: a presidential advisory from the American

Heart Association. *Circulation.* (2022) 146:e18–43. doi: 10.1161/CIR.00000000000 01078

84. Khan SS, Ning H, Wilkins JT, Allen N, Carnethon M, Berry JD, et al. Association of body mass index with lifetime risk of cardiovascular disease and compression of morbidity. *JAMA Cardiol.* (2018) 3:280–7. doi: 10.1001/jamacardio.2018.0022

85. Zhou Z, Macpherson J, Gray SR, Gill JMR, Welsh P, Celis-Morales C, et al. Are people with metabolically healthy obesity really healthy? A prospective cohort study of 381,363 UK Biobank participants. *Diabetologia.* (2021) 64:1963–72. doi: 10.1007/s00125-021-05484-6

86. Savini I, Catani MV, Evangelista D, Gasperi V, Avigliano L. Obesity-associated oxidative stress: strategies finalized to improve redox state. *Int J Mol Sci.* (2013) 14:10497–538 doi: 10.3390/ijms140510497

87. Galindo Muñoz JS, Morillas-Ruiz JM, Gómez Gallego M, Díaz Soler I, Barberá Ortega MDC, Martínez CM, et al. Cognitive training therapy improves the effect of hypocaloric treatment on subjects with overweight/obesity: a randomised clinical trial. *Nutrients.* (2019) 11:925. doi: 10.3390/nu11040925

88. Salminen P, Grönroos S, Helmiö M, Hurme S, Juuti A, Juusela R, et al. Effect of laparoscopic sleeve gastrectomy vs Roux-en-Y gastric bypass on weight loss, comorbidities, and reflux at 10 years in adult patients with obesity. *JAMA Surg.* (2022) 157:656–66. doi: 10.1001/jamasurg.2022.2229

89. Gagliardi AC, Miname MH, Santos RD. Uric acid: a marker of increased cardiovascular risk. *Atherosclerosis.* (2009) 202:11–7. doi: 10.1016/j.atherosclerosis.2008.05.022

90. Gaubert M, Bardin T, Cohen-Solal A, Diévart F, Fauvel JP, Guieu R, et al. Hyperuricemia and hypertension, coronary artery disease, kidney disease: from concept to practice. *Int J Mol Sci.* (2020) 21:4066. doi: 10.3390/ijms21114066

91. Liu N, Xu H, Sun Q, Yu X, Chen W, Wei H, et al. The role of oxidative stress in hyperuricemia and xanthine oxidoreductase (XOR) inhibitors. *Oxid Med Cell Longev.* (2021) 2021:1–15. doi: 10.1155/2021/1470380

92. Monroy MA. Chronic kidney disease alters vascular smooth muscle cell phenotype. *Front Biosci.* (2015) 20:784–95. doi: 10.2741/4337

93. Gianos E, Jackson EA, Tejpal A, Aspry K, O'Keefe J, Aggarwal M, et al. Oral health and atherosclerotic cardiovascular disease: a review. *Am J Prev Cardiol.* (2021) 7:100179. doi: 10.1016/j.ajpc.2021.100179

94. Bale BF, Doneen AL, Vigerust DJ. High-risk periodontal pathogens contribute to the pathogenesis of atherosclerosis. *Postgrad Med J.* (2016) 93:215–20. doi: 10.1136/postgradmedj-2016-134279

95. Zhang B, Khalaf H, Sirsjo A, Bengtsson T. Gingipains from the periodontal pathogen porphyromonas gingivalis play a significant role in regulation of angiopoietin 1 and angiopoietin 2 in human aortic smooth muscle cells. *Infect Immun.* (2015) 83:4256–65. doi: 10.1128/IAI.00498-15

96. Sharma P, Fenton A, Dias IH, Heaton B, Brown CL, Sidhu A, et al. Oxidative stress links periodontal inflammation and renal function. *J Clin Periodontol.* (2021) 48:357–67. doi: 10.1111/jcpe.13414

97. da Silva JC, Muniz WMG F, Oballe HJR, Andrades M, Rösing CK, Cavagni J. The effect of periodontal therapy on oxidative stress biomarkers: a systematic review. *J Clin Periodontol.* (2018) 45:1222–37. doi: 10.1111/jcpe.12993

98. Eke PI, Dye BA, Wei L, Slade GD, Thornton-Evans GO, Borgnakke WS, et al. Update on prevalence of periodontitis in adults in the United States: NHANES 2009 to 2012. *J Periodontol.* (2015) 86:611–22. doi: 10.1902/jop.2015.140520

99. Eke PI, Wei L, Borgnakke WS, Thornton-Evans G, Zhang X, Lu H, et al. Periodontitis prevalence in adults ≥ 65 years of age, in the USA. *Periodontol 2000.* (2016) 72:76–95. doi: 10.1111/prd.12145

100. Kassebaum NJ, Bernabé E, Dahiya M, Bhandari B, Murray CJ, Marcenes W. Global burden of severe periodontitis in 1990-2010: a systematic review and meta-regression. *J Dent Res.* (2014) 93:1045–53. doi: 10.1177/0022034514552491

101. Domont F, Cacoub P. Chronic hepatitis C virus infection, a new cardiovascular risk factor? *Liver International.* (2016) 36:621–7. doi: 10.1111/liv.13064

102. Farrugia PM, Lucariello R, Coppola JT. Human immunodeficiency virus and atherosclerosis. *Cardiol Rev.* (2009) 17:211–5. doi: 10.1097/CRD.0b013e3181b151a3

103. Ivanov AV, Bartosch B, Isaguliants MG. Oxidative stress in infection and consequent disease. *Oxid Med Cell Longev.* (2017) 2017:3496043. doi: 10.1155/2017/3496043

104. Roguljic H, Nincevic V, Bojanic K, Kuna L, Smolic R, Vcev A, et al. Impact of DAA treatment on cardiovascular disease risk in chronic HCV infection: an update. *Front Pharmacol.* (2021) 12:678546. doi: 10.3389/fphar.2021.678546

105. Domingues EAM, Ferrit-Martín M, Calleja-Hernández MÁ. Impact of pharmaceutical care on cardiovascular risk among older

HIV patients on antiretroviral therapy. *Int J Clin Pharm.* (2017) 39:52–60. doi: 10.1007/s11096-016-0387-1

106. Loke YK, Brown JW, Kwok CS, Niruban A, Myint PK. Association of obstructive sleep apnea with risk of serious cardiovascular events: a systematic review and meta-analysis. *Circ Cardiovasc Qual Outcomes.* (2012) 5:720–8. doi: 10.1161/CIRCOUTCOMES.111.964783

107. Drager LF, Togeiro SM, Polotsky VY, Lorenzi-Filho G. Obstructive sleep apnea: a cardiometabolic risk in obesity and the metabolic syndrome. *J Am Coll Cardiol.* (2013) 62:569–76. doi: 10.1016/j.jacc.2013.05.045

108. Salman LA, Shulman R, Cohen JB. Obstructive sleep apnea, hypertension, and cardiovascular risk: epidemiology, pathophysiology, and management. *Curr Cardiol Rep.* (2020) 22:6. doi: 10.1007/s11886-020-1257-y

109. Linz D, McEvoy RD, Cowie MR, Somers VK, Nattel S, Levy P, et al. Associations of obstructive sleep apnea with atrial fibrillation and continuous positive airway pressure treatment: a review. *JAMA Cardiol.* (2018) 3:532–40. doi: 10.1001/jamacardio.2018.0095

110. Khattak HK, Hayat F, Pamboukian SV, Hahn HS, Schwartz BP, Stein PK. Obstructive sleep apnea in heart failure: review of prevalence, treatment with continuous positive airway pressure, and prognosis. *Tex Heart Inst J.* (2018) 45:151–61. doi: 10.14503/THIJ-15-5678

111. Arnaud C, Bochaton T, Pepin JL, Belaidi E. Obstructive sleep apnoea and cardiovascular consequences: pathophysiological mechanisms. *Arch Cardiovasc Dis.* (2020) 113:350–8. doi: 10.1016/j.acvd.2020.01.003

112. Punjabi NM. The epidemiology of adult obstructive sleep apnea. *Proc Am Thorac Soc.* (2008) 5:136–43. doi: 10.1513/pats.200709-155MG

113. American Psychiatric Association. *Diagnostic Statistical Manual of Mental Disorders: DSM-5-TR.* Washington, DC: American Psychiatric Association Publishing (2022).

114. Orru G, Storari M, Scano A, Piras V, Taibi R, Viscuso D. Obstructive Sleep Apnea, oxidative stress, inflammation and endothelial dysfunction-an overview of predictive laboratory biomarkers. *Eur Rev Med Pharmacol Sci.* (2020) 24:6939–48. doi: 10.26355/eurrev_202006_21685

115. Javaheri S, Barbe F, Campos-Rodriguez F, Dempsey JA, Khayat R, Javaheri S, et al. Sleep apnea: types, mechanisms, and clinical cardiovascular consequences. *J Am Coll Cardiol.* (2017) 69:841–58. doi: 10.1016/j.jacc.2016.11.069

116. Lorenzi-Filho G, Almeida FR, Strollo PJ. Treating OSA: current and emerging therapies beyond CPAP. *Respirology.* (2017) 22:1500–7. doi: 10.1111/resp.13144

117. Tóthová L, Celec P, Mucska I, Hodosy J. Short-term effects of continuous positive airway pressure on oxidative stress in severe sleep apnea. *Sleep Breath.* (2019) 23:857–63. doi: 10.1007/s11325-018-01777-0

118. Halaris A, Leonard BE. Preface. *Mod Trends Pharmacopsychiatry.* (2013) 28:VII–VIII. doi: 10.1159/isbn.978-3-318-02311-4

119. Celano CM, Daunis DJ, Lokko HN, Campbell KA, Huffman JC. Anxiety disorders and cardiovascular disease. *Curr Psychiatry Rep.* (2016) 18:101. doi: 10.1007/s11920-016-0739-5

120. Vavakova M, Durackova Z, Trebaticka J. Markers of oxidative stress and neuroprogression in depression disorder. *Oxid Med Cell Longev.* (2015) 2015:898393. doi: 10.1155/2015/898393

121. Juszczyk G, Mikulska J, Kasperek K, Pietrzak D, Mrozek W, Herbet M. Chronic stress and oxidative stress as common factors of the pathogenesis of depression and Alzheimer's disease: the role of antioxidants in prevention and treatment. *Antioxidants.* (2021) 10:1439. doi: 10.3390/antiox10091439

122. Steenkamp LR, Hough CM, Reus VI, Jain FA, Epel ES, James SJ, et al. Severity of anxiety– but not depression– is associated with oxidative stress in Major Depressive Disorder. *J Affect Disord.* (2017) 219:193–200. doi: 10.1016/j.jad.2017.04.042

123. Fedoce ADG, Ferreira F, Bota RG, Bonet-Costa V, Sun PY, Davies KJA. The role of oxidative stress in anxiety disorder: cause or consequence? *Free Radic Res.* (2018) 52:737–50. doi: 10.1080/10715762.2018.1475733

124. Liu T, Zhong S, Liao X, Chen J, He T, Lai S, et al. A meta-analysis of oxidative stress markers in depression. *PLoS One.* (2015) 10:e0138904. doi: 10.1371/journal.pone.0138904

125. Panahi D, Pirposhteh EA, Moradi B, Poursadeqiyan M, Sahlabadi AS. Effectiveness of educational intervention on reducing oxidative stress caused by occupational stress in nurses: a health promotion approach. *J Educ Health Promot.* (2022) 55:56. doi: 10.4103/jehp.jehp_1425_21

126. Verdoia M, Schaffer A, Sartori C, Barbieri L, Cassetti E, et al. Vitamin D deficiency is independently associated with the extent of coronary artery disease. *Eur J Clin Invest.* (2014) 44:634–42. doi: 10.1111/eci.12281

127. Wang Y, Zhang H. Serum 25-hydroxyvitamin D3 levels are associated with carotid intima-media thickness and carotid atherosclerotic plaque in type 2 diabetic patients. *J Diabetes Res.* (2017) 2017:3510275. doi: 10.1155/2017/3510275

128. Holick MF. Vitamin D status: measurement, interpretation, clinical application. *Ann Epidemiol.* (2009) 19:73–8. doi: 10.1016/j.annepidem.2007.12.001

129. Lavie CJ, Lee JH, Milani RV. Vitamin D and cardiovascular disease will it live up to its hype? *J Am Coll Cardiol.* (2011) 58:1547–56. doi: 10.1016/j.jacc.2011.07.008

130. Wimalawansa SJ. Vitamin D deficiency: effects on oxidative stress, epigenetics, gene regulation, and aging. *Biology.* (2019) 8:30. doi: 10.3390/biology8020030

131. Ricca C, Aillon A, Bergandi L, Alotto D, Castagnoli C, Silvagno F. Vitamin D receptor is necessary for mitochondrial function and cell health. *Int J Mol Sci.* (2018) 19:1672. doi: 10.3390/ijms19061672

132. Salamanna F, Maglio M, Sartori M, Landini MP, Fini M. Vitamin D and platelets: a menacing duo in COVID-19 and potential relation to bone remodeling. *Int J Mol Sci.* (2021) 22:10010. doi: 10.3390/ijms221810010

133. Zhou W, Wang W, Yuan XJ, Xiao CC, Xing Y, Ye SD, et al. The effects of RBP4 and vitamin D on the proliferation and migration of vascular smooth muscle cells via the JAK2/STAT3 signaling pathway. *Oxid Med Cell Longev.* (2022) 2022:3046777. doi: 10.1155/2022/3046777

134. Kim D-H, Meza CA, Clarke H, Kim J-S, Hickner RC. Vitamin D and endothelial function. *Nutrients.* (2020) 12:575. doi: 10.3390/nu12020575

135. Cimmino G, Conte S, Morello M, Pellegrino G, Marra L, Morello A, et al. Vitamin D inhibits IL-6 pro-atherothrombotic effects in human endothelial cells: a potential mechanism for protection against COVID-19 infection? *J Cardiovasc Dev Dis.* (2022) 9:27. doi: 10.3390/jcdd9010027

136. Uberti F, Lattuada D, Morsanuto V, Nava U, Bolis G, Vacca G, et al. Vitamin D protects human endothelial cells from oxidative stress through the autophagic and survival pathways. *J Clin Endocrinol Metab.* (2014) 99:1367–1374. doi: 10.1210/jc.2013-2103

137. de la Guía-Galipienso F, Martínez-Ferran M, Vallecillo N, Lavie CJ, Sanchis-Gomar F, Pareja-Galeano H. Vitamin D and cardiovascular health. *Clin Nutr.* (2021) 40:2946–57. doi: 10.1016/j.clnu.2020.12.025

138. Boucher BJ, Grant WB. Difficulties in designing randomised controlled trials of vitamin D supplementation for reducing acute cardiovascular events and in the analysis of their outcomes. *Int J Cardiol Heart Vasculat.* (2020) 29:100564. doi: 10.1016/j.ijcha.2020.100564

139. Witkowski M, Weeks TL, Hazen SL. Gut microbiota and cardiovascular disease. *Circ Res.* (2020) 127:553–70. doi: 10.1161/CIRCRESAHA.120.316242

140. Jie Z, Xia H, Zhong S-L, Feng Q, Li S, Liang S, et al. The gut microbiome in atherosclerotic cardiovascular disease. *Nat Commun.* (2017) 8:845. doi: 10.1038/s41467-017-00900-1

141. Zhu Q, Gao R, Zhang Y, Pan D, Zhu Y, Zhang X, et al. Dysbiosis signatures of gut microbiota in coronary artery disease. *Physiol Genomics.* (2018) 50:893–903. doi: 10.1152/physiolgenomics.00070.2018

142. Ascher S, Reinhardt C. The gut microbiota: an emerging risk factor for cardiovascular and cerebrovascular disease. *Eur J Immunol.* (2018) 48:564–75. doi: 10.1002/eji.201646879

143. Hamer HM, Jonkers DM, Bast A, Vanhoutvin SA, Fischer MA, Kodde A, et al. Butyrate modulates oxidative stress in the colonic mucosa of healthy humans. *Clin Nutr.* (2009) 28:88–93. doi: 10.1016/j.clnu.2008.11.002

144. Valladares R, Sankar D, Li N, Williams E, Lai KK, Abdelgeliel AS, et al. Lactobacillus johnsonii N6.2 mitigates the development of type 1 diabetes in BB-DP rats. *PLoS ONE.* (2010) 5:e10507. doi: 10.1371/journal.pone.0010507

145. Leschelle X, Goubern M, Andriamihaja M, Blottière HM, Couplan E, Gonzalez-Barroso MD, et al. Adaptative metabolic response of human colonic epithelial cells to the adverse effects of the luminal compound sulfide. *Biochim Biophys Acta.* (2005) 1725:201–12. doi: 10.1016/j.bbagen.2005.06.002

146. Qiao Y, Sun J, Ding Y, Le G, Shi Y. Alterations of the gut microbiota in high-fat diet mice is strongly linked to oxidative stress. *Appl Microbiol Biotechnol.* (2013) 97:1689–97. doi: 10.1007/s00253-012-4323-6

147. Xu CC, Yang SF, Zhu LH, Cai X, Sheng YS, Zhu SW, et al. Regulation of N-acetyl cysteine on gut redox status and major microbiota in weaned piglets. *J Anim Sci.* (2014) 92:1504–11. doi: 10.2527/jas.2013-6755

148. Shandilya S, Kumar S, Kumar Jha N, Kumar Kesari K, Ruokolainen J. Interplay of gut microbiota and oxidative stress: perspective on neurodegeneration and neuroprotection. *J Adv Res.* (2022) 38:223–44. doi: 10.1016/j.jare.2021.09.005

149. Rahman MM, Islam F, Or-Rashid MH, Mamun AA, Rahaman MS, Islam MM, et al. The gut microbiota (microbiome) in cardiovascular disease and its therapeutic regulation. *Front Cell Infect Microbiol.* (2022) 12:903570. doi: 10.3389/fcimb.2022.903570

150. Dregan A, Charlton J, Chowienczyk P, Gulliford MC. Chronic inflammatory disorders and risk of type 2 diabetes mellitus, coronary heart disease, and stroke: a population-based cohort study. *Circulation.* (2014) 130:837–44. doi: 10.1161/CIRCULATIONAHA.114.009990

151. Crowson CS, Liao KP, Davis JM 3rd, Solomon DH, Matteson EL, Knutson KL, et al. Rheumatoid arthritis and cardiovascular disease. *Am Heart J.* (2013) 166:622–8.e1. doi: 10.1016/j.ahj.2013.07.010

152. Asanuma YF. Accelerated atherosclerosis and inflammation in systemic lupus erythematosus. *Nihon Rinsho Meneki Gakkai Kaishi.* (2012) 35:470–80. doi: 10.2177/jsci.35.470

153. Smallwood MJ, Nissim A, Knight AR, Whiteman M, Haigh R, Winyard PG. Oxidative stress in autoimmune rheumatic diseases. *Free Radic Biol Med.* (2018) 125:3–14. doi: 10.1016/j.freeradbiomed.2018.05.086

154. López-Armada MJ, Fernández-Rodríguez JA, Blanco FJ. Mitochondrial dysfunction and oxidative stress in rheumatoid arthritis. *Antioxidants.* (2022) 11:1151. doi: 10.3390/antiox11061151

155. Danesh Yazdi M, Wang Y, Di Q, Wei Y, Requia WJ, Shi L, et al. Long-term association of air pollution and hospital admissions among medicare participants using a doubly robust additive model. *Circulation.* (2021) 143:1584–96. doi: 10.1161/CIRCULATIONAHA.120.050252

156. Lelieveld J, Klingmuller K, Pozzer A, Poschl U, Fnais M, Daiber A, et al. Cardiovascular disease burden from ambient air pollution in Europe reassessed using novel hazard ratio functions. *Eur Heart J.* (2019) 40:1590–6. doi: 10.1093/eurheartj/ehz135

157. Leni Z, Künzi L, Geiser M. Air pollution causing oxidative stress. *Curr Opin Toxicol.* (2020) 20–21:1–8. doi: 10.1016/j.cotox.2020.02.006

158. Hahad O, Lelieveld J, Birklein F, Lieb K, Daiber A, Münzel T. Ambient air pollution increases the risk of cerebrovascular and neuropsychiatric disorders through induction of inflammation and oxidative stress. *Int J Mol Sci.* (2020) 21:4306. doi: 10.3390/ijms21124306

159. Abohashem S, Osborne MT, Dar T, Naddaf N, Abbasi T, Ghoneem A, et al. A leucopoietic-arterial axis underlying the link between ambient air pollution and cardiovascular disease in humans. *Eur Heart J.* (2021) 42:761–72. doi: 10.1093/eurheartj/ehaa982

160. Zhao M, Hoek G, Strak M, Grobbee DE, Graham I, Klipstein-Grobusch K, et al. A global analysis of associations between fine particle air pollution and cardiovascular risk factors: feasibility study on data linkage. *Glob Heart.* (2020) 15:53. doi: 10.5334/gh.877

161. Huang C, Moran AE, Coxson PG, Yang X, Liu F, Cao J, et al. Potential cardiovascular and total mortality benefits of air pollution control in urban China. *Circulation.* (2017) 136:1575–84. doi: 10.1161/CIRCULATIONAHA.116.026487

162. Sarnak MJ, Levey AS, Schoolwerth AC, Coresh J, Culleton B, Hamm LL, et al. Kidney disease as a risk factor for development of cardiovascular disease. *Circulation.* (2003) 108:2154–69. doi: 10.1161/01.CIR.0000095676.90936.80

163. Mafham M, Emberson J, Landray MJ, Wen CP, Baigent C. Estimated glomerular filtration rate and the risk of major vascular events and all-cause mortality: a meta-analysis. *PLoS ONE.* (2011) 6:e25920. doi: 10.1371/journal.pone.0025920

164. van der Velde M, Matsushita K, Coresh J, Astor BC, Woodward M, Levey A, et al. Lower estimated glomerular filtration rate and higher albuminuria are associated with all-cause and cardiovascular mortality. A collaborative meta-analysis of high-risk population cohorts. *Kidney Int.* (2011) 79:1341–52. doi: 10.1038/ki.2010.536

165. Yuan J, Zou X-R, Han S-P, Cheng H, Wang L, Wang J-W, et al. Prevalence and risk factors for cardiovascular disease among chronic kidney disease patients: results from the Chinese cohort study of chronic kidney disease (C-STRIDE). *BMC Nephrol.* (2017) 18:23. doi: 10.1186/s12882-017-0441-9

166. Vallianou NG, Mitesh S, Gkogkou A, Geladari E. Chronic kidney disease and cardiovascular disease: is there any relationship? *Curr Cardiol Rev.* (2018) 15:55–63. doi: 10.2174/1573403X14666180711124825

167. Umbro I, Fabiani V, Fabiani M, Angelico F, Del Ben M. A systematic review on the association between obstructive sleep apnea and chronic kidney disease. *Sleep Med Rev.* (2020) 53:101337. doi: 10.1016/j.smrv.2020.101337

168. Jean G, Souberbielle J, Chazot C. Vitamin D in chronic kidney disease and dialysis patients. *Nutrients.* (2017) 9:328. doi: 10.3390/nu9040328

169. Chen Y, Cao F, Xiao J-P, Fang X-Y, Wang X-R, Ding L-H, et al. Emerging role of air pollution in chronic kidney disease. *Environ Sci Pollut Res.* (2021) 28:52610–24. doi: 10.1007/s11356-021-16031-6

170. Feng Z, Wang T, Dong S, Jiang H, Zhang J, Raza HK, et al. Association between gut dysbiosis and chronic kidney disease: a narrative review of the literature. *J Int Med Res.* (2021) 49:030006052110532. doi: 10.1177/03000605211053276

171. Simoes e Silva AC, Miranda AS, Rocha NP, Teixeira AL. Neuropsychiatric disorders in chronic kidney disease. *Front Pharmacol.* (2019) 10:932. doi: 10.3389/fphar.2019.00932

172. Chang A, Van Horn L, Jacobs DR, Liu K, Muntner P, Newsome B, et al. Lifestyle-related factors, obesity, and incident microalbuminuria: the CARDIA (coronary artery risk development in young adults) study. *Am J Kidney Dis.* (2013) 62:267–75. doi: 10.1053/j.ajkd.2013.02.363

173. Okabayashi Y, Tsuboi N, Sasaki T, Haruhara K, Kanzaki G, Koike K, et al. Glomerulopathy associated with moderate obesity. *Kidney Int Rep.* (2016) 1:250–5. doi: 10.1016/j.ekir.2016.08.006

174. Minutolo R, De Nicola L, Mazzaglia G, Postorino M, Cricelli C, Mantovani LG, et al. Detection and awareness of moderate to advanced CKD by primary care practitioners: a cross-sectional study from Italy. *Am J Kidney Dis.* (2008) 52:444–53. doi: 10.1053/j.ajkd.2008.03.002

175. Chen Y-C, Lin H-Y, Li C-Y, Lee M-S, Su YC. A nationwide cohort study suggests that hepatitis C virus infection is associated with increased risk of chronic kidney disease. *Kidney Int.* (2014) 85:1200–7. doi: 10.1038/ki.2013.455

176. Gherghina ME, Peride I, Tiglis M, Neagu TP, Niculae A, Checherita IA. Uric acid and oxidative stress-relationship with cardiovascular, metabolic, and renal impairment. *Int J Mol Sci.* (2022) 23:3188. doi: 10.3390/ijms23063188

177. Duni A, Liakopoulos V, Roumeliotis S, Peschos D, Dounousi E. Oxidative stress in the pathogenesis and evolution of chronic kidney disease: Untangling Ariadne's thread. *Int J Mol Sci.* (2019) 20:3711 doi: 10.3390/ijms20153711

178. Ferrer LM, Monroy AM, Lopez-Pastrana J, Nanayakkara G, Cueto R, Li Y-F, et al. Caspase-1 plays a critical role in accelerating chronic kidney disease-promoted neointimal hyperplasia in the carotid artery. *J Cardiovasc Transl Res.* (2016) 9:135–144. doi: 10.1007/s12265-016-9683-3

179. Bray G. Obesity increases risk for diabetes. *Int J Obesity Relat Metab Disord.* (1992) 16:S13–7.

180. Sami W, Ansari T, Butt NS, Ab Hamid RM. Effect of diet on type 2 diabetes mellitus: a review. *Int J Health Sci.* (2017) 11:65. doi: 10.1002/dmrr.2515

181. Aune D, Norat T, Leitzmann M, Tonstad S, Vatten LJ. Physical activity and the risk of type 2 diabetes: a systematic review and dose–response meta-analysis. *Eur J Epidemiol.* (2015) 30:529–42. doi: 10.1007/s10654-015-0056-z

182. Suez J, Korem T, Zeevi D, Zilberman-Schapira G, Thaiss CA, Maza O, et al. Artificial sweeteners induce glucose intolerance by altering the gut microbiota. *Nature.* (2014) 514:181–6. doi: 10.1038/nature13793

183. Thomas C, Wurzer L, Malle E, Ristow M, Madreiter-Sokolowski CT. Modulation of reactive oxygen species homeostasis as a pleiotropic effect of commonly used drugs. *Front Aging.* (2022) 3:905261. doi: 10.3389/fragi.2022.905261

184. Newman CB, Preiss D, Tobert JA, Jacobson TA, Page RL 2nd, Goldstein LB, et al. Statin safety and associated adverse events: a scientific statement from the American Heart Association. *Arterioscler Thromb Vasc Biol.* (2019) 39:e38–e81. doi: 10.1161/ATV.0000000000000073

185. Pignatelli P, Carnevale R, Pastori D, Cangemi R, Napoleone L, Bartimoccia S, et al. Immediate antioxidant and antiplatelet effect of atorvastatin via inhibition of Nox2. *Circulation.* (2012) 126:92–103. doi: 10.1161/CIRCULATIONAHA.112.095554

186. Margaritis M, Sanna F, Antoniades C. Statins and oxidative stress in the cardiovascular system. *Curr Pharm Des.* (2018) 23:7040–7. doi: 10.2174/1381612823666170926130338

187. Zinellu A, Mangoni AA. A systematic review and meta-analysis of the effect of statins on glutathione peroxidase, superoxide dismutase, and catalase. *Antioxidants.* (2021) 10:1841. doi: 10.3390/antiox10111841

188. Chen S, Liu B, Kong D, Li S, Li C, Wang H, et al. Atorvastatin calcium inhibits phenotypic modulation of PDGF-BB-induced VSMCs via down-regulation the Akt signaling pathway. *PLoS ONE.* (2015) 10:e0122577. doi: 10.1371/journal.pone.0122577

189. Ferguson JF, Hinkle CC, Mehta NN, Bagheri R, Derohannessian SL, Shah R, et al. Translational studies of lipoprotein-associated phospholipase A in inflammation and atherosclerosis. *J Am Coll Cardiol.* (2012) 59:764–72. doi: 10.1016/j.jacc.2011.11.019

190. White HD, Simes J, Stewart RAH, Blankenberg S, Barnes EH, Marschner IC, et al. Changes in lipoprotein-associated phospholipase A2 activity predict coronary events and partly account for the treatment effect of pravastatin: results from the long-term intervention with pravastatin in ischemic disease study. *J Am Heart Assoc.* (2013) 2:e000360. doi: 10.1161/JAHA.113.000360

191. Pinkosky SL, Newton RS, Day EA, Ford RJ, Lhotak S, Austin RC, et al. Liver-specific ATP-citrate lyase inhibition by bempedoic acid decreases LDL-C and attenuates atherosclerosis. *Nat Commun.* (2016) 7:13457. doi: 10.1038/ncomms13457

192. Ballantyne CM, Laufs U, Ray KK, Leiter LA, Bays HE, Goldberg AC, et al. Bempedoic acid plus ezetimibe fixed-dose combination in patients with hypercholesterolemia and high CVD risk treated with maximally tolerated statin therapy. *Eur J Prev Cardiol.* (2020) 27:593–603. doi: 10.1177/2047487319864671

193. Goldberg AC, Leiter LA, Stroes ESG, Baum SJ, Hanselman JC, Bloedon LT, et al. Effect of bempedoic acid vs placebo added to maximally tolerated statins on low-density lipoprotein cholesterol in patients at high risk for cardiovascular disease. *JAMA.* (2019) 322:1780. doi: 10.1001/jama.2019.16585

194. Zhao X, Ma X, Luo X, Shi Z, Deng Z, Jin Y, et al. Efficacy and safety of bempedoic acid alone or combining with other lipid-lowering therapies in hypercholesterolemic patients: a meta-analysis of randomized controlled trials. *BMC Pharmacol Toxicol.* (2020) 21:86. doi: 10.1186/s40360-020-00463-w

195. Bays HE, Baum SJ, Brinton EA, Plutzky J, Hanselman JC, Teng R, et al. Effect of bempedoic acid plus ezetimibe fixed-dose combination vs ezetimibe or placebo on low-density lipoprotein cholesterol in patients with type 2 diabetes and hypercholesterolemia not treated with statins. *Am J Prevent Cardiol.* (2021) 8:100278. doi: 10.1016/j.ajpc.2021.100278

196. Lloyd-Jones DM, Morris PB, Ballantyne CM, Birtcher KK, Covington AM, DePalma SM, et al. Wilkins: 2022 ACC Expert Consensus Decision Pathway on the Role of Nonstatin Therapies for LDL-Cholesterol Lowering in the Management of Atherosclerotic Cardiovascular Disease Risk: A Report of the American College of Cardiology Solution Set Oversight Committee. *J Am Coll Cardiol.* (2022) 80:1366–418. doi: 10.1016/j.jacc.2022.07.006

197. Marston NA, Giugliano RP, Im K, Silverman MG, O'Donoghue ML, Wiviott SD, et al. Association between triglyceride lowering and reduction of cardiovascular risk across multiple lipid-lowering therapeutic classes: a systematic review and meta-regression analysis of randomized controlled trials. *Circulation.* (2019) 140:1308–17. doi: 10.1161/CIRCULATIONAHA.119.041998

198. Prasad A. Biochemistry and molecular biology of mechanisms of action of fibrates–an overview. *Int J Biochem Res Rev.* (2019) 26:1–12 doi: 10.9734/ijbcrr/2019/v26i230094

199. Raslová K, Nagyová A, Dobiásová M, Ptáčková K, Dusinská M. Effect of ciprofibrate on lipoprotein metabolism and oxidative stress parameters in patients with type 2 diabetes mellitus and atherogenic lipoprotein phenotype. *Acta Diabetol.* (2000) 37:131–4. doi: 10.1007/s005920070015

200. Sabatine MS, Giugliano RP, Wiviott SD, Raal FJ, Blom DJ, Robinson J, et al. Open-label study of long-term evaluation against: efficacy and safety of evolocumab in reducing lipids and cardiovascular events. *N Engl J Med.* (2015) 372:1500–9. doi: 10.1056/NEJMoa1500858

201. Robinson JG, Farnier M, Krempf M, Bergeron J, Luc G, Averna M, et al. Efficacy and safety of alirocumab in reducing lipids and cardiovascular events. *N Engl J Med.* (2015) 372:1489–99. doi: 10.1056/NEJMoa1501031

202. Schwartz GG, Steg PG, Szarek M, Bhatt DL, Bittner VA, Diaz R, et al. Alirocumab and cardiovascular outcomes after acute coronary syndrome. *N Engl J Med.* (2018) 379:2097–107. doi: 10.1056/NEJMoa1801174

203. Cammisotto V, Baratta F, Simeone PG, Barale C, Lupia E, Galardo G, et al. Proprotein convertase subtilisin kexin type 9 (PCSK9) beyond lipids: the role in oxidative stress and thrombosis. *Antioxidants.* (2022) 11:569. doi: 10.3390/antiox11030569

204. Third report of the national cholesterol education program (NCEP) expert panel on detection, evaluation, and treatment of high blood cholesterol in adults (Adult Treatment Panel III) final report. *Circulation.* (2002) 106:3143–421 doi: 10.1161/circ.106.25.3143

205. Ganji SH, Qin S, Zhang L, Kamanna VS, Kashyap ML. Niacin inhibits vascular oxidative stress, redox-sensitive genes, and monocyte adhesion to human aortic endothelial cells. *Atherosclerosis.* (2009) 202:68–75. doi: 10.1016/j.atherosclerosis.2008.04.044

206. Hamoud S, Kaplan M, Meilin E, Hassan A, Torgovicky R, Cohen R, et al. Niacin administration significantly reduces oxidative stress in patients with hypercholesterolemia and low levels of high-density lipoprotein cholesterol. *Am J Med Sci.* (2013) 345:195–9. doi: 10.1097/MAJ.0b013e3182548c28

207. Romani M, Hofer DC, Katsyuba E, Auwerx J. Niacin: an old lipid drug in a new NAD+ dress. *J Lipid Res.* (2019) 60:741–6. doi: 10.1194/jlr.S092007

208. Ilkhani F, Hosseini B, Saedisomeolia A. Niacin and oxidative stress: a mini-review. *J Nutr Med Diet Care.* (2016) 2:014. doi: 10.23937/2572-3278.1510014

209. Skulas-Ray AC, Wilson PWF, Harris WS, Brinton EA, Kris-Etherton PM, Richter CK, et al. Omega-3 fatty acids for the management of hypertriglyceridemia: a science advisory from the American Heart Association. *Circulation.* (2019) 140:e673–91. doi: 10.1161/CIR.0000000000000709

210. Heshmati J, Morvaridzadeh M, Maroufizadeh S, Akbari A, Yavari M, Amirinejad A, et al. Omega-3 fatty acids supplementation and oxidative stress parameters: a systematic review and meta-analysis of clinical trials. *Pharmacol Res.* (2019) 149:104462. doi: 10.1016/j.phrs.2019.104462

211. Rahimi K, Bidel Z, Nazarzadeh M, Copland E, Canoy D, Ramakrishnan R, et al. Pharmacological blood pressure lowering for primary and secondary prevention of cardiovascular disease across different levels of blood pressure: an individual participant-level data meta-analysis. *Lancet.* (2021) 397:1625–36. doi: 10.1016/S0140-6736(21)00590-0

212. Snow V, Barry P, Fihn SD, Gibbons RJ, Owens DK, Williams SV, et al. Primary care management of chronic stable angina and asymptomatic suspected or known coronary artery disease: a clinical practice guideline from the American College of Physicians. *Ann Intern Med.* (2004) 141:562–7. doi: 10.7326/0003-4819-141-7-200410050-00014

213. Vukelic S, Griendling KK. Angiotensin II, from vasoconstrictor to growth factor: a paradigm shift. *Circ Res.* (2014) 114:754–7. doi: 10.1161/CIRCRESAHA.114.303045

214. Hornig B, Landmesser U, Kohler C, Ahlersmann D, Spiekermann S, Christoph A, et al. Comparative effect of ACE inhibition and angiotensin II type 1 receptor antagonism on bioavailability of nitric oxide in patients with coronary artery disease. *Circulation.* (2001) 103:799–805. doi: 10.1161/01.CIR.103.6.799

215. Liang W, Tan CY, Ang L, Sallam N, Granville DJ, Wright JM, et al. Ramipril improves oxidative stress-related vascular endothelial dysfunction in db/db mice. *J Physiol Sci.* (2008) 58:405–11. doi: 10.2170/physiolsci.RP012808

216. Mason RP. Mechanisms of plaque stabilization for the dihydropyridine calcium channel blocker amlodipine: review of the evidence. *Atherosclerosis.* (2002) 165:191–9. doi: 10.1016/S0021-9150(01)00729-8

217. Kim HJ, Han SJ, Kim DJ, Jang HC, Lim S, Choi SH, et al. Effects of valsartan and amlodipine on oxidative stress in type 2 diabetic patients with hypertension: a randomized, multicenter study. *Korean J Intern Med.* (2017) 32:497–504. doi: 10.3904/kjim.2015.404

218. Matsuda Y, Akita H, Terashima M, Shiga N, Kanazawa K, Yokoyama M. Carvedilol improves endothelium-dependent dilatation in patients with coronary artery disease. *Am Heart J.* (2000) 140:753–9. doi: 10.1067/mhj.2000.110093

219. Kametani R, Miura T, Harada N, Shibuya M, Wang R, Tan H, et al. Carvedilol inhibits mitochondrial oxygen consumption and superoxide production during calcium overload in isolated heart mitochondria. *Circ J.* (2006) 70:321–6. doi: 10.1253/circj.70.321

220. Zepeda RJ, Castillo R, Rodrigo R, Prieto JC, Aramburu I, Brugere S, et al. Effect of carvedilol and nebivolol on oxidative stress-related parameters and endothelial function in patients with essential hypertension. *Basic Clin Pharmacol Toxicol.* (2012) 111:309–16. doi: 10.1111/j.1742-7843.2012.00911.x

221. Sudano I, Osto E, Ruschitzka F. *Blood Pressure-Lowering Therapy.* Berlin Heidelberg: Springer (2020).

222. Yaribeygi H, Atkin SL, Sahebkar A. A review of the molecular mechanisms of hyperglycemia-induced free radical generation leading to oxidative stress. *J Cell Physiol.* (2019) 234:1300–12. doi: 10.1002/jcp.27164

223. Li FF, Fu LY, Xu XH, Su XF, Wu JD, Ye L, et al. Analysis of the add-on effect of α-glucosidase inhibitor, acarbose in insulin therapy: a pilot study. *Biomed Rep.* (2016) 5:461–6. doi: 10.3892/br.2016.744

224. Rizzo MR, Barbieri M, Marfella R, Paolisso G. Reduction of oxidative stress and inflammation by blunting daily acute glucose fluctuations in patients with type 2 diabetes: role of dipeptidyl peptidase-IV inhibition. *Diabetes Care.* (2012) 35:2076–82. doi: 10.2337/dc12-0199

225. Del Guerra S, Grupillo M, Masini M, Lupi R, Bugliani M, Torri S, et al. Gliclazide protects human islet beta-cells from apoptosis induced by intermittent high glucose. *Diabetes Metab Res Rev.* (2007) 23:234–8. doi: 10.1002/dmrr.680

226. Owen MR, Doran E, Halestrap AP. Evidence that metformin exerts its anti-diabetic effects through inhibition of complex 1 of the mitochondrial respiratory chain. *Biochem J.* (2000) 348:607–14 doi: 10.1042/bj3480607

227. Ashabi G, Khalaj L, Khodagholi F, Goudarzvand M, Sarkaki A. Pre-treatment with metformin activates Nrf2 antioxidant pathways and inhibits inflammatory responses through induction of AMPK after transient global cerebral ischemia. *Metab Brain Dis.* (2015) 30:747–54. doi: 10.1007/s11011-014-9632-2

228. D. Diniz Vilela D, Gomes Peixoto L, Teixeira RR, Belele Baptista N, Carvalho Caixeta D, Vieira de Souza A, et al. The role of metformin in controlling oxidative stress in muscle of diabetic rats. *Oxid Med Cell Longev.* (2016) 2016:6978625. doi: 10.1155/2016/6978625

229. Zhu Q, Ni XQ, Lu WW, Zhang JS, Ren JL, Wu D, et al. Intermedin reduces neointima formation by regulating vascular smooth muscle cell phenotype via cAMP/PKA pathway. *Atherosclerosis.* (2017) 266:212–22. doi: 10.1016/j.atherosclerosis.2017.10.011

230. Krasner NM, Ido Y, Ruderman NB, Cacicedo JM. Glucagon-like peptide-1 (GLP-1) analog liraglutide inhibits endothelial cell inflammation through a calcium and AMPK dependent mechanism. *PLoS ONE.* (2014) 9:e97554. doi: 10.1371/journal.pone.0097554

231. Uthman L, Baartscheer A, Schumacher CA, Fiolet JWT, Kuschma MC, Hollmann MW, et al. Direct cardiac actions of sodium glucose cotransporter 2 inhibitors target pathogenic mechanisms underlying heart failure in diabetic patients. *Front Physiol.* (2018) 9:1575. doi: 10.3389/fphys.2018.01575

232. Osman I, Segar L. Pioglitazone, a PPARgamma agonist, attenuates PDGF-induced vascular smooth muscle cell proliferation through AMPK-dependent and AMPK-independent inhibition of mTOR/p70S6K and ERK signaling. *Biochem Pharmacol.* (2016) 101:54–70. doi: 10.1016/j.bcp.2015.11.026

233. Redondo S, Ruiz E, Santos-Gallego CG, Padilla E, Tejerina T. Pioglitazone induces vascular smooth muscle cell apoptosis through a peroxisome proliferator-activated receptor-γ, transforming growth factor-β1, and a Smad2-dependent mechanism. *Diabetes.* (2005) 54:811–7. doi: 10.2337/diabetes.54.3.811

234. Mazzone T, Meyer PM, Feinstein SB, Davidson MH, Kondos GT, D'Agostino RB, et al. Effect of pioglitazone compared with glimepiride on carotid intima-media thickness in type 2 diabetes: a randomized trial. *JAMA.* (2006) 296:2572–81. doi: 10.1001/jama.296.21.joc60158

235. Nissen SE, Nicholls SJ, Wolski K, Nesto R, Kupfer S, Perez A, et al. Comparison of pioglitazone vs glimepiride on progression of coronary atherosclerosis in patients with type 2 diabetes: the periscope randomized controlled trial. *JAMA.* (2008) 299:1561–73. doi: 10.1001/jama.299.13.1561

236. Saremi A, Schwenke DC, Buchanan TA, Hodis HN, Mack WJ, Banerji M, et al. Pioglitazone slows progression of atherosclerosis in prediabetes independent of changes in cardiovascular risk factors. *Arterioscler Thromb Vasc Biol.* (2013) 33:393–9. doi: 10.1161/ATVBAHA.112.300346

237. Yang HB, Zhao XY, Zhang JY, Du YY, Wang XF. Pioglitazone induces regression and stabilization of coronary atherosclerotic plaques in patients with impaired glucose tolerance. *Diabet Med.* (2012) 29:359–65. doi: 10.1111/j.1464-5491.2011.03458.x

238. Tuttolomondo A, Di Raimondo D, Pecoraro R, Arnao V, Pinto A, Licata G. Atherosclerosis as an Inflammatory Disease. *Curr Pharm Des.* (2012) 18:4266–88. doi: 10.2174/138161212802481237

239. Xiang P, Blanchard V, Francis GA. Smooth muscle cell-macrophage interactions leading to foam cell formation in atherosclerosis: location, location, location. *Front Physiol.* (2022) 13:921597. doi: 10.3389/fphys.2022.921597

240. Augé N, Maupas-Schwalm FO, Elbaz M, Thiers J-C, Waysbort A, Itohara S, et al. Role for matrix metalloproteinase-2 in oxidized low-density lipoprotein–induced activation of the sphingomyelin/ceramide pathway and smooth muscle cell proliferation. *Circulation.* (2004) 110:571–8. doi: 10.1161/01.CIR.0000136995.83451.1D

241. Wilkins JT, Li RC, Sniderman A, Chan C, Lloyd-Jones DM. Discordance between apolipoprotein B and LDL-cholesterol in young adults predicts coronary artery calcificationthe CARDIA study. *J Am Coll Cardiol.* (2016) 67:193–201. doi: 10.1016/j.jacc.2015.10.055

242. Otarigho B, Aballay A. Cholesterol regulates innate immunity via nuclear hormone receptor NHR-8. *iScience.* (2020) 23:101068. doi: 10.1016/j.isci.2020.101068

243. Meijaard E, Abrams JF, Slavin JL, Sheil D. Dietary fats, human nutrition and the environment: balance and sustainability. *Front Nutr.* (2022) 9:878644. doi: 10.3389/fnut.2022.878644

244. Sachdeva A, Cannon CP, Deedwania PC, Labresh KA, Smith SC, Jr., et al. Lipid levels in patients hospitalized with coronary artery disease: an analysis of 136,905 hospitalizations in get with the guidelines. *Am Heart J.* (2009) 157:111–7.e2. doi: 10.1016/j.ahj.2008.08.010

245. Walldius G, Jungner I, Aastveit AH, Holme I, Furberg CD, Sniderman AD. The apoB/apoA-I ratio is better than the cholesterol ratios to estimate the balance between plasma proatherogenic and antiatherogenic lipoproteins and to predict coronary risk. *Clin Chem Lab Med.* (2004) 42:1355–63. doi: 10.1515/CCLM.2004.254

246. Ridker PM, Everett BM, Thuren T, MacFadyen JG, Chang WH, Ballantyne C, et al. Antiinflammatory therapy with canakinumab for atherosclerotic disease. *N Engl J Med.* (2017) 377:1119–31. doi: 10.1056/NEJMoa1707914

247. Gustafsson M, Borén J. Mechanism of lipoprotein retention by the extracellular matrix. *Curr Opin Lipidol.* (2004) 15:505–14. doi: 10.1097/00041433-200410000-00003

248. Yoshida T, Owens GK. Molecular determinants of vascular smooth muscle cell diversity. *Circ Res.* (2005) 96:280–91. doi: 10.1161/01.RES.0000155951.62152.2e

249. Liu R, Jin Y, Tang WH, Qin L, Zhang X, Tellides G, et al. Ten-eleven translocation-2 (TET2) is a master regulator of smooth muscle cell plasticity. *Circulation.* (2013) 128:2047–57. doi: 10.1161/CIRCULATIONAHA.113.002887

250. Zeng Z, Xia L, Fan S, Zheng J, Qin J, Fan X, et al. Circular RNA CircMAP3K5 acts as a MicroRNA-22-3p sponge to promote resolution of intimal hyperplasia via TET2-mediated smooth muscle cell differentiation. *Circulation.* (2021) 143:354–71. doi: 10.1161/CIRCULATIONAHA.120.049715

251. Rask-Madsen C, King GL. Proatherosclerotic mechanisms involving protein kinase C in diabetes and insulin resistance. *Arterioscler Thromb Vasc Biol.* (2005) 25:487–96. doi: 10.1161/01.ATV.0000155325.41507.e0

252. Feng X, Liu P, Zhou X, Li M-T, Li F-L, Wang Z, et al. Thromboxane A2 activates YAP/TAZ protein to induce vascular smooth muscle cell proliferation and migration. *J Biol Chem.* (2016) 291:18947–58. doi: 10.1074/jbc.M116.739722

253. Rade JJ, Barton BA, Vasan RS, Kronsberg SS, Xanthakis V, Keaney JF, et al. Association of thromboxane generation with survival in aspirin users and nonusers. *J Am Coll Cardiol.* (2022) 80:233–50. doi: 10.1016/j.jacc.2022.04.034

254. Patrono C, Rocca B. Measurement of thromboxane biosynthesis in health and disease. *Front Pharmacol.* (2019) 10:1244. doi: 10.3389/fphar.2019.01244

255. Rudijanto A. The role of vascular smooth muscle cells on the pathogenesis of atherosclerosis. *Acta Med Indones.* (2007) 39:86-93

256. Williams H, Mill CA, Monk BA, Hulin-Curtis S, Johnson JL, George SJ. Wnt2 and WISP-1/CCN4 induce intimal thickening via promotion of smooth muscle cell migration. *Arterioscler Thromb Vasc Biol.* (2016) 36:1417–24. doi: 10.1161/ATVBAHA.116.307626

257. Bale BF, Doneen AL. A guarantee of arterial wellness: new era of cardiovascular medicine. *J Clin Exp Cardiolog.* (2014) 5:298. doi: 10.4172/2155-9880.1000298

258. Feng D, Esperat MC, Doneen AL, Bale B, Song H, Green AE. 8-year outcomes of a program for early prevention of cardiovascular events: a growth-curve analysis. *J Cardiovasc Nurs.* (2014) 30:281–91. doi: 10.1097/JCN.0000000000000141

259. Madder RD, Husaini M, Davis AT, VanOosterhout S, Khan M, Wohns D, et al. Large lipid-rich coronary plaques detected by near-infrared spectroscopy at non-stented sites in the target artery identify patients likely to experience future major adverse cardiovascular events. *Eur Heart J Cardiovasc Imaging.* (2016) 17:393–9. doi: 10.1093/ehjci/jev340

260. Sun J, Zhao X-Q, Balu N, Neradilek MB, Isquith DA, Yamada K, et al. Carotid plaque lipid content and fibrous cap status predict systemic CV outcomes. The MRI Substudy in AIM-HIGH. *JACC Cardiovasc Imaging.* (2017) 10:241–9. doi: 10.1016/j.jcmg.2016.06.017

261. Xing L, Higuma T, Wang Z, Aguirre AD, Mizuno K, Takano M, et al. Clinical significance of lipid-rich plaque detected by optical coherence tomography: a 4-year follow-up study. *J Am Coll Cardiol.* (2017) 69:2502–13. doi: 10.1016/S0735-1097(17)34364-4

262. Cheng HG, Patel BS, Martin SS, Blaha M, Doneen A, Bale B, et al. Effect of comprehensive cardiovascular disease risk management on longitudinal changes in carotid artery intima-media thickness in a community-based prevention clinic. *Arch Med Sci.* (2016) 12:728–35. doi: 10.5114/aoms.2016.60955

263. Bartlett VL, Dhruva SS, Shah ND, Ryan P, Ross JS. Feasibility of using real-world data to replicate clinical trial evidence. *JAMA*

Netw Open. (2019) 2:e1912869. doi: 10.1001/jamanetworkopen.2019.12869

264. Hiramatsu K, Barrett A, Miyata Y. Current status, challenges, and future perspectives of real-world data and real-world evidence in Japan. *Drugs Real World Outcomes.* (2021) 8:459–80. doi: 10.1007/s40801-021-00266-3

265. Wehrle K, Tozzi V, Braune S, Roßnagel F, Dikow H, Paddock S, et al. Implementation of a data control framework to ensure confidentiality, integrity, and availability of high-quality real-world data (RWD) in the NeuroTransData (NTD) registry. *JAMIA Open.* (2022) 5:ooac017. doi: 10.1093/jamiaopen/ooac017

266. Willeit P, Tschiderer L, Allara E, Reuber K, Seekircher L, Gao L, et al. Carotid intima-media thickness progression as surrogate marker for cardiovascular risk. *Circulation.* (2020) 142:621–42. doi: 10.1161/CIRCULATIONAHA.120.046361

267. Arbab-Zadeh A, Nakano M, Virmani R, Fuster V. Acute coronary events. *Circulation.* (2012) 125:1147–56. doi: 10.1161/CIRCULATIONAHA.111.047431

268. Baber U, Mehran R, Sartori S, Schoos MM, Sillesen H, Muntendam P, et al. Prevalence, impact, and predictive value of detecting subclinical coronary and carotid atherosclerosis in asymptomatic adults: the BioImage study. *J Am Coll Cardiol.* (2015) 65:1065–74. doi: 10.1016/j.jacc.2015.01.017

269. Nicolaides A, Panayiotou AG. Screening for atherosclerotic cardiovascular risk using ultrasound. *J Am Coll Cardiol.* (2016) 67:1275–7. doi: 10.1016/j.jacc.2016.01.016

270. Doneen AL, Bale BF, Vigerust DJ, Leimgruber PP. Cardiovascular prevention: migrating from a binary to a ternary classification. *Front Cardiovasc Med.* (2020) 7:92. doi: 10.3389/fcvm.2020.00092

271. Näslund U, Ng N, Lundgren A, Fhärm E, Grönlund C, Johansson H, et al. Visualization of asymptomatic atherosclerotic disease for optimum cardiovascular prevention (VIPVIZA): a pragmatic, open-label, randomised controlled trial. *Lancet.* (2019) 393:133–42. doi: 10.1016/S0140-6736(18)32818-6

272. Sabatine MS, Morrow DA, Jablonski KA, Rice MM, Warnica JW, Domanski MJ, et al. Prognostic significance of the centers for disease control/American Heart Association high-sensitivity C-reactive protein cut points for cardiovascular and other outcomes in patients with stable coronary artery disease. *Circulation.* (2007) 115:1528–36. doi: 10.1161/CIRCULATIONAHA.106.649939

273. Bakris GL. Microalbuminuria: what is it? Why is it important? What should be done about it? *J Clin Hypertens.* (2001) 3:99–102 doi: 10.1111/j.1524-6175.2001.00442.x

274. Nicholls SJ, Hazen SL. Myeloperoxidase and cardiovascular disease. *Arterioscler Thromb Vasc Biol.* (2005) 25:1102–11. doi: 10.1161/01.ATV.0000163262.83456.6d

275. Morrow JD. Quantification of isoprostanes as indices of oxidant stress and the risk of atherosclerosis in humans. *Arteriosclerosis, Thrombosis, Vascular Biology.* (2005) 25:279–86. doi: 10.1161/01.ATV.0000152605.64964.c0

276. Evans MK, Graves Jr JL, Shim RS, Tishkoff SA, Williams WW. Race in medicine—genetic variation, social categories, and paths to health equity. *New Engl J Med.* (2021) 385:e45. doi: 10.1056/NEJMp2113749

277. Wilkins CH, Schindler SE, Morris JC. Addressing health disparities among minority populations. *JAMA Neurol.* (2020) 77:1063. doi: 10.1001/jamaneurol.2020.1614

Network pharmacology and molecular docking-based analysis of protective mechanism of MLIF in ischemic stroke

Mengting Lv[1†], Qiuzhen Zhu[2†], Xinyu Li[1], Shanshan Deng[1], Yuchen Guo[3], Junqing Mao[4]* and Yuefan Zhang[1]*

[1]School of Medicine, Shanghai University, Shanghai, China, [2]The Seventh People's Hospital of Shanghai University of Traditional Chinese Medicine, Shanghai, China, [3]College of Pharmacology, Anhui University of Chinese Medicine, Hefei, China, [4]Department of Clinical Pharmacy, Jiading Branch of Shanghai General Hospital, Shanghai Jiao Tong University School of Medicine, Shanghai, China

Objective: This study aimed to evaluate the potential mechanism by which Monocyte locomotion inhibitory factor (MLIF) improves the outcome of ischemic stroke (IS) inflammatory injury.

Methods: Potential MLIF-related targets were predicted using Swiss TargetPrediction and PharmMapper, while IS-related targets were found from GeneCards, PharmGKB, and Therapeutic Target Database (TTD). After obtaining the intersection from these two datasets, the Search Tool for Retrieval of Interacting Genes/Protein (STRING11.0) database was used to analyze the protein-protein interaction (PPI) network of the intersection and candidate genes for MLIF treatment of IS. The candidate genes were imported into the Metascape database for Gene Ontology (GO) functional analysis and Kyoto Encyclopedia of Genes and Genomes (KEGG) pathway enrichment. The top 20 core genes and the "MLIF-target-pathway" network were mapped using the Cytoscape3.9.1. Using AutoDock Vina1.1.2, the molecular docking validation of the hub targets and MLIF was carried out. In the experimental part, transient middle cerebral artery occlusion (tMCAO) and oxygen and glucose deprivation (OGD) models were used to evaluate the protective efficacy of MLIF and the expression of inflammatory cytokines and the putative targets.

Results: MLIF was expected to have an effect on 370 targets. When these targets were intersected with 1,289 targets for ischemic stroke, 119 candidate therapeutic targets were found. The key enriched pathways were PI3K-Akt signaling pathway and MAPK signaling pathway, etc. The GO analysis yielded 1,677 GO entries ($P < 0.01$), such as hormone stimulation, inflammatory response, etc. The top 20 core genes included AKT1, EGFR, IGF1, MAPK1, MAPK10, MAPK14, etc. The result of molecular docking demonstrated that MLIF had the strong binding capability to JNK (MAPK10). The *in vitro* and *in vivo* studies also confirmed that MLIF protected against IS by lowering JNK (MAPK10) and AP-1 levels and decreasing pro-inflammatory cytokines (IL-1, IL-6).

Conclusion: MLIF may exert a cerebral protective effect by inhibiting the inflammatory response through suppressing the JNK/AP-1 signaling pathway.

Introduction

Stroke is a group of acute and serious cerebral vascular diseases with a high incidence, disability, death, and recurrence rate (1). More than 80% of all conditions result in ischemic stroke (IS), which is triggered by arterial blockage (2). However, the mechanisms involved in the stroke process are complex, such as excitotoxicity, calcium overload, oxidative stress, inflammatory and apoptosis (3, 4). Dyslipidemia is an important risk factor for IS and contributes to IS by several of these mechanisms (5). Elevated blood lipid levels can cause oxidative stress by increasing the production of excess oxygen free radicals, which can alter the arterial and microcirculatory systems (6). Thrombolysis is the most effective treatment for stroke worldwide, although its therapeutic efficacy is greatly controlled by time, and the prognosis is dismal because the majority of patients incur various degrees of neurological impairment after treatment (7). In summary, it is crucial to create effective neuroprotective medications in order to reduce brain damage in stroke patients and improve their prognosis.

Entamoeba histolytica produces a pentapeptide known as monocyte locomotion inhibitory factor (MLIF), which has blatant anti-inflammatory properties (8), such as inhibition of human monocyte motility and immune responses of monocytes and neutrophils, increase of anti-inflammatory cytokines (9), downregulation of LPS-induced IL-1β in U-937 cells (10), and inflammation and matrix metalloproteinases in a collagen-induced arthritis (CIA) mouse model. According to our findings (11), the amount of cerebral ischemia in the temporary middle cerebral artery occlusion (tMCAO) model is greatly decreased

FIGURE 1
Flowchart of the mechanisms of MLIF against IS.
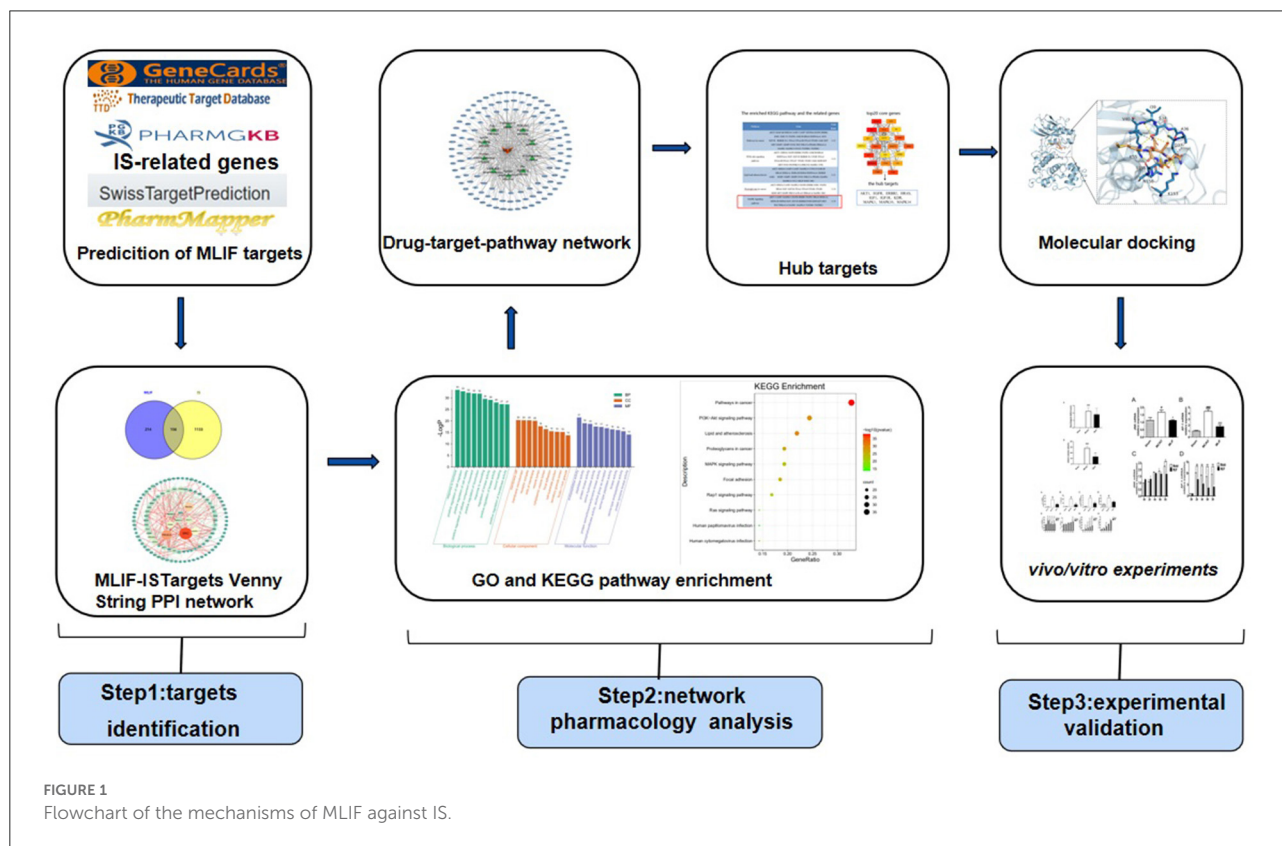
by MLIF. Currently, as an experimental novel medication with potential for neuroprotection in acute ischemic stroke, MLIF has been approved (11), but the exact mechanism is unknown.

The network pharmacology approach combines high-throughput data incorporation, metadata search, data analysis, target prediction, and simulation labs to independently present the "drug-target-pathway" associated with a particular disease and to show the connections and interactions between drugs and targets from a systematic perspective (12). It provides a novel tool for innovative drug discovery (13). The process of "molecular docking" involves interacting a drug molecule with a receptor to design new drugs (14), which has become frequently employed in drug discovery (15). Therefore, this study used Swiss TargetPrediction, PharmMapper databases to forecast the MLIF-related targets, and GeneGards, PharmGKB, and Therapeutic Target Database (TTD) to search for targets of IS. After obtaining common targets, the protein-protein interaction (PPI) network, Gene Ontology (GO) functional analysis, and pathway enrichment from the Kyoto Encyclopedia of Genes and Genomes (KEGG) were performed using online analytic platforms like STRING11.0, Metascape, and combined with the cytoHubba plug-in in Cytoscape3.9.1 to extract the top20 core genes. Finally, molecular docking was performed by AutoDock Vina1.1.2. The probable targets of MLIF were further confirmed by tests based on the findings of network pharmacology analysis and molecular docking analysis. From the perspective of network pharmacology, the scientific connotation of the anti-inflammatory effect of MLIF in stroke was elucidated in order to serve as a reference for its use in treating post-stroke neurological damage and to lay the foundation for further studies on its mechanism of action (the flow of the study is shown in Figure 1).

Materials and methods

Network pharmacology analysis

Prediction of MLIF and IS-related targets

The MLIF structural data was retrieved from the PubChem database (https://pubchem.ncbi.nlm.nih.gov/) (16), and the MLIF-related targets were predicted in PharmMapper (http://www.lilab-ecust.cn/pharmmapper/) and the Swiss TargetPrediction databases (http://www.swisstargetprediction.ch/) (17, 18), respectively. To create a collection of MLIF-related targets, the targets from the two databases were combined and standardized with the Uniprot database (https://www.uniprot.org/) (19). The IS-related targets were looked for in GeneCards (https://www.genecards.org/) (20), PharmGKB (https://www.pharmgkb.org/) (21) and TTD (http://db.idrblab.net/ttd/) (22) databases

using "ischemic stroke" and "cerebral ischemia" as the keywords, respectively.

Protein interaction network (PPI) and the core genes finding

The intersection of MLIF-related targets and the IS-related targets datasets was obtained by Venny diagram. The STRING11.0 database (https://cn.string-db.org/) was updated with the integrated target data to obtain the protein-protein interaction (PPI) network and the species must be restricted to "Homo sapiens," with the confidence score of at least 0.9 (23). The PPI network was made visible by using Cytoscape 3.9.1 (https://cytoscape.org/) (24) and topology analysis was performed using the CytoHubba plug-in to obtain the top 20 targets in terms of degree as the core genes (25).

Gene function and pathway enrichment analysis

The Metascape database (https://metascape.org/gp/index.html#/main/step1) was used to import the targets of MLIF treatment IS for Kyoto Encyclopedia of Genes and Genomes (KEGG) pathway enrichment and Gene Ontology (GO) functional analysis with $P < 0.01$ (26).

TABLE 1 Sequence of the qRT-PCR primers.

Gene	Sequence of primers
Mouse IL-1	F CAACCAACAAGTGATATTCTCCATG R GATCCACACTCTCCAGCTGCA
Mouse IL-6	F TCCAGTTGCCTTCTTGGGAC R GTGTAATTAAGCCTCCGACTTG
Mouse AP-1	F TGGTGGCGTTCGTTTC R CACTGACTTGCTCTTCCCTC
Mouse JNK	F AGTGACAGTAAAAGCGATGG R TTTAGGAGGACAAGTTCACG
Rat IL-1	F AGGCTGACAGACCCCAAAAG R CTCCACGGGCAAGACATAGG
Rat IL-6	F CAGCCACTGCCTTCCCTACTTC R TAGCCACTCCTTCTGTGACTCTAACT
Rat AP-1	F GACTGCAAAGATGGAAACGACC R AGAAGGTCCGAGTTCTTGGC
Rat JNK	F CCAAGAGAGCTTATCGGGAAC R TCCCAAGATGACTTCTGGAGC
GAPDH	F ACCACAGTCCATGCCATCAC R TCCACCACCCTGTTGCTGTA

Drug-target-pathway network construction

The "MLIF-target-pathway" network was created using the data from the aforementioned procedures and Cytoscape 3.9.1 software (https://cytoscape.org/) (24), allowing us to see how each node interacts with the active substance (MLIF), potential targets, and enriched KEGG pathways.

Molecular docking

The 3D structures of target proteins were obtained from the RCSB protein database (https://www.rcsb.org/) (27), and the 2D structure of MLIF was obtained using the PubChem database (https://pubchem.ncbi.nlm.nih.gov/), drawn in 3D using ChemDraw20 (https://www.chemdraw.com.cn/) (28) and converted to pdb file format using OpenBabel 3.1.1 (http://openbabel.org/wiki/Main_Page) (29). MLIF was set as a ligand and the hub targets were set as receptors. In order to delete water molecules and heteroatoms and add charge and hydrogen atoms, the drug and receptor proteins were added to PyMOL 2.4 (https://pymol.org/2/) and AutoDock 4.2.6 (https://autodock.scripps.edu/). Using AutoDock Vina 1.1.2 (https://autodock.scripps.edu/), the produced medication was molecularly docked to the target protein. PyMOL 2.4 was used to visualize the final conformation, which was chosen based on its best binding energy (30).

Experimental verification

Animals and reagents

The rats were kept in a controlled setting with a 12-h cycle of light and dark and were fed a conventional rat diet along with water. The Institutional Animal Care and Use Committee at Shanghai University oversaw all animal studies and surgical operations to ensure that they adhered to international standards for the humane use of experimental animals. Male Sprague-Dawley rats weighing between 250 and 280 g were randomly assigned to one of three groups ($N = 3$–6): the Sham group (Sham), the MCAO group (MCAO), and the MLIF group (MLIF). Five minutes before reperfusion, 1 mg/kg of MLIF was injected into the tail vein for the MLIF group. Both the Sham group and the MCAO group received the identical dosage of normal saline by tail intravenous injection at the same time.

MLIF was created by the Chinese Peptide Company (Hangzhou, China), with a purity level of above 98% and in accordance with the recognized amino acid sequence (Met-Gln-Cys-Asn-Ser). 2,3,5-triphenyl tetrazolium chloride (TTC) was provided by Jiancheng Biotech Co. (Nanjing, China). The peptide was dissolved to its final concentration (50 g/ml) in PBS (pH 7.4) before being employed for cell therapy. Hyclone (Logan, Utah, USA) provided high/low glucose versions of Dulbecco's modified Eagle's medium (DMEM). Fetal bovine serum (FBS) and 0.25% tryptase were purchased from Gibco (Carlsbad, CA, USA). Penicillin-streptomycin solution was purchased from Biosera (France). R&D (Minneapolis, MN, USA) provided the enzyme-linked immunosorbent assay (ELISA) kits for IL-1 and IL-6, and Takara (Shiga, Japan) provided the kits for total RNA. All the other chemicals were bought from businesses.

Cell culture

Brain microvascular endothelial cells (bEnd3 cells) were purchased from the American Type Culture Collection (ATCC). The DMEM with high glucose, 10% fetal bovine serum, and 100
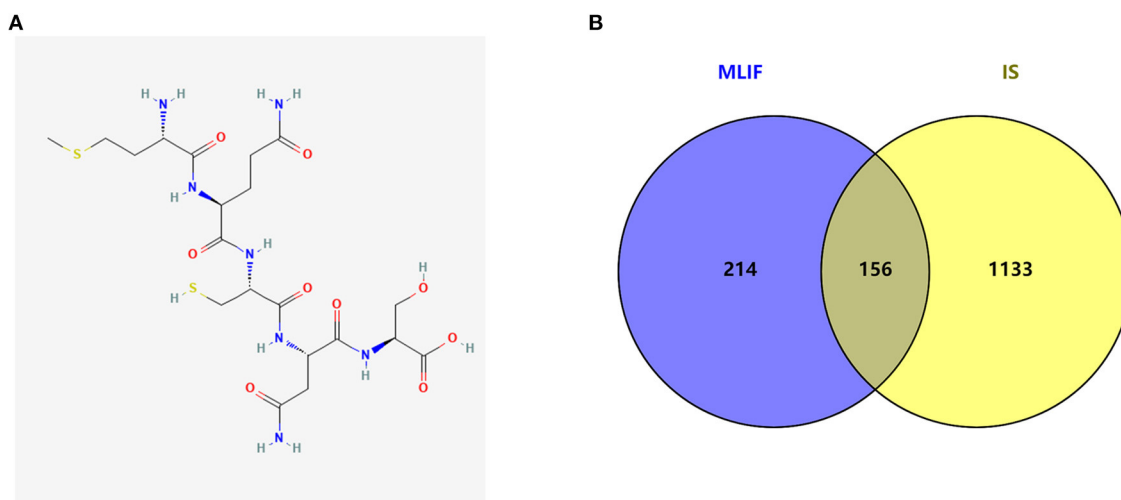

FIGURE 2
The graph structure of MLIF **(A)** and target intersections for MLIF and IS **(B)**.

g/ml penicillin-streptomycin solution was used to cultivate the bEnd3 cells. At 37°C, cells were grown in 5% CO_2 and 95% air.

Transient middle cerebral artery occlusion

Procedures for tMCAO were previously described (31). In a nutshell, pentobarbitone (350 mg/kg, i.p.) was used to anesthetize rats during surgery. The internal carotid artery was used to insert an 11-mm silicone-coated 8–0 filament into the left common carotid artery for 2 h. The filament was then gently removed to complete a 24-h reperfusion period. A heating lamp

was used to keep the subject's body temperature at $37.5 \pm 0.5°C$. After reperfusion for 24 h, we assessed the efficacy of MLIF by TTC staining and neurological deficit score and measured pro-inflammatory cytokines, including IL-1 and IL-6, in the ischemic penumbra.

Oxygen and glucose deprivation

According to a prior description by Yang et al., an ischemic model was created *in vitro* by depriving cells of oxygen and glucose (32). The bEnd3 cells was planted in cell culture plates

FIGURE 3
PPI network, where nodes stand in for proteins and edges for connections.
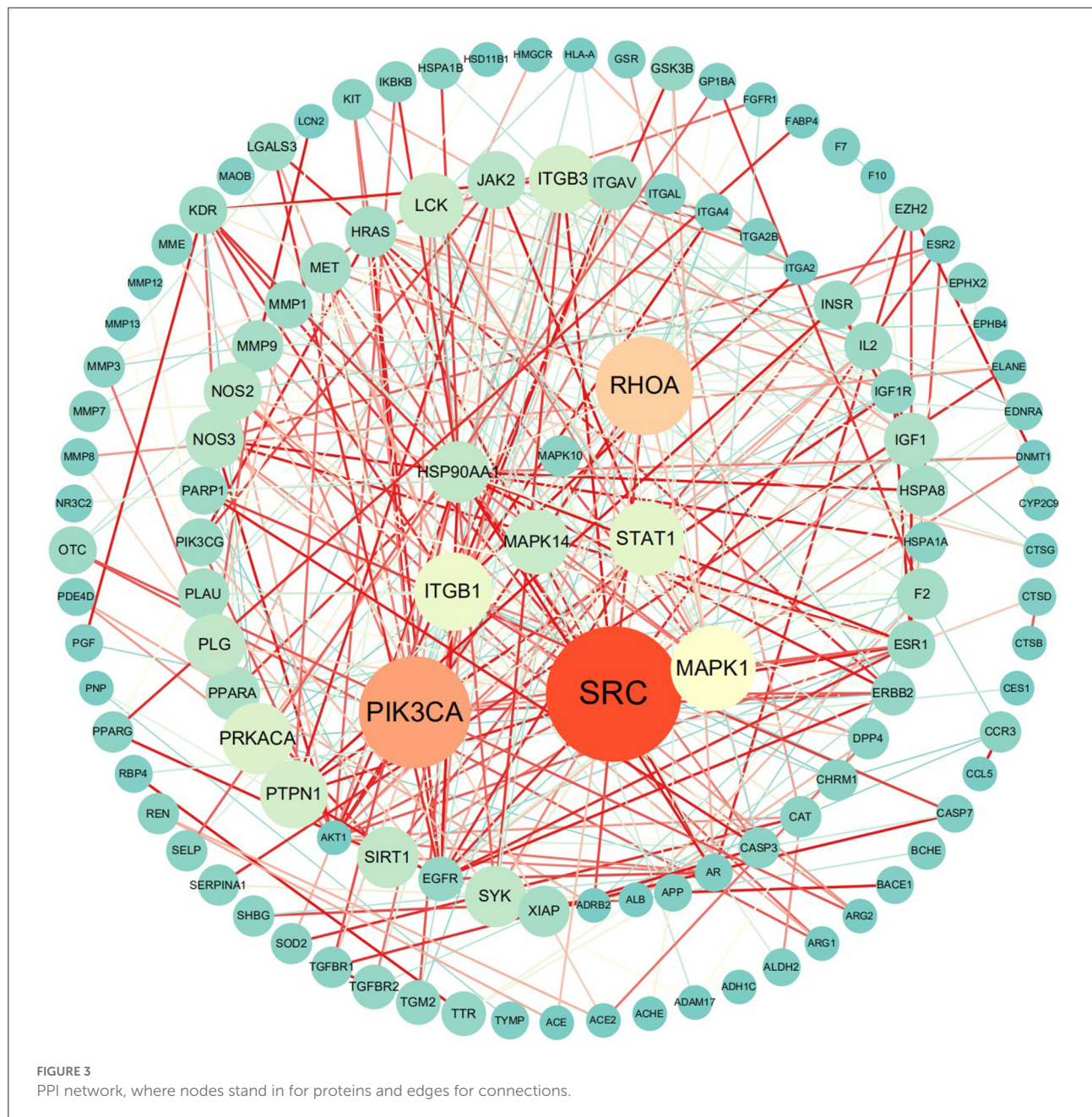
with 5% CO_2 at 37°C at a density of 3×10^5 cells/ml. When the confluency reached to 80%, the pure culture was quickly changed to low glucose DMEM without FBS and quinolone solution, The cells were then starved for 2 h in a 95% atmosphere, 5% carbon dioxide atmosphere at 37°C. The OGD insult was administered after MLIF (50 g/ml) administration, and the cells were placed under hypoxic conditions (5% CO_2 and 95% N_2) for various time periods (0, 2, 4, 6, and 8 h) in different experiments. The ELISA assay and Quantitative real-time PCR (qRT-PCR) were performed after OGD to detect the inflammatory cytokines (IL-1 and IL-6).

Evaluation of neurological deficit score

We used Longa's approach to calculate the neurological deficit score for rats (0 = no neurological deficit, 1 = unable to extend left front paw, 2 = rats' crawling motion circled to the left, 3 = rats stood with a left-leaning posture, 4 = rats lost consciousness and were unable to walk on its own) (33).

Staining with 2,3,5-triphenyl-tetrazolium chloride

Each group's brains were taken out and preserved for 15 min at −20°C. The brains were divided into six sections, each about 2 mm thick. The sections were immersed in 1% 2,3,5-triphenyl-tetrazolium chloride (TTC) for 30 min at 37°C. Sections were rotated every 5 min and then washed three times with ddH2O. Images were gathered for additional examination.

FIGURE 4
Top 20 core genes in terms of degree.

Enzyme-linked immunosorbent assay

According to the instructions provided by the kit's manufacturer (R&D), the ELISA was used to measure the amounts of inflammatory cytokines (IL-1 and IL-6) in the hydrolysates of ischemic brain tissue and the effluent of the bEnd3 cells. The reactions were placed in ELISA plates, and the results were examined at a wave length of 450 nm. The standard curve was used to determine the concentrations of IL-1 and IL-6.

Quantitative real-time PCR

To evaluate the RNA levels of IL-1, IL-6, JNK, and AP-1, qRT-PCR was utilized. Total RNA was extracted from brain tissues and bEnd3 cells using the Total RNA Kit (Takara, Shiga, Japan). According to the manufacturer's instructions, cDNAs were created using 5 ×Primescript reverse transcription reagents (Takara, Shiga, Japan). Table 1 displayed the primers being used in quantitative RT-PCR (qRT-PCR). qRT-PCR was carried out using SYBR Premix Ex Taq^{TM} (Tli RnaseH Plus) (Takara, Shiga, Japan) on 7500 Real-Time PCR System (Applied Biosystems). The level of expression for each target genes was normalized to the control (GAPDH).

Statistical analysis

Every piece of data was reported as mean±SD. Using one-way analysis of variance (ANOVA), statistical analysis was carried out. The Student's t-test was applied to compare the two groups. Statistics were judged significant at $P < 0.05$. With GraphPad Prism 9.0 (SPSS Inc., United States), all statistical analysis was completed.

Results

Prediction of drug and disease targets

The MLIF 2D structure from the pubchem database (CID: 10325914 Figure 2A), MLIF-related targets prediction was performed using the Swiss TargetPrediction platform and PharmMapper databases, and 370 action objectives in total were found after de-duplication screening (Supplementary Table 1). After deleting entries with duplicate information from the GeneCards, PharmGKB, and TTD databases, 1,289 targets associated to IS were found.

Construction of PPI network

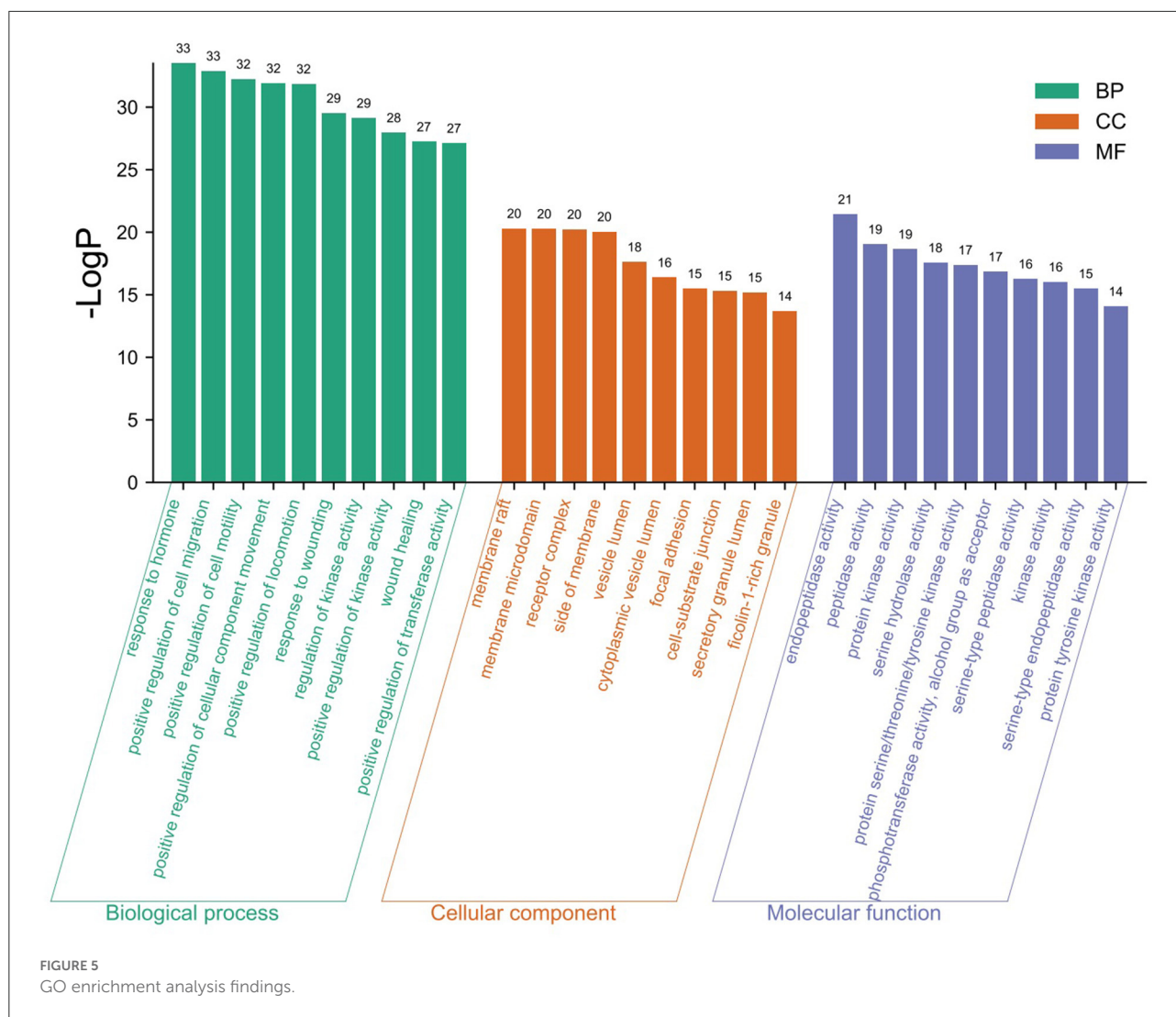The MLIF-related targets and IS-related targets were intersected to obtain 156 common targets between drug and
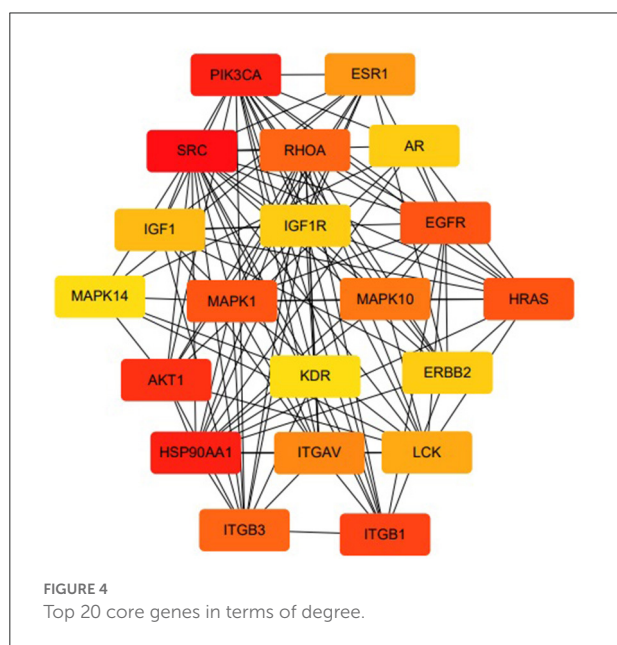
FIGURE 5
GO enrichment analysis findings.

disease (Figure 2B). The 156 common targets were imported into the STRING11.0 database, and targets with the confidence score > 0.9 were screened out, and isolated targets were excluded to obtain a PPI network containing 119 targets. It is suggested that these 119 shared targets may be candidate targets for MLIF treatment of IS. The PPI network was shown in Figure 3, where each edge represented a protein interaction and each node represented a target. The size of the nodes indicates the degree's magnitude. The network diagram demonstrates the intimate ties between the targets, demonstrating the complexity and diversity of the MLIF for the treatment of IS and the synergy between various targets. The top 20 core genes were determined using Cytoscape 3.9.1's cytoHubba plug-in, and they were shown in Figure 4. The node color and score are correlated, with darker and more red nodes signifying higher scores.

GO and KEGG enrichment analysis of candidate targets

The GO analysis by Metascape database yielded 1,677 GO entries ($P < 0.01$), including 1,437 entries for biological process (BP), such as positive regulation of cell migration, hormone stimulation, positive regulation of cellular component movement, etc, 97 entries for cellular component (CC), such as cell membrane, cytoplasm, cytosol, nucleus, etc., 143 entries for molecular function (MF), such as endopeptidase activity, peptidase activity, protein kinase activity, etc. For visualization, the best 10 submissions for each category were selected and shown in Figure 5. The KEGG pathway enrichment of 119 candidate targets yielded 181 signaling pathways with $P < 0.01$, mainly involving neural, vascular, inflammation, oxidative stress, apoptosis and lipid metabolism. Ten pathways with more

FIGURE 6
Top ten KEGG pathway enrichment findings.
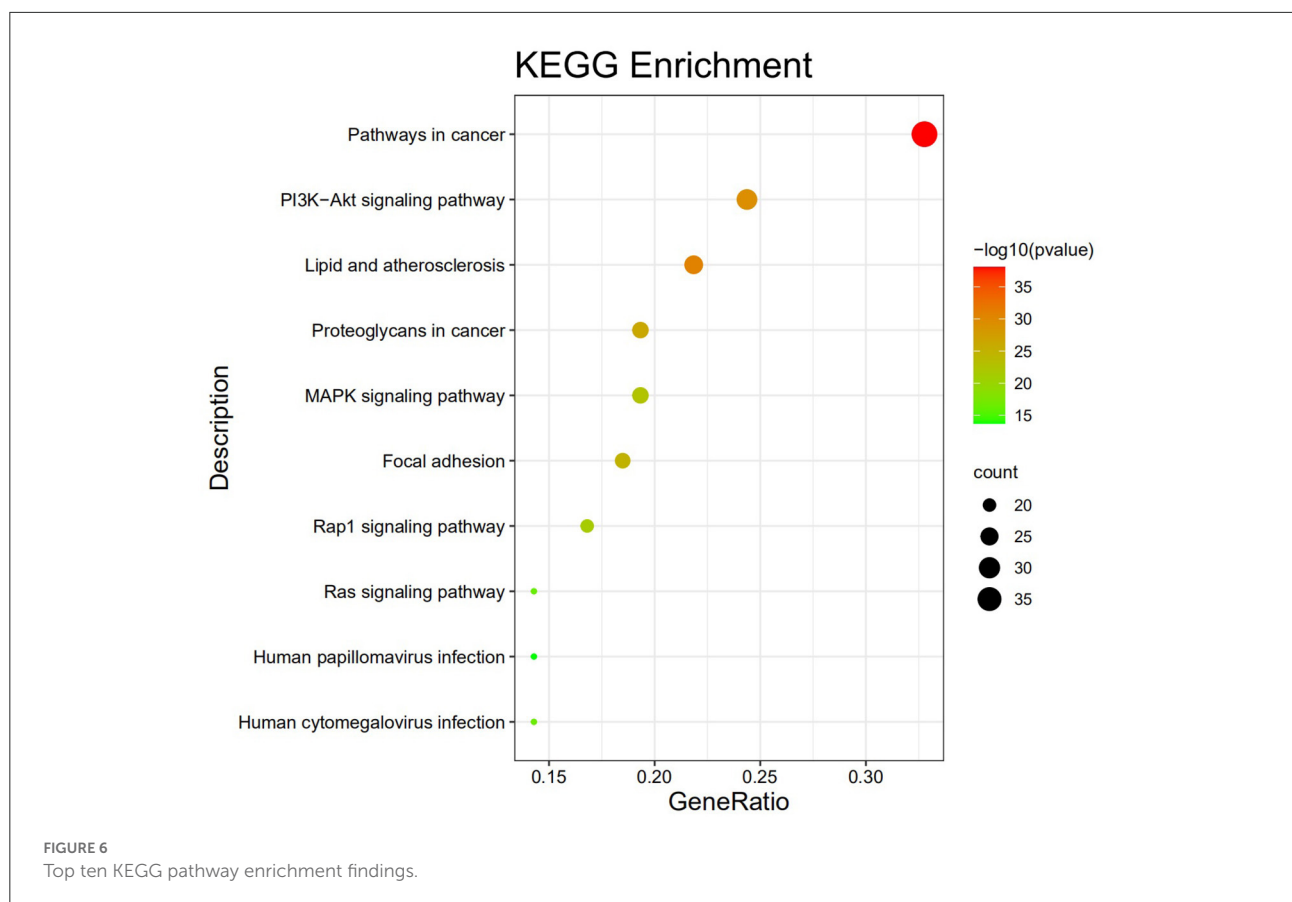
significant gene ratio in the enrichment results were selected for display (Figure 6), those related to other diseases including cancer signaling pathways, human papillomavirus infection, human cytomegalovirus infection, lipids and atherosclerosis. And those related to apoptosis: PI3K-Akt signaling pathway, RAS signaling pathway, two related to adhesion: Rap1 signaling pathways and Focal adhesion. The inflammation-related pathways: PI3K-Akt signaling pathway and mitogen-activated protein kinase (MAPK) signaling pathway. A total of 23 targets were involved in the MAPK signaling pathway (Table 2). The "MLIF -target-pathway" network was further built using nodes of various colors and shapes to represent various active compound, targets, and pathways. One compound (red V-shape), 119 targets (blue circles), and 10 KEGG pathways (green triangles) are among the nodes that represent active compounds, targets, and pathways (Figure 7).

Molecular docking results

Based on the results of KEGG analysis and top20 core genes analysis, AKT1 (PDB ID: 6s9w), EGFR (PDB ID:5Y9T), ERBB2 (PDB ID:2a91), HRAS (PDB ID:5P21), IGF1 (PDB ID:1b9g), IGF1R (PDB ID:6PYH), KDR/VEGFR2 (PDB ID:1y6a) MAPK1/ERK (PDB ID:6G54), MAPK10/JNK (PDB ID:7S1N), MAPK14/P38 (PDB ID:5ETI) were selected as the hub targets (Figure 8). As shown in Table 3, MLIF was selected as the ligand and the hub targets were selected as receptors. There's a strong possibility that MLIF binds well to the JNK receptor ($\leq$-7.0 kcal/mol) (Figure 9), a protein corresponding to MAPK10, and this indicates that MLIF has good binding potential to key targets of the JNK signaling pathway.

MLIF played a protective role against neurological damage on the MCAO rats

The neurological deficit score of the MCAO group was considerably higher than that of the Sham group, as can be seen in Figure 10A ($P < 0.01$). Although the MLIF group's neurological deficit score was lower than the MCAO group's, there was no discernible difference between the two. The focal infarct volume was also measured 24 h following reperfusion. As shown in Figure 10B, the percentage of infarct volume in the MCAO group was considerably higher than that in the

TABLE 2 The top 10 KEGG pathways that are enriched and the associated genes.

Pathway	Gene	Gene ratio
Pathways in cancer	AKT1 XIAP AR RHOA CASP3 CASP7 EDNRA EGFR ERBB2 ESR1 ESR2 F2 FGFR1 GSK3B HRAS HSP90AA1 IGF1 IGF1R IKBKB IL2 ITGA2 ITGA2B ITGAV ITGB1 JAK2 KIT MET MMP1 MMP9 NOS2 PGF PIK3CA PPARG PRKACA MAPK1 MAPK10 STAT1 TGFBR1 TGFBR2	0.32
PI3K-Akt signaling pathway	AKT1 CHRM1 EGFR ERBB2 FGFR1 GSK3B HRAS HSP90AA1 IGF1 IGF1R IKBKB IL2 INSR ITGA2 ITGA2B ITGA4 ITGAV ITGB1 ITGB3 JAK2 KDR KIT MET NOS3 PGF PIK3CA PIK3CG MAPK1 SYK	0.24
Lipid and atherosclerosis	AKT1 RHOA CASP3 CASP7 MAPK14 CYP2C9 GSK3B HRAS HSPA1A HSPA1B HSPA8 HSP90AA1 IKBKB JAK2 MMP1 MMP3 MMP9 NOS3 PIK3CA PPARG MAPK1 MAPK10 CCL5 SELP SOD2 SRC	0.21
Proteoglycans in cancer	AKT1 RHOA CASP3 MAPK14 EGFR ERBB2 ESR1 FGFR1 HRAS IGF1 IGF1R ITGA2 ITGAV ITGB1 ITGB3 KDR MET MMP9 PIK3CA PLAU PRKACA MAPK1 SRC	0.19
MAPK signaling pathway	AKT1 CASP3 MAPK14 EGFR ERBB2 FGFR1 HRAS HSPA1A HSPA1B HSPA8 IGF1 IGF1R IKBKB INSR KDR KIT MET PGF PRKACA MAPK1 MAPK10 TGFBR1 TGFBR2	0.19
Focal adhesion	AKT1 XIAP RHOA EGFR ERBB2 GSK3B HRAS IGF1 IGF1R ITGA2 ITGA2B ITGA4 ITGAV ITGB1 ITGB3 KDR MET PGF PIK3CA MAPK1 MAPK10 SRC	0.18
Rap1 signaling pathway	AKT1 RHOA MAPK14 EGFR FGFR1 HRAS IGF1 IGF1R INSR ITGA2B ITGAL ITGB1 ITGB3 KDR KIT MET PGF PIK3CA MAPK1 SRC	0.17
Ras signaling pathway	AKT1 RHOA EGFR FGFR1 HRAS IGF1 IGF1R IKBKB INSR KDR KIT MET PGF PIK3CA PRKACA MAPK1 MAPK10	0.14
Human cytomegalovirus infection	AKT1 RHOA CASP3 CCR3 MAPK14 EGFR GSK3B HLAA HRAS IKBKB ITGAV ITGB3 PIK3CA PRKACA MAPK1 CCL5 SRC	0.14
Human papillomavirus infection	AKT1 CASP3 EGFR GSK3B HLAA HRAS IKBKB ITGA2 ITGA2B ITGA4 ITGAV ITGB1 ITGB3 PIK3CA PRKACA MAPK1 STAT1	0.14

Sham group ($P < 0.01$), and MLIF significantly decreased the percentage of infarct volume in the MCAO group ($P < 0.01$).
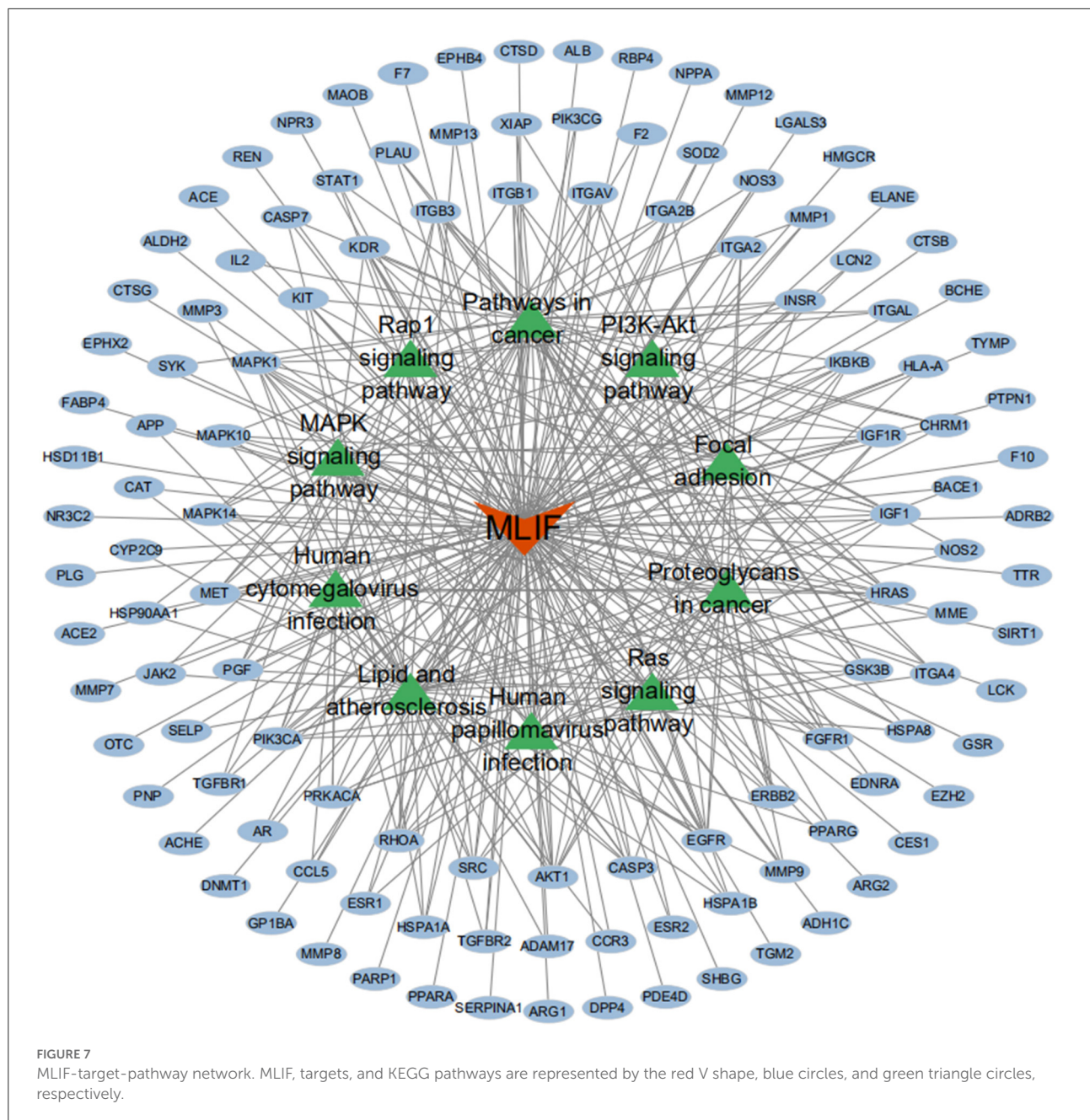
MLIF reduced the expression of the IL-1 and IL-6 in the MCAO rat's brain and OGD insulted BEnd3 cells

The expansion of the area with brain injury brought on by the release of pro-inflammatory cytokines into the extracellular space raises the neurological deficit and has a detrimental effect on the prognosis for survival (34). IL-1 receptor antagonist (IL-1Ra) administration significantly reduced peripheral markers of inflammation in patients with ischemic stroke (35, 36). We determined the effect of MLIF on cytokines which promote inflammation (IL-1 and IL-6) expression in the pathological process of brain ischemia by qRT-PCR and ELISA analysis *in vivo* and *in vitro*, respectively. We found that MLIF (1 mg/kg) could reduce the relative IL-1 and IL-6 mRNA expression ($P < 0.05$) in the MCAO rats (Figures 11A,B). It also showed a significant reduction of IL-1 ($P < 0.01$) and IL-6 ($P < 0.05$) in the MCAO rats (Figures 11C,D). In this *in vitro* study,

we used the OGD model and found that the relative mRNA expression of IL-1 and IL-6 were significantly upregulated at the different time (2, 4, 6, and 8 h) after OGD (Figures 11E,G). Administration of MLIF (50 μg/ml) remarkably reduced the expression of IL-1 compared with the OGD model group (2, 4, 6, and 8 h) ($P < 0.01$). As for IL-6, MLIF has the similar effect at 2 h ($P < 0.05$),4 h, 6 h, and 8 h ($P < 0.01$) after OGD insult. Moreover, we also assessed protein expression of IL-1 and IL-6 in bEnd3 cells supernatant after OGD by ELISA. As shown in Figures 11F,H, MLIF significantly decreased the level of IL-1 ($P < 0.05$) at 8 h and IL-6 at 4 h ($P < 0.05$) in bEnd3 cells' supernatant after OGD insult. These results showed the anti-inflammatory effect of MLIF on brain ischemia.

MLIF inhibited the JNK/AP-1 signaling pathway in the MCAO rats and OGD insulted BEnd3 cells

Studies have suggested that the JNK pathway's most significant downstream, AP-1 activation, may have a role in the

FIGURE 7
MLIF-target–pathway network. MLIF, targets, and KEGG pathways are represented by the red V shape, blue circles, and green triangle circles, respectively.

expression of numerous genes linked to cell survival or death in ischemic brain injury (37). So we further measured JNK, AP-1 levels in the rats brain tissue after MCAO and bEnd3 cells during the OGD insult. MLIF (1 mg/kg) could reduce the relative mRNA expression of JNK ($P < 0.05$) (Figure 12A) and AP-1 ($P < 0.001$) (Figure 12B) *in vivo*. Treatment of MLIF (50 μg/ml) resulted in a significant reduction in the transcriptional level of JNK in bEnd3 cells after OGD insult when it was at 8 h ($P < 0.05$) (Figure 12C). And MLIF (50 μg/ml) could remarkably decreased OGD-induced the gene expression of AP-1 at 2, 4, 6, and 8 h ($P < 0.01$) (Figure 12D).

These findings suggested that MLIF may inhibit inflammatory responses after IS *in vivo* and *in vitro* through the JNK/AP-1 signaling pathways.

Discussion

According to some researchers, the heightened inflammatory response may have a role in the development of stroke (38). In general, inflammatory indicators like IL-6 produce cardiovascular remodeling and arterial resistance

FIGURE 8
The hub targets.

TABLE 3 The docking information of hub targets with MLIF.

Gene	Binding energy (kcal/mol)
MAPK10	−7.2
EGFR	−5.9
ERBB2	−6.3
IGF1	−4.5
IGF1R	−5.6
KDR	−5.7
AKT1	−3.9
HRAS	−2.7
MAPK1	−1.5
MAPK14	−0.5

(39) and increase the incidence of cardiovascular disease (CVD) (40).

Entamoeba Histolytica produces the heat-stable pentapeptide MLIF, which has a variety of anti-inflammatory effects (9, 41, 42), including regulating inflammation and immune responses through the NF-κB and MAPK pathways (43). The anti-inflammatory effect of MLIF makes the its increasing research on brain ischemia (44). Our previous study has proved that MLIF can reduce the risk

of brain ischemia injury by focusing on the eEF1A1/eNOS pathway (45).

In recent years, network pharmacology has become frequently employed to forecast novel drug targets and pathways, lessening the blindness of research and improving the efficiency of drug discovery (46). Molecular docking techniques have been used to validate the predictions of network pharmacology by combining components with target proteins in a virtual evaluation (47). The network pharmacology was used in the study to further analyze the possible targets and pathways of MLIF for the treatment of IS and found that MLIF acts on top20 core genes, includingAKT1, EGFR, ERBB2, HRAS, IGF1, MAPK1, MAPK10, MAPK14, etc. The "MLIF-target-pathway" network analysis revealed that the effect of MLIF on IS therapy PI3K/AKT, MAPK, and other signaling pathways were involved. PI3K/AKT signaling pathway is a pro-cell survival pathway that regulates cell proliferation, differentiation, metabolism, and anti-apoptosis (48). This pathway is activated in the early stages of cerebral ischemia, inducing apoptosis and inflammatory response, and its activity is gradually inhibited as ischemia increases (49). The MAPK signaling pathway is crucial for controlling inflammation, neuronal apoptosis, brain edema, and ischemia-reperfusion injury. It also affects the development of stroke (50). Stress-activated protein kinase (SAPK) or Jun amino-terminal kinase (JNK) is a member of the MAPK family and is activated by a
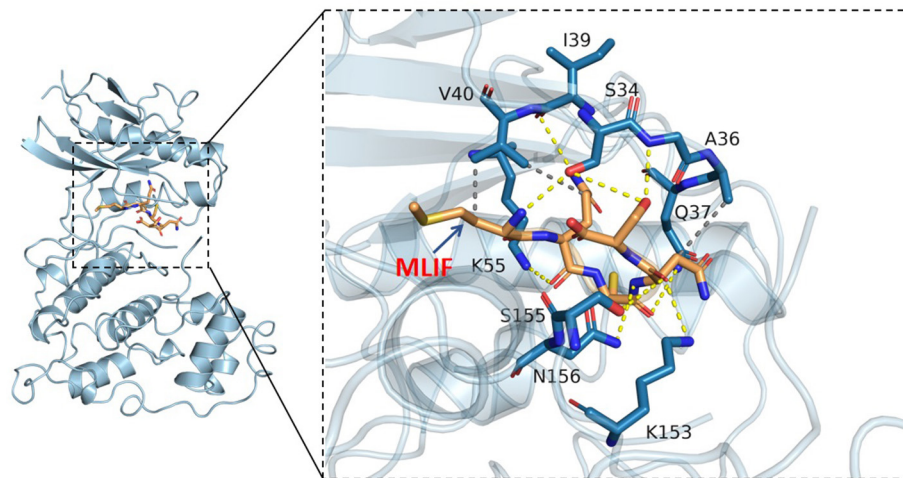
FIGURE 9
3D docking conformation of MLIF with JNK (MAPK10). The **orange** stick in the diagram is a small molecule (MLIF), the **blue** cartoon is a protein (JNK), the **yellow** dashed line indicates hydrogen bonding and the **gray** dashed line indicates hydrophobic interactions.
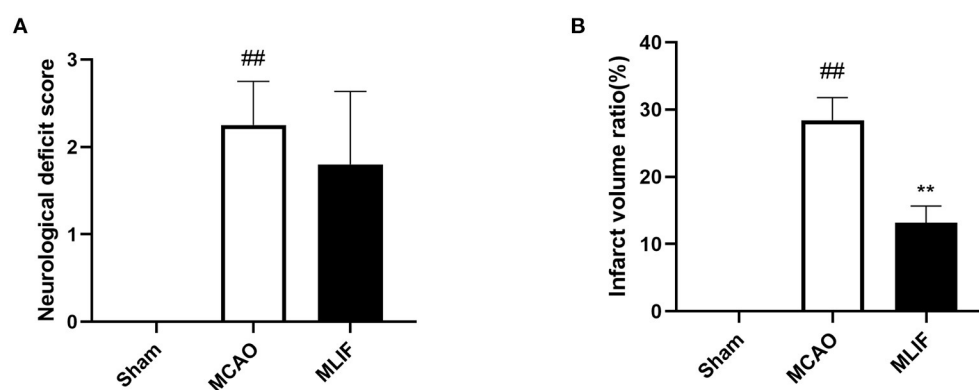
FIGURE 10
MLIF played a protective role against neurological damage on the MCAO rats. Neurological deficit score **(A)** and infarct volume statistical results **(B)** of brain tissue in rats. ($N = 6$, $^{\#\#}P < 0.01$ vs. Sham group, $^{**}P < 0.01$ vs. MCAO group).

range of environmental stresses, inflammatory cytokines, and growth factors. It is crucial for stress reactions like apoptosis and inflammation (51). The JNK pathway is thought to be a marker of neuronal cell death. JNK phosphorylation can result in the transcription of inflammatory mediators like nitric oxide (NO), inducible nitric oxide synthase (iNOS), cyclooxygenase-2 (COX-2), prostaglandin E2 (PGE2), and the pro-inflammatory cytokines IL-6 and IL-1, which in turn can result in neuronal degeneration.

Based on the results of the network pharmacology, the study was conducted to validate the hub targets of the MAPK signaling pathway using molecular docking techniques and *vivo/vitro* experiments, respectively. And MLIF showed strong binding capacity ($\leq$-7.0 kcal/mol) to JNK (MAPK10). In addition, *in vitro* and *in vivo* experiments demonstrated that JNK and AP-1 RNA levels were considerably decreased in the MLIF group, and the transcript and expression of inflammatory factors (IL-1, IL-6) were reduced, further suggesting that MLIF has a therapeutic effect on IS inflammation, possibly by regulating the JNK/AP-1 signaling pathway (52).
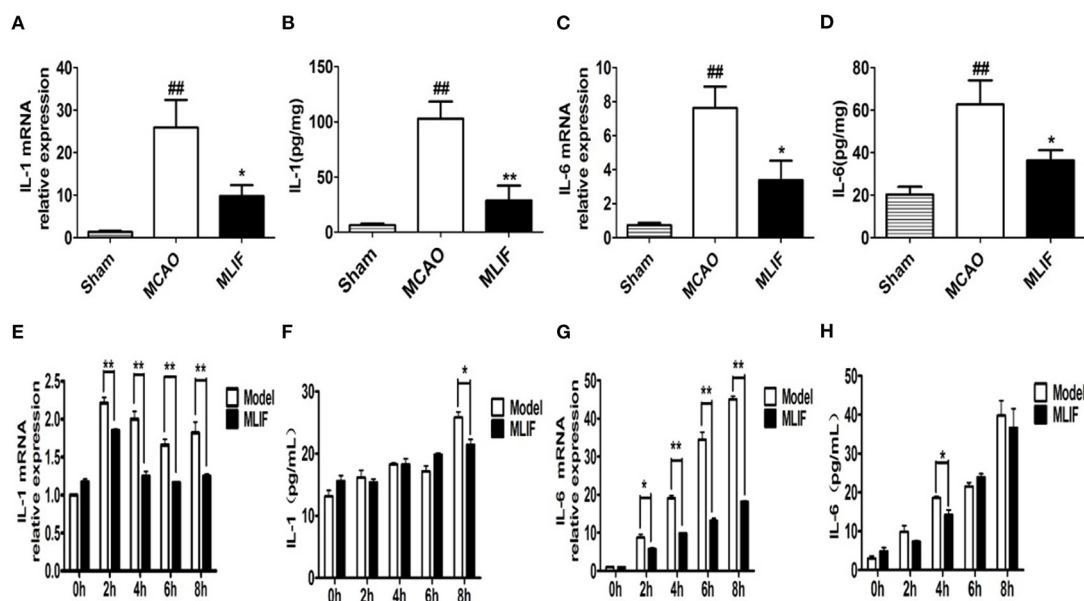
FIGURE 11

MLIF reduced the expression of the pro-inflammatory cytokines IL-1 and IL-6 in the MCAO rats and bEnd3 cells at the different time after OGD. The relative mRNA expression levels of IL-1 **(A,E)** and IL-6 **(C,G)** in the MCAO rats and bEnd3 cells were determined by qRT-PCR. IL-1 **(B,F)** and IL-6 **(D,H)** in the rat brain tissue homogenate and OGD-insulted bEnd3 cells supernatant was measured by ELISA assay ($N = 3$, $^{\#\#}P < 0.01$ vs. Sham group, $^{**}P < 0.01$ vs. MCAO group, $^{*}P < 0.05$ vs. MCAO group).
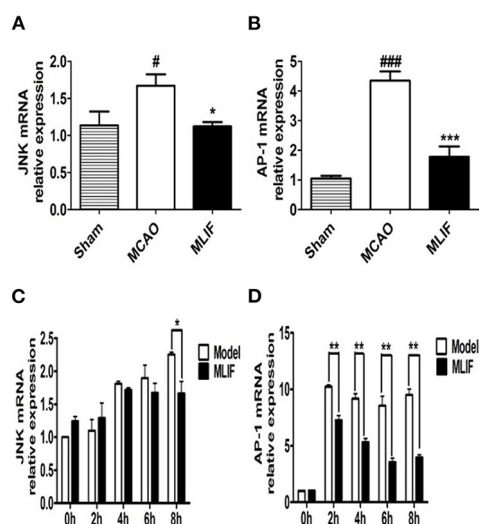

FIGURE 12

JNK/AP-1 signaling pathways contributes to the anti-inflammatory effect of MLIF. The relative mRNA levels of JNK **(A,C)** and AP-1 **(B,D)** in rat's brain and bEnd3 cells were determined by qRT-PCR at the different time (0, 2, 4, 6, and 8 h) after OGD ($N = 3$, $^{\#\#\#}P < 0.001$ vs. Sham group, $^{\#}P < 0.05$ vs. Sham group, $^{***}P < 0.001$ vs. MCAO group, $^{**}P < 0.01$ vs. MCAO group, $^{*}P < 0.05$ vs. MCAO group).

Data availability statement

The datasets presented in this study can be found in online repositories. The names of the repository/repositories and accession number(s) can be found in the article/Supplementary material.

Ethics statement

The animal study was reviewed and approved by the Shanghai University Ethics Committee.

Author contributions

The tests were designed by YZ and JM. Data analysis, figure creation, and manuscript writing were all done by ML. The animal model was built by ML, QZ, XL, SD, and YG. The Western blot and cell tests were carried out by ML. The article's submission was reviewed and approved by all authors.

Funding

Conflict of interest

The authors declare that the research was conducted in the absence of any commercial or financial relationships that could be construed as a potential conflict of interest.

Publisher's note

All claims expressed in this article are solely those of the authors and do not necessarily represent those of their affiliated organizations, or those of the publisher, the editors and the reviewers. Any product that may be evaluated in this article, or claim that may be made by its manufacturer, is not guaranteed or endorsed by the publisher.

Supplementary material

The Supplementary Material for this article can be found online at: https://www.frontiersin.org/articles/10.3389/fcvm.2022.1071533/full#supplementary-material

References

1. Vos T, Lim SS, Abbafati C, Abbas KM, Abbasi M, Abbasifard M, et al. Global Burden of 369 Diseases and Injuries in 204 Countries and Territories, 1990–2019: A Systematic Analysis for the Global Burden of Disease Study 2019. *Lancet.* (2020) 396:1204–22. doi: 10.1016/S0140-6736(20)30925-9

2. Feske SK. Ischemic stroke. *Am J Med.* (2021) 134:1457–64. doi: 10.1016/j.amjmed.2021.07.027

3. Kelly PJ, Lemmens R, Tsivgoulis G. Inflammation and stroke risk: a new target for prevention. *Stroke.* (2021) 52:2697–706. doi: 10.1161/STROKEAHA.121.034388

4. Kuriakose D, Xiao Z. Pathophysiology and treatment of stroke: present status and future perspectives. *Int J Mol Sci.* (2020) 21:7609. doi: 10.3390/ijms21207609

5. Li Z, Zhang J, Luo Y. Impact of triglyceride playing on stroke severity correlated to bilirubin. *Medicine (Baltimore).* (2020) 99:e21792. doi: 10.1097/MD.0000000000021792

6. Ross R. Atherosclerosis–an Inflammatory disease. *N Engl J Med.* (1999) 340:115–26. doi: 10.1056/NEJM199901143400207

7. Ernst E, Matrai A, Paulsen F. Leukocyte rheology in recent stroke. *Stroke.* (1987) 18:59–62. doi: 10.1161/01.STR.18.1.59

8. Utrera-Barillas D, Velazquez JR, Enciso A, Cruz SM, Rico G, Curiel-Quesada E, et al. An Anti-inflammatory oligopeptide produced by entamoeba histolytica down-regulates the expression of pro-inflammatory chemokines. *Parasite Immunol.* (2003) 25:475–82. doi: 10.1111/j.1365-3024.2003.00657.x

9. Rojas-Dotor S, Araujo-Monsalvo VM, Sanchez-Rojas MJ, Dominguez-Hernandez VM. The monocyte locomotion inhibitory factor inhibits the expression of inflammation-induced cytokines following experimental contusion in rat tibia. *Scand J Immunol.* (2018) 88:e12702. doi: 10.1111/sji.12702

10. Hayward JA, Mathur A, Ngo C, Man SM. Cytosolic recognition of microbes and pathogens: inflammasomes in action. *Microbiol Mol Biol Rev.* (2018) 82:e00015–18. doi: 10.1128/MMBR.00015-18

11. Liu X, Hu P, Wang Y, Wang X, Huang J, Li J, et al. A validated Uplc-Ms/Ms Method for the quantitation of an unstable peptide, monocyte locomotion inhibitory factor (Mlif) in human plasma and its application to a pharmacokinetic study. *J Pharm Biomed Anal.* (2018) 157:75–83. doi: 10.1016/j.jpba.2018.04.009

12. Song X, Zhang Y, Dai E, Du H, Wang L. Mechanism of action of celastrol against rheumatoid arthritis: a network pharmacology analysis. *Int Immunopharmacol.* (2019) 74:105725. doi: 10.1016/j.intimp.2019.105725

13. Kibble M, Saarinen N, Tang J, Wennerberg K, Makela S, Aittokallio T. Network pharmacology applications to map the unexplored target space and therapeutic potential of natural products. *Nat Prod Rep.* (2015) 32:1249–66. doi: 10.1039/C5NP00005J

14. Pinzi L, Rastelli G. Molecular docking: shifting paradigms in drug discovery. *Int J Mol Sci.* (2019) 20:4331. doi: 10.3390/ijms20184331

15. Ferreira LG, Dos Santos RN, Oliva G, Andricopulo AD. Molecular docking and structure-based drug design strategies. *Molecules.* (2015) 20:13384–421. doi: 10.3390/molecules200713384

16. Li Q, Cheng T, Wang Y, Bryant SH. Pubchem as a public resource for drug discovery. *Drug Discov Today.* (2010) 15:1052–7. doi: 10.1016/j.drudis.2010.10.003

17. Zoete V, Daina A, Bovigny C, Michielin O. Swisssimilarity: a web tool for low to ultra high throughput ligand-based virtual screening. *J Chem Inf Model.* (2016) 56:1399–404. doi: 10.1021/acs.jcim.6b00174

18. Wang X, Shen Y, Wang S, Li S, Zhang W, Liu X, et al. Pharmmapper 2017 update: a web server for potential drug target identification with a comprehensive target pharmacophore database. *Nucleic Acids Res.* (2017) 45:W356–W60. doi: 10.1093/nar/gkx374

19. Zaru R, Magrane M, O'Donovan C, UniProt C. From the research laboratory to the database: the caenorhabditis elegans kinome in uniprotkb. *Biochem J.* (2017) 474:493–515. doi: 10.1042/BCJ20160991

20. Rebhan M, Chalifa-Caspi V, Prilusky J, Lancet D. Genecards: a novel functional genomics compendium with automated data mining and query reformulation support. *Bioinformatics.* (1998) 14:656–64. doi: 10.1093/bioinformatics/14.8.656

21. Barbarino JM, Whirl-Carrillo M, Altman RB, Klein TE. Pharmgkb: a worldwide resource for pharmacogenomic information. *Wiley Interdiscip Rev Syst Biol Med.* (2018) 10:e1417. doi: 10.1002/wsbm.1417

22. Wang Y, Zhang S, Li F, Zhou Y, Zhang Y, Wang Z, et al. Therapeutic target database 2020: enriched resource for facilitating research and early development of targeted therapeutics. *Nucleic Acids Res.* (2020) 48:D1031–D41. doi: 10.1093/nar/gkz981

23. Szklarczyk D, Gable AL, Nastou KC, Lyon D, Kirsch R, Pyysalo S, et al. The string database in 2021: customizable protein-protein networks, and functional characterization of user-uploaded gene/measurement sets. *Nucleic Acids Res.* (2021) 49:D605–D12. doi: 10.1093/nar/gkaa1074

24. Shannon P, Markiel A, Ozier O, Baliga NS, Wang JT, Ramage D, et al. Cytoscape: a software environment for integrated models of biomolecular interaction networks. *Genome Res.* (2003) 13:2498–504. doi: 10.1101/gr.1239303

25. Chin CH, Chen SH, Wu HH, Ho CW, Ko MT, Lin CY. Cytohubba: identifying hub objects and sub-networks from complex interactome. *BMC Syst Biol.* (2014) 8 Suppl 4:S11. doi: 10.1186/1752-0509-8-S4-S11

26. Zhou Y, Zhou B, Pache L, Chang M, Khodabakhshi AH, Tanaseichuk O, et al. Metascape provides a biologist-oriented resource for the analysis of systems-level datasets. *Nat Commun.* (2019) 10:1523. doi: 10.1038/s41467-019-09234-6

27. Goodsell DS, Zardecki C, Di Costanzo L, Duarte JM, Hudson BP, Persikova I, et al. Rcsb protein data bank: enabling biomedical research and drug discovery. *Protein Sci.* (2020) 29:52–65. doi: 10.1002/pro.3730

28. Evans DA. History of the harvard chemdraw project. *Angew Chem Int Ed Engl.* (2014) 53:11140–5. doi: 10.1002/anie.201405820

29. O'Boyle NM, Banck M, James CA, Morley C, Vandermeersch T, Hutchison GR. Open babel: an open chemical toolbox. *J Cheminform.* (2011) 3:33. doi: 10.1186/1758-2946-3-33

30. Nguyen NT, Nguyen TH, Pham TNH, Huy NT, Bay MV, Pham MQ, et al. Autodock Vina adopts more accurate binding poses but Autodock4 forms better binding affinity. *J Chem Inf Model.* (2020) 60:204–11. doi: 10.1021/acs.jcim.9b00778

31. Zhu Q, Zhang Y, Liu Y, Cheng H, Wang J, Zhang Y, et al. Mlif alleviates Sh-Sy5y neuroblastoma injury induced by oxygen-glucose deprivation by targeting eukaryotic translation elongation factor 1a2. *PLoS ONE.* (2016) 11:e0149965. doi: 10.1371/journal.pone.0149965

32. Chen YJ, Hsu CC, Shiao YJ, Wang HT, Lo YL, Lin AMY. Anti-inflammatory effect of afatinib (an Egfr-Tki) on ogd-induced neuroinflammation. *Sci Rep.* (2019) 9:2516. doi: 10.1038/s41598-019-38676-7

33. Longa EZ, Weinstein PR, Carlson S, Cummins R. Reversible middle cerebral artery occlusion without craniectomy in rats. *Stroke.* (1989) 20:84–91. doi: 10.1161/01.STR.20.1.84

34. Malone K, Amu S, Moore AC, Waeber C. The immune system and stroke: from current targets to future therapy. *Immunol Cell Biol.* (2019) 97:5–16. doi: 10.1111/imcb.12191

35. Levard D, Buendia I, Lanquetin A, Glavan M, Vivien D, Rubio M. Filling the gaps on stroke research: focus on inflammation and immunity. *Brain Behav Immun.* (2021) 91:649–67. doi: 10.1016/j.bbi.2020.09.025

36. Smith CJ, Hulme S, Vail A, Heal C, Parry-Jones AR, Scarth S, et al. Scil-stroke (Subcutaneous Interleukin-1 Receptor Antagonist in Ischemic Stroke). *Stroke.* (2018) 49:1210–6. doi: 10.1161/STROKEAHA.118.020750

37. Dong Y, Liu HD, Zhao R, Yang CZ, Chen XQ, Wang XH, et al. Ischemia activates Jnk/C-Jun/Ap-1 pathway to up-Regulate 14-3-3gamma in astrocyte. *J Neurochem.* (2009) 109 Suppl 1:182–8. doi: 10.1111/j.1471-4159.2009.05974.x

38. Tuttolomondo A, Di Raimondo D, Pecoraro R, Serio A, D'Aguanno G, Pinto A, et al. Immune-inflammatory markers and arterial stiffness indexes in subjects with acute ischemic stroke. *Atherosclerosis.* (2010) 213:311–8. doi: 10.1016/j.atherosclerosis.2010.08.065

39. Laurent S, Boutouyrie P, Asmar R, Gautier I, Laloux B, Guize L, et al. Aortic stiffness is an independent predictor of all-cause and cardiovascular mortality in hypertensive patients. *Hypertension.* (2001) 37:1236–41. doi: 10.1161/01.HYP.37.5.1236

40. Guerin AP, Blacher J, Pannier B, Marchais SJ, Safar ME, London GM. Impact of aortic stiffness attenuation on survival of patients in end-stage renal failure. *Circulation.* (2001) 103:987–92. doi: 10.1161/01.CIR.103.7.987

41. Scheiblecker L, Kollmann K, Sexl V. Cdk4/6 and Mapk-crosstalk as opportunity for cancer treatment. *Pharmaceuticals (Basel).* (2020) 13:418. doi: 10.3390/ph13120418

42. Godina-Gonzalez S, Furuzawa-Carballeda J, Utrera-Barillas D, Alcocer-Varela J, Teran LM, Vazquez-del Mercado M, et al. Amebic monocyte locomotion inhibitory factor peptide ameliorates inflammation in cia mouse model by downregulation of cell adhesion, inflammation/chemotaxis, and matrix metalloproteinases genes. *Inflamm Res.* (2010) 59:1041–51. doi: 10.1007/s00011-010-0224-2

43. Silva-Garcia R, Estrada-Garcia I, Ramos-Payan R, Torres-Salazar A, Morales-Martinez ME, Arenas-Aranda D, et al. The effect of an anti-inflammatory pentapeptide produced by entamoeba histolytica on gene expression in the U-937 monocytic cell line. *Inflamm Res.* (2008) 57:145–50. doi: 10.1007/s00011-007-6199-y

44. Wang X, Wang C, Yang Y, Ni J. New monocyte locomotion inhibitory factor analogs protect against cerebral ischemia-reperfusion injury in rats. *Bosn J Basic Med Sci.* (2017) 17:221–7. doi: 10.17305/bjbms.2017.1622

45. Zhang Y, Chen J, Li F, Li D, Xiong Q, Lin Y, et al. A pentapeptide monocyte locomotion inhibitory factor protects brain ischemia injury by targeting the Eef1a1/endothelial nitric oxide synthase pathway. *Stroke.* (2012) 43:2764–73. doi: 10.1161/STROKEAHA.112.657908

46. Zhou Z, Chen B, Chen S, Lin M, Chen Y, Jin S, et al. Applications of network pharmacology in traditional chinese medicine research. *Evid Based Complement Alternat Med.* (2020) 2020:1646905. doi: 10.1155/2020/1646905

47. Li T, Guo R, Zong Q, Ling G. Application of molecular docking in elaborating molecular mechanisms and interactions of supramolecular cyclodextrin. *Carbohydr Polym.* (2022) 276:118644. doi: 10.1016/j.carbpol.2021.118644

48. Hou Y, Wang K, Wan W, Cheng Y, Pu X, Ye X. Resveratrol provides neuroprotection by regulating the Jak2/Stat3/Pi3k/Akt/Mtor pathway after stroke in rats. *Genes Dis.* (2018) 5:245–55. doi: 10.1016/j.gendis.2018.06.001

49. Zhang Q, An R, Tian X, Yang M, Li M, Lou J, et al. Beta-caryophyllene pretreatment alleviates focal cerebral ischemia-reperfusion injury by activating Pi3k/Akt signaling pathway. *Neurochem Res.* (2017) 42:1459–69. doi: 10.1007/s11064-017-2202-3

50. Alam S, Liu Q, Liu S, Liu Y, Zhang Y, Yang X, et al. Up-regulated cathepsin C induces macrophage M1 polarization through Fak-Triggered P38 Mapk/Nf-Kappab pathway. *Exp Cell Res.* (2019) 382:111472. doi: 10.1016/j.yexcr.2019.06.017

51. Weston CR, Davis RJ. The Jnk signal transduction pathway. *Curr Opin Cell Biol.* (2007) 19:142–9. doi: 10.1016/j.ceb.2007.02.001

52. Besirli CG, Wagner EF, Johnson EM Jr. The limited Role of Nh2-Terminal C-Jun phosphorylation in neuronal apoptosis: identification of the nuclear pore complex as a potential target of the Jnk pathway. *J Cell Biol.* (2005) 170:401–11. doi: 10.1083/jcb.200501138

Von Willebrand factor in diagnostics and treatment of cardiovascular disease: Recent advances and prospects

Sergey Kozlov[1]*, Sergey Okhota[1], Yuliya Avtaeva[2],
Ivan Melnikov[2,3], Evgeny Matroze[2,4] and Zufar Gabbasov[2]*

[1]Department of Problems of Atherosclerosis, National Medical Research Centre of Cardiology
Named After Academician E.I. Chazov of the Ministry of Health of the Russian Federation, Moscow,
Russia, [2]Laboratory of Cell Hemostasis, National Medical Research Centre of Cardiology Named
After Academician E.I. Chazov of the Ministry of Health of the Russian Federation, Moscow, Russia,
[3]Laboratory of Gas Exchange, Biomechanics and Barophysiology, State Scientific Center of the
Russian Federation—The Institute of Biomedical Problems of the Russian Academy of Sciences,
Moscow, Russia, [4]Department of Innovative Pharmacy, Medical Devices and Biotechnology,
Moscow Institute of Physics and Technology, Moscow, Russia

Von Willebrand factor (VWF) is a large multimeric glycoprotein involved in hemostasis. It is essential for platelet adhesion to the subendothelium of the damaged endothelial layer at high shear rates. Such shear rates occur in small-diameter arteries, especially at stenotic sites. Moreover, VWF carries coagulation factor VIII and protects it from proteolysis in the bloodstream. Deficiency or dysfunction of VWF predisposes to bleeding. In contrast, an increase in the concentration of high molecular weight multimers (HMWM) of VWF is closely associated with arterial thrombotic events. Severe aortic stenosis (AS) or hypertrophic obstructive cardiomyopathy (HOCM) can deplete HMWM of VWF and lead to cryptogenic, gastrointestinal, subcutaneous, and mucosal bleeding. Considering that VWF facilitates primary hemostasis and a local inflammatory response at high shear rates, its dysfunction may contribute to the development of coronary artery disease (CAD) and its complications. However, current diagnostic methods do not allow for an in-depth analysis of this contribution. The development of novel diagnostic techniques, primarily microfluidic, is underway. Such methods can provide physiologically relevant assessments of VWF function at high shear rates; however, they have not been introduced into clinical practice. The development and use of agents targeting VWF interaction with the vessel wall and/or platelets may be reasonable in prevention of CAD and its complications, given the prominent role of VWF in arterial thrombosis.

KEYWORDS

von Willebrand factor, ADAMTS-13, cardiovascular disease, Heyde syndrome, coronary artery disease

Introduction

Von Willebrand factor (VWF) owes its name to a Finnish physician Erik von Willebrand, who described an inherited bleeding disorder in 1924, which was later called Von Willebrand disease (VWD). In the 1950s it became clear that the disease was due to a deficiency of some blood protein. This protein was first purified in the early 1970s and its complete sequence was described in 1986 (1). Later research showed that VWF function is shear-rate dependent and is crucial for primary hemostasis in arteries (2, 3). Recent years have seen a surge in studies of VWF role in a number of pathologies other than VWD, as well as introduction of anti-VWF agents.

VWF is a large multimeric glycoprotein that is involved in hemostasis (4). It is essential for platelet adhesion to the subendothelium of the damaged endothelial layer at high shear rates occurring in small-diameter arteries, especially at stenotic sites. Moreover, VWF carries coagulation factor VIII and protects it from proteolysis in the bloodstream. Unprotected by VWF, coagulation factor VIII is unstable and degrades rapidly.

The structure and functions of the von Willebrand factor

VWF is a large, complex multimeric protein composed of a varying number of dimers that polymerize into high-molecular-weight multimers (HMWM). The more dimers a VWF molecule contains, the more potent it is in causing hemostasis. Smaller multimers mainly function as carriers of coagulation factor VIII, whereas HMWM are involved in cell adhesion (5, 6). Monomers that form dimers consist of functionally different parts, or domains, of VWF (**Figures 1**, **2**). Each domain contains binding sites for specific cells and molecules. Thus, the A1 domain contains a binding site for the glycoprotein complex Ib/IX/V (GP Ib) of platelets, the only receptor on non-activated platelets with a high affinity for VWF. Additionally, the A1 domain contains binding sites for collagen types I, IV, VI, and heparin. The A2 domain contains binding sites for the ADAMTS-13 (a disintegrin and metalloproteinase with a thrombospondin type 1 motif 13) metalloprotease and VWF molecules. The A3

domain contains binding sites for collagen types I and III. The C4 domain contains a binding site for the platelet integrin αIIbβ3 (GPIIb/IIIa). C domains facilitate VWF flexibility. The D′D3 domain contains a binding site for coagulation factor VIII. The C-terminal cysteine knot (CTCK) is involved in the dimerization of VWF. All D domains are involved in the formation of disulfide bonds between dimers (7).

VWF is mainly produced in the endothelial cells and is densely packed in endothelial Weibel–Palade bodies with P-selectin. Some VWF is produced by megakaryocytes. When mature platelets detach from megakaryocytes, VWF remains inside α-granules (8, 9). VWF is constantly released into the bloodstream from Weibel-Palade bodies of non-activated endothelial cells (basal secretion). Activation of the endothelium upregulates VWF secretion. Further, up to 20% of VWF may be secreted from α-granules upon platelet activation (10, 11). However, the role of platelet VWF in hemostasis has not been fully established, and studies are limited.

VWF exists in two forms in the bloodstream: inactive globular and active unfolded (**Figure 3**), which are determined by the shear rate of the flowing blood. Blood is a heterogeneous liquid, and as it flows through the vessels, it encounters an internal friction force, causing different layers to move at different velocities. The velocity of the flow at the center of the vessel is higher than that at its walls. The magnitude of the difference in the velocities of adjacent layers is quantitatively expressed as the shear rate, measured in reciprocal seconds (s^{-1}). At low shear rates, which occur in the veins or large arteries, VWF remains in the globular form. This form conceals VWF domains and prevents interaction with the circulating platelets. At high shear rates, which occur in the small arteries and arterioles, especially at stenotic sites, VWF unfolds and exposes the domains with binding sites (9, 12).

Unfolded VWF strains can self-associate through the A2 domain and form complex mesh structures that significantly increase the number of platelet binding sites. The ability of the unfolded VWF to self-associate at high shear rates was studied *in vitro* by Zheng et al. (13). Schneider et al. reported the formation of mesh structures from VWF strains that unfolded at high shear rates (2).

Upon unfolding, VWF presents binding sites for ADAMTS-13 on A2 domains. This interaction results in the proteolytic cleavage of HMWM of VWF, reducing its hemostatic activity (14). ADAMTS-13 is synthesized exclusively in stellate cells of the liver, and its plasma level is negatively associated with that of VWF (15).

VWF carries coagulation factor VIII in the bloodstream. This factor is involved in the intrinsic coagulation pathway, interacting with factor IXa as a cofactor to form intrinsic tenase, an enzyme complex that converts inactive coagulation factor X into active Xa. Without VWF, coagulation factor VIII is susceptible to rapid degradation. A globular conformation of VWF protects against proteolysis and prolongs the half-life of
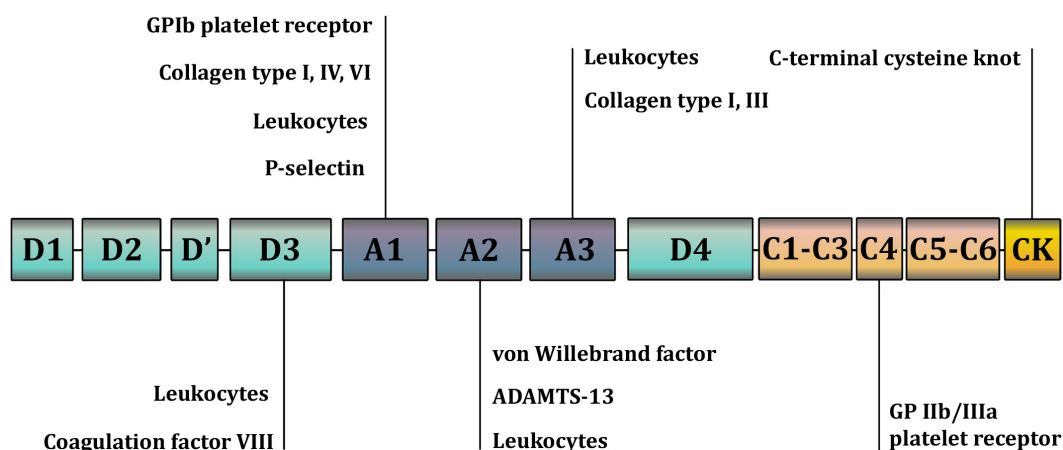
FIGURE 1
A schematic representation of the domains and binding sites of the Von Willebrand factor (VWF) monomer. The A1 domain contains a binding site for the glycoprotein complex Ib/IX/V (GP Ib) of platelets; collagen types I, IV, VI; and heparin. The A2 domain contains binding sites for the ADAMTS-13 (a disintegrin and metalloproteinase with a thrombospondin type 1 motif 13) metalloprotease and VWF molecules. The A3 domain contains binding sites for collagen types I and III. The C4 domain contains a binding site for the platelet integrin αIIbβ3 (GPIIb/IIIa). C domains facilitate VWF flexibility. The D'D3 domain contains a binding site for coagulation factor VIII. The C-terminal cysteine knot (CTCK) is involved in the dimerization of VWF. All D domains are involved in the formation of disulfide bonds between VWF dimers.

coagulation factor VIII, ultimately delivering it to the sites of vascular damage (16).

Diseases associated with von Willebrand factor and ADAMTS-13 deficiency or dysfunction

VWF deficiency or dysfunction predisposes to bleeding. VWD is a congenital disorder caused by quantitative deficiency and/or qualitative changes in the structure of VWF. VWD is one of the most common hemostatic disorders, with the prevalence of severe cases being 1:10,000 in the general population (17). VWD presents with symptoms similar to those observed in hemophilia such as nasal and gingival bleeding, subcutaneous and muscle hematomas, prolonged skin bleeding, and metrorrhagia. Acquired von Willebrand syndrome is a rare disease associated with acquired quantitative and/or qualitative VWF deficiency in lymphoproliferative (chronic lymphocytic leukemia), myeloproliferative (thrombocythemia), cardiovascular (AS and HOCM), and immunological (hypothyroidism) diseases (18).
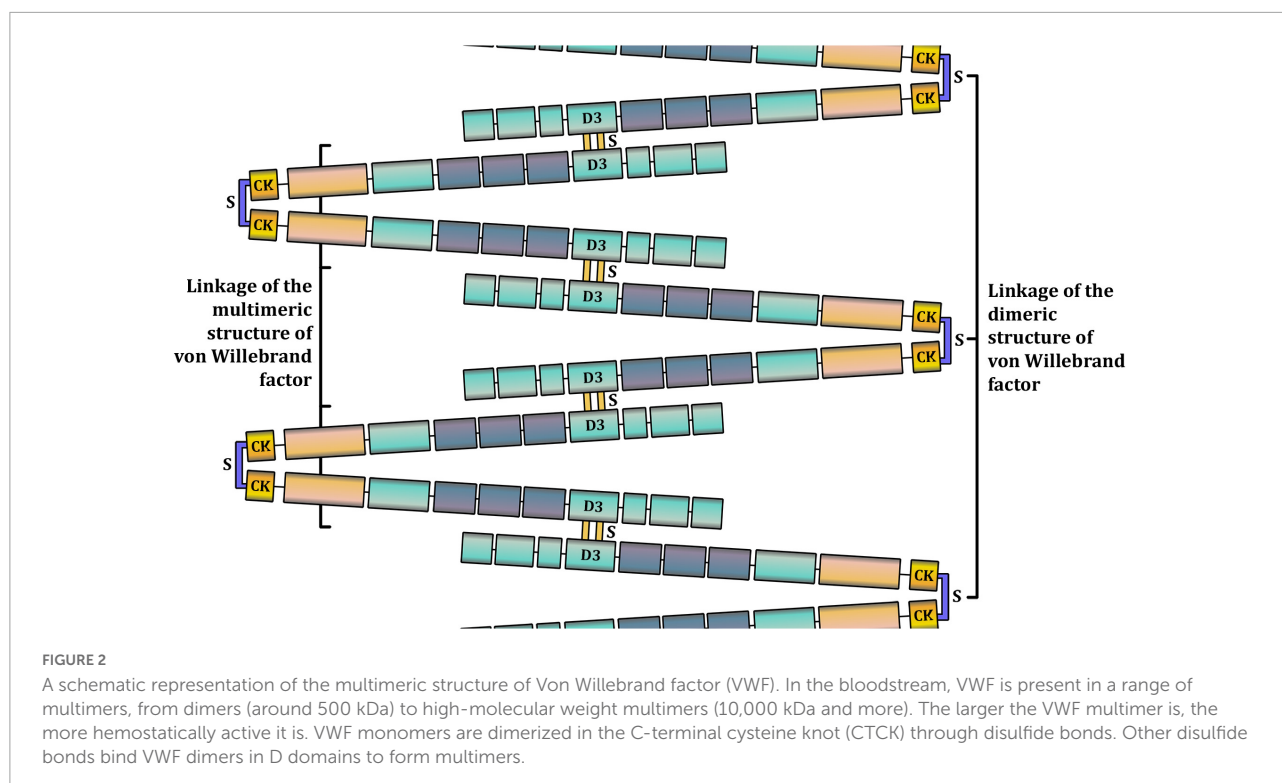
The increase in the level of HMWM of VWF due to ADAMTS-13 deficiency causes thrombotic thrombocytopenic purpura (TTP), characterized by microvascular thrombosis and platelet pool depletion (19). Quantitative deficiency of ADAMTS-13 in TTP can develop due to a congenital defect or production of autoantibodies that enhance ADAMTS-13 clearance. Functional deficiency can also develop due to autoantibodies that inhibit ADAMTS-13 activity without

affecting its plasma level (20). Thrombosis in TTP may manifest as acute kidney injury, neurological and mental disorders, fever, hemolytic anemia, and thrombocytopenia with purpura.

Diagnostic testing of deficiency and dysfunction of von Willebrand factor

The diagnosis of VWD requires various tests (21). The VWF plasma level, also known as the von Willebrand factor antigen (VWF:Ag), is measured using an enzyme-linked immunosorbent assay (ELISA), which involves a highly specific antigen-antibody reaction. VWF:Ag measures the concentration of plasma VWF molecules, ranging from dimers to HMWM. Normal values of VWF:Ag range from 50 to 150 IU/dL, but levels can vary over a wide range in the same individual on separate occasions (22). Proteolytic cleavage of HMWM of VWF into smaller multimers impairs its hemostatic function without affecting VWF:Ag values. Therefore, VWF:Ag reflects the total amount of this protein in the blood rather than its functional state.

VWF level in the blood depends on blood group (23). This complicates the distinction between healthy individuals with low VWF levels and those with mild VWD (24). Individuals with blood group O have lower VWF:Ag levels than that of those with other blood groups (25, 26). In a study involving 1,117 blood donors, Gill et al. showed that the mean VWF:Ag level in the donors with blood group O was 74.8 IU/dL. The mean VWF:Ag level in donors with blood groups A (105.9 IU/dL) and

FIGURE 2

A schematic representation of the multimeric structure of Von Willebrand factor (VWF). In the bloodstream, VWF is present in a range of multimers, from dimers (around 500 kDa) to high-molecular weight multimers (10,000 kDa and more). The larger the VWF multimer is, the more hemostatically active it is. VWF monomers are dimerized in the C-terminal cysteine knot (CTCK) through disulfide bonds. Other disulfide bonds bind VWF dimers in D domains to form multimers.

B (116.9 IU/dL) was higher. The highest VWF:Ag level was seen in donors with blood group AB (123.3 IU/dL) (27). The half-life of VWF may differ depending on the blood group (11).

Ristocetin cofactor activity assay (VWF:RCo) is the gold standard for assessing VWF activity. In this assay, the antibiotic ristocetin causes the A1 domains of VWF to bind platelet GPIb receptors, inducing platelet agglutination. In VWF:RCo, standardized formalin-fixed or lyophilized platelets are added to a sample of platelet-poor plasma containing VWF and ristocetin. This leads to VWF-dependent platelet agglutination, which is measured using an aggregometer. VWF:RCo induces VWF activation by a non-physiological chemical agent. This test is used to diagnose VWD. It is especially sensitive in severe cases, such as VWD type 3, in which VWF is almost or completely absent from the blood. Studies revealed that normal values of VWF:RCo were blood group-dependent. In a study on 167 healthy donors, Moeller et al. showed that VWF:RCo values were 67.7 ± 19, 81.2 ± 27.7, 95.5 ± 24.5, and $102.3 \pm 19.1\%$ in blood groups O, A, B, and AB, respectively (28). In a study on 200 healthy children, Akin et al. demonstrated that VWF:RCo values were 89 ± 23 and $103 \pm 17\%$ in blood groups O and non-O, respectively (29).

Structural analysis of VWF multimers using agarose gel electrophoresis remains the gold standard for assessing HMWM deficiency (6, 30). This assessment is critical to the identification of VWD type 2 subtypes. It can also be applied to the diagnosis of HMWM deficiency due to acquired von Willebrand syndrome in patients with severe valvular disease. Additionally,

VWF collagen binding assay (VWF:CB) can be used to assess HMWM deficiency (24).

The platelet function analyzer-100 (PFA-100), a device that assesses primary hemostasis, has often been used in VWD screening (31). The analysis is performed in a chamber consisting of a narrow tube and membrane with a 150 μm aperture. A whole blood sample is drawn via the tube and through the aperture into the membrane, and coated with collagen and platelet activators, such as adenosine diphosphate (ADP) and epinephrine, or ADP and prostaglandin E1. The shear rate in the aperture can reach $6,000 \text{ s}^{-1}$, which is sufficient to unfold and activate VWF. A PFA-100 test measures the time to occlusion of the aperture by thrombus formation (closure time). This complex process involves numerous interactions that lead to platelet adhesion and aggregation. Therefore, PFA-100 does not allow isolation of the contribution of shear rate-dependent VWF activation to thrombus formation (31). Currently, PFA-100 is often employed in research.

Von Willebrand factor and cardiovascular disease

Aortic stenosis

Aortic stenosis (AS) is a valvular heart disease eventually resulting in the left ventricular outflow tract (LVOT) obstruction. The most common cause of AS is chronic
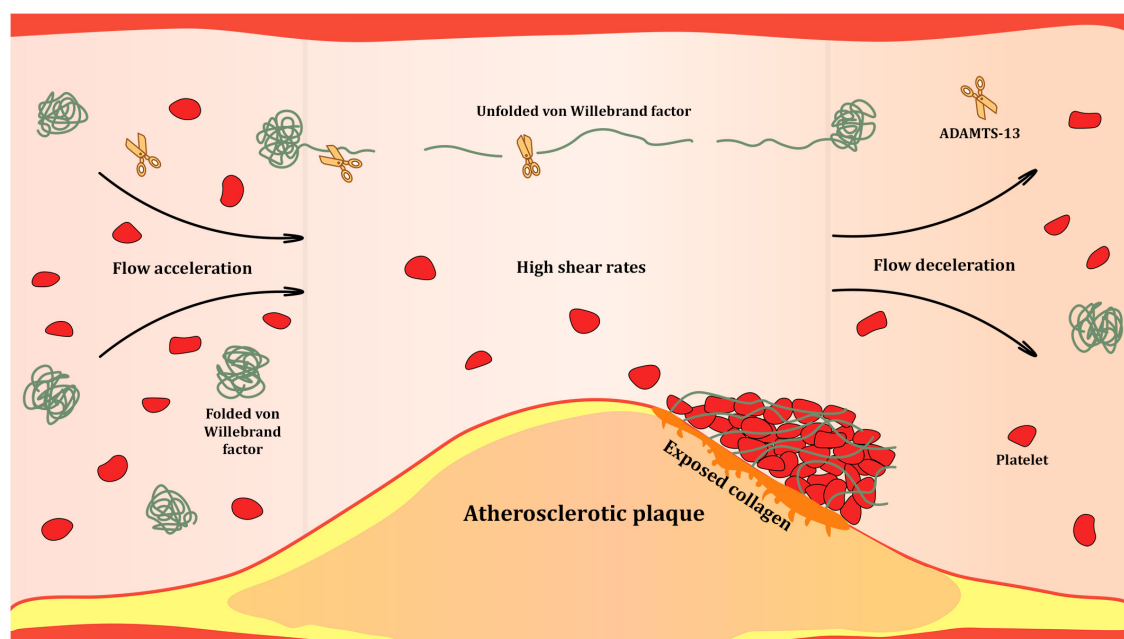
FIGURE 3
Shear-rate dependent activation of Von Willebrand factor (VWF) at the site of atherosclerotic stenosis. High shear rates occurring in the bloodstream at sites of significant atherosclerotic narrowing of the arterial lumen trigger unfolding of VWF multimers. Unfolded VWF presents a range of binding sites for proteins of subendothelial matrix, platelets and leukocytes. It is also subjected to proteolysis by ADAMTS-13 that cleaves unfolded VWF multimers at the A2 domains and reduces their hemostatic activity.

inflammatory degeneration and calcification of aortic valve leaflets. Severe AS may result in a number of life-threatening conditions, including heart failure, myocardial ischemia, arrhythmias, and cardiac arrest. The treatment of severe AS, especially after the onset of symptoms, usually involves aortic valve replacement (32).

Cryptogenic gastrointestinal bleeding in patients with AS was first described by Heyde in 1958 (33). In 1992, Warkentin et al. suggested that bleeding from gastrointestinal angiodysplasia was caused by the loss of HMWM of VWF due to AS or hypertrophic cardiomyopathy (HCM) (34). In 2002, Warkentin et al. reported two cases of severe AS with gastrointestinal bleeding that resolved after aortic valve replacement (35). Platelet count, activated partial thromboplastin time, coagulation factor VIII, VWF:Ag level, and VWF:RCo values were normal preoperatively. However, a pronounced reduction in HMWM of VWF was present, which recovered after aortic valve replacement and remained normal during the 10-year follow-up period (35). The level of HMWM of VWF can decrease by 50% in severe AS (36). Moreover, low pulse pressure in AS contributes to a decrease in the endothelial basal secretion of VWF (37, 38).

The primary reason for the loss of HMWM of VWF is that AS increases the shear rate at the aortic valve orifice. As the entire volume of circulating blood passes through the stenotic orifice, all HMWM of VWF are subjected to unfolding and proteolysis by ADAMTS-13. This eventually results in a quantitative deficiency of HMWM of VWF (acquired von Willebrand syndrome type 2A), which manifests as bleeding (39). The combination of AS, acquired von Willebrand syndrome type 2A, and bleeding from gastrointestinal angiodysplasia is known as Heyde syndrome. Additionally, patients with severe AS report subcutaneous and mucosal bleeding. The severity of bleeding increases with AS progression (39). The HMWM of VWF recovers within several hours following surgical valve replacement, which normalizes the shear rate in the valve orifice and pulse pressure (38, 40). The loss of HMWM of VWF does not occur in severe coronary or peripheral artery stenosis, because only a small portion of the blood is subjected to high shear rates.

The loss of HMWM of VWF in severe AS and recovery after aortic valve replacement has been demonstrated in a number of studies. Panzer et al. studied 47 patients with severe AS who underwent aortic valve replacement (41). Initially, the level of HMWM of VWF decreased in all patients. It recovered after aortic valve replacement in most patients. The PFA-100 closure time was prolonged preoperatively and normalized thereafter. The authors showed that the loss of HMWM of VWF affected platelet adhesion and ADP-induced platelet aggregation (41). Vincentelli et al. reported subcutaneous and mucosal hemorrhages in 21% of patients with severe AS (42). The VWF:Ag level was within normal range in all patients. The

PFA-100 test demonstrated prolonged closure time. The levels of HMWM of VWF and VWF:CB were reduced. The closure time and level of HMWM of VWF normalized 1 day after valve replacement (42). Patients with severe AS who underwent aortic valve replacement presented the same pattern in a study by Frank et al. (36). The PFA-100 closure time was prolonged, and the level of HMWM of VWF was reduced preoperatively. Both parameters normalized following successful valve replacement. The 18-month follow-up showed that the level of HMWM of VWF did not decrease again after aortic valve replacement. This observation was supported by several other studies with a follow-up period of 2 weeks–6 months (36). However, HMWM of VWF may not be replenished if severe aortic regurgitation occurs after aortic valve replacement (42). Despite bleeding, VWF:Ag and VWF:RCo values were within the normal range in patients with Heyde syndrome (36). Acquired von Willebrand and Heyde syndromes were reported in patients with aortic and mitral regurgitation (38, 43–45).

Hypertrophic obstructive cardiomyopathy

Hypertrophic obstructive cardiomyopathy (HOCM) is a genetic disorder, most frequently transmitted through an autosomal dominant pattern. It results in asymmetric myocardial hypertrophy of the left ventricle that may lead to LVOT. HOCM is a significant cause of sudden cardiac death, arrhythmias and heart failure in young people. In severe cases, septal reduction therapy either with surgical septal myectomy or alcohol ablation can be used to reduce LVOT (46).

LVOT obstruction exposes HMWM of VWF to proteolysis by ADAMTS-13, similarly to AS. Blackshear et al. studied five patients with symptomatic HOCM (47). Spontaneous gastrointestinal, mucosal, or excessive postoperative bleeding was observed in all patients. VWF: Ag and VWF: RCo values were within normal range, whereas electrophoresis showed the loss of HMWM and an excess of low-molecular weight multimers of VWF. Bleeding ceased, and HMWM of VWF recovered following septal myectomy in all patients (47). In another study of 28 patients with HOCM, the VWF:Ag level was normal in all patients (48). The PFA-100 closure time was prolonged in all but one patient. Loss of HMWM of VWF was detected in all patients. A strong positive correlation was found between the peak pressure gradient in the LVOT and percentage loss of HMWM of VWF, relative to all VWF multimers. The peak pressure gradient 15 mmHg in the LVOT at rest was sufficient to reduce the HMWM of VWF (48).

Left ventricular assist devices

Left ventricular assist devices (LVAD) are pumping systems used in patients with the end-stage heart failure refractory to

medical therapy as a bridge-to-transplant or an alternative to heart transplantation option (49). Gastrointestinal bleeding is among the most common complications associated with LVAD use. Pump construction may cause the loss of HMWM of VWF due to increased shear rates in the LVAD-driven circulation. LVAD explantation is associated with the recovery of HMWM of VWF, within a few hours (50).

Coronary artery disease

Coronary artery disease (CAD) is a chronic condition characterized by atherosclerotic plaque accumulation in the epicardial arteries. Retention of atherogenic lipoproteins in arterial intima and low-grade vascular inflammation are recognized as the main drivers of atherosclerosis development (51). Oxidation of low-density lipoproteins may link lipoprotein retention and proinflammatory macrophage activation in the vessel wall (52). Recently, the role of mitochondrial DNA mutations was suggested in induction of sterile vascular inflammation (53). Atherosclerotic plaques in epicardial arteries can eventually rupture or erode, resulting in acute coronary syndrome (ACS) in a form of myocardial infarction (MI) or unstable angina. Plaques can also gradually progress to significant narrowing of arterial lumen, causing angina pectoris, heart failure, or remain asymptomatic. CAD usually follows a pattern of long stable periods intermitted by unstable episodes due to atherothrombotic events (54).

Impairment of the hemostatic role of VWF may contribute to the development of CAD and its complications. In addition, VWF may contribute to inflammation in atherosclerosis. VWF facilitates leukocyte recruitment and extravasation at high shear rates (55). VWF may modulate the inflammatory response at the sites of atherosclerotic lesions through this function.

CAD is less prevalent in patients with VWD than in healthy individuals. The prevalence of atherosclerotic cardiovascular disease (CAD, MI, brain ischemia, and peripheral artery disease) was assessed in 7,556 patients with VWD and 19,918,970 patients without VWD (56). The prevalence of CAD was 15.0% in patients with VWD vs. 26.0% in patients without VWD. The risk factor-adjusted odds ratio was 0.86 [95% confidence interval (CI), 0.80–0.94] for CAD and 0.69 (95% CI, 0.61–0.79) for MI in patients with VWD (56).

In a study by Xu et al., the VWF:Ag level, which differed between patients with CAD and healthy individuals, was 141.78 ± 20.53 IU/dL in patients with CAD vs. 111.95 ± 17.15 IU/dL in healthy controls (57). Kaikita et al. reported that the VWF:Ag level was $2,151 \pm 97$ mU/mL in patients hospitalized within 72 h from the onset of MI, $1,445 \pm 93$ mU/mL in patients with exertional angina and 90% narrowing of a major coronary artery, and $1,425 \pm 76$ mU/mL in patients with chest pain without stenotic coronary atherosclerosis on diagnostic cardiac catheterization (58). In contrast, the ADAMTS-13 level was the

lowest in patients experiencing acute MI (799 ± 29 mU/mL), and higher in patients experiencing exertional angina (996 ± 31 mU/mL) and in those without significant coronary artery stenosis (967 ± 31 mU/mL) (58). In another study, the VWF:Ag level was almost 1.5-fold higher in 1,026 patients with ST-segment elevation myocardial infarction (STEMI) than in 652 control patients (378.2 ng/mL vs. 264.4 ng/mL, respectively), whereas ADAMTS-13 activity was lower in patients with STEMI than in the controls (90 and 97%, respectively) (59). No association was observed between VWF:Ag and ADAMTS-13 levels in the SMILE study, which included 560 men who experienced a MI at least 6 months prior and 646 healthy men. ADAMTS-13 (101 and 100%, respectively) and VWF:Ag (138 and 135%, respectively) levels did not differ between the groups (60).

The time to recovery of the VWF:Ag level after STEMI was studied in 57 male rats in which the anterior descending artery was permanently ligated approximately 2 mm from its origin (61). The rats were divided into four groups. Blood was initially collected from the coronary sinus and inferior vena cava in all groups, 1 h after the onset of MI in the first group, 24 h after the onset of MI in the second group, 7 days after the onset of MI in the third group. The fourth group was the control sham-operated group. Compared with the initial values, the VWF:Ag level in the blood from the coronary sinus increased 1.31-fold 1 h after MI and 0.88-fold 24 h later. The VWF:Ag level in the blood from the inferior vena cava increased 0.37-fold 1 h after MI and 0.18-fold 24 h later. The VWF:Ag level normalized 7 days after MI (61).

The association between the VWF:Ag level and CAD risk was studied in an initially CAD-free population (62). In a prospective study, 1,411 men without CAD were divided into tertiles depending on the VWF:Ag level, and followed up for 16 years. After adjusting for cardiovascular risk factors, the odds ratio was 1.53 (95% CI, 1.10–2.12) for CAD in the upper tertile when compared with the lower tertile (62). Another prospective study followed up approximately 10,000 healthy men for 5 years (63). CAD developed in 296 patients (158 developed MI and 142 developed stable and unstable angina). The baseline VWF:Ag level was higher in patients who developed MI (129.2 ± 53.1 IU/dL) compared with the control patients (115.9 ± 41.8 IU/dL). The relative risk of MI was 3.04-fold (95% CI, 1.59–5.80) higher in participants with a VWF:Ag level in the upper quartile when compared with the lower quartile (63). The prospective Reykjavik study enrolled 1,925 patients without CAD who subsequently developed MI or fatal CAD during the 19.4-year follow-up and 3,616 controls (64). The baseline VWF:Ag level was higher in patients with major adverse cardiovascular events (MACE) than it was in the control group. After adjusting for cardiovascular risk factors, the increase by one standard deviation above baseline VWF:Ag level corresponded to an odds ratio of 1.08 (95% CI, 1.02–1.15) for MI or lethal CAD (64). However, according to the large ARIC study on 14,477

participants initially free from CAD, an elevated VWF:Ag did not provide added value for cardiovascular risk assessment when adjusted to traditional cardiovascular risk factors (65). Several other studies reported that the VWF:Ag level assessment did not improve predicting MACE when adjusted to traditional cardiovascular risk factors (66–68). Therefore, the low predictive value of the VWF:Ag level in cardiovascular risk assessment in CAD-free individuals can be partially explained by confounding cardiovascular risk factors (69).

Contrary to studies on the general CAD-free population, studies on patients with preexisting CAD found a direct relationship between the VWF:Ag level and MACE rate (70–72). The prospective ECAT study followed up 3,043 patients with angina pectoris for 2 years. Those who subsequently developed MI or sudden cardiac death had higher baseline VWF:Ag levels. Patients were divided into quintiles depending on the VWF:Ag level. The relative risk of MACE in the upper quintile was 1.85-fold higher than it was in the lower quintile (70). The ENTIRE-TIMI 23 study enrolled 314 patients with STEMI who had VWF:Ag levels measured before and 48–72 h after fibrinolysis (71). The study showed that the VWF:Ag level in the upper quartile was associated with a higher incidence of repeated MI and death in the subsequent 30 days, than that in the lower quartile (11.2 and 4.1%, respectively) (71). Another study followed up 123 MI survivors under the age of 70 years for 4.9 years (72). The VWF:Ag level was measured 3 months after the onset of MI. A higher VWF:Ag level was independently associated with recurrent MI and death (72).

A VWF:Ag level increase can be caused by factors that contribute to CAD development, such as age (73, 74) and smoking (73, 75). Patients with diabetes mellitus (DM) had higher VWF:Ag levels than those without DM in the ASCET study (74). According to Stehouwer et al., increased VWF:Ag levels in patients with DM type 2 occurred in response to microalbuminuria (76). Several studies have addressed the relationship between arterial hypertension and the VWF:Ag level. In a study by Lip et al., The VWF:Ag level was higher in hypertensive patients than in healthy controls (113 and 98 IU/dL, respectively) (77). In a study by Lee et al., 73 patients with stable CAD and arterial hypertension and 35 healthy controls underwent 24-h ambulatory blood pressure (BP) monitoring (78). The patients were divided into four groups: The first group included patients with high arterial pulse pressure, the second included those with low arterial pulse pressure, the third included dippers, and the fourth included non-dippers. In all groups the VWF:Ag level was higher than the in the control subjects (197 ± 58 and 120 ± 18 IU/dL, respectively). Patients with high arterial pulse pressure and non-dippers had the highest VWF:Ag level (219 ± 58 and 222 ± 55 IU/dL, respectively) (78).

VWF:Ag levels increase in response to stress. Stress signals induce the release of vasopressin, which stimulates the release

of VWF from endothelial Weibel-Palade bodies. Desmopressin, a vasopressin analog, is used to sustain the VWF plasma level in VWD treatment (79). A treatment-induced VWF:Ag level increase can occur due to the use of diuretics, digoxin, unfractionated heparin, and oral anticoagulants (57). Unlike unfractionated heparin, enoxaparin reduces VWF release (71, 80).

CAD can affect the VWF:Ag level. Endothelial dysfunction is crucial to the pathogenesis of atherosclerosis, increasing the risk of MACE (81). Considering the predominantly endothelial source of VWF in the bloodstream, higher VWF:Ag levels in patients with CAD may be associated with characteristic endothelial dysfunction and endothelial damage. An increase in the concentration of circulating VWF can propagate chronic local inflammation of the arterial wall. An increase in VWF:Ag levels in response to inflammation was found in patients with systemic inflammatory diseases. The VWF:Ag level was higher in patients with rheumatoid arthritis, scleroderma, and systemic vasculitis than in healthy controls (82). The VWF:Ag level and VWF:RCo values were higher in patients with systemic lupus erythematosus (primarily in those with serositis) than those in healthy controls. However, higher VWF:Ag levels were not associated with clinical manifestations of the disease, including thrombotic complications (83). The VWF:Ag level increases and decreases simultaneously with C-reactive protein in acute inflammation (84). Various inflammatory agents influence the endothelial secretion of VWF. Interleukin-6 (IL-6), IL-8, and tumor necrosis factor-α significantly stimulate the release of VWF from endothelial Weibel-Palade bodies. IL-6 prevents proteolytic cleavage of VWF by ADAMTS-13 (85).

Most studies that addressed the role of VWF in the development of CAD and its complications used ELISA-based VWF:Ag measurements. This assay cannot provide information on the functional state of VWF. Some studies used VWF:RCo, which activated VWF multimers using a non-physiological chemical agent. These laboratory methods failed to reproduce physiologically relevant conditions for platelet adhesion and aggregation. In recent years, microfluidic systems have been popularized. These devices can model hemodynamic conditions, such as different shear rates, which are characteristic of the arterial or venous bed; turbulent flow; complex vessel anatomy, such as bi- or trifurcations; and vessel narrowing by a stenotic plaque, etc. Among the advantages of these devices is that they require small volumes of blood to obtain reproducible results. Moreover, they can examine individual links of hemostasis such as platelet adhesion in isolation from aggregation (86). In future, these devices may be used to diagnose various hemostatic disorders and to test the effectiveness and dose adjustment of antiplatelet drugs. However, such microfluidic systems are not currently standardized and are uncommon in clinical practice (13, 86–90).

Advances and prospects for agents targeting von Willebrand factor and ADAMTS-13 in cardiovascular disease

The development and use of agents targeting VWF interaction with the vessel wall and/or platelets may be reasonable in prevention of CAD and its complications, given the prominent role of VWF in arterial thrombosis. Most agents used in the primary and secondary prevention of CAD do not affect VWF or ADAMTS-13. Only heparins interfere with GPIb-mediated platelet adhesion by binding to the A1 domain of VWF (91).

At the turn of the twenty-first century, AJvW-2 and AJW200 antibodies targeting the GPIb binding sites on the A1 domain of VWF were developed. A study on dogs with induced occlusive thrombosis in the left coronary artery compared the efficacy of AJW200 and the GPIIb/IIIa antagonist abciximab in thrombosis prevention. AJW200 inhibited thrombus formation without affecting bleeding time and showed a better safety profile than abciximab (92). Similar results were obtained with AJvW-2 in another canine study (93).

Eto et al. studied the effect of AJvW-2 on platelet aggregation at high shear rates in patients with unstable angina or MI and control subjects (94). Platelet aggregation was 2- and 1.3-fold higher in patients with MI and unstable angina, respectively, than in the controls. AJvW-2 completely inhibited platelet adhesion in all groups (94).

Aptamers targeting GPIb interaction with the A1 domain of VWF have been developed. These are small single-stranded RNA or DNA molecules that are capable of high-affinity binding to a target molecule. The first-generation aptamer, ARC1779, produced dose-dependent inhibition of VWF activity in healthy individuals (95). The antithrombotic effect of ARC1779 was studied in 36 patients who underwent carotid endarterectomy. ARC1779 reduced the availability of A1 domains of VWF and the rate of embolic signals detected using doppler ultrasonography; however, perioperative bleeding and anemia were increased (96). Further research on ARC1779 was halted owing to a lack of funding. A second-generation aptamer, TAGX-0004, inhibited the binding of GPIb to the A1 domain of VWF by 10-fold compared to ARC1779. TAGX-0004 inhibited thrombus formation in a flow chamber by 20-fold compared to ARC1779 (97). The third-generation aptamer, BT200, reduced the availability of the A1 domains of VWF in a dose-dependent manner and prolonged PFA-100 closure time by more than 300 s (98). Additionally, BT200 reduced the availability of the A1 domains of VWF in a dose-dependent manner in 320 patients with ACS (99). Another aptamer, DTRI-031, produced a dose-dependent decrease in platelet adhesion (up to complete inhibition) at high shear rates in a microfluidic system. DTRI-031 prevented arterial thrombosis and facilitated thrombus

recanalization in murine and canine models of carotid artery injury (100).

Anfibatide is a reversible platelet GP Ib receptor antagonist. In a murine model of focal cerebral ischemia, anfibatide administration resulted in smaller infarct size, a less severe neurological deficit, and histopathological brain tissue changes compared to sham-treated mice (101). Results of anfibatide administration were comparable to that of the GPIIb/IIIa inhibitor tirofiban; however, anfibatide caused less intracerebral hemorrhage and had shorter bleeding time (101). Similar results have been reported by Chu et al. (102). Anfibatide suppressed ristocetin-induced platelet aggregation without affecting bleeding time or coagulation in 94 healthy individuals (103). Another study comprised 90 patients with non-ST elevation MI who were divided into groups of 30 depending on the anfibatide dose and 30 controls (104). Anfibatide was administered in addition to standard dual antiplatelet therapy. Ristocetin-induced platelet aggregation decreased by 47, 16, and 21%, in the high-, medium-, and low-dose groups, respectively, and by 0% in the placebo group. During the 30-day follow-up, death, MI, and major bleeding were rare and the outcomes were comparable between the anfibatide and placebo groups (104).

ALX-0081 (caplacizumab) is the only agent approved for clinical use that targets the VWF-platelet interaction (105). It is a humanized bivalent nanoparticle that targets the GPIb binding sites on the A1 domains of VWF. It was approved for clinical use in the European Union and United States for the treatment of adult patients with TTP, following the results of the HERCULES trial. In this trial, caplacizumab administration resulted in a lower incidence of the composite endpoint of TTP-related death, recurrent TTP, and thromboembolism (105).

Few studies have investigated the efficacy and safety of caplacizumab in patients with CAD. The efficacy of caplacizumab was studied in 9 patients with CAD who were scheduled for elective percutaneous coronary intervention (PCI) and 11 healthy controls (106). Caplacizumab completely inhibited platelet adhesion to collagen at high shear rates in patients with CAD and in healthy controls. However, complete inhibition of adhesion in the patients with CAD required high doses of caplacizumab. The effectiveness of caplacizumab was unaffected by antithrombotic drugs, including acetylsalicylic acid, clopidogrel, and heparin (106). In a study of 46 patients with stable CAD scheduled for elective PCI, caplacizumab was safe and resulted in complete inhibition of platelet aggregation (107). In 2009, caplacizumab was studied in 380 high-risk patients with ACS scheduled for elective PCI. Compared to the GPIIb/IIIa inhibitor abciximab, caplacizumab was not beneficial in reducing the risk of bleeding and had comparable antithrombotic effectiveness (108).

Administration of recombinant human ADAMTS-13 reduced endothelial dysfunction and improved cardiac remodeling in a murine model of left ventricular pressure overload (109). Another study showed that recombinant human ADAMTS-13 administration reduced infarct size, neutrophil infiltration of the ischemic myocardium, and troponin-I release in a murine model of ischemia/reperfusion injury (110).

A novel agent, Revacept, is a fusion protein of the extracellular domain of GPVI, a major platelet collagen receptor, and the human Fc fragment (111). It coats exposed collagen at the sites of vessel injury and prevents platelet adhesion and subsequent aggregation. Similarly, Revacept may interfere with the binding of VWF to collagen (111). In a murine cerebral ischemia/reperfusion injury model, Revacept administered immediately before reperfusion reduced cerebral infarct size, edema, and inflammation, and did not increase the incidence of intracranial bleeding. However, there were no differences in the recovery of neurological functions 24 h after the onset of stroke between mice treated with Revacept and those treated with fibrinolytic rtPA (111). The ISAR-PLASTER study investigated the safety and efficacy of Revacept in 334 patients with stable CAD scheduled for elective PCI (112). Patients received Revacept at a dose of 160 mg, 80 mg, or placebo in addition to standard antiplatelet therapy. Revacept did not show a benefit over standard therapy regarding the primary endpoint of death or myocardial injury and did not affect the incidence of bleeding at 30 days (112). Currently, a clinical trial on the safety and efficacy of Revacept in patients with symptomatic carotid atherosclerosis is underway (113).

Microlyse, a fusion protein consisting of an antibody fragment targeting the CTCK domain of VWF and the protease domain of urokinase plasminogen activator, was described in 2022 (114). This novel agent triggers destruction of platelet-VWF complexes by plasmin on endothelial cells. Antithrombotic effect of Microlyse was more potent than that of caplacizumab in the murine model of TTP. Microlyse also attenuated thrombocytopenia and tissue damage without affecting hemostasis in a tail-clip bleeding murine model (114).

Conclusion

Severe AS or HOCM predisposes to a deficiency in HMWM of VWF and leads to gastrointestinal, subcutaneous, or mucosal bleeding. Considering that VWF facilitates primary hemostasis and a local inflammatory response at high shear rates, dysfunction of this protein may putatively contribute to the development of CAD and its complications. However, few methods allow for in-depth analysis of this contribution. The development and use of agents targeting VWF interaction with the vessel wall and/or platelets may be reasonable in prevention of CAD and its complications, given the prominent role of VWF in arterial thrombosis.

Author contributions

Funding

Conflict of interest

The authors declare that the research was conducted in the absence of any commercial or financial relationships that could be construed as a potential conflict of interest.

Publisher's note

All claims expressed in this article are solely those of the authors and do not necessarily represent those of their affiliated organizations, or those of the publisher, the editors and the reviewers. Any product that may be evaluated in this article, or claim that may be made by its manufacturer, is not guaranteed or endorsed by the publisher.

References

1. Sadler J. Biochemistry and genetics of von Willebrand factor. *Annu Rev Biochem.* (1998) 67:395–424. doi: 10.1146/annurev.biochem.67.1.395

2. Schneider S, Nuschele S, Wixforth A, Gorzelanny C, Alexander-Katz A, Netz R, et al. Shear-induced unfolding triggers adhesion of von Willebrand factor fibers. *Proc Natl Acad Sci USA.* (2007) 104:7899–903. doi: 10.1073/pnas.0608422104

3. Springer T. von Willebrand factor, Jedi knight of the bloodstream. *Blood.* (2014) 124:1412–25. doi: 10.1182/blood-2014-05-378638

4. Ruggeri Z. von Willebrand factor. *J Clin Invest.* (1997) 99:559–64. doi: 10.1172/JCI119195

5. Zhang Q, Zhou Y, Zhang C, Zhang X, Lu C, Springer T. Structural specializations of A2, a force-sensing domain in the ultralarge vascular protein von Willebrand factor. *Proc Natl Acad Sci USA.* (2009) 106:9226–31. doi: 10.1073/pnas.0903679106

6. Stockschlaeder M, Schneppenheim R, Budde U. Update on von Willebrand factor multimers: focus on high-molecular-weight multimers and their role in hemostasis. *Blood Coagul Fibrinolysis.* (2014) 25:206–16. doi: 10.1097/MBC.0000000000000065

7. Zhou Y, Eng E, Zhu J, Lu C, Walz T, Springer T. Sequence and structure relationships within von Willebrand factor. *Blood.* (2012) 120:449–58. doi: 10.1182/blood-2012-01-405134

8. Chen J, Chung D. Inflammation, von Willebrand factor, and ADAMTS13. *Blood.* (2018) 132:141–7. doi: 10.1182/blood-2018-02-769000

9. Wijeratne S, Botello E, Yeh H, Zhou Z, Bergeron A, Frey E, et al. Mechanical activation of a multimeric adhesive protein through domain conformational change. *Phys Rev Lett.* (2013) 110:108102. doi: 10.1103/PhysRevLett.110.108102

10. Blair P, Flaumenhaft R. Platelet α-granules: basic biology and clinical correlates. *Blood Rev.* (2009) 23:177–89. doi: 10.1016/j.blre.2009.04.001

11. Lenting P, Christophe O, Denis C. von Willebrand factor biosynthesis, secretion, and clearance: connecting the far ends. *Blood.* (2015) 125:2019–28. doi: 10.1182/blood-2014-06-528406

12. Rana A, Westein E, Niego B, Hagemeyer C. Shear-dependent platelet aggregation: mechanisms and therapeutic opportunities. *Front Cardiovasc Med.* (2019) 6:141. doi: 10.3389/fcvm.2019.00141

13. Zheng Y, Chen J, López J. Flow-driven assembly of VWF fibres and webs in in vitro microvessels. *Nat Commun.* (2015) 6:7858. doi: 10.1038/ncomms8858

14. Crawley J, de Groot R, Xiang Y, Luken B, Lane D. Unraveling the scissile bond: how ADAMTS13 recognizes and cleaves von Willebrand factor. *Blood.* (2011) 118:3212–21. doi: 10.1182/blood-2011-02-306597

15. Mannucci P, Capoferri C, Canciani M. Plasma levels of von Willebrand factor regulate ADAMTS-13, its major cleaving protease: von Willebrand factor regulates ADAMTS-13. *Br J Haematol.* (2004) 126:213–8. doi: 10.1111/j.1365-2141.2004.05009.x

16. Pendu R, Terraube V, Christophe O, Gahmberg C, de Groot P, Lenting P, et al. P-selectin glycoprotein ligand 1 and β2-integrins cooperate in the adhesion of leukocytes to von Willebrand factor. *Blood.* (2006) 108:3746–52. doi: 10.1182/blood-2006-03-010322

17. Smith L. Laboratory diagnosis of von Willebrand disease. *Clin Lab Sci.* (2017) 30:65–74. doi: 10.29074/ascls.30.2.65

18. Federici A. Acquired von Willebrand syndrome: is it an extremely rare disorder or do we see only the tip of the iceberg? *J Thromb Haemost.* (2008) 6:565–8. doi: 10.1111/j.1538-7836.2008.02917.x

19. Rizzo C, Rizzo S. Thrombotic thrombocytopenic purpura: a review of the literature in the light of our experience with plasma exchange. *Blood Transfus.* (2012) 10:521–32. doi: 10.2450/2012.0122-11

20. Kramer M, Rittersma S, de Winter R, Ladich E, Fowler D, Liang Y, et al. Relationship of thrombus healing to underlying plaque morphology in sudden coronary death. *J Am Coll Cardiol.* (2010) 55:122–32. doi: 10.1016/j.jacc.2009.09.007

21. James P, Connell N, Ameer B, Di Paola J, Eikenboom J, Giraud N, et al. ASH ISTH NHF WFH 2021 guidelines on the diagnosis of von Willebrand disease. *Blood Adv.* (2021) 5:280–300. doi: 10.1182/bloodadvances.2020003265

22. Ng C, Motto D, Di Paola J. Diagnostic approach to von Willebrand disease. *Blood.* (2015) 125:2029–37. doi: 10.1182/blood-2014-08-528398

23. Franchini M, Capra F, Targher G, Montagnana M, Lippi G. Relationship between ABO blood group and von Willebrand factor levels: from biology to clinical implications. *Thrombosis J.* (2007) 5:14. doi: 10.1186/1477-9560-5-14

24. Roberts J, Flood V. Laboratory diagnosis of von Willebrand disease. *Int J Lab Hem.* (2015) 37:11–7. doi: 10.1111/ijlh.12345

25. Jager A, van Hinsbergh V, Kostense P, Emeis J, Yudkin J, Nijpels G, et al. von Willebrand factor, C-reactive protein, and 5-year mortality in diabetic and nondiabetic subjects: the Hoorn study. *Arterioscler Thromb Vasc Biol.* (1999) 19:3071–8. doi: 10.1161/01.ATV.19.12.3071

26. Budde U, Schneppenheim R. von Willebrand factor and von Willebrand disease. *Rev Clin Exp Hematol.* (2001) 5:335–68. doi: 10.1046/j.1468-0734.2001.00048.x

27. Gill J, Endres-Brooks J, Bauer P, Marks W, Montgomery R. The effect of ABO blood group on the diagnosis of von Willebrand disease. *Blood.* (1987) 69:1691–5.

28. Moeller A, Weippert-Kretschmer M, Prinz H, Kretschmer V. Influence of ABO blood groups on primary hemostasis. *Transfusion.* (2001) 41:56–60. doi: 10.1046/j.1537-2995.2001.41010056.x

29. Akin M, Balkan C, Karapinar D, Kavakli K. The influence of the ABO blood type on the distribution of von Willebrand factor in healthy children with no bleeding symptoms. *Clin Appl Thromb Hemost.* (2012) 18:316–9. doi: 10.1177/1076029611422364

30. Budde U, Pieconka A, Will K, Schneppenheim R. Laboratory testing for von Willebrand disease: contribution of multimer analysis to diagnosis and classification. *Semin Thromb Hemost.* (2006) 32:514–21. doi: 10.1055/s-2006-947866

31. Harrison P. The role of PFA-100R testing in the investigation and management of haemostatic defects in children and adults. *Br J Haematol.* (2005) 130:3–10. doi: 10.1111/j.1365-2141.2005.05511.x

32. Carabello B. Introduction to aortic stenosis. *Circ Res.* (2013) 113:179–85. doi: 10.1161/CIRCRESAHA.113.300156

33. Heyde E. Gastrointestinal bleeding in aortic stenosis. *N Engl J Med.* (1958) 259:196–196. doi: 10.1056/NEJM195807242590416

34. Warkentin T, Morgan D, Moore J. Aortic stenosis and bleeding gastrointestinal angiodysplasia: is acquired von Willebrand's disease the link? *Lancet.* (1992) 340:35–7. doi: 10.1016/0140-6736(92)92434-H

35. Warkentin T, Moore J, Morgan D. Gastrointestinal angiodysplasia and aortic stenosis. *N Engl J Med.* (2002) 347:858–9. doi: 10.1056/NEJM200209123471122

36. Frank R, Lanzmich R, Haager P, Budde U. Severe aortic valve stenosis: sustained cure of acquired von Willebrand syndrome after surgical valve replacement. *Clin Appl Thromb Hemost.* (2017) 23:229–34. doi: 10.1177/1076029616660759

37. Miller L. The development of the von Willebrand syndrome with the use of continuous flow left ventricular assist devices. *J Am Coll Cardiol.* (2010) 56:1214–5. doi: 10.1016/j.jacc.2010.06.009

38. Van Belle E, Vincent F, Rauch A, Casari C, Jeanpierre E, Loobuyck V, et al. von Willebrand factor and management of heart valve disease. *J Am Coll Cardiol.* (2019) 73:1078–88. doi: 10.1016/j.jacc.2018.12.045

39. Yasar S, Abdullah O, Fay W, Balla S. Von Willebrand factor revisited. *J Interven Cardiol.* (2018) 31:360–7. doi: 10.1111/joic.12478

40. Van Belle E, Rauch A, Vincent F, Robin E, Kibler M, Labreuche J, et al. von Willebrand factor multimers during transcatheter aortic-valve replacement. *N Engl J Med.* (2016) 375:335–44. doi: 10.1056/NEJMoa1505643

41. Panzer S, Eslam R, Schneller A, Kaider A, Koren D, Eichelberger B, et al. Loss of high-molecular-weight von Willebrand factor multimers mainly affects platelet aggregation in patients with aortic stenosis. *Thromb Haemost.* (2010) 103:408–14. doi: 10.1160/TH09-06-0391

42. Vincentelli A, Susen S, Le Tourneau T, Six I, Fabre O, Juthier F, et al. Acquired von Willebrand syndrome in aortic stenosis. *N Engl J Med.* (2003) 349:343–9. doi: 10.1056/NEJMoa022831

43. Blackshear J, Wysokinska E, Safford R, Thomas C, Shapiro B, Ung S, et al. Shear stress-associated acquired von Willebrand syndrome in patients with mitral regurgitation. *J Thromb Haemost.* (2014) 12:1966–74. doi: 10.1111/jth.12734

44. Solomon C, Budde U, Schneppenheim S, Czaja E, Hagl C, Schoechl H, et al. Acquired type 2A von Willebrand syndrome caused by aortic valve disease corrects during valve surgery. *Br J Anaesth.* (2011) 106:494–500. doi: 10.1093/bja/aeq413

45. Susen S, Vincentelli A, Le Tourneau T, Caron C, Zawadzki C, Prat A, et al. Severe aortic and mitral valve regurgitation are associated with von Willebrand factor defect. *Blood.* (2005) 106:1790–1790. doi: 10.1182/blood.V106.11.1790.1790

46. Nishimura R, Seggewiss H, Schaff H. Hypertrophic obstructive cardiomyopathy: surgical myectomy and septal ablation. *Circ Res.* (2017) 121:771–83. doi: 10.1161/CIRCRESAHA.116.309348

47. Blackshear J, Schaff H, Ommen S, Chen D, Nichols W. Hypertrophic obstructive cardiomyopathy, bleeding history, and acquired von Willebrand syndrome: response to septal myectomy. *Mayo Clin Proc.* (2011) 86:219–24. doi: 10.4065/mcp.2010.0309

48. Le Tourneau T, Susen S, Caron C, Millaire A, Maréchaux S, Polge A, et al. Functional impairment of von Willebrand factor in hypertrophic cardiomyopathy: relation to rest and exercise obstruction. *Circulation.* (2008) 118:1550–7. doi: 10.1161/CIRCULATIONAHA.108.786681

49. Han J, Acker M, Atluri P. Left Ventricular assist devices: synergistic model between technology and medicine. *Circulation.* (2018) 138:2841–51. doi: 10.1161/CIRCULATIONAHA.118.035566

50. Davis M, Haglund N, Tricarico N, Matafonov A, Gailani D, Maltais S. Immediate recovery of acquired von Willebrand syndrome after left ventricular assist device explantation: implications for heart transplantation. *ASAIO J.* (2015) 61:e1–4. doi: 10.1097/MAT.0000000000000157

51. Soehnlein O, Libby P. Targeting inflammation in atherosclerosis–from experimental insights to the clinic. *Nat Rev Drug Discov.* (2021) 20:589–610. doi: 10.1038/s41573-021-00198-1

52. Mushenkova N, Bezsonov E, Orekhova V, Popkova T, Starodubova A, Orekhov A. Recognition of oxidized lipids by macrophages and its role in atherosclerosis development. *Biomedicines.* (2021) 9:915. doi: 10.3390/biomedicines9080915

53. Bezsonov E, Sobenin I, Orekhov A. Immunopathology of atherosclerosis and related diseases: focus on molecular biology. *Int J Mol Sci.* (2021) 22:4080. doi: 10.3390/ijms22084080

54. Severino P, D'Amato A, Pucci M, Infusino F, Adamo F, Birtolo L, et al. Ischemic heart disease pathophysiology paradigms overview: from plaque activation to microvascular dysfunction. *Int J Mol Sci.* (2020) 21:8118. doi: 10.3390/ijms21218118

55. Kawecki C, Lenting P, Denis C. von Willebrand factor and inflammation. *J Thromb Haemost.* (2017) 15:1285–94. doi: 10.1111/jth.13696

56. Seaman C, Yabes J, Comer D, Ragni M. Does deficiency of von Willebrand factor protect against cardiovascular disease? Analysis of a national discharge register. *J Thromb Haemost.* (2015) 13:1999–2003. doi: 10.1111/jth.13142

57. Xu A, Xu R, Lu C, Yao M, Zhao W, Fu X, et al. Correlation of von Willebrand factor gene polymorphism and coronary heart disease. *Mol Med Rep.* (2012) 6:1107–10. doi: 10.3892/mmr.2012.1037

58. Kaikita K, Soejima K, Matsukawa M, Nakagaki T, Ogawa H. Reduced von Willebrand factor-cleaving protease (ADAMTS13) activity in acute myocardial infarction. *J Thromb Haemost.* (2006) 4:2490–3. doi: 10.1111/j.1538-7836.2006.02161.x

59. Rutten B, Maseri A, Cianflone D, Laricchia A, Cristell N, Durante A, et al. Plasma levels of active von Willebrand factor are increased in patients with first ST-segment elevation myocardial infarction: a multicenter and multiethnic study. *Eur Heart J Acute Cardiovasc Care.* (2015) 4:64–74. doi: 10.1177/2048872614534388

60. Chion C, Doggen C, Crawley J, Lane D, Rosendaal F. ADAMTS13 and von Willebrand factor and the risk of myocardial infarction in men. *Blood.* (2007) 109:1998–2000. doi: 10.1182/blood-2006-07-038166

61. Li Y, Li L, Dong F, Guo L, Hou Y, Hu H, et al. Plasma von Willebrand factor level is transiently elevated in a rat model of acute myocardial infarction. *Exp Ther Med.* (2015) 10:1743–9. doi: 10.3892/etm.2015.2721

62. Whincup P, Danesh J, Walker M, Lennon L, Thompson A, Appleby P, et al. von Willebrand factor and coronary heart disease. Prospective study and meta-analysis. *Eur Heart J.* (2002) 23:1764–70. doi: 10.1053/euhj.2001.3237

63. Morange P, Simon C, Alessi M, Luc G, Arveiler D, Ferrieres J, et al. Endothelial cell markers and the risk of coronary heart disease: the prospective epidemiological study of myocardial infarction (PRIME) study. *Circulation.* (2004) 109:1343–8. doi: 10.1161/01.CIR.0000120705.55512.EC

64. Willeit P, Thompson A, Aspelund T, Rumley A, Eiriksdottir G, Lowe G, et al. Hemostatic factors and risk of coronary heart disease in general populations: new prospective study and updated meta-analyses. *PLoS One.* (2013) 8:e55175. doi: 10.1371/journal.pone.0055175

65. Folsom A, Wu K, Rosamond W, Sharrett A, Chambless L. Prospective study of hemostatic factors and incidence of coronary heart disease: the atherosclerosis risk in communities (ARIC) study. *Circulation.* (1997) 96:1102–8. doi: 10.1161/01.CIR.96.4.1102

66. Rumley A, Lowe G, Sweetnam P, Yarnell J, Ford R. Factor VIII, von Willebrand factor and the risk of major ischaemic heart disease in the Caerphilly heart study. *Br J Haematol.* (1999) 105:110–6.

67. Thögersen A, Jansson J, Boman K, Nilsson T, Weinehall L, Huhtasaari F, et al. High plasminogen activator inhibitor and tissue plasminogen activator levels in plasma precede a first acute myocardial infarction in both men and women: evidence for the fibrinolytic system as an independent primary risk factor. *Circulation.* (1998) 98:2241–7. doi: 10.1161/01.CIR.98.21.2241

68. Smith F, Lee A, Fowkes F, Price J, Rumley A, Lowe G. Hemostatic factors as predictors of ischemic heart disease and stroke in the Edinburgh artery study. *Arterioscler Thromb Vasc Biol.* (1997) 17:3321–5. doi: 10.1161/01.ATV.17.11.3321

69. Vischer U. von Willebrand factor, endothelial dysfunction, and cardiovascular disease. *J Thromb Haemost.* (2006) 4:1186–93. doi: 10.1111/j.1538-7836.2006.01949.x

70. Thompson S, Kienast J, Pyke S, Haverkate F, van de Loo J. Hemostatic factors and the risk of myocardial infarction or sudden death in patients with angina pectoris. *N Engl J Med.* (1995) 332:635–41. doi: 10.1056/NEJM199503093321003

71. Ray K, Morrow D, Gibson C, Murphy S, Antman E, Braunwald E. Predictors of the rise in vWF after ST elevation myocardial infarction: implications for treatment strategies and clinical outcome. *Eur Heart J.* (2005) 26:440–6. doi: 10.1093/eurheartj/ehi104

72. Jansson J, Nilsson T, Johnson O. von Willebrand factor in plasma: a novel risk factor for recurrent myocardial infarction and death. *Heart.* (1991) 66:351–5. doi: 10.1136/hrt.66.5.351

73. Danesh J, Wheeler J, Hirschfield G, Eda S, Eiriksdottir G, Rumley A, et al. Reactive protein and other circulating markers of inflammation in the prediction of coronary heart disease. *N Engl J Med.* (2004) 350:1387–97. doi: 10.1056/NEJMoa032804

74. Warlo E, Pettersen A, Arnesen H, Seljeflot I. vWF/ADAMTS13 is associated with on-aspirin residual platelet reactivity and clinical outcome in patients with stable coronary artery disease. *Thrombosis J.* (2017) 15:28. doi: 10.1186/s12959-017-0151-3

75. Price J, Mowbray P, Lee A, Rumpley A, Lowe G, Fowkes F. Relationship between smoking and cardiovascular risk factors in the development of peripheral arterial disease and coronary artery disease; Edinburgh artery study. *Eur Heart J.* (1999) 20:344–53. doi: 10.1053/euhj.1998.1194

76. Stehouwer C, Zeldenrust G, den Ottolander G, Hackeng W, Donker A, Nauta J. Urinary albumin excretion, cardiovascular disease, and endothelial dysfunction in non-insulin-dependent diabetes mellitus. *Lancet.* (1992) 340:319–23. doi: 10.1016/0140-6736(92)91401-S

77. Lip G, Blann A, Jones A, Lip P, Beevers D. Relation of endothelium, thrombogenesis, and hemorheology in systemic hypertension to ethnicity and left ventricular hypertrophy. *Am J Cardiol.* (1997) 80:1566–71. doi: 10.1016/S0002-9149(97)00749-2

78. Lee K, Blann A, Lip G. High pulse pressure and nondipping circadian blood pressure in patients with coronary artery disease: relationship to thrombogenesis and endothelial damage/dysfunction. *Am J Hypertens.* (2005) 18:104–15. doi: 10.1016/j.amjhyper.2004.09.003

79. Kaufmann J, Oksche A, Wollheim C, Günther G, Rosenthal W, Vischer U. Vasopressin-induced von Willebrand factor secretion from endothelial cells involves V2 receptors and cAMP. *J Clin Invest.* (2000) 106:107–16. doi: 10.1172/JCI9516

80. Montalescot G, Philippe F, Ankri A, Vicaut E, Bearez E, Poulard J, et al. Early Increase of von Willebrand factor predicts adverse outcome in unstable coronary artery disease: beneficial effects of enoxaparin. *Circulation.* (1998) 98:294–9. doi: 10.1161/01.CIR.98.4.294

81. Bonetti P, Lerman L, Lerman A. Endothelial dysfunction: a marker of atherosclerotic risk. *Arterioscler Thromb Vasc Biol.* (2003) 23:168–75. doi: 10.1161/01.ATV.0000051384.43104.FC

82. Blann A, Herrick A, Jayson M. Altered levels of soluble adhesion molecules in rheumatoid arthritis, vasculitis and systemic sclerosis. *Rheumatology.* (1995) 34:814–9. doi: 10.1093/rheumatology/34.9.814

83. Nossent J, Raymond W, Eilertsen G. Increased von Willebrand factor levels in patients with systemic lupus erythematosus reflect inflammation rather than increased propensity for platelet activation. *Lupus Sci Med.* (2016) 3:e000162. doi: 10.1136/lupus-2016-000162

84. Kefer J, Galanti L, Desmet S, Deneys V, Hanet C. Time course of release of inflammatory markers after coronary stenting: comparison between bare metal stent and sirolimus-eluting stent. *Coron Artery Dis.* (2005) 16:505–9. doi: 10.1097/00019501-200512000-00009

85. Pottinger B, Read R, Paleolog E, Higgins P, Pearson J. von Willebrand factor is an acute phase reactant in man. *Thromb Res.* (1989) 53:387–94. doi: 10.1016/0049-3848(89)90317-4

86. Gabbasov Z, Avtaeva Y, Melnikov I, Okhota S, Caprnda M, Mozos I, et al. Kinetics of platelet adhesion to a fibrinogen-coated surface in whole blood under flow conditions. *J Clin Lab Anal.* (2021) 35:e23939. doi: 10.1002/jcla.23939

87. Schoeman R, Lehmann M, Neeves K. Flow chamber and microfluidic approaches for measuring thrombus formation in genetic bleeding disorders. *Platelets.* (2017) 28:463–71. doi: 10.1080/09537104.2017.1306042

88. Brazilek R, Tovar-Lopez F, Wong A, Tran H, Davis A, McFadyen J, et al. Application of a strain rate gradient microfluidic device to von Willebrand's disease screening. *Lab Chip.* (2017) 17:2595–608. doi: 10.1039/C7LC00498B

89. Kim D, Ashworth K, Di Paola J, Ku D. Platelet α-granules are required for occlusive high-shear-rate thrombosis. *Blood Adv.* (2020) 4:3258–67. doi: 10.1182/bloodadvances.2020002117

90. Hosokawa K, Ohnishi T, Kondo T, Fukasawa M, Koide T, Maruyama I, et al. A novel automated microchip flow-chamber system to quantitatively evaluate thrombus formation and antithrombotic agents under blood flow conditions: thrombus formation and antithrombotic interventions under flow. *J Thromb Haemost.* (2011) 9:2029–37. doi: 10.1111/j.1538-7836.2011.04464.x

91. Sobel M, McNeill P, Carlson P, Kermode J, Adelman B, Conroy R, et al. Heparin inhibition of von Willebrand factor-dependent platelet function in vitro and in vivo. *J Clin Invest.* (1991) 87:1787–93. doi: 10.1172/JCI115198

92. Kageyama S, Matsushita J, Yamamoto H. Effect of a humanized monoclonal antibody to von Willebrand factor in a canine model of coronary arterial thrombosis. *Eur J Pharmacol.* (2002) 443:143–9. doi: 10.1016/S0014-2999(02)01590-X

93. Kageyama S, Yamamoto H, Nakazawa H, Yoshimoto R. Anti-human vWF monoclonal antibody, AJvW-2 fab, inhibits repetitive coronary artery thrombosis without bleeding time prolongation in dogs. *Thromb Res.* (2001) 101:395–404. doi: 10.1016/S0049-3848(00)00430-8

94. Eto K, Isshiki T, Yamamoto H, Takeshita S, Ochiai M, Yokoyama N, et al. AJvW-2, an anti-vWF monoclonal antibody, inhibits enhanced platelet aggregation induced by high shear stress in platelet-rich plasma from patients with acute coronary syndromes. *Arterioscler Thromb Vasc Biol.* (1999) 19:877–82. doi: 10.1161/01.ATV.19.4.877

95. Gilbert J, DeFeo-Fraulini T, Hutabarat R, Horvath C, Merlino P, Marsh H, et al. First-in-human evaluation of anti–von Willebrand factor therapeutic aptamer ARC1779 in healthy volunteers. *Circulation.* (2007) 116:2678–86. doi: 10.1161/CIRCULATIONAHA.107.724864

96. Markus H, McCollum C, Imray C, Goulder M, Gilbert J, King A. The von Willebrand inhibitor ARC1779 reduces cerebral embolization after carotid endarterectomy: a randomized trial. *Stroke.* (2011) 42:2149–53. doi: 10.1161/STROKEAHA.111.616649

97. Sakai K, Someya T, Harada K, Yagi H, Matsui T, Matsumoto M. Novel aptamer to von Willebrand factor A1 domain (TAGX-0004) shows total inhibition of thrombus formation superior to ARC1779 and comparable to caplacizumab. *Haematologica.* (2019) 105:2631–8. doi: 10.3324/haematol.2019.235549

98. Kovacevic K, Buchtele N, Schoergenhofer C, Derhaschnig U, Gelbenegger G, Brostjan C, et al. The aptamer BT200 effectively inhibits von Willebrand factor (VWF) dependent platelet function after stimulated VWF release by desmopressin or endotoxin. *Sci Rep.* (2020) 10:11180. doi: 10.1038/s41598-020-68125-9

99. Kovacevic K, Jilma B, Zhu S, Gilbert J, Winter M, Toma A, et al. von Willebrand factor predicts mortality in ACS patients treated with potent P2Y12 antagonists and is inhibited by aptamer BT200 ex vivo. *Thromb Haemost.* (2020) 120:1282–90. doi: 10.1055/s-0040-1713888

100. Nimjee S, Dornbos D, Pitoc G, Wheeler D, Layzer J, Venetos N, et al. Preclinical development of a vWF aptamer to limit thrombosis and engender arterial recanalization of occluded vessels. *Mol Ther.* (2019) 27:1228–41. doi: 10.1016/j.ymthe.2019.03.016

101. Li T, Fan M, Hou S, Li X, Barry D, Jin H, et al. A novel snake venom-derived GPIb antagonist, anfibatide, protects mice from acute experimental ischaemic stroke and reperfusion injury: anfibatide protects mice from ischaemic stroke and reperfusion injury. *Br J Pharmacol.* (2015) 172:3904–16. doi: 10.1111/bph.13178

102. Chu W, Sun X, Zhu X, Zhao Y, Zhang J, Kong Q, et al. Blockade of platelet glycoprotein receptor Ib ameliorates blood-brain barrier disruption following ischemic stroke via Epac pathway. *Biomed Pharmacother.* (2021) 140:111698. doi: 10.1016/j.biopha.2021.111698

103. Li B, Dai X, Xu X, Adili R, Neves M, Lei X, et al. In vitro assessment and phase I randomized clinical trial of anfibatide a snake venom derived anti-thrombotic agent targeting human platelet GPIbα. *Sci Rep.* (2021) 11:11663. doi: 10.1038/s41598-021-91165-8

104. Zheng B, Li J, Jiang J, Xiang D, Chen Y, Yu Z, et al. Safety and efficacy of a platelet glycoprotein Ib inhibitor for patients with non-ST segment elevation myocardial infarction: a phase Ib/IIa study. *Pharmacotherapy.* (2021) 41:828–36. doi: 10.1002/phar.2620

105. Scully M, Cataland S, Peyvandi F, Coppo P, Knöbl P, Kremer Hovinga J, et al. Caplacizumab treatment for acquired thrombotic thrombocytopenic purpura. *N Engl J Med.* (2019) 380:335–46. doi: 10.1056/NEJMoa1806311

106. van Loon J, de Jaegere P, van Vliet H, de Maat M, de Groot P, Simoons M, et al. The in vitro effect of the new antithrombotic drug candidate ALX-0081 on blood samples of patients undergoing percutaneous coronary intervention. *Thromb Haemost.* (2011) 106:165–71. doi: 10.1160/TH10-12-0804

107. Bartunek J, Barbato E, Vercruysse K, Duby C, Wijns W, Heyndrickx G, et al. Abstract 15084: safety and efficacy of anti-von Willebrand factor nanobody® ALX-0081 in stable angina patients undergoing percutaneous coronary intervention. *Circulation.* (2010) 122:A15084.

108. Bartunek J, Barbato E, Heyndrickx G, Vanderheyden M, Wijns W, Holz J. Novel antiplatelet agents: ALX-0081, a nanobody directed towards von Willebrand factor. *J Cardiovasc Trans Res.* (2013) 6:355–63. doi: 10.1007/s12265-012-9435-y

109. Witsch T, Martinod K, Sorvillo N, Portier I, De Meyer S, Wagner D. Recombinant human ADAMTS13 treatment improves myocardial remodeling and functionality after pressure overload injury in mice. *J Am Heart Assoc.* (2018) 7:e007004. doi: 10.1161/JAHA.117.007004

110. De Meyer S, Savchenko A, Haas M, Schatzberg D, Carroll M, Schiviz A, et al. Protective anti-inflammatory effect of ADAMTS13 on myocardial ischemia/reperfusion injury in mice. *Blood.* (2012) 120:5217–23. doi: 10.1182/blood-2012-06-439935

111. Goebel S, Li Z, Vogelmann J, Holthoff H, Degen H, Hermann D, et al. The GPVI-Fc fusion protein revacept improves cerebral infarct volume and functional outcome in stroke. *PLoS One.* (2013) 8:e66960. doi: 10.1371/journal.pone.0066960

112. Mayer K, Hein-Rothweiler R, Schüpke S, Janisch M, Bernlochner I, Ndrepepa G, et al. Efficacy and safety of revacept, a novel lesion-directed competitive antagonist to platelet glycoprotein VI, in patients undergoing elective percutaneous coronary intervention for stable ischemic heart disease: the randomized, double-blind, placebo-controlled ISAR-PLASTER phase 2 trial. *JAMA Cardiol.* (2021) 6:753. doi: 10.1001/jamacardio.2021.0475

113. Gröschel K, Uphaus T, Loftus I, Poppert H, Diener H, Zobel J, et al. Revacept, an inhibitor of platelet adhesion in symptomatic carotid artery stenosis: design and rationale of a randomized phase II clinical trial. *TH Open.* (2020) 04:e393–9. doi: 10.1055/s-0040-1721078

114. de Maat S, Clark C, Barendrecht A, Smits S, van Kleef N, El Otmani H, et al. Microlyse: a thrombolytic agent that targets VWF for clearance of microvascular thrombosis. *Blood.* (2022) 139:597–607. doi: 10.1182/blood.2021011776

Check for updates

Paradoxical reduction of plasma lipids and atherosclerosis in mice with adenine-induced chronic kidney disease and hypercholesterolemia

Mugdha V. Padalkar[1], Alexandra H. Tsivitis[1], Ylona Gelfman[1], Mariya Kasiyanyk[1], Neil Kaungumpillil[1], Danyang Ma[1], Michael Gao[1], Kelly A. Borges[1], Puneet Dhaliwal[1], Saud Nasruddin[1], Sruthi Saji[1], Hina Gilani[1], Eric J. Schram[1], Mohnish Singh[1], Maria M. Plummer[2] and Olga V. Savinova[1]*

[1]Department of Biomedical Sciences, New York Institute of Technology College of Osteopathic Medicine, Old Westbury, NY, United States, [2]Department of Clinical Specialties, New York Institute of Technology College of Osteopathic Medicine, Old Westbury, NY, United States

Background: Atherosclerotic cardiovascular disease is prevalent among patients with chronic kidney disease (CKD). In this study, we initially aimed to test whether vascular calcification associated with CKD can worsen atherosclerosis. However, a paradoxical finding emerged from attempting to test this hypothesis in a mouse model of adenine-induced CKD.

Methods: We combined adenine-induced CKD and diet-induced atherosclerosis in mice with a mutation in the low-density lipoprotein receptor gene. In the first study, mice were co-treated with 0.2% adenine in a western diet for 8 weeks to induce CKD and atherosclerosis simultaneously. In the second study, mice were pre-treated with adenine in a regular diet for 8 weeks, followed by a western diet for another 8 weeks.

Results: Co-treatment with adenine and a western diet resulted in a reduction of plasma triglycerides and cholesterol, liver lipid contents, and atherosclerosis in co-treated mice when compared with the western-only group, despite a fully penetrant CKD phenotype developed in response to adenine. In the two-step model, renal tubulointerstitial damage and polyuria persisted after the discontinuation of adenine in the adenine-pre-treated mice. The mice, however, had similar plasma triglycerides, cholesterol, liver lipid contents, and aortic root atherosclerosis after being fed a western diet, irrespective of adenine pre-treatment. Unexpectedly, adenine pre-treated mice consumed twice the calories from the diet as those not pre-treated without showing an increase in body weight.

Conclusion: The adenine-induced CKD model does not recapitulate accelerated atherosclerosis, limiting its use in pre-clinical studies. The results indicate that excessive adenine intake impacts lipid metabolism.

KEYWORDS

triglycerides, cholesterol, chronic kidney disease, mouse model, atherosclerosis

1. Introduction

Chronic kidney disease (CKD) confers an increased risk of mortality from cardiovascular causes, including atherosclerotic cardiovascular disease (ASCVD) (1). CKD is considered a risk-enhancing factor for ASCVD (2, 3). Vascular calcification, another independent predictor of ASCVD used for risk stratification, is prevalent in patients with CKD (4, 5). It is currently unknown whether calcification directly contributes to an increased ASCVD burden or severity in patients with CKD (6). A better understanding of the complex interplay between calcification and atherosclerosis in patients with CKD could help develop new strategies to reduce ASCVD and mortality in these patients (6).

Animal models demonstrate that increased uremic toxins accelerate ASCVD (7). Uremic toxins induce endothelial dysfunction, inflammation, and oxidative stress, promoting atherosclerosis, while premature senescence and cell death contribute to plaque vulnerability (8–11). We hypothesized that a causal relationship exists between calcification and atherosclerosis in CKD and sought to test this hypothesis in an animal model.

Animal models of CKD and atherosclerosis almost exclusively use a 5/6 kidney ablation in mice deficient in the apolipoprotein E (*apoE*) or low-density lipoprotein receptor (*ldlr*) (12–15). The 5/6 nephrectomy model, however, has several limitations, including variable surgical success rate, inter-laboratory variations, and irreversibility of the procedure (16). On the other hand, several recent vascular calcification studies not concerned with atherosclerosis have been conducted using a non-surgical adenine-induced model of CKD (17–20). Excessive oral intake of adenine leads to the accumulation of 2,8-dihydroxyadenine crystals in the renal tubules that cause progressive tubulointerstitial nephropathy (21). Adenine-induced CKD is thought to be reversible, with kidney function fully or partially restored upon discontinuation of adenine treatment (22). The reversibility of the adenine model of CKD might provide an opportunity to study the effects of calcification on the progression of atherosclerosis independently of uremic blood toxins.

In this study, we explored two scenarios. The first experiment involved a concurrent induction of CKD and atherosclerosis by feeding *ldlr* mutant mice with a western diet supplemented with adenine to confirm the interaction between CKD and atherosclerosis. In the second study, CKD was established prior to atherosclerosis. Adenine was used as a pre-treatment and discontinued during a western diet treatment. Unexpectedly, we observed a striking reduction of plasma lipids and atherosclerosis in mice co-treated with adenine and a western diet despite all other manifestations of CKD. The development of atherosclerosis was no longer impeded after the discontinuation of adenine. Although the effect of adenine on lipid metabolism precluded testing of the central hypothesis of this study, the results point to a previously unrecognized mechanism of modulating atherosclerosis.

2. Materials and methods

2.1. Animal studies

Animal studies were approved by the Institutional Animal Care and Use Committee (IACUC) of the New York Institute of Technology College of Osteopathic Medicine (Protocol number 2020-OS-01) and complied with the National Institutes of Health Office of Laboratory Animal Welfare guidelines.

Ldlr mutant mice were initially obtained from the Jackson Laboratory (C57BL/6J-Ldlr^{Hlb301}/J; strain #005061; Bar Harbor, ME, USA) in 2015 and kept in our colony. These mice carry a familial hypercholesterolemia mutation (C699Y) in the *ldlr* gene. At the time of discovery, the mutation was nicknamed "wicked high cholesterol" (*WHC*) (23). We used *WHC* mice in our earlier studies and reported their lipid profiles, atherosclerosis, and vascular calcification phenotypes (24, 25).

Mice were kept under a 12:12-h light/dark cycle with unrestricted access to food and water. A control diet (LabDiet 5001) was obtained from W.F Fisher and Son Inc. (Somerville, NJ, USA); a western diet (TD.88137) was obtained from Envigo (Madison, WI, USA). CKD was induced by adenine (Sigma, cat. #A8626; St. Louis, MO, USA) supplementation in a western diet (experiment 1) or a control diet (experiment 2).

In the first experiment, 24 10-week-old mice (50% males) were divided into two groups. One group was fed a western diet alone (W) for 8 weeks; the other group was fed a western diet supplemented with 0.2% adenine (W + A) for 8 weeks. In the second experiment, 82 10-week-old mice (50% males) were divided into four groups. The first group was fed a control diet for 8 weeks (C) and the second group was fed a control diet supplemented with adenine for 8 weeks (A). Due to high mortality in this experiment, the adenine dose for male mice was adjusted to 0.1%, whereas females received 0.2% adenine supplementation (26). Mice in the remaining two groups were fed a control diet with or without adenine for 8 weeks and then switched to a western diet without adenine supplementation for another 8 weeks (C→W and A→W).

2.2. Blood and urine chemistry

Blood was collected at terminal time points by cardiac puncture. Mice were fasted for 5 h prior to blood collection. Lithium heparin plasma was prepared and kept frozen until the analysis. Total cholesterol, triglycerides, and glucose were measured in whole plasma to evaluate lipid and carbohydrate metabolism. Blood urea nitrogen (BUN), a biomarker of kidney function, along with liver enzymes (indicative of hepatocellular death) alanine aminotransferase (ALT) and aspartate aminotransferase (AST) were measured after clearing the plasma with a Lipoclear reagent (Beckman Coulter, Inc., Brea, CA, USA) to reduce interference from lipemia. Urine samples were collected *via* metabolic cages (Techniplast, West Chester, PA, USA) to calculate 24-h glucose and protein excretion. All reagents were from Pointe Scientific (Lincoln Park, MI, USA) and used according to the manufacturer's instructions. A mouse/rat Cystatin C Quantikine ELISA kit was obtained from R&D Systems (Minneapolis, MN, USA) as another measure of kidney function. Plasma IL-6 and TNF-α were measured using LEGEND MAX^{TM} Mouse IL-6 and TNF-α ELISA kits (San Diego, CA, USA) as biomarkers of systemic inflammation.

2.3. Fecal fat content

Fresh fecal samples were collected after placing a mouse in a clean cage for 15–20 min. Fecal dry weight was determined following
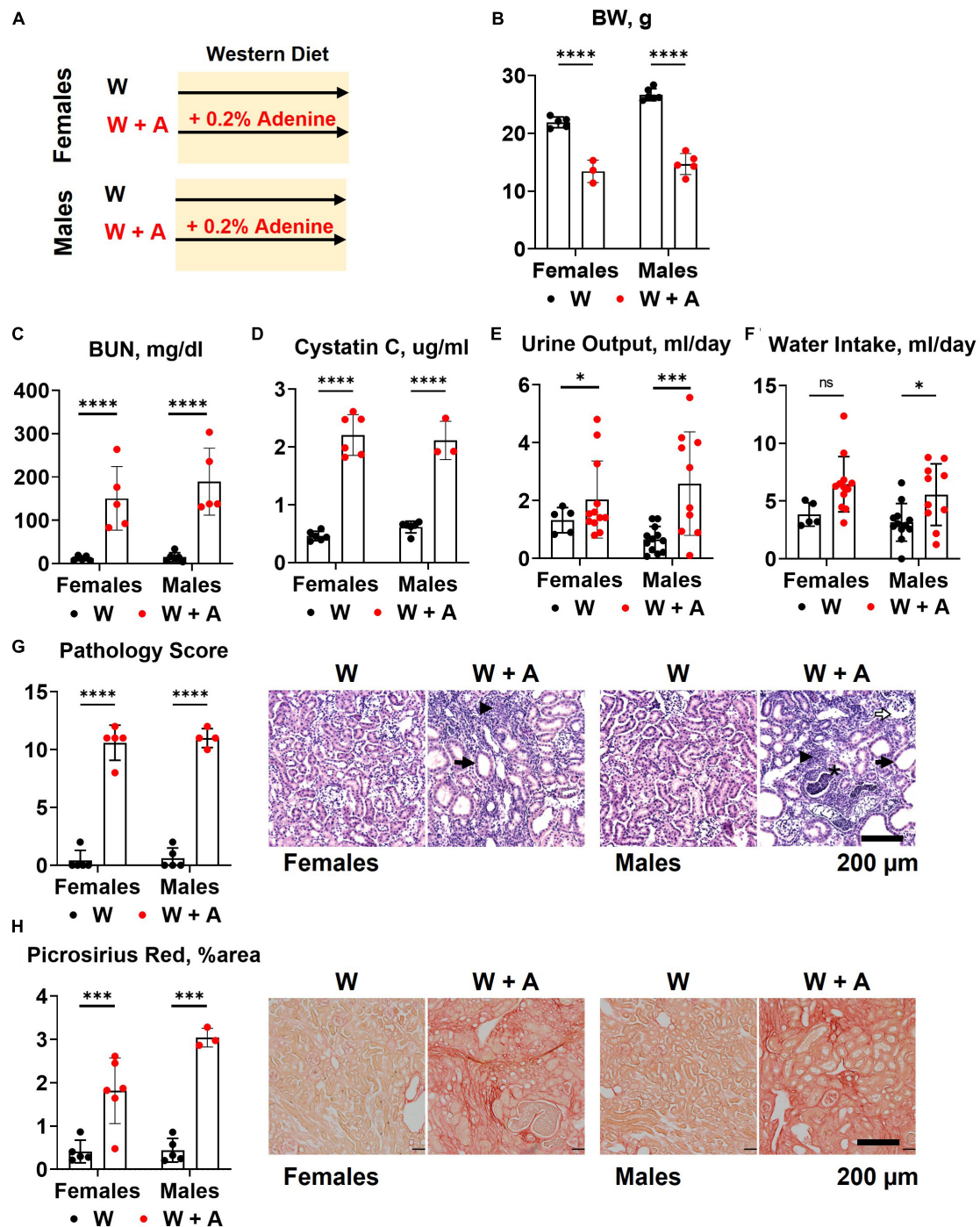
FIGURE 1

Chronic kidney disease in *WHC* mice fed a western diet supplemented with 0.2% adenine. **(A)** Treatment groups: male and female mice (*n* = 6 per group) were treated with a western diet (W) or a western diet supplemented with 0.2% adenine (W + A). **(B)** Body weight (BW). **(C)** Blood urea nitrogen (BUN). **(D)** Plasma Cystatin C. **(E)** 24-h urine output. **(F)** 24-h water intake. **(G)** Renal histology scores and representative images of H&E stained slides; tubular dilatation (arrow), inflammation (arrowhead), pus casts (asterisk), enlarged Bowman's space (open arrow). **(H)** Quantification of kidney fibrosis and representative images of picrosirius red staining. *n* = 4–10 per group; two-way ANOVA; ns, not significant; *$p < 0.05$; ***$p < 0.001$; ****$p < 0.0001$.

an overnight incubation at 42°C, and the samples were rehydrated with an equal volume (v/w) of saline. Lipids were extracted according to the Folch method and reconstituted in 0.1% Triton X-100 in saline. Cholesterol and free (non-esterified) fatty acids (FFA) were determined using Pointe Scientific cholesterol reagents and WAKO non-esterified fatty acids (NEFA) kit (FUJIFILM Medical Systems U.S.A. Inc., Lexington, MA, USA).

2.4. Histology

Tissues were harvested *via* whole-body perfusion and stored in 10% neutral formalin (Sigma, cat. #HT501320; St. Louis, MO, USA). The left kidneys were dissected, and transverse slices were made at the level of the renal pelvis. Cross-sectional slices of the liver (perpendicular to the central vein) were obtained from the medial
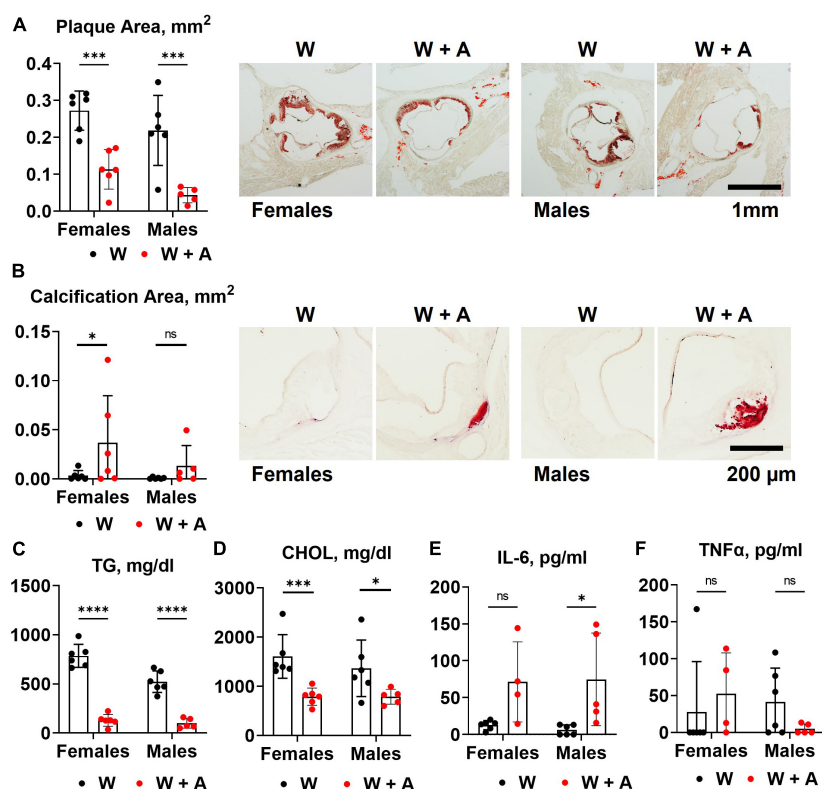
FIGURE 2
Aortic root atherosclerosis, plasma lipids, and inflammatory cytokines in *WHC* mice treated with a western with or without adenine. **(A)** Representative images and quantification of Oil red O staining of the aortic root. **(B)** Representative images and quantification of alizarin red staining of the aortic root. **(C)** Plasma triglycerides (TG). **(D)** Cholesterol (CHOL). **(E)** Interleukin-6 (IL-6). **(F)** Tumor necrosis factor alpha (TNFα). $n = 4–6$ per group; two-way ANOVA; ns, not significant; $*p < 0.05$; $***p < 0.001$; $****p < 0.0001$.
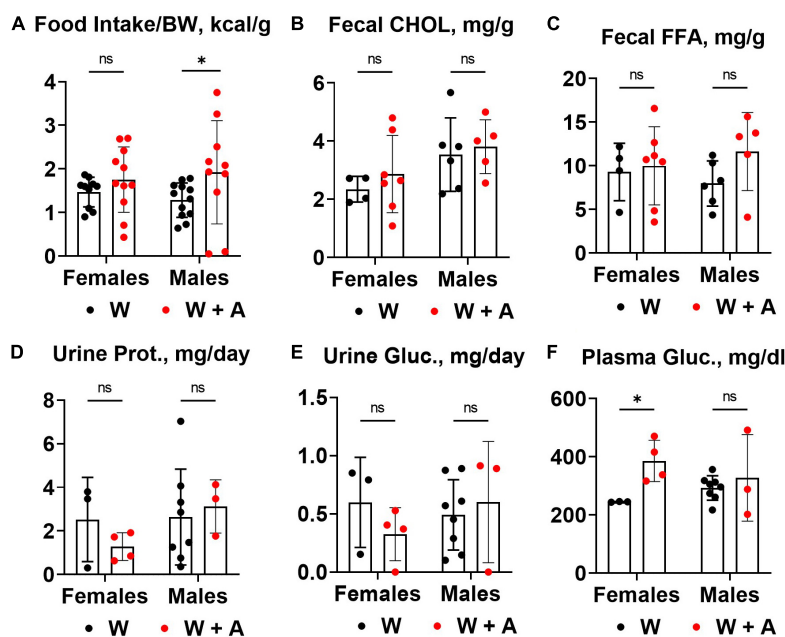

FIGURE 3
Food consumption and macronutrient excretion in feces and urine of WHC mice co-treated with adenine and a western diet. **(A)** Caloric intake per body weight (BW). **(B)** Fecal cholesterol (CHOL) content. **(C)** Fecal free fatty acids (FFA) content. **(D)** 24-h urine protein excretion. **(E)** 24-h urine glucose excretion. **(F)** Plasma glucose concentration. $n = 3–11$ per group; two-way ANOVA; ns, not significant; $*p < 0.05$.
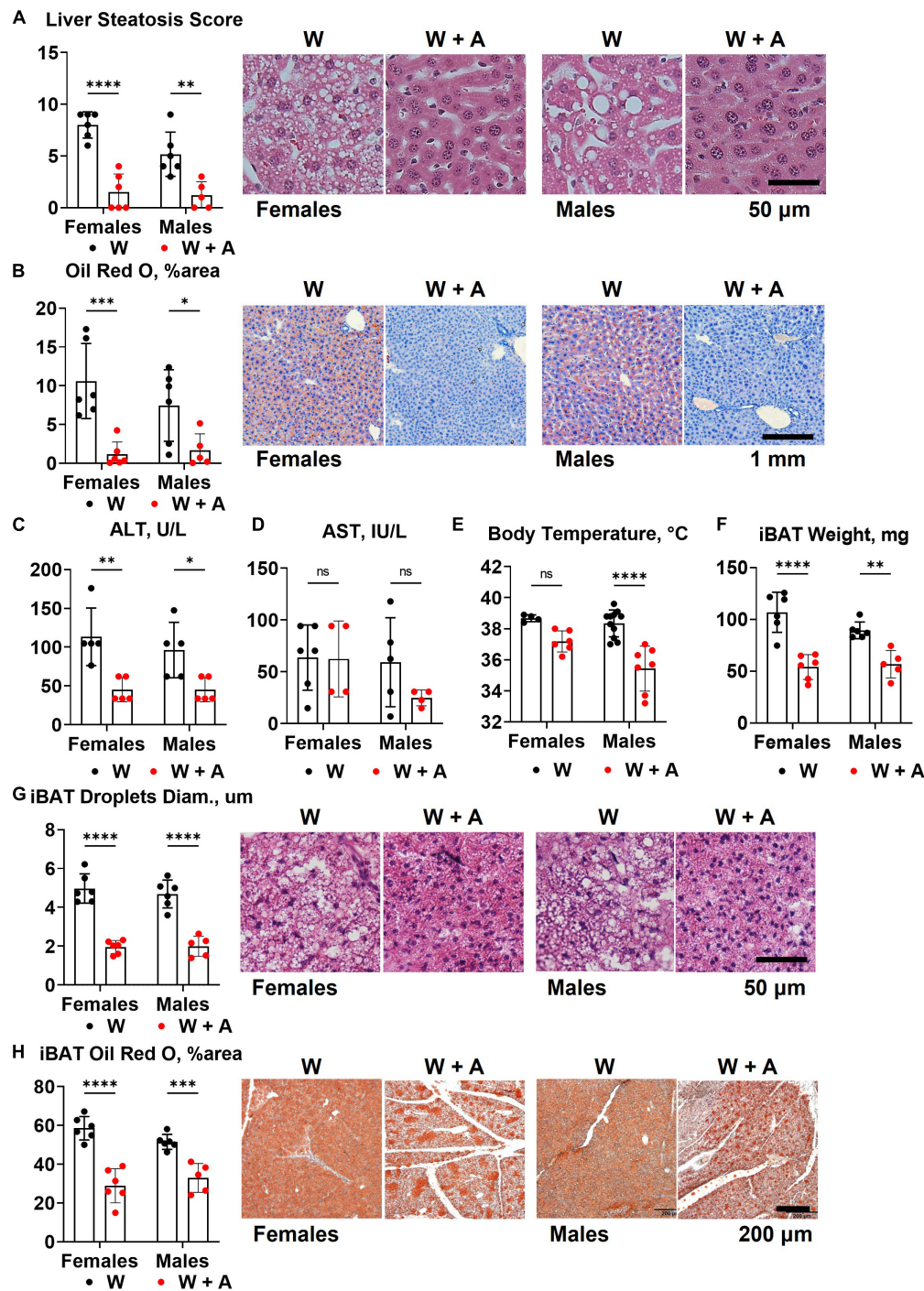
FIGURE 4
Liver and brown adipose tissue phenotypes of *WHC* mice treated with a western diet with or without adenine. **(A)** Pathology scores and representative images of H&E staining of the liver. **(B)** Representative images and quantification of Oil red O staining of the liver. **(C)** Plasma alanine transaminase (ALT). **(D)** Plasma aspartate transaminase (AST). **(E)** Core body temperature. **(F)** Interscapular brown adipose tissue (iBAT) weight. **(G)** Average diameter of lipid droplets in iBAT and representative images of iBAT stained with H&E. **(H)** iBAT lipis content detected by Oil red O staining. $n = 4–11$ per group; two-way ANOVA; ns, not significant; *$p < 0.05$; **$p < 0.01$; ***$p < 0.001$; ****$p < 0.0001$.

lobes. Grossed tissues were equilibrated in 30% sucrose in phosphate-buffered saline (PBS), embedded in an Optimal Cutting Temperature (OCT) compound (Sakura Finetek USA, Inc., Torrance, CA, USA), and frozen in liquid nitrogen vapor. Ten μm-thick cryosections were prepared using a cryostat and mounted on positively-charged slides. Slides were stained with hematoxylin and eosin (H&E), picrosirius red (kidneys), and Oil red O (liver). Four high-power

microscopic fields were imaged for each sample using an Olympus BX53 microscope (Olympus Co., Breinigsville, PA, USA). Kidney damage was assessed on a semi-quantitative pathological scale (0, 1, 2, 3) in H&E stained slides: 0 = no visible lesions; 1 = mild dilation of some tubules, luminal debris (casts), and partial nuclear loss in <1/3 tubules in a high-power field; 2 = apparent dilation of many tubules, nuclear loss, and cast in <2/3 tubules in a high-power field;
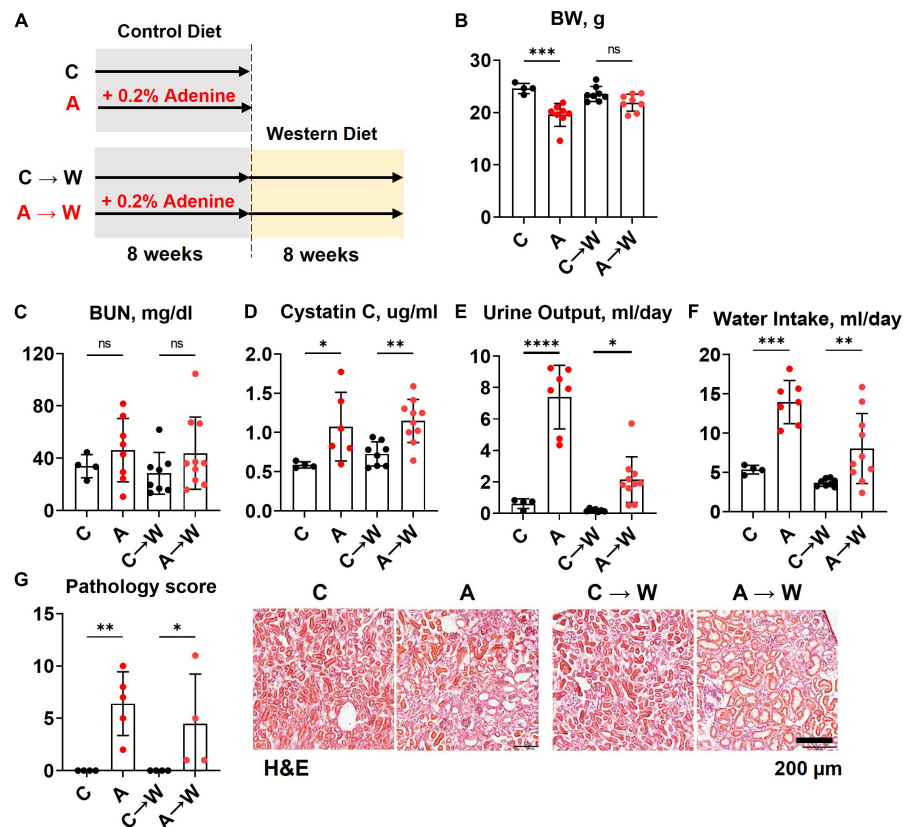
FIGURE 5

Chronic kidney disease in *WHC* female mice pre-treated with 0.2% adenine before a western diet. **(A)** Schematics of the experiment: control diet (C), 0.2% adenine in a control diet (A), control diet followed by a western diet (C→W), adenine diet followed by a western diet (A→W). **(B)** Body weight (BW). **(C)** Blood urea nitrogen (BUN). **(D)** Plasma Cystatin C. **(E)** 24-h urine output. **(F)** 24-h water intake. **(G)** Renal histology scores and representative images of H&E stained slides. $n = 4-10$ per group; two-way ANOVA. ns, not significant; *$p < 0.05$; **$p < 0.01$; ***$p < 0.001$; ****$p < 0.0001$.

3 = severe dilation of most tubules, casts, and interstitial proliferation in >2/3 of the cortex (27). Kidney fibrosis was estimated as an average Picrosirius red-positive area. Liver damage was graded by analyzing hepatocellular vesicular steatosis on a scale (0, 1, 2, 3) from 0 = no damage to 3 > 75% affected area (28). Liver lipid content was measured as an Oil red O positive percent area. Interscapular brown adipose tissue (iBAT) was dissected. Ten μm-thick cryosections were prepared and mounted on TruBond360 adhesion slides and stained with H&E and Oil red O. Atherosclerosis was assessed at the aortic root level. Cryosections of the aortic roots were prepared over the as per recommended protocol (29). We collected 72 consecutive 10 μm sections as an array on eight slides. Slides were stained with Oil red O and Alizarin red. Atherosclerosis in the aortic root was quantified by measuring the Oil red O-positive area using ImageJ software Similarly, calcification was quantified by measuring the alizarin red positive area in sections of the aortic root.

2.5. Statistical analysis

Data were analyzed in GraphPad Prism 9 statistical software (San Diego, CA, USA). A two-way ANOVA was used to determine the main effects and the interactions between sex and adenine treatment (experiment 1) or adenine pre-treatment and a western diet (experiment 2). Not normally distributed non-zero data were log-transformed to meet the assumptions of the two-way ANOVA.

Post hoc pair-wise comparisons were calculated using Sidak's multiple comparison test. In addition, a *t*-test or a Mann–Whitney test were applied to investigate specific effects. Survival curves were compared by a log-rank (Mantel–Cox) test. Data were reported as means and standard deviations (SD). A *p*-value of <0.05 was considered statistically significant.

3. Results

3.1. Tubulointerstitial disease in *WHC* mice co-treated with adenine and a western diet

Both male and female mice ($n = 6$ per group) were started on a western diet with or without 0.2% adenine supplementation when 10 weeks of age (**Figure 1A**). At the end of the 8-week treatment period, a significant loss of body weight (BW) was observed in both sexes ($p < 0.0001$, **Figure 1B**; **Supplementary Table 1**); one male mouse died. Adenine treatment was associated with a significant increase in plasma BUN and Cystatin C ($p < 0.0001$, two-way ANOVA; **Figures 1C, D**; **Supplementary Table 2**). A significant increase in 24-h water consumption and urine output was also observed in adenine-supplemented mice compared to those treated with a western diet alone ($p < 0.0001$, two-way
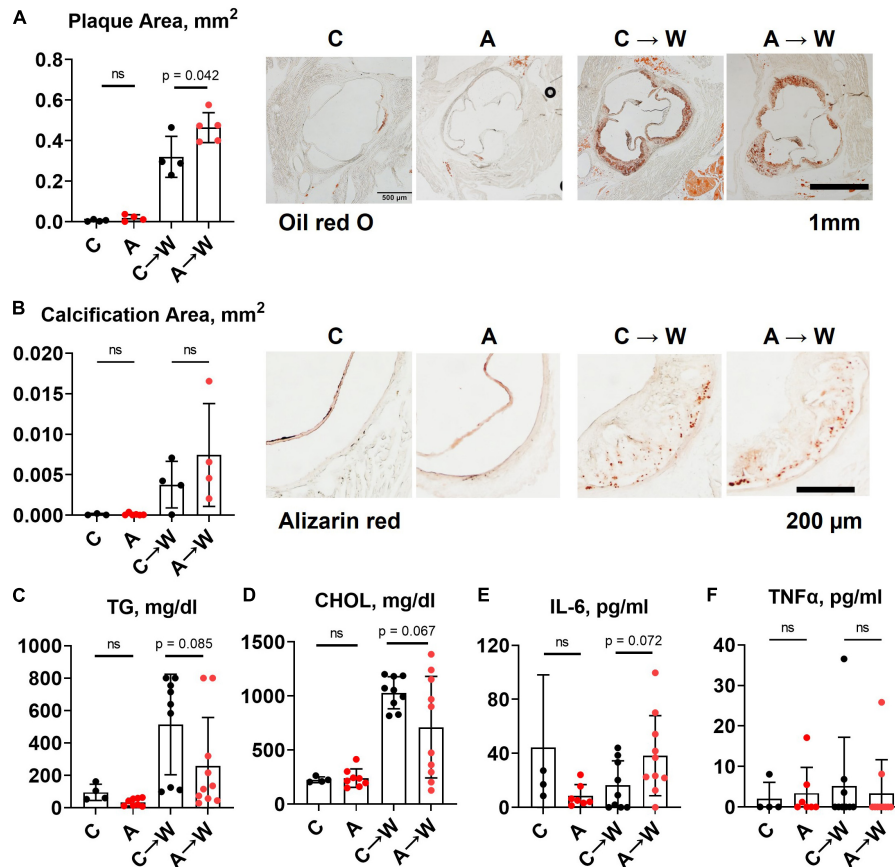
FIGURE 6

Aortic root atherosclerosis, plasma lipids, and inflammatory cytokines in *WHC* mice pre-treated with 0.2% adenine before a western diet.
(A) Representative images and quantification of Oil red O staining of the aortic root. **(B)** Representative images and quantification of alizarin red staining of the aortic root. **(C)** Plasma triglycerides (TG). **(D)** Cholesterol (CHOL). **(E)** Interleukin-6 (IL-6). **(F)** Tumor necrosis factor alpha (TNFα). $n = 4-6$ per group; two-way ANOVA; ns, not significant.

ANOVA; **Figures 1E, F**; **Supplementary Table 1**). After 8 weeks on a diet, H&E staining of the renal cortex displayed hallmark features of adenine-induced CKD, including tubular dilation, granulomatous inflammation, pus casts, and enlarged Bowman's space resulting in a significantly higher pathology score ($p < 0.0001$, two-way ANOVA; **Figure 1G**; **Supplementary Table 1**). The area positive for picrosirius red staining was also increased, indicating the development of interstitial fibrosis ($p < 0.0001$, two-way ANOVA; **Figure 1H**; **Supplementary Table 1**). Overall, these data confirmed the expected renal phenotype in mice treated with 0.2% adenine on a western diet (30).

3.2. Aortic root atherosclerosis, plasma lipids, and inflammation in *WHC* mice co-treated with adenine and a western diet

Unexpectedly, we found that adenine pre-treatment had a lowering effect on the aortic root atherosclerosis ($p < 0.0001$, two-way ANOVA; **Figure 2A**; **Supplementary Table 3**), despite the significant increase in vascular calcification ($p < 0.05$, two-way ANOVA; **Figure 2B**; **Supplementary Table 3**). In addition, plasma triglycerides and cholesterol were significantly reduced in

adenine-treated mice compared with those treated with a western diet only ($p < 0.0001$, two-way ANOVA, **Figures 2C, D**; **Supplementary Table 2**). Because it was reported that adenine might suppress inflammatory cytokines secretion (31) and, thus, explain a reduction in atherosclerosis, we tested plasma levels of interleukin 6 (IL-6) and tumor necrosis factor alpha (TNFα). Contrary to this potential explanation, we found an increase in IL-6 level in mice co-treated with adenine and a western diet ($p < 0.01$, two-way ANOVA; **Figure 2E**; **Supplementary Table 2**). No significant changes in TNF-α were observed, with several mice displaying TNF-α levels below the detection limit in all groups (**Figure 2F**; **Supplementary Table 2**).

3.3. Food consumption and macronutrient excretion in feces and urine of *WHC* mice co-treated with adenine and a western diet

We noted that mice treated with adenine had increased food consumption compared to mice from the western-only group ($p < 0.05$, two-way ANOVA; **Figure 3A**; **Supplementary Table 4**). There were no significant differences in fecal cholesterol or free fatty acids excretion in adenine treated mice compared to mice on a western diet alone (**Figures 3B, C**; **Supplementary Table 4**). No
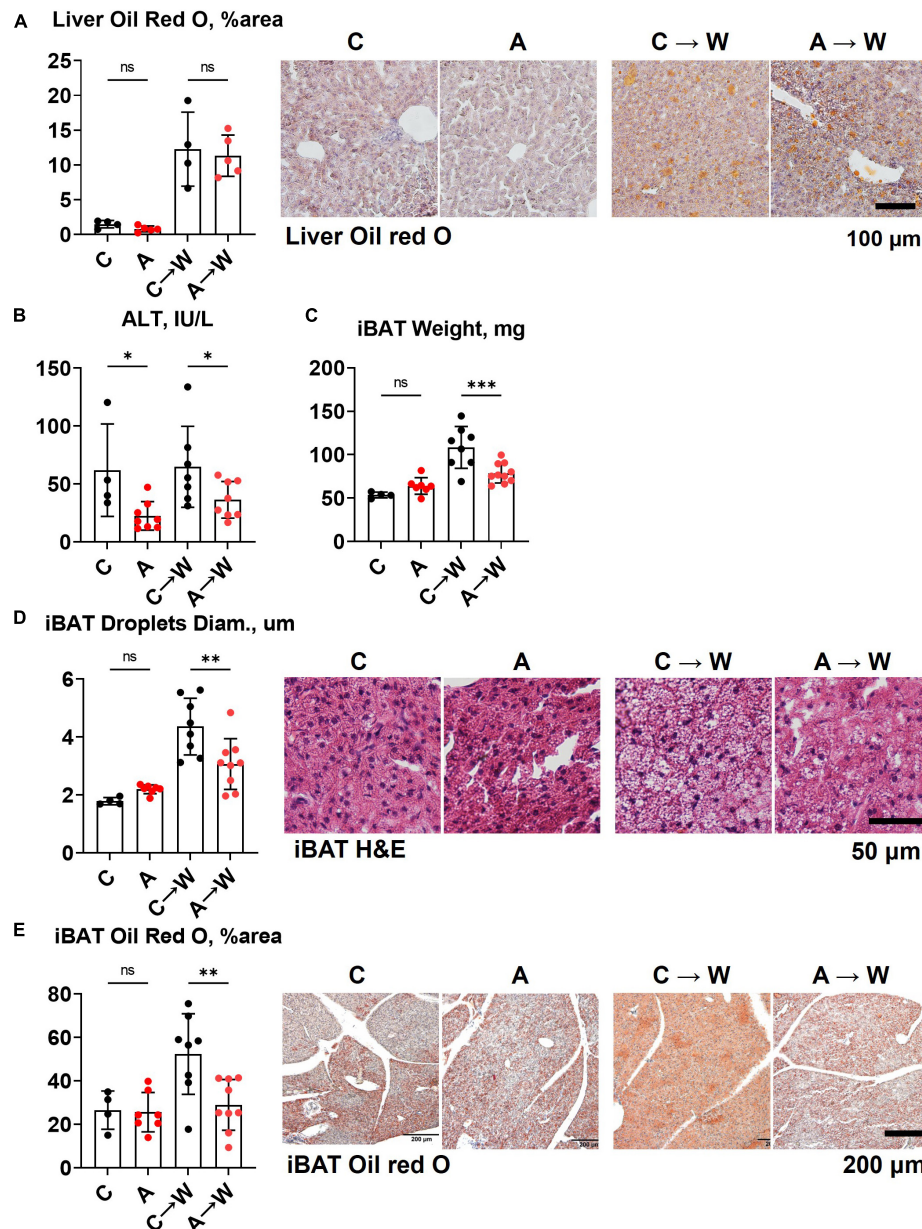
FIGURE 7
Liver and brown adipose tissue phenotypes in *WHC* mice pre-treated with adenine before a western diet. **(A)** Representative images and quantification of Oil red O staining of the liver. **(B)** Plasma alanine transaminase (ALT). **(C)** Interscapular brown adipose tissue (iBAT) weight. **(D)** Average diameter of lipid droplets in iBAT and representative images of iBAT stained with H&E. **(E)** iBAT lipis content detected by Oil red O staining. $n = 4–9$ per group; two-way ANOVA; ns, not significant; *$p < 0.05$; **$p < 0.01$; ***$p < 0.001$.

increase in urine protein or glucose excretion was found in adenine-treated mice compared to the western-only group (**Figures 3D, E**; **Supplementary Table 4**). An elevation in blood glucose was found in female mice co-treated with adenine and western; however, the overall effect was insignificant (**Figure 3F**; **Supplementary Table 4**).

3.4. Liver and brown adipose tissue phenotypes in *WHC* mice co-treated with adenine and a western diet

The reduction of triglycerides and cholesterol in fasted plasma may result from liver toxicity and an imbalance in the secretion of triglyceride-rich, very low-density lipoproteins (VLDL) due to liver steatosis (32). Since liver steatosis is likely to develop in *WHC* mice fed a western diet for 8 weeks, we investigated whether adenine could have worsened steatosis. Contrary to this idea, H&E staining unequivocally showed that instead of worsening, adenine prevented steatosis ($p < 0.0001$, **Figure 4A**; **Supplementary Table 5**). Furthermore, analyzing Oil red O staining of the liver, we found very little accumulation of lipids in the liver of adenine-treated mice compared to the western-only group ($p < 0.001$, females; $p < 0.05$, males; **Figure 4B**; **Supplementary Table 5**). Conversely, no significant elevation of ALT or AST were detected in adenine-treated mice (**Figures 4C, D**); in fact, lower ALT levels were observed in adenine-treated mice compared to mice on a western diet alone
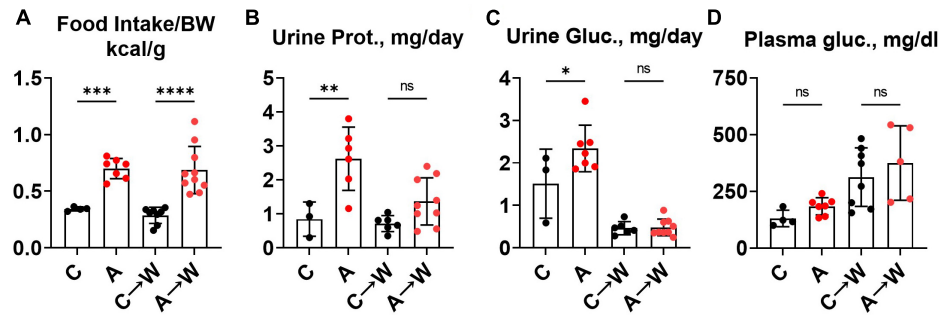
FIGURE 8

Food intake, urinary macromolecule loss, and plasma glucose in *WHC* mice pre-treated with adenine before a western diet. **(A)** 24-h calorie intake from food (control diet—LabDiets 5001; western—Envigo TD.88137). **(B)** 24-h urine protein excretion. **(C)** 24-h urine glucose excretion. **(D)** Fasted plasma glucose. *n* = 4−10 per group; two-way ANOVA; ns, not significant; *p < 0.05; **p < 0.01; ***p < 0.001; ****p < 0.0001.

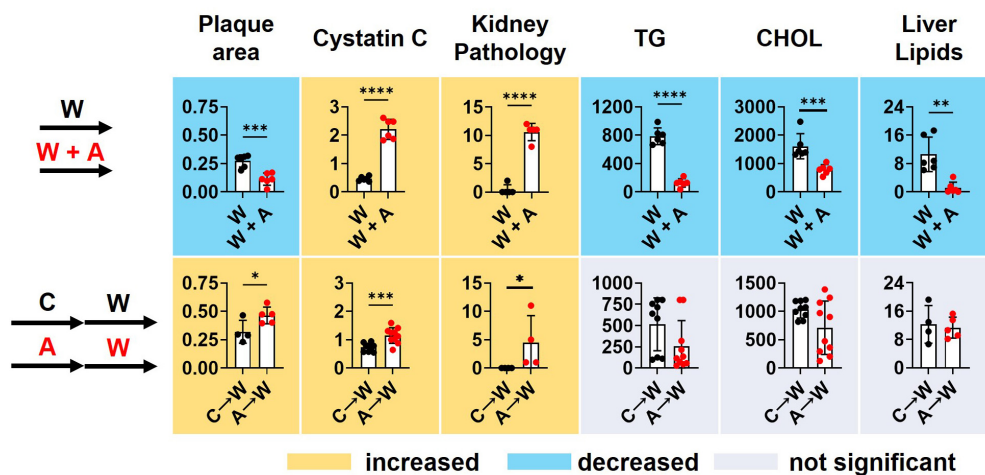**FIGURE 9**

Summary of key findings. *T*-test; *p < 0.05; **p < 0.01; ***p < 0.001; ****p < 0.0001.

($p < 0.001$, two-way ANOVA; **Figure 4C**; **Supplementary Table 2**). Thus, the direct hepatotoxicity of adenine as a cause of lipid reduction was ruled out.

Reduction in body weight and inability to accumulate lipids in the liver in mice treated with adenine could indicate an increase in thermogenesis. To address this possibility, we measured core body temperature and interscapular brown adipose tissue (iBAT) mass and lipid content. We found that mice treated with adenine had lower body temperatures than mice from the western-only group ($p < 0.0001$, two-way ANOVA; **Figure 4E**; **Supplementary Table 5**). Adenine-treated animals also had smaller iBAT mass, the diameter of lipid droplets within iBAT tissue, and the overall lipid content of iBAT ($p < 0.0001$ for all, two-way ANOVA; **Figures 4F–H**; **Supplementary Table 5**). Thus, there was no evidence of increased thermogenesis of BAT hyperplasia in mice treated with adenine.

3.5. Two-step model of adenine-induced CKD and atherosclerosis

Unfortunately, the profound effect of adenine on lipid metabolism has precluded testing our central hypothesis regarding the interaction between vascular calcification and atherosclerosis in CKD. Although the lipid-lowering effect associated with adenine supplementation was serendipitous, it was interesting and potentially clinically relevant. Therefore, we proceeded with the second study to better understand the mechanism of the lipid-lowering effect of adenine (**Figure 5A**).

Both male and female mice were included in the study. However, despite a reduced adenine dose (0.1%), the mortality in male mice was prohibitively high (**Supplementary Figure 1**), and we could not complete the study in males. Therefore, the remaining data represent the findings in females only. Data were collected at the end of the adenine pre-treatment and after western diet treatment.

3.6. Kidney disease in *WHC* mice pre-treated with adenine before a western diet

Mice were treated with a control diet with or without adenine for 8 weeks and then switched to a western diet without adenine supplementation for another 8 weeks. At the end of the first 8-week treatment, a significant loss of body weight was observed in the adenine-supplemented mice compared to those on a regular

diet ($p < 0.001$); the difference in body weight was not significant at the end of the western diet treatment ($p = 0.0681$, **Figure 5B**; **Supplementary Table 6**).

The BUN was not significantly affected by adenine in this experiment (**Figure 5C**; **Supplementary Table 7**). However, adenine pre-treated mice showed significant increases in plasma Cystatin C ($p < 0.05$), which persisted after discontinuation of adenine treatment ($p < 0.01$, **Figure 5D**; **Supplementary Table 7**). In addition, these mice also displayed significant polyuria and polydipsia immediately after the adenine treatment period and 8 weeks after they were switched to a western diet without adenine supplementation (**Figures 5E, F**; **Supplementary Table 6**).

H&E staining of the renal cortex revealed tubulointerstitial damage immediately after adenine pre-treatment ($p < 0.01$) that persisted until the end of the western diet treatment (**Figure 5G**; **Supplementary Table 6**).

3.7. Aortic root atherosclerosis and plasma lipids in *WHC* mice pre-treated with adenine before a western diet

Adenine pre-treatment did not affect aortic root plaque size (**Figure 6A**; **Supplementary Table 8**). However, a *t*-test comparison between adenine pre-treated and untreated mice detected a slight increase in plaque size in pre-treated mice compared to those not pre-treated ($p = 0.0418$). There was no significant difference in vascular calcification between the groups on the same diet (**Figure 6B**; **Supplementary Table 8**). Plasma triglycerides and cholesterol in adenine pre-treated mice were not significantly different compared to untreated mice on a western diet (**Figures 6C, D**; **Supplementary Table 7**). There were no differences in plasma inflammatory cytokines IL-6 and TNFα (**Figures 6E, F**; **Supplementary Table 7**) between adenine pre-treated and untreated mice on a western diet. This experiment demonstrated that the lipid-lowering effect of adenine in the setting of a western diet is reversible upon discontinuation of adenine and that adenine pre-treatment did not interfere with the development of aortic root atherosclerosis in *WHC* mice on a western diet.

3.8. Liver and brown adipose tissue phenotypes of *WHC* mice pre-treated with adenine before a western diet

In contrast to the first experiment involving the co-administration of adenine and a western diet, the liver lipid content quantified by Oil red O staining was similar between adenine pre-treated and untreated mice on a western diet (**Figure 7A**; **Supplementary Table 9**). Interestingly, ALT levels remained significantly lower in the adenine pre-treated mice compared to those untreated at both time points (**Figure 7B**; **Supplementary Table 7**). This experiment showed that the attenuation of hepatic steatosis by adenine appeared fully reversible upon its discontinuation. The size of interscapular brown adipose tissue (iBAT), lipid droplets diameter, and lipid content iBAT, however, was significantly reduced in adenine pre-treated mice 8 weeks after mice were switched to a western diet without adenine supplementation (**Figures 7C–E**; **Supplementary Table 9**).

3.9. Increased food intake and urinary macronutrient loss in *WHC* mice pre-treated with adenine before a western diet

We noted in the first experiment that mice co-treated with adenine and a western diet consumed more calories from food than non-exposed mice (**Supplementary Table 4**). The increase in food consumption was also significant in mice pre-treated with adenine compared to those untreated, and this difference persisted after discontinuation of adenine (**Figure 8A**; **Supplementary Table 10**). This phenotype was striking because adenine-exposed mice did not gain weight (**Figure 5B**), suggesting that adenine exposure accelerated metabolism. A plausible explanation was that mice were losing calories due to their kidney disease. Indeed, mice had significant proteinuria and glucosuria while on the adenine treatment; however, both effects were not significant after the discontinuation of adenine (**Figures 8B, C**; **Supplementary Table 10**). Of note, although increased on a western, as expected (33), plasma glucose concentration was not affected by adenine treatment (**Figure 8D**; **Supplementary Table 7**).

3.10. Summary of findings

Supplementing a western diet with 0.2% adenine for 8 weeks resulted in the development of CKD in *ldlr* mutant mice that was manifested as tubulointerstitial kidney damage and elevated plasma Cystatin C, a marker of kidney disease. In addition, adenine exposure suppressed hyperlipidemia and liver steatosis in *ldlr* mutant WHC mice on a western diet. Adenine-induced kidney disease persisted after its discontinuation. Plasma lipids and lipid metabolism in the liver appeared to rebound after discontinuation of adenine in *ldlr* mutant WHC mice consequently exposed to a western diet (**Figure 9**).

4. Discussion

The goal of this study was to model CKD in the background of hyperlipidemia using a non-surgical approach and then investigate the long-term effects of CKD-induced vascular calcification on the course of atherosclerosis. However, we were unable to test this hypothesis because of the unanticipated effect of adenine on lipid metabolism that masked the effect of vascular calcification on the extent of atherosclerosis. Adenine supplemented diet were used to induce CKD without surgery as previously described (30).

In the first experiment with a western diet and adenine co-treatment, we documented the reduction of renal function and tubulointerstitial pathology in male and female mice as expected. Surprisingly we found reduced plasma triglycerides, cholesterol, and atherosclerotic plaque formation, the findings that were opposite to a phenotype in a model of surgical kidney mass reduction (33, 34). In addition, we found a striking reduction of lipids in the liver without any signs of liver toxicity of adenine. Our observation raised the possibility that adenine might affect lipid metabolism.

While our manuscript was in preparation, two studies reported on atherosclerosis in adenine-treated *apoE* knockout mice. One

study showed an increase in plasma lipids without an increase in atherosclerosis, attributed by the authors to an overall reduction in inflammation (35). In our experiment, we observed an increase in plasma IL-6 and TNFα suggesting that the reduction of atherosclerosis was independent of inflammation in *ldlr* mutant WHC mice. In the other study, *apoE* knockout mice were treated with adenine in a western diet supplemented with sodium cholate. In this study, the authors observed no changes in plasma or liver lipids but reduced atherosclerosis, which was explained by the increased cholesterol and triglycerides excretion in feces and increased bile acid synthesis (36). We investigated the fecal excretion of cholesterol and free fatty acids in *ldlr* mutant WHC mice and found no evidence of the increased fecal fat in adenine-treated mice under the conditions of our experiment on a western diet without sodium cholate.

In our follow-up experiment, we administered adenine and western diets sequentially. We observed a tubulointerstitial injury, polydipsia, and polyuria in adenine pre-treated mice that persisted after 8 weeks of adenine washout. Plasma lipids were highly variable between individual mice within the adenine-pretreated mice, and the liver lipid content increased after mice were switched from an adenine-supplemented diet to a western diet. Moreover, mice pre-treated with adenine had significantly increased food intake, consuming twice as many calories without significant weight gain or blood glucose elevation.

Various metabolic effects could potentially explain the paradoxical reduction of atherosclerosis in the adenine-induced model of CKD. We can speculate that adenine-induced tubular damage results in macronutrient wasting and negative energy balance that leads to the reduction of synthesis of triglycerides and lipoproteins in the liver. As renal function improves following the withdrawal of adenine (as indicated by the resolution of proteinuria and glucosuria), the liver lipid metabolism rebounds and correlates with an increase in atherosclerosis in WHC mice after discontinuing adenine treatment. Such a mechanism suggests an indirect effect of renal tubular function of lipid metabolism and atherosclerosis. Alternatively, as discussed below, adenine might directly impact energy metabolism and triglyceride synthesis.

Several studies demonstrate the beneficial effects of adenine (31, 37–40). Adenine can act as an allosteric activator of a fuel-sensing enzyme AMP-activated protein kinase (AMPK), increasing cellular glucose metabolism (37); it can delay senescence of cultured cells (38), reduce inflammatory cytokines secretion and adhesion of monocytes to endothelial cells (31, 39), and improve wound healing (40). In addition, activation of AMPK has been shown to reduce hyperlipidemia and hepatic steatosis, plausibly explaining the liver and plasma lipid findings (41).

We observed that mice either co-treated or pre-treated with adenine neither exhibited histologic evidence of liver damage nor elevated ALT levels, suggesting that adenine was not toxic to the liver. Our results support findings from other studies showing a lack of adenine hepatotoxicity (42, 43). However, another study reported a hepatotoxic effect of adenine as demonstrated by elevated liver enzymes in response to inflammation (44). This is in contrast with the results of our study, in which increased systemic inflammation was not associated with elevated liver enzymes in adenine-treated animals.

Our study was not without limitations. Unfortunately, we could not test our hypothesis regarding the interaction between vascular calcification and atherosclerosis because of the unanticipated effects of adenine-induced CKD on lipid metabolism. Thus, the results of our study can only generate additional hypotheses. In the pre-treatment experiment, a more extended adenine clearance period and the assessment of the levels of adenine in plasma before administrating the western diet could have helped differentiate between the direct effects of adenine and tubulointerstitial injury on lipid metabolism or atherosclerosis. Alternatively, a different nephrotoxic agent acting on the proximal tubule, such as aminoglycosides (45), could be used to rule out the direct effects of adenine on metabolism. Lastly, the lack of direct measurements of energy expenditure and brown adipose tissue remains a significant limitation for the mechanistic understanding of the described lipid-lowering effect of adenine. Unfortunately, developing these timelines and experimental designs was outside the scope of this study.

Adenine-induced CKD has a metabolic effect on lipid and energy metabolism, and it may not be an appropriate model to study the effect of CKD on atherosclerosis in animals. Nevertheless, our findings can help design future hypothesis-driven research to understand the pathophysiology of increased metabolism and reduced atherosclerosis in adenine-treated mice.

Data availability statement

The raw data supporting the conclusions of this article will be made available by the authors, without undue reservation.

Ethics statement

The animal study was reviewed and approved by Institutional Animal Care and Use Committee (IACUC) of the New York Institute of Technology College of Osteopathic Medicine.

Author contributions

Funding

Acknowledgments

Conflict of interest

The authors declare that the research was conducted in the absence of any commercial or financial relationships that could be construed as a potential conflict of interest.

Publisher's note

All claims expressed in this article are solely those of the authors and do not necessarily represent those of their affiliated organizations, or those of the publisher, the editors and the reviewers. Any product that may be evaluated in this article, or claim that may be made by its manufacturer, is not guaranteed or endorsed by the publisher.

Supplementary material

The Supplementary Material for this article can be found online at: https://www.frontiersin.org/articles/10.3389/fcvm.2023.1088015/full#supplementary-material

References

1. Mathew R, Bangalore S, Lavelle M, Pellikka P, Sidhu M, Boden W, et al. Diagnosis and management of atherosclerotic cardiovascular disease in chronic kidney disease: a review. *Kidney Int.* (2017) 91:797–807.

2. Arnett D, Blumenthal R, Albert M, Buroker A, Goldberger Z, Hahn E, et al. 2019 ACC/AHA Guideline on the primary prevention of cardiovascular disease: executive summary: a report of the American College of Cardiology/American Heart Association Task Force on Clinical Practice Guidelines. *Circulation.* (2019) 140:e563–95.

3. Valdivielso J, Rodríguez-Puyol D, Pascual J, Barrios C, Bermúdez-López M, Sánchez-Niño M, et al. Atherosclerosis in chronic kidney disease: more, less, or just different? *Arterioscler Thromb Vasc Biol.* (2019) 39:1938–66.

4. Cainzos-Achirica M, Quispe R, Dudum R, Greenland P, Lloyd-Jones D, Rana J, et al. CAC for risk stratification among individuals with hypertriglyceridemia free of clinical atherosclerotic cardiovascular disease. *JACC Cardiovasc Imaging.* (2022) 15:641–51. doi: 10.1016/j.jcmg.2021.10.017

5. Fang Y, Ginsberg C, Sugatani T, Monier-Faugere M, Malluche H, Hruska K. Early chronic kidney disease-mineral bone disorder stimulates vascular calcification. *Kidney Int.* (2014) 85:142–50.

6. Vervloet M, Cozzolino M. Vascular calcification in chronic kidney disease: different bricks in the wall? *Kidney Int.* (2017) 91:808–17. doi: 10.1016/j.kint.2016.09.024

7. El Chamieh C, Liabeuf S, Massy Z. Uremic toxins and cardiovascular risk in chronic kidney disease: what have we learned recently beyond the past findings? *Toxins.* (2022) 14:280. doi: 10.3390/toxins14040280

8. Bi X, Du C, Wang X, Wang X, Han W, Wang Y, et al. Mitochondrial damage-induced innate immune activation in vascular smooth muscle cells promotes chronic kidney disease-associated plaque vulnerability. *Adv Sci.* (2021) 8:2002738. doi: 10.1002/advs.202002738

9. Lee T, Lu T, Chen C, Guo B, Hsu C. Hyperuricemia induces endothelial dysfunction and accelerates atherosclerosis by disturbing the asymmetric dimethylarginine/dimethylarginine dimethylaminotransferase 2 pathway. *Redox Biol.* (2021) 46:102108. doi: 10.1016/j.redox.2021.102108

10. Nakano T, Katsuki S, Chen M, Decano J, Halu A, Lee L, et al. Uremic toxin indoxyl sulfate promotes proinflammatory macrophage activation via the interplay of OATP2B1 and Dll4-notch signaling. *Circulation.* (2019) 139:78–96. doi: 10.1161/CIRCULATIONAHA.118.034588

11. Sun K, Tang X, Song S, Gao Y, Yu H, Sun N, et al. Hyperoxalemia leads to oxidative stress in endothelial cells and mice with chronic kidney disease. *Kidney Blood Press Res.* (2021) 46:377–86. doi: 10.1159/000516013

12. Mathew A, Zeng L, Atkins K, Sadri K, Byun J, Fujiwara H, et al. Deletion of bone marrow myeloperoxidase attenuates chronic kidney disease accelerated atherosclerosis. *J Biol Chem.* (2021) 296:100120. doi: 10.1074/jbc.RA120.014095

13. Lu X, Li H, Wang S. Hydrogen sulfide protects against uremic accelerated atherosclerosis via nPKCδ/Akt signal pathway. *Front Mol Biosci.* (2020) 7:615816. doi: 10.3389/fmolb.2020.615816

14. Wang J, Tsai P, Tseng K, Chen F, Yang W, Shen M. Sesamol ameliorates renal injury-mediated atherosclerosis via inhibition of oxidative stress/IKKα/p53. *Antioxidants.* (2021) 10:1519. doi: 10.3390/antiox10101519

15. Fujino Y, Yasuda-Yamahara M, Tanaka-Sasaki Y, Kuwagata S, Yamahara K, Tagawa A, et al. Limited effects of systemic or renal lipoprotein lipase deficiency on renal physiology and diseases. *Biochem Biophys Res Commun.* (2022) 620:15–20.

16. Shobeiri N, Adams M, Holden R. Vascular calcification in animal models of CKD: a review. *Am J Nephrol.* (2010) 31:471–81.

17. Oe Y, Mitsui S, Sato E, Shibata N, Kisu K, Sekimoto A, et al. Lack of endothelial nitric oxide synthase accelerates ectopic calcification in uremic mice fed an adenine and high phosphorus diet. *Am J Pathol.* (2021) 191:283–93. doi: 10.1016/j.ajpath.2020.10.012

18. Dargam V, Ng H, Nasim S, Chaparro D, Irion C, Seshadri S, et al. S2 heart sound detects aortic valve calcification independent of hemodynamic changes in mice. *Front Cardiovasc Med.* (2022) 9:809301. doi: 10.3389/fcvm.2022.809301

19. Tani T, Fujiwara M, Orimo H, Shimizu A, Narisawa S, Pinkerton A, et al. Inhibition of tissue-nonspecific alkaline phosphatase protects against medial arterial calcification and improves survival probability in the CKD-MBD mouse model. *J Pathol.* (2020) 250:30–41. doi: 10.1002/path.5346

20. Yang L, Dai R, Wu H, Cai Z, Xie N, Zhang X, et al. Unspliced XBP1 counteracts β-catenin to inhibit vascular calcification. *Circ Res.* (2022) 130:213–29. doi: 10.1161/CIRCRESAHA.121.319745

21. Tamura M, Aizawa R, Hori M, Ozaki H. Progressive renal dysfunction and macrophage infiltration in interstitial fibrosis in an adenine-induced tubulointerstitial nephritis mouse model. *Histochem Cell Biol.* (2009) 131:483–90. doi: 10.1007/s00418-009-0557-5

22. Diwan V, Brown L, Gobe G. Adenine-induced chronic kidney disease in rats. *Nephrology.* (2018) 23:5–11.

23. Svenson K, Ahituv N, Durgin R, Savage H, Magnani P, Foreman O, et al. A new mouse mutant for the LDL receptor identified using ENU mutagenesis. *J Lipid Res.* (2008) 49:2452–62. doi: 10.1194/jlr.M800303-JLR200

24. Romanelli F, Corbo A, Salehi M, Yadav M, Salman S, Petrosian D, et al. Overexpression of tissue-nonspecific alkaline phosphatase (TNAP) in endothelial cells accelerates coronary artery disease in a mouse model of familial hypercholesterolemia. *PLoS One.* (2017) 12:e0186426. doi: 10.1371/journal.pone.0186426

25. Rodionov R, Begmatov H, Jarzebska N, Patel K, Mills M, Ghani Z, et al. Homoarginine supplementation prevents left ventricular dilatation and preserves systolic function in a model of coronary artery disease. *J Am Heart Assoc.* (2019) 8:e012486. doi: 10.1161/JAHA.119.012486

26. Diwan V, Small D, Kauter K, Gobe G, Brown L. Gender differences in adenine-induced chronic kidney disease and cardiovascular complications in rats. *Am J Physiol Renal Physiol.* (2014) 307:F1169–78. doi: 10.1152/ajprenal.00676.2013

27. Di Giusto G, Anzai N, Endou H, Torres A. Oat5 and NaDC1 protein abundance in kidney and urine after renal ischemic reperfusion injury. *J Histochem Cytochem.* (2009) 57:17–27. doi: 10.1369/jhc.2008.951582

28. Liang W, Menke A, Driessen A, Koek G, Lindeman J, Stoop R, et al. Establishment of a general NAFLD scoring system for rodent models and comparison to human liver pathology. *PLoS One.* (2014) 9:e115922. doi: 10.1371/journal.pone.0115922

29. Daugherty A, Tall A, Daemen M, Falk E, Fisher E, Garcia-Cardena G, et al. Recommendation on design, execution, and reporting of animal atherosclerosis studies: a scientific statement from the American Heart Association. *Arterioscler Thromb Vasc Biol.* (2017) 37:e131–57.

30. Jia T, Olauson H, Lindberg K, Amin R, Edvardsson K, Lindholm B, et al. A novel model of adenine-induced tubulointerstitial nephropathy in mice. *BMC Nephrol.* (2013) 14:116. doi: 10.1186/1471-2369-14-116

31. Wu T, Chen C, Lin J, Young G, Wang H, Chen H. The anti-inflammatory function of adenine occurs through AMPK activation and its downstream transcriptional regulation in THP-1 cells. *Biosci Biotechnol Biochem.* (2019) 83:2220–9. doi: 10.1080/09168451.2019.1650632

32. Ress C, Kaser S. Mechanisms of intrahepatic triglyceride accumulation. *World J Gastroenterol.* (2016) 22:1664–73.

33. Bro S, Bentzon J, Falk E, Andersen C, Olgaard K, Nielsen L. Chronic renal failure accelerates atherogenesis in apolipoprotein E-deficient mice. *J Am Soc Nephrol.* (2003) 14:2466–74. doi: 10.1097/01.asn.0000088024.72216.2e

34. Massy Z, Ivanovski O, Nguyen-Khoa T, Angulo J, Szumilak D, Mothu N, et al. Uremia accelerates both atherosclerosis and arterial calcification in apolipoprotein E knockout mice. *J Am Soc Nephrol.* (2005) 16:109–16.

35. Zhang W, Miikeda A, Zuckerman J, Jia X, Charugundla S, Zhou Z, et al. Inhibition of microbiota-dependent TMAO production attenuates chronic kidney disease in mice. *Sci Rep.* (2021) 11:518.

36. Scherler L, Verouti S, Ackermann D, Vogt B, Escher G. Adenine-induced nephropathy reduces atherosclerosis in ApoE knockout mice. *Biomolecules.* (2022) 12:1147. doi: 10.3390/biom12081147

37. Young G, Lin J, Cheng Y, Huang C, Chao C, Nong J, et al. Identification of adenine modulating AMPK activation in NIH/3T3 cells by proteomic approach. *J Proteomics.* (2015) 120:204–14. doi: 10.1016/j.jprot.2015.03.012

38. Cheng Y, Young G, Chiu T, Lin J, Huang P, Kuo C, et al. Adenine supplement delays senescence in cultured human follicle dermal papilla cells. *Exp Dermatol.* (2016) 25:162–4. doi: 10.1111/exd.12881

39. Cheng Y, Young G, Lin J, Jang H, Chen C, Nong J, et al. Activation of AMP-activated protein kinase by adenine alleviates TNF-alpha-induced inflammation in human umbilical vein endothelial cells. *PLoS One.* (2015) 10:e0142283. doi: 10.1371/journal.pone.0142283

40. Young G, Lin J, Cheng Y, Ho C, Kuok Q, Hsu R, et al. Modulation of adenine phosphoribosyltransferase-mediated salvage pathway to accelerate diabetic wound healing. *FASEB J.* (2021) 35:e21296. doi: 10.1096/fj.202001736RR

41. Lian Z, Li Y, Gao J, Qu K, Li J, Hao L, et al. A novel AMPK activator, WS070117, improves lipid metabolism discords in hamsters and HepG2 cells. *Lipids Health Dis.* (2011) 10:67. doi: 10.1186/1476-511X-10-67

42. Feere D, Velenosi T, Urquhart B. Effect of erythropoietin on hepatic cytochrome P450 expression and function in an adenine-fed rat model of chronic kidney disease. *Br J Pharmacol.* (2015) 172:201–13. doi: 10.1111/bph.12932

43. Tokunaga A, Miyamoto H, Fumoto S, Nishida K. Effect of chronic kidney disease on hepatic clearance of drugs in rats. *Biol Pharm Bull.* (2020) 43:1324–30.

44. Al Za'abi M, Shalaby A, Manoj P, Ali B. The in vivo effects of adenine-induced chronic kidney disease on some renal and hepatic function and CYP450 metabolizing enzymes. *Physiol Res.* (2017) 66:263–71. doi: 10.33549/physiolres.933374

45. Rodríguez Salgueiro S, González Núñez L. Animal models mimicking aminoglycoside-induced renal damage. *J Nephropharmacol.* (2016) 5:1–3.

Frontiers in
Cardiovascular Medicine

Innovations and improvements in cardiovascular treatment and practice

Focuses on research that challenges the status quo of cardiovascular care, or facilitates the translation of advances into new therapies and diagnostic tools.

Discover the latest Research Topics

See more →

frontiers | Research Topics